

E-ISSN: 2148-6247



Turkish Journal of PHARMACEUTICAL SCIENCES

An Official Journal of the Turkish Pharmacists' Association, Academy of Pharmacy

Volume: **19** Issue: **2** April **2022**



www.turkjps.org

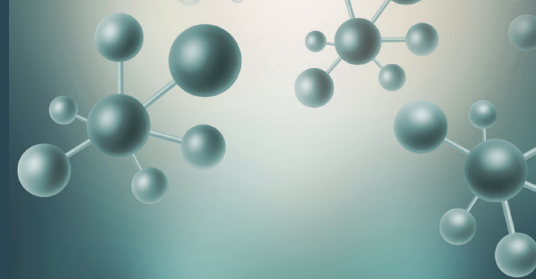


PubMed
Central

PublMed

Scopus

TRDIZIN



Turkish Journal of PHARMACEUTICAL SCIENCES

Editor-in-Chief

Prof. İlkey Erdoğan Orhan, Ph.D.

ORCID: <https://orcid.org/0000-0002-7379-5436>

Gazi University, Faculty of Pharmacy,
Department of Pharmacognosy, Ankara, TURKEY
iorhan@gazi.edu.tr

Associate Editors

Prof. Bensu Karahalil, Ph.D.

ORCID: <https://orcid.org/0000-0003-1625-6337>

Gazi University, Faculty of Pharmacy,
Department of Pharmaceutical Toxicology, Ankara, TURKEY
bensu@gazi.edu.tr

Assoc. Prof. Sinem Aslan Erdem, Ph.D.

ORCID: <https://orcid.org/0000-0003-1504-1916>

Ankara University, Faculty of Pharmacy, Department of
Pharmacognosy, Ankara, TURKEY
saslan@pharmacy.ankara.edu.tr

Editorial Board

MPharm, MSc, Afonso Miguel CAVACO, Ph.D.

ORCID: orcid.org/0000-0001-8466-0484

Lisbon University, Faculty of Pharmacy, Lisboa,
PORTUGAL
acavaco@campus.ul.pt

Prof. Bezhan CHANKVETADZE, Ph.D.

ORCID: orcid.org/0000-0003-2379-9815

Ivane Javakhishvili Tbilisi State University, Institute of
Physical and Analytical Chemistry, Tbilisi, GEORGIA
jpba_bezhan@yahoo.com

Prof. Blanca LAFFON, Ph.D.

ORCID: orcid.org/0000-0001-7649-2599

DICOMOSA group, Advanced Scientific Research
Center (CICA), Department of Psychology, Area
Psychobiology, University of A Coruña, Central
Services of Research Building (ESCI), Campus Elviña
s/n, A Coruña, SPAIN
blanca.laffon@udc.es

Prof. Christine LAFFORGUE, Ph.D.

ORCID: orcid.org/0000-0001-7798-2565

Paris Saclay University, Faculty of Pharmacy,
Department of Dermopharmacology and
Cosmetology, Paris, FRANCE
christine.lafforgue@universite-paris-saclay.fr

Prof. Dietmar FUCHS, Ph.D.

ORCID: orcid.org/0000-0003-1627-9563

Innsbruck Medical University, Center for Chemistry
and Biomedicine, Institute of Biological Chemistry,
Biocenter, Innsbruck, AUSTRIA
dietmar.fuchs@i-med.ac.at

Prof. Francesco EPIFANO, Ph.D.

ORCID: [0000-0002-0381-7812](https://orcid.org/0000-0002-0381-7812)

Università degli Studi G. d'Annunzio Chieti e Pescara,
Chieti CH, Italy
francesco.epifano@unich.it

Prof. Fernanda BORGES, Ph.D.

ORCID: orcid.org/0000-0003-1050-2402

Porto University, Faculty of Sciences, Department of
Chemistry and Biochemistry, Porto, PORTUGAL
fborges@fc.up.pt

Prof. Göksel ŞENER, Ph.D.

ORCID: orcid.org/0000-0001-7444-6193

Fenerbahçe University, Faculty of Pharmacy,
Department of Pharmacology, İstanbul, TURKEY
gseiner@marmara.edu.tr

Prof. Gülbin ÖZÇELİKAY, Ph.D.

ORCID: orcid.org/0000-0002-1580-5050

Ankara University, Faculty of Pharmacy, Department
of Pharmacy Management, Ankara, TURKEY
gozcelikay@ankara.edu.tr

Prof. Hermann BOLT, Ph.D.

ORCID: orcid.org/0000-0002-5271-5871

Dortmund University, Leibniz Research Centre,
Institute of Occupational Physiology, Dortmund,
GERMANY
bolt@ifado.de

Prof. Hildebert WAGNER, Ph.D.

Ludwig-Maximilians University, Center for
Pharmaceutical Research, Institute of Pharmacy,
Munich, GERMANY
H.Wagner@cup.uni-muenchen.de

Prof. İ. İrem ÇANKAYA, Ph.D.

ORCID: orcid.org/0000-0001-8531-9130

Hacettepe University, Faculty of Pharmacy, Department
of Pharmaceutical Botany, Ankara, TURKEY
itatli@hacettepe.edu.tr

Prof. K. Arzum ERDEM GÜRSAN, Ph.D.

ORCID: orcid.org/0000-0002-4375-8386

Ege University, Faculty of Pharmacy, Department of
Analytical Chemistry, İzmir, TURKEY
arzum.erdem@ege.edu.tr

Prof. Bambang KUSWANDI, Ph.D.

ORCID: [0000-0002-1983-6110](https://orcid.org/0000-0002-1983-6110)

Chemo and Biosensors Group, Faculty of Pharmacy
University of Jember, East Java, Indonesia
b_kuswandi.farmasi@unej.ac.id

Prof. Luciano SASO, Ph.D.

ORCID: orcid.org/0000-0003-4530-8706

Sapienze University, Faculty of Pharmacy
and Medicine, Department of Physiology and
Pharmacology "Vittorio Erspamer", Rome, ITALY
luciano.saso@uniroma1.it

Prof. Maarten J. POSTMA, Ph.D.

ORCID: orcid.org/0000-0002-6306-3653

University of Groningen (Netherlands), Department
of Pharmacy, Unit of Pharmacoepidemiology &
Pharmacoeconomics, Groningen, HOLLAND
m.j.postma@rug.nl

Prof. Meriç KÖKSAL AKKOÇ, Ph.D.

ORCID: orcid.org/0000-0001-7662-9364

Yeditepe University, Faculty of Pharmacy,
Department of Pharmaceutical Chemistry, İstanbul,
TURKEY
merickoksal@yeditepe.edu.tr

Prof. Mesut SANCAR, Ph.D.

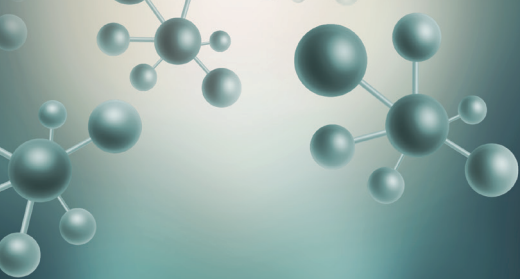
ORCID: orcid.org/0000-0002-7445-3235

Marmara University, Faculty of Pharmacy,
Department of Clinical Pharmacy, İstanbul, TURKEY
mesut.sancar@marmara.edu.tr

Assoc. Prof. Nadja Cristhina de SOUZA PINTO, Ph.D.

ORCID: orcid.org/0000-0003-4206-964X

University of São Paulo, Institute of Chemistry, São
Paulo, BRAZIL
nadja@iq.usp.br



Turkish Journal of PHARMACEUTICAL SCIENCES

Assoc. Prof. Neslihan AYGÜN KOCABAŞ, Ph.D. E.R.T.

ORCID: orcid.org/0000-0000-0000-0000
Total Research & Technology Feluy Zone
Industrielle Feluy, Refining & Chemicals, Strategy
– Development - Research, Toxicology Manager,
Seneffe, BELGIUM
neslihan.aygun.kocabas@total.com

Prof. Rob VERPOORTE, Ph.D.

ORCID: orcid.org/0000-0001-6180-1424
Leiden University, Natural Products Laboratory,
Leiden, NETHERLANDS
verpoort@chem.leidenuniv.nl

Prof. Robert RAPOPORT, Ph.D.

ORCID: orcid.org/0000-0001-8554-1014
Cincinnati University, Faculty of Pharmacy,
Department of Pharmacology and Cell Biophysics,
Cincinnati, USA
robertrapoport@gmail.com

Prof. Satyajit D. SARKER, Ph.D.

ORCID: orcid.org/0000-0003-4038-0514
Liverpool John Moores University, Liverpool,
UNITED KINGDOM
S.Sarker@ljmu.ac.uk

Prof. Tayfun UZBAY, Ph.D.

ORCID: orcid.org/0000-0002-9784-5637
Üsküdar University, Faculty of Medicine,
Department of Medical Pharmacology, Istanbul,
TURKEY
tayfun.uzbay@uskudar.edu.tr

Prof. Wolfgang SADEE, Ph.D.

ORCID: orcid.org/0000-0003-1894-6374
Ohio State University, Center for Pharmacogenomics, Ohio,
USA
wolfgang.sadee@osumc.edu

Advisory Board

Prof. Yusuf ÖZTÜRK, Ph.D.

Anadolu University, Faculty of Pharmacy,
Department of Pharmacology, Eskişehir, TURKEY
ORCID: 0000-0002-9488-0891

Prof. Tayfun UZBAY, Ph.D.

Üsküdar University, Faculty of Medicine,
Department of Medical Pharmacology, Istanbul,
TURKEY
ORCID: orcid.org/0000-0002-9784-5637

Prof. K. Hüsnü Can BAŞER, Ph.D.

Anadolu University, Faculty of Pharmacy,
Department of Pharmacognosy, Eskişehir, TURKEY
ORCID: 0000-0003-2710-0231

Prof. Erdem YEŞİLADA, Ph.D.

Yeditepe University, Faculty of Pharmacy,
Department of Pharmacognosy, Istanbul, TURKEY
ORCID: 0000-0002-1348-6033

Prof. Yılmaz ÇAPAN, Ph.D.

Hacettepe University, Faculty of Pharmacy,
Department of Pharmaceutical Technology, Ankara,
TURKEY
ORCID: 0000-0003-1234-9018

Prof. Sibel A. ÖZKAN, Ph.D.

Ankara University, Faculty of Pharmacy,
Department of Analytical Chemistry, Ankara,
TURKEY
ORCID: 0000-0001-7494-3077

Prof. Ekrem SEZİK, Ph.D.

Istanbul Health and Technology University, Faculty
of Pharmacy, Department of Pharmacognosy,
Istanbul, TURKEY
ORCID: 0000-0002-8284-0948

Prof. Gönül ŞAHİN, Ph.D.

Eastern Mediterranean University, Faculty of
Pharmacy, Department of Pharmaceutical
Toxicology, Famagusta, CYPRUS
ORCID: 0000-0003-3742-6841

Prof. Sevda ŞENEL, Ph.D.

Hacettepe University, Faculty of Pharmacy,

Department of Pharmaceutical Technology, Ankara,
TURKEY

ORCID: 0000-0002-1467-3471

Prof. Sevim ROLLAS, Ph.D.

Marmara University, Faculty of Pharmacy,
Department of Pharmaceutical Chemistry, Istanbul,
TURKEY
ORCID: 0000-0002-4144-6952

Prof. Göksel ŞENER, Ph.D.

Fenerbahçe University, Faculty of Pharmacy,
Department of Pharmacology, Istanbul, TURKEY
ORCID: 0000-0001-7444-6193

Prof. Erdal BEDİR, Ph.D.

İzmir Institute of Technology, Department of
Bioengineering, İzmir, TURKEY
ORCID: 0000-0003-1262-063X

Prof. Nurşen BAŞARAN, Ph.D.

Hacettepe University, Faculty of Pharmacy,
Department of Pharmaceutical Toxicology, Ankara,
TURKEY
ORCID: 0000-0001-8581-8933

Prof. Bensu KARAHALİL, Ph.D.

Gazi University, Faculty of Pharmacy, Department
of Pharmaceutical Toxicology, Ankara, TURKEY
ORCID: 0000-0003-1625-6337

Prof. Betül DEMİRCİ, Ph.D.

Anadolu University, Faculty of Pharmacy,
Department of Pharmacognosy, Eskişehir, TURKEY
ORCID: 0000-0003-2343-746X

Prof. Bengi USLU, Ph.D.

Ankara University, Faculty of Pharmacy,
Department of Analytical Chemistry, Ankara,
TURKEY
ORCID: 0000-0002-7327-4913

Prof. Ahmet AYDIN, Ph.D.

Yeditepe University, Faculty of Pharmacy,
Department of Pharmaceutical Toxicology, Istanbul,
TURKEY
ORCID: 0000-0003-3499-6435

Prof. İlkay ERDOĞAN ORHAN, Ph.D.

Gazi University, Faculty of Pharmacy, Department
of Pharmacognosy, Ankara, TURKEY
ORCID: 0000-0002-7379-5436

Prof. Ş. Güniz KÜÇÜKGÜZEL, Ph.D.

Fenerbahçe University Faculty of Pharmacy,
Department of Pharmaceutical Chemistry, Istanbul,
TURKEY
ORCID: 0000-0001-9405-8905

Prof. Engin Umut AKKAYA, Ph.D.

Dalian University of Technology, Department of
Chemistry, Dalian, CHINA
ORCID: 0000-0003-4720-7554

Prof. Esra AKKOL, Ph.D.

Gazi University, Faculty of Pharmacy, Department
of Pharmacognosy, Ankara, TURKEY
ORCID: 0000-0002-5829-7869

Prof. Erem BİLENSOY, Ph.D.

Hacettepe University, Faculty of Pharmacy,
Department of Pharmaceutical Technology, Ankara,
TURKEY
ORCID: 0000-0003-3911-6388

Prof. Uğur TAMER, Ph.D.

Gazi University, Faculty of Pharmacy, Department
of Analytical Chemistry, Ankara, TURKEY
ORCID: 0000-0001-9989-6123

Prof. Gülaçtı TOPÇU, Ph.D.

Bezmialem Vakıf University, Faculty of Pharmacy,
Department of Pharmacognosy, Istanbul, TURKEY
ORCID: 0000-0002-7946-6545

Prof. Hasan KIRMIZİBEKMEZ, Ph.D.

Yeditepe University, Faculty of Pharmacy,
Department of Pharmacognosy, Istanbul, TURKEY
ORCID: 0000-0002-6118-8225

**Members of the Advisory Board consist of the scientists
who received Science Award presented by TEB Academy
of Pharmacy in chronological order.*



Turkish Journal of PHARMACEUTICAL SCIENCES

AIMS AND SCOPE

The Turkish Journal of Pharmaceutical Sciences is the only scientific periodical publication of the Turkish Pharmacists' Association and has been published since April 2004.

Turkish Journal of Pharmaceutical Sciences journal is regularly published 6 times in a year (February, April, June, August, October, December). The issuing body of the journal is Galenos Yayınevi/Publishing House level. The aim of Turkish Journal of Pharmaceutical Sciences is to publish original research papers of the highest scientific and clinical value at an international level. The target audience includes specialists and professionals in all fields of pharmaceutical sciences.

The editorial policies are based on the "Recommendations for the Conduct, Reporting, Editing, and Publication of Scholarly Work in Medical Journals (ICMJE Recommendations)" by the International Committee of Medical Journal Editors (20, archived at <http://www.icmje.org/>) rules.

Editorial Independence

Turkish Journal of Pharmaceutical Sciences is an independent journal with independent editors and principles and has no commercial relationship with the commercial product, drug or pharmaceutical company regarding decisions and review processes upon articles.

ABSTRACTED/INDEXED IN

PubMed
PubMed Central
Web of Science-Emerging Sources Citation Index (ESCI)
SCOPUS SJR
TÜBİTAK/ULAKBİM TR Dizin
ProQuest
Chemical Abstracts Service (CAS)
EBSCO
EMBASE
GALE
Index Copernicus
Analytical Abstracts
International Pharmaceutical Abstracts (IPA)
Medicinal & Aromatic Plants Abstracts (MAPA)
British Library
CSIR INDIA
GOALI
Hinari
OARE
ARDI
AGORA
Türkiye Atıf Dizini
Türk Medline
UDL-EDGE
J- Gate
Idealonline
CABI

OPEN ACCESS POLICY

This journal provides immediate open access to its content on the principle that making research freely available to the public supports a greater global exchange of knowledge.

Open Access Policy is based on the rules of the Budapest Open Access Initiative (BOAI) <http://www.budapestopenaccessinitiative.org/>. By "open access" to peer-reviewed research literature, we mean its free availability on the public internet, permitting any users to read, download, copy, distribute, print, search, or link to the full texts of these articles, crawl them for indexing, pass them as data to software, or use them for any other lawful purpose, without financial, legal, or technical barriers other than those inseparable from gaining access to the internet itself. The only constraint on reproduction and distribution, and the only role for copyright in this domain, should be to give authors control over the integrity of their work and the right to be properly acknowledged and cited.

CORRESPONDENCE ADDRESS

All correspondence should be directed to the Turkish Journal of Pharmaceutical Sciences Editorial Board

Post Address: Turkish Pharmacists' Association, Mustafa Kemal Mah 2147.Sok No:3 06510 Çankaya/Ankara, TURKEY
Phone: +90 (312) 409 81 00
Fax: +90 (312) 409 81 09
Web Page: <http://turkjps.org>
E-mail: turkjps@gmail.com

PERMISSIONS

Requests for permission to reproduce published material should be sent to the publisher.

Publisher: Erkan Mor
Address: Molla Gürani Mah. Kaçamak Sok. 21/1 Fındıkzade, Fatih, İstanbul, Turkey
Telephone: +90 212 621 99 25
Fax: +90 212 621 99 27
Web page: <http://www.galenos.com.tr/en>
E-mail: info@galenos.com.tr

ISSUING BODY CORRESPONDING ADDRESS

Issuing Body : Galenos Yayınevi
Address: Molla Gürani Mah. Kaçamak Sk. No: 21/, 34093 İstanbul, Turkey
Phone: +90 212 621 99 25 Fax: +90 212 621 99 27
E-mail: info@galenos.com.tr

MATERIAL DISCLAIMER

The author(s) is (are) responsible for the articles published in the JOURNAL. The editors, editorial board and publisher do not accept any responsibility for the articles.

This work is licensed under a Creative Commons Attribution-NonCommercial-NoDerivatives 4.0 International License.



Galenos Publishing House
Owner and Publisher
Derya Mor
Erkan Mor
Publication Coordinator
Burak Sever
Web Coordinators
Fuat Hocalar
Turgay Akpınar
Graphics Department
Ayda Alaca
Çiğdem Birinci
Gülşah Özgül
Finance Coordinator
Sevinç Çakmak
Emre Kurtulmuş

Project Coordinators
Aysel Balta
Duygu Yıldırım
Gamze Aksoy
Gülşah Akın
Hatice Sever
Melike Eren
Özlem Çelik Çekil
Pınar Akpınar
Rabia Palazoğlu
Sümeyye Karadağ

Research&Development
Melisa Yiğitoğlu
Nihan Karamanlı
Digital Marketing Specialist
Ümit Topluoğlu

Publisher Contact
Address: Molla Gürani Mah. Kaçamak Sk. No: 21/1
34093 İstanbul, Turkey
Phone: +90 (212) 621 99 25 Fax: +90 (212) 621 99 27
E-mail: info@galenos.com.tr | yayin@galenos.com.tr
Web: www.galenos.com.tr | Publisher Certificate Number: 14521
Publication Date: April 2022
E-ISSN: 2148-6247
International scientific journal published bimonthly.



Turkish Journal of PHARMACEUTICAL SCIENCES

INSTRUCTIONS TO AUTHORS

Turkish Journal of Pharmaceutical Sciences journal is published 6 times (February, April, June, August, October, December) per year and publishes the following articles:

- Research articles
- Reviews (only upon the request or consent of the Editorial Board)
- Preliminary results/Short communications/Technical notes/Letters to the Editor in every field of pharmaceutical sciences.

The publication language of the journal is English.

The Turkish Journal of Pharmaceutical Sciences does not charge any article submission or processing charges.

A manuscript will be considered only with the understanding that it is an original contribution that has not been published elsewhere.

The Journal should be abbreviated as "Turk J Pharm Sci" when referenced.

The scientific and ethical liability of the manuscripts belongs to the authors and the copyright of the manuscripts belongs to the Journal. Authors are responsible for the contents of the manuscript and accuracy of the references. All manuscripts submitted for publication must be accompanied by the Copyright Transfer Form [copyright transfer]. Once this form, signed by all the authors, has been submitted, it is understood that neither the manuscript nor the data it contains have been submitted elsewhere or previously published and authors declare the statement of scientific contributions and responsibilities of all authors.

Experimental, clinical and drug studies requiring approval by an ethics committee must be submitted to the JOURNAL with an ethics committee approval report including approval number confirming that the study was conducted in accordance with international agreements and the Declaration of Helsinki (revised 2013) (<http://www.wma.net/en/30publications/10policies/b3/>). The approval of the ethics committee and the fact that informed consent was given by the patients should be indicated in the Materials and Methods section. In experimental animal studies, the authors should indicate that the procedures followed were in accordance with animal rights as per the Guide for the Care and Use of Laboratory Animals (<http://oacu.od.nih.gov/regs/guide/guide.pdf>) and they should obtain animal ethics committee approval.

Authors must provide disclosure/acknowledgment of financial or material support, if any was received, for the current study.

If the article includes any direct or indirect commercial links or if any institution provided material support to the study, authors must state in the cover letter that they have no relationship with the commercial product, drug, pharmaceutical company, etc. concerned; or specify the type of relationship (consultant, other agreements), if any.

Authors must provide a statement on the absence of conflicts of interest among the authors and provide authorship contributions.

All manuscripts submitted to the journal are screened for plagiarism using the 'iThenticate' software. Results indicating plagiarism may result in manuscripts being returned or rejected.

The Review Process

This is an independent international journal based on double-blind peer-review principles. The manuscript is assigned to the Editor-

in-Chief, who reviews the manuscript and makes an initial decision based on manuscript quality and editorial priorities. Manuscripts that pass initial evaluation are sent for external peer review, and the Editor-in-Chief assigns an Associate Editor. The Associate Editor sends the manuscript to at least two reviewers (internal and/or external reviewers). The Associate Editor recommends a decision based on the reviewers' recommendations and returns the manuscript to the Editor-in-Chief. The Editor-in-Chief makes a final decision based on editorial priorities, manuscript quality, and reviewer recommendations. If there are any conflicting recommendations from reviewers, the Editor-in-Chief can assign a new reviewer.

The scientific board guiding the selection of the papers to be published in the Journal consists of elected experts of the Journal and if necessary, selected from national and international authorities. The Editor-in-Chief, Associate Editors may make minor corrections to accepted manuscripts that do not change the main text of the paper.

In case of any suspicion or claim regarding scientific shortcomings or ethical infringement, the Journal reserves the right to submit the manuscript to the supporting institutions or other authorities for investigation. The Journal accepts the responsibility of initiating action but does not undertake any responsibility for an actual investigation or any power of decision.

The Editorial Policies and General Guidelines for manuscript preparation specified below are based on "Recommendations for the Conduct, Reporting, Editing, and Publication of Scholarly Work in Medical Journals (ICMJE Recommendations)" by the International Committee of Medical Journal Editors (20, archived at <http://www.icmje.org/>).

Preparation of research articles, systematic reviews and meta-analyses must comply with study design guidelines:

CONSORT statement for randomized controlled trials (Moher D, Schultz KF, Altman D, for the CONSORT Group. The CONSORT statement revised recommendations for improving the quality of reports of parallel group randomized trials. JAMA 2001; 285: 1987-91) (<http://www.consort-statement.org/>);

PRISMA statement of preferred reporting items for systematic reviews and meta-analyses (Moher D, Liberati A, Tetzlaff J, Altman DG, The PRISMA Group. Preferred Reporting Items for Systematic Reviews and Meta-Analyses: The PRISMA Statement. PLoS Med 2009; 6(7): e1000097.) (<http://www.prisma-statement.org/>);

STARD checklist for the reporting of studies of diagnostic accuracy (Bossuyt PM, Reitsma JB, Bruns DE, Gatsonis CA, Glasziou PP, Irwig LM, et al., for the STARD Group. Towards complete and accurate reporting of studies of diagnostic accuracy: the STARD initiative. Ann Intern Med 2003;138:40-4.) (<http://www.stard-statement.org/>);

STROBE statement, a checklist of items that should be included in reports of observational studies (<http://www.strobe-statement.org/>);

MOOSE guidelines for meta-analysis and systemic reviews of observational studies (Stroup DF, Berlin JA, Morton SC, et al. Meta-analysis of observational studies in epidemiology: a proposal for reporting Meta-analysis of observational Studies in Epidemiology (MOOSE) group. JAMA 2000; 283: 2008-12).



Turkish Journal of PHARMACEUTICAL SCIENCES

INSTRUCTIONS TO AUTHORS

GENERAL GUIDELINES

Manuscripts can only be submitted electronically through the Journal Agent website (<http://journalagent.com/tjps/>) after creating an account. This system allows online submission and review.

Format: Manuscripts should be prepared using Microsoft Word, size A4 with 2.5 cm margins on all sides, 12 pt Arial font and 1.5 line spacing.

Abbreviations: Abbreviations should be defined at first mention and used consistently thereafter. Internationally accepted abbreviations should be used; refer to scientific writing guides as necessary.

Cover letter: The cover letter should include statements about manuscript type, single-Journal submission affirmation, conflict of interest statement, sources of outside funding, equipment (if applicable), for original research articles.

ETHICS COMMITTEE APPROVAL

The editorial board and our reviewers systematically ask for ethics committee approval from every research manuscript submitted to the Turkish Journal of Pharmaceutical Sciences. If a submitted manuscript does not have ethical approval, which is necessary for every human or animal experiment as stated in international ethical guidelines, it must be rejected on the first evaluation.

Research involving animals should be conducted with the same rigor as research in humans; the Turkish Journal of Pharmaceutical Sciences asks original approval document to show implements the 3Rs principles. If a study does not have ethics committee approval or authors claim that their study does not need approval, the study is consulted to and evaluated by the editorial board for approval.

SIMILARITY

The Turkish Journal of Pharmaceutical Sciences is routinely looking for similarity index score from every manuscript submitted before evaluation by the editorial board and reviewers. The journal uses iThenticate plagiarism checker software to verify the originality of written work. There is no acceptable similarity index; but, exceptions are made for similarities less than 15 %.

REFERENCES

Authors are solely responsible for the accuracy of all references.

In-text citations: References should be indicated as a superscript immediately after the period/full stop of the relevant sentence. If the author(s) of a reference is/are indicated at the beginning of the sentence, this reference should be written as a superscript immediately after the author's name. If relevant research has been conducted in Turkey or by Turkish investigators, these studies should be given priority while citing the literature.

Presentations presented in congresses, unpublished manuscripts, theses, Internet addresses, and personal interviews or experiences should not be indicated as references. If such references are used, they should be indicated in parentheses at the end of the relevant sentence in the text, without reference number and written in full, in order to clarify their nature.

References section: References should be numbered consecutively in the order in which they are first mentioned in the text. All authors should be listed regardless of number. The titles of Journals should be abbreviated according to the style used in the Index Medicus.

Reference Format

Journal: Last name(s) of the author(s) and initials, article title, publication title and its original abbreviation, publication date, volume, the inclusive page numbers. Example: Collin JR, Rathbun JE. Involuntal entropion: a review with evaluation of a procedure. Arch Ophthalmol. 1978;96:1058-1064.

Book: Last name(s) of the author(s) and initials, book title, edition, place of publication, date of publication and inclusive page numbers of the extract cited.

Example: Herbert L. The Infectious Diseases (1st ed). Philadelphia; Mosby Harcourt; 1999:11;1-8.

Book Chapter: Last name(s) of the author(s) and initials, chapter title, book editors, book title, edition, place of publication, date of publication and inclusive page numbers of the cited piece.

Example: O'Brien TP, Green WR. Periocular Infections. In: Feigin RD, Cherry JD, eds. Textbook of Pediatric Infectious Diseases (4th ed). Philadelphia; W.B. Saunders Company; 1998:1273-1278.

Books in which the editor and author are the same person: Last name(s) of the author(s) and initials, chapter title, book editors, book title, edition, place of publication, date of publication and inclusive page numbers of the cited piece. Example: Solcia E, Capella C, Kloppel G. Tumors of the exocrine pancreas. In: Solcia E, Capella C, Kloppel G, eds. Tumors of the Pancreas. 2nd ed. Washington: Armed Forces Institute of Pathology; 1997:145-210.

TABLES, GRAPHICS, FIGURES, AND IMAGES

All visual materials together with their legends should be located on separate pages that follow the main text.

Images: Images (pictures) should be numbered and include a brief title. Permission to reproduce pictures that were published elsewhere must be included. All pictures should be of the highest quality possible, in JPEG format, and at a minimum resolution of 300 dpi.

Tables, Graphics, Figures: All tables, graphics or figures should be enumerated according to their sequence within the text and a brief descriptive caption should be written. Any abbreviations used should be defined in the accompanying legend. Tables in particular should be explanatory and facilitate readers' understanding of the manuscript, and should not repeat data presented in the main text.

MANUSCRIPT TYPES

Original Articles

Clinical research should comprise clinical observation, new techniques or laboratories studies. Original research articles should include title, structured abstract, key words relevant to the content of the article, introduction, materials and methods, results, discussion, study limitations, conclusion references, tables/figures/images and



Turkish Journal of PHARMACEUTICAL SCIENCES

INSTRUCTIONS TO AUTHORS

acknowledgement sections. Title, abstract and key words should be written in both Turkish and English. The manuscript should be formatted in accordance with the above-mentioned guidelines and should not exceed 16 A4 pages.

Title Page: This page should include the title of the manuscript, short title, name(s) of the authors and author information. The following descriptions should be stated in the given order:

1. Title of the manuscript (Turkish and English), as concise and explanatory as possible, including no abbreviations, up to 135 characters
2. Short title (Turkish and English), up to 60 characters
3. Name(s) and surname(s) of the author(s) (without abbreviations and academic titles) and affiliations
4. Name, address, e-mail, phone and fax number of the corresponding author
5. The place and date of scientific meeting in which the manuscript was presented and its abstract published in the abstract book, if applicable

Abstract: A summary of the manuscript should be written in both Turkish and English. References should not be cited in the abstract. Use of abbreviations should be avoided as much as possible; if any abbreviations are used, they must be taken into consideration independently of the abbreviations used in the text. For original articles, the structured abstract should include the following sub-headings:

Objectives: The aim of the study should be clearly stated.

Materials and Methods: The study and standard criteria used should be defined; it should also be indicated whether the study is randomized or not, whether it is retrospective or prospective, and the statistical methods applied should be indicated, if applicable.

Results: The detailed results of the study should be given and the statistical significance level should be indicated.

Conclusion: Should summarize the results of the study, the clinical applicability of the results should be defined, and the favorable and unfavorable aspects should be declared.

Keywords: A list of minimum , but no more than 5 key words must follow the abstract. Key words in English should be consistent with "Medical Subject Headings (MESH)" (www.nlm.nih.gov/mesh/MBrowser.html). Turkish key words should be direct translations of the terms in MESH.

Original research articles should have the following sections:

Introduction: Should consist of a brief explanation of the topic and indicate the objective of the study, supported by information from the literature.

Materials and Methods: The study plan should be clearly described, indicating whether the study is randomized or not, whether it is retrospective or prospective, the number of trials, the characteristics, and the statistical methods used.

Results: The results of the study should be stated, with tables/figures given in numerical order; the results should be evaluated according to the statistical analysis methods applied. See General Guidelines for details about the preparation of visual material.

Discussion: The study results should be discussed in terms of their favorable and unfavorable aspects and they should be compared with the literature. The conclusion of the study should be highlighted.

Study Limitations: Limitations of the study should be discussed. In addition, an evaluation of the implications of the obtained findings/ results for future research should be outlined.

Conclusion: The conclusion of the study should be highlighted.

Acknowledgements: Any technical or financial support or editorial contributions (statistical analysis, English/Turkish evaluation) towards the study should appear at the end of the article.

References: Authors are responsible for the accuracy of the references. See General Guidelines for details about the usage and formatting required.

Review Articles

Review articles can address any aspect of clinical or laboratory pharmaceuticals. Review articles must provide critical analyses of contemporary evidence and provide directions of or future research. Most review articles are commissioned, but other review submissions are also welcome. Before sending a review, discussion with the editor is recommended.

Reviews articles analyze topics in depth, independently and objectively. The first chapter should include the title in Turkish and English, an unstructured summary and key words. Source of all citations should be indicated. The entire text should not exceed 25 pages (A, formatted as specified above).



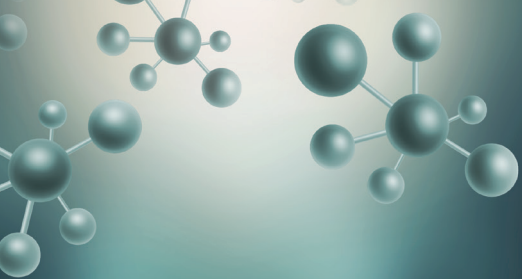
CONTENTS

Original Articles

- 116 Ameliorative Effect of Marine Macroalgae on Carbon Tetrachloride-Induced Hepatic Fibrosis and Associated Complications in Rats
Maria AZAM, Khan HIRA, Shamim A. QURESHI, Nasira KHATOON, Jehan ARA, Syed EHTESHAMUL-HAQUE
- 125 Design, Development, Optimization and Evaluation of Ranolazine Extended Release Tablets
Raghavendra Kumar GUNDA, Prasada Rao MANCHINENI, Dhachinamoorthi DURAISWAMY, Koteswara Rao GSN
- 132 Protective Role of *Diospyros lotus* L. in Cisplatin-Induced Cardiotoxicity: Cardiac Damage and Oxidative Stress in Rats
Neşe BAŞAK TÜRKMEN, Dilan AŞKIN ÖZEK, Aslı TAŞLIDERE, Osman ÇİFTÇİ, Özlem SARAL, Cemile Ceren GÜL
- 138 A Combination of Virgin Coconut Oil and Extra Virgin Olive Oil Elicits Superior Protection Against Doxorubicin Cardiotoxicity in Rats
Andi Ulfiana UTARI, Yulia Yusrini DJABIR, Bogie Putra PALINGGI
- 145 Phytochemical, Histochemical and *In Vitro* Antimicrobial Study of Various Solvent Extracts of *Costus speciosus* (J. Koenig) Sm. and *Costus pictus* D. Don
Sana Saffiruddin SHAIKH, Abubakar Salam BAWAZIR, Barrawaz Aateka YAHYA
- 153 Formulation and Development of Aqueous Film Coating for Moisture Protection of Hygroscopic *Herniaria glabra* L. Tablets
Hakim EL MABROUKI, Irina Evgenievna KAUKHOVA
- 161 Vitamin D with Calcium Supplementation Managing Glycemic Control with HbA1c and Improve Quality of Life in Patients with Diabetes
Sanjana MEHTA, Parminder NAIN, Bimal K. AGRAWAL, Rajinder Pal SINGH
- 168 Preparation and Characterization of Orlistat Bionanocomposites Using Natural Carriers
Santosh PAYGHAN, Vaishali PAYGHAN, Kavita NANGARE, Lalita DAHIWADE, Karna KHAVANE, Ram PHALKE
- 180 13, 14-Epoxyoleanan-3-ol-acetate: A Male Fertility-Enhancing Constituent from Hexane Fraction of *Momordica charantia* L. (Cucurbitaceae)
Oluwasegun ADEDOKUN, Adebayo GBOLADE, Bunyaminu AYINDE
- 187 Chitosan-Based Microparticle Encapsulated *Acinetobacter baumannii* Phage Cocktail in Hydrogel Matrix for the Management of Multidrug Resistant Chronic Wound Infection
Margaret O. ILOMUANYA, Nkechi V. ENWURU, Emmanuella ADENOKUN, Abigail FATUNMBI, Adebawale ADELUOLA, Cecilia I. IGWILLO
- 196 Creatine and Alpha-Lipoic Acid Antidepressant-Like Effect Following Cyclosporine A Administration
Mehdi ALIOMRANI, Azadeh MESRIPOUR, Abolfazl Saleki MEHRJARDI
- 202 Potential Inhibitors of SARS-CoV-2 from *Neocarya macrophylla* (Sabine) Prance ex F. White: Chemoinformatic and Molecular Modeling Studies for Three Key Targets
Amina Jega YUSUF, Musa Ismail ABDULLAHI, Aliyu Muhammad MUSA, Hassan ABUBAKAR, Abubakar Muhammad AMALI, Asma'u Hamza NASIR

Short Communication

- 213 Simple and Sensitive RP-HPLC and UV Spectroscopic Methods for the Determination of Remogliflozin Etabonate in Pure and Pharmaceutical Formulations
Nandeeshia ITIGIMATHA, Kailash S. CHADCHAN, Basappa C. YALLUR, Manjunatha D. HADAGALI



Turkish Journal of PHARMACEUTICAL SCIENCES

CONTENTS

Reviews

- 220 A Brief Discussion of Multi-Component Organic Solids: Key Emphasis on Co-Crystallization
Braham DUTT, Manjusha CHOUDHARY, Vikas BUDHWAR
- 232 Challenges Faced by Hospital Pharmacists in Low-Income Countries Before COVID-19 Vaccine Roll-Out:
Handling Approaches and Implications for Future Pandemic Roles
Rajeev SHRESTHA, Sunil SHRESTHA, Binaya SAPKOTA, Saval KHANAL, Bhuvan KC



Ameliorative Effect of Marine Macroalgae on Carbon Tetrachloride-Induced Hepatic Fibrosis and Associated Complications in Rats

✉ Maria AZAM¹, ✉ Khan HIRA^{1,2}, ✉ Shamim A. QURESHI¹, ✉ Nasira KHATOON³, ✉ Jehan ARA⁴, ✉ Syed EHTESHAMUL-HAQUE^{5*}

¹Karachi University, Faculty of Science, Department of Biochemistry, Karachi, Pakistan

²Dow University of Health Sciences, Dow College of Pharmacy, Department of Pharmacology, Karachi, Pakistan

³Karachi University, Faculty of Science, Department of Zoology, Karachi, Pakistan

⁴Karachi University, Faculty of Science, Department of Food Science and Technology, Karachi, Pakistan

⁵Karachi University, Faculty of Science, Department of Botany, Karachi, Pakistan

ABSTRACT

Objectives: Liver fibrosis is one of the serious health concern around the globe. Persistent exposure to drugs, toxicants, and pathogens may induce liver fibrosis. Marine macroalgae are globally consumed because of nutritive and medicinal value. This study was conducted to evaluate the protective role of two seaweeds *Padina pavonia* and *Caulerpa racemosa* in carbon tetrachloride (CCl₄)-induced liver fibrosis in rats.

Materials and Methods: Animal model of hepatic fibrosis was developed by injecting 40% CCl₄ dissolved in olive oil [2 mL/kg, body weight (b.w.), i.p.] on alternate days for 30 days. Water extracts (WE) [200 mg/kg b.w., p.o.] of *P. pavonia* and *C. racemosa* were given to rats daily for 30 days. On day 31, rats were sacrificed after 12 h fasting. Serum was used for biochemical estimation. 10% neutral buffered formalin was used to preserve the liver sample for histopathological examination, while the other portion was used for the preparation of tissue homogenate to estimate antioxidant enzymes and malondialdehyde levels.

Results: WEs of both marine macro-algae significantly abrogate the elevated serum concentrations of aminotransferases (alanine aminotransferase and aspartate aminotransferases), alkaline phosphatase and lactate dehydrogenase along with a substantial ($p < 0.05$) reduction in serum bilirubin levels. They also showed positive effects on oxidative stress, evident by improvement in reduced glutathione, catalase, and glutathione peroxidase activities and down regulation of lipid peroxidation level, with stabilizing the destructive cellular morphology of liver induced by repeated CCl₄ injection. Both algal extracts also improved kidney function (urea and creatinine) along with lipid metabolism (triglycerides and cholesterol).

Conclusion: WE of *C. racemosa* has shown great potential in attenuating liver fibrosis induced by CCl₄.

Key words: *Padina pavonia*, *Caulerpa racemosa*, bilirubin, glutathione, lipid peroxidation, kidney

INTRODUCTION

The liver is the metabolic hub for the degradation, synthesis, detoxification and transformation of drugs and biomolecules. Along with all vital functions it performs, it is also prone to toxicity.¹ The liver comprises various cells, such as hepatocytes, hepatic stellate cells (HSCs), which work as a reservoir of lipid droplet (vitamin A) and Kupffer cells, usually known as resident macrophages of liver.² Viral infections, chemical/drug intoxication, or any malfunctioning of liver lead to damage of hepatocytes.³ HSCs, release extracellular matrix

(ECM) components around the injured area to prevent the further damage to the liver.⁴ Chronic exposure of the liver with toxicants resulting in continuous activation of HSCs, forming scar tissues in the liver, lead to conditions such as; fibrosis, cirrhosis, and hepatocellular carcinoma.⁵ Liver fibrosis is one of the serious health concern around the globe⁶ and it is an early stage of cirrhosis.⁷ It has been reported that the fibrotic liver contains more ECM components, which contains collagens (I, III, and IV), fibronectin, elastin, laminin, hyaluronic acid, and proteoglycans.⁸ The earlier diagnosis of liver fibrosis is

*Correspondence: sehaq@uok.edu.pk, Phone: +923012420634, ORCID-ID: orcid.org/0000-0002-8540-4068

Received: 15.03.2021, Accepted: 04.07.2021

©Turk J Pharm Sci, Published by Galenos Publishing House.

important since it is treatable and termed as reversible liver fibrosis.⁹

Carbon tetrachloride (CCl_4) has been widely used for developing animal models of hepatic fibrosis, cirrhosis, and hepatocellular carcinoma for many decades.¹⁰ The lipid-soluble nature of CCl_4 allows it to cross the lipid bilayer membrane, produces hindrance in cellular activities by promoting the lipid peroxidation, activating reactive oxygen species (ROS).¹¹ Persistent exposure of CCl_4 promotes accumulation of ECM components, which either damages the cellular structures and/or disturbs the cellular integrity.¹²

Among different marine sources, macroalgae have drawn the attention of many researchers as an interesting and unique source of bioactive natural products, besides, a great source of proteins, carbohydrates, minerals and vitamins.¹³ They have medicinal importance, including anticancer, antibacterial, anticoagulant, nephroprotective, anti-inflammatory and antioxidant activities.^{14,15} Green seaweeds are a rich source of carotenoids, phenolics, terpenoids, essential proteins, vitamins, minerals and sulfated polysaccharides (SP).¹⁶ *Ulva* and *Caulerpa* species contain higher contents of SP and rare sugars (arabinose, rhamnose and iduronic acid).¹⁷ *Caulerpa racemosa*, an edible green seaweed, has number of biological activities such as antibacterial and hypolipidemic activities against triton-induced hyperlipidemic rats.^{18,19} However, the hepatoprotective role of this seaweed against CCl_4 induced hepatic injury has not been evaluated. Brown seaweeds contain phenolic compounds and SP (alginates, fucoidans, and laminarins) and possess tremendous biological activities such as hepatoprotective, anticancer, anticoagulant, wound healing, and antiviral.¹⁴ *Padina pavonia*, has been previously reported to have anti-proliferative and pro-apoptotic activities.²⁰ Its hepatoprotective activity against azoxymethane-induced hepatotoxicity has been reported.²¹ However, its hepatoprotective activity against CCl_4 has not been explored, yet. The current study was designed to elucidate the hepatoprotective potential of *C. racemosa* and *P. pavonia* against CCl_4 -induced liver fibrosis. The study also describes the effect of these seaweeds on liver fibrosis associated complications, including renal dysfunction and lipid metabolism.

MATERIALS AND METHODS

Algal materials

Seaweeds were collected from the Karachi coast (Buleji Beach) at low tide during the month of November–April. Collected algal samples were identified by a taxonomist (Dr. Aisha Begum, Associate Professor, Department of Botany, University of Karachi). The algal material was washed using running tap water and air dried under a green shade. The dried samples were ground and stored for further use.

Water extracts

Water extract (WE) was obtained by soaking dry powder (250 g) of each seaweed in 1 L of deionized water under continuous shaking for 3 h. The filtrate obtained was lyophilized using a lyophilizer (Eyela FD-1, Japan). The dry powders were stored separately at -20°C until used according to Ismail and Tan.²²

Experimental animals

Female Wistar rats (120–200 g) acquired from Dow University of Health Sciences, Karachi. Animals were accommodated in polypropylene cages under standard laboratory conditions ($23 \pm 2^\circ\text{C}$ and 12 h light/dark cycle). The cages were bedded with wood shaving and the rats had free access to a normal pellet diet and tap water. Rats were acclimatized for 7 days under the guidelines of the Institutional Bioethical Committee University of Karachi (IBC-KU-132/2020) before the experimental protocol.

Induction of fibrosis

The method of Iredale et al.²³ was followed to develop hepatic fibrosis in rats with slight modification. Rats received 40% CCl_4 intraperitoneally (*i.p.*) at 2 mL/kg body weight (b.w.), dissolved in olive oil, on alternative days for 30 days.

Experimental design

Effect of the WE of seaweeds in normal and liver fibrotic rat model

To evaluate the efficacy of seaweed extracts in rats, they were randomly divided into 8 groups (n= 6).

Group 1; Normal control: Rats received distilled water at 1 mL/kg b.w., daily for 30 days.

Group 2; WE of *P. pavonia*-treated rats: WE of *P. pavonia* was supplemented to rats at 200 mg/kg/mL, b.w., in distilled water, daily for 30 days.

Group 3; WE of *C. racemosa*-treated rats: WE of *C. racemosa* was supplemented to rats at 200 mg/kg /mL, b.w., in distilled water, daily for 30 days.

Group 4; Silymarin-treated rats: Rats were supplemented with silymarin [Sigma-aldrich (50 mg/kg b.w., suspended in normal saline)] daily for 30 days.²⁴

Group 5; CCl_4 control: Rats were intraperitoneally (*i.p.*) injected 40% CCl_4 (in olive oil) 2 mL/kg b.w., on alternate days for 30 days.

Group 6; WE of *P. pavonia* + CCl_4 -induced liver fibrosis: WE of *P. pavonia* was supplemented to rats at 200 mg/kg/mL, b.w., in distilled water, along with the administration of CCl_4 (*i.p.*, 2 mL/kg, b.w.), on alternate days for 30 days.

Group 7; WE of *C. racemosa* + CCl_4 -induced liver fibrosis: WE of *C. racemosa* was supplemented to rats at 200 mg/kg /mL, b.w., in distilled water daily, along with the administration of CCl_4 (*i.p.*, 2 mL/kg, b.w.), on alternate days for 30 days.

Group 8; Silymarin treatment + CCl_4 -induced liver fibrosis: Rats were supplemented with silymarin [Sigma-aldrich (50 mg/kg b.w., suspended in normal saline)] daily, along with the administration of CCl_4 (*i.p.*, 2 mL/kg, b.w.), on alternate days for 30 days.

Assessment of hepatotoxicity and associated complications

To determine the effect of seaweed on liver fibrosis and other associated complications; rats were fasted for 12 h and decapitated on the 31st day. Blood was centrifuged at 3000 rpm for 15 min to obtain serum. Liver enzymes, viz; alanine aminotransferase (ALAT) (INO-17531) aspartate

aminotransferase (ASAT) (INO-17521), lactate dehydrogenases (LDH) (INO-17653), alkaline phosphatases (ALP) (INO-17541), and other liver markers, viz; total-bilirubin (INO-17645) and direct-bilirubin (INO-17646); lipid parameters including cholesterol (INO-17501) and triglycerides (TGs) (INO-17511), renal function markers such as urea (INO-17611) & creatinine (INO-17551) and blood glucose (INO-17602) were estimated on blood chemistry analyzer (Microlab-300, Merck, France) using kits from Merck (Innoline), France as *per* manufacturer's instructions.

For histopathological studies, the liver was excised, washed with normal saline. The right lobe was preserved in 10% neutral buffered formalin. The remaining portion of liver was used for the preparation of liver tissue homogenate [Tris-HCl buffer (pH: 7.4) using Polytron (Kinematica) PT-MR 2100 homogenizer]. Tissue homogenate was used for measuring the antioxidant parameters reduced glutathione (GSH), catalase (CAT), malondialdehyde (MDA), and glutathione peroxidase (Gpx).

Assessment of hepatic reduce glutathione

Reduced GSH was estimated using the method of Moron et al.²⁵ Brief 0.1 mL homogenate was mixed with 0.1 mL trichloroacetic acid (25%) and allowed to stand at room temperature for 5 min. The mixture sample was centrifuged at 3000 rpm for 10 minutes the supernatant was collected and mixed with 1.8 mL of 0.1 mM 5,5'-dithiobis(2-nitrobenzoic acid) (DTNB). Samples were allowed to incubate in dark at room temperature for 10 min and absorbance was recorded at 412 nm against the reagent blank.

Assessment of hepatic glutathione peroxidase

The activity of GPx was estimated by the method Flohé and Günzler.²⁶ Briefly 300 μ L of liver homogenate was mixed with 300 μ L of phosphate buffer (pH: 7.4), 200 μ L of GSH (2 mM), 100 μ L of sodium azide (1 mM) and 100 μ L of hydrogen peroxide (1 mM). The mixture was allowed to stand for 15 min at 37°C in a water bath. 500 μ L TCA (15%) was added in the mixture and centrifuged at 1500 rpm for 5 min, supernatant was mixed with 200 μ L of phosphate buffer and 700 μ L of DTNB (0.1 mM). The absorbance was recorded at 412 nm against the reagent blank.

Assessment of hepatic catalase

The CAT activity was evaluated by the method of Sinha.²⁷ Briefly, 100 μ L of the homogenate was mixed with 1 mL of phosphate buffer (pH: 7.4) and 500 μ L of hydrogen peroxide (0.2 M). The mixture was allowed to incubate 37°C for 15 min. 2 mL of dichromate solution (5%) was added to the mixture and absorbance was recorded at 570 nm against the reagent blank.

Assessment of lipid peroxidation (LPO)

MDA the end product of LPO was estimated by the method of Ohkawa et al.²⁸ Briefly, 100 μ L of tissue homogenate was mixed with 100 μ L of sodium dodecyl sulphate (8.1%) and incubated at room temperature for 10 min. 750 μ L of 20% acetic acid and 750 μ L thiobarbituric acid (0.8%) were added to the mixture and volume was adjusted up to 2 mL. The mixture was allowed to stand at 95°C for 1 hour. A 2.5 mL butanol and pyridine (1:1) solution was added to a mixture and the volume was adjusted

up to 5 mL with distilled water, and centrifuged (4000 rpm) for 10 min. The upper organic layer was collected and absorbance was recorded at 532 nm against the reagent blank.

Histological study

The liver tissue was preserved in 10% neutral buffered formalin and embedded in paraffin wax. Then, 3-4 μ m thin sections were cut using a microtome. The tissues were either stained with hematoxylin and eosin or Masson's trichrome for evaluating architectural changes and evaluate the abundance of collagen in the liver tissue.²⁹ The slides were studied under the light microscope (Nikon FX-35A, Japan) and pictures were taken from an attached Nikon camera (DS FI1). The Batts and Ludwig³⁰ scoring system was used to grade hepatic fibrosis.

Statistical analysis

The data were represented as a means \pm standard deviation. Statistical analysis was executed using SPSS software (version 16). The differences between the means were subjected to One-Way ANOVA followed by Tukey's *post-hoc* test. *P* value ≤ 0.05 was considered a level of significance.

RESULTS

Effect of water extracts of *P. pavonia* and *C. racemosa* on liver profile

CCl₄ remarkably increased levels of serum aminotransferases ALAT (623.8%) and ASAT (246.3%) and ALP (392.4%), serum LDH (228.2%), total bilirubin (370%), and direct bilirubin (552.1%) levels compared to those of normal control rats. Intoxicated rats treated with WE of *P. pavonia* decreased ALAT (-62.0%), ASAT (-49.0%), ALP (-29.3%), LDH (-65.7%), total bilirubin (-70%), and direct bilirubin (-79.3%) as compared to CCl₄-treated control rats. The same pattern was observed in intoxicated rats treated with WE of *C. racemosa*, which significantly ($p \leq 0.05$) reduced the elevation of ALAT (-82.2%), ASAT (-46.7%), ALP (-41.3%), LDH (-25.8%), total bilirubin (-69.6%), and direct bilirubin (-69.3%) levels. Fibrotic rats concomitantly treated with silymarin showed a significant reduction in serum ALAT (-71.0%), ASAT (-41.3%), ALP (-40.7%), LDH (-45.6%), total bilirubin (-31.2%), and direct bilirubin (-43.3%). In general, WE of *C. racemosa* showed a more promising effect as compared to WE of *P. pavonia* on liver function markers in CCl₄-induced liver fibrotic rats. Further, fibrotic rats showed a significant elevation in blood glucose (25%) levels as compared with normal rats. Besides, treatment with WE, *P. pavonia* reversed the elevated blood glucose level (-51.3%) (Tables 1, 2). Overall results demonstrated that WE of both seaweeds may reciprocate the elevated level of hepatic enzymes, metabolites and also ameliorates increased blood glucose levels in response to persistent liver assault.

Effect of water extracts of *P. pavonia* and *C. racemosa* on renal function and lipid profile

Table 3 demonstrated that CCl₄ has significantly ($p \leq 0.05$) impaired the kidney function and glucose metabolism by increasing serum urea (151.8%) and creatinine (816%) levels. CCl₄ was also responsible for reducing the serum cholesterol (-75%) and TGs (-62.5%), when compared with normal rats.

Table 1. Effect of water extracts of *Padina pavonia* and *Caulerpa racemosa* on liver enzymes in normal and CCl₄-intoxicated rats

Treatments	Normal rat model				Fibrotic rat model			
	Normal control	<i>P. padina</i> (WE)	<i>C. racemosa</i> (WE)	Silymarin	CCl ₄ control	<i>P. padina</i> (WE) + CCl ₄	<i>C. racemosa</i> (WE) + CCl ₄	Silymarin + CCl ₄
ALAT (u/L)	42 ± 7.3	50.5 ± 3.25 ^a (20.2%)	44.5 ± 6.59 ^a (5.9%)	38.02 ± 0.28 ^a (-9.4%)	304.2 ± 34.06 ^{a*} (623.8%)	115.5 ± 14.45 ^{b*} (-62.0%)	54.6 ± 7.2 ^{b*} (-82.2%)	88.2 ± 5.03 ^{b*} (-71.0%)
ASAT (u/L)	123 ± 16.11	100.5 ± 15.5 ^a (-18.6%)	64 ± 8.6 ^a (-47%)	64.6 ± 5.2 ^{a*} (-47.4%)	426 ± 54.39 ^{a*} (246%)	217 ± 23.7 ^{b*} (-49.0%)	227 ± 28.34 ^{b*} (-46.7%)	140 ± 7.2 ^{b*} (-65.7%)
ALP (u/L)	79 ± 8.85	114 ± 14.5 ^a (44.3%)	72 ± 14.36 ^a (-8.8%)	67.6 ± 5.2 ^a (-15.1%)	389 ± 49.1 ^{a*} (392.4%)	275 ± 14.6 ^{b*} (-29.3%)	250 ± 1.5 ^{b*} (-41.3%)	230.3 ± 47.5 ^{b*} (-40.7%)
LDH (u/L)	124.6 ± 8.1	146.3 ± 19.6 ^a (17.4%)	184.0 ± 25.4 ^a (48.1%)	170.3 ± 0.57 ^a (36.9%)	409.1 ± 15.07 ^{a*} (228.25%)	162.3 ± 15.6 ^{b*} (-58.3%)	303.33 ± 24.9 ^{b*} (-25.8%)	222.3 ± 14.04 ^{b*} (-45.6%)

The data were analyzed by One-Way ANOVA followed by Tukey's *post-hoc* test. **p*<0.05, ^aIndicates the comparison with control rats, ^bIndicates the comparison with CCl₄ control rats.

Data were expressed in means ± standard deviation (n= 6). The values in parenthesis represent percentage (%) increased or decreased as compared to their respective control. CCl₄: Carbon tetrachloride, ALAT: Alanine aminotransferase, ASAT: Aspartate aminotransferase, ALP: Alkaline phosphatases, LDH: Lactate dehydrogenases, WE: Water extract

Table 2. Effect of water extracts of *Padina pavonia* and *Caulerpa racemosa* on liver metabolite and blood glucose in normal and CCl₄-intoxicated rats

Treatments	Normal rats model				Fibrotic rats model			
	Normal control	<i>P. padina</i> (WE)	<i>C. racemosa</i> (WE)	Silymarin	CCl ₄ control	<i>P. padina</i> (WE) + CCl ₄	<i>C. racemosa</i> (WE) + CCl ₄	Silymarin + CCl ₄
Glucose (mg/dL)	116.18 ± 8.07	89.16 ± 5.7 ^a (-23.3%)	115 ± 14.30 ^a (0.94%)	98 ± 3.0 ^a (-15.59%)	146.3 ± 14.3 ^{a*} (25.8%)	71.16 ± 7.55 ^{b*} (-51.3%)	147 ± 22.4 ^b (-0.47%)	100 ± 1.5 ^{b*} (-31.64%)
Total bilirubin (mg/dL)	0.34 ± 0.04	0.21 ± 0.04 ^a (-38.2%)	0.23 ± 0.05 ^a (-32.3%)	0.6 ± 0.05 ^a (76.4%)	1.6 ± 0.12 ^{a*} (370%)	0.48 ± 0.08 ^{b*} (-70%)	0.5 ± 0.06 ^{b*} (-69.6%)	1.1 ± 0.05 ^{b*} (-31.2%)
Direct bilirubin (mg/dL)	0.23 ± 0.05	0.21 ± 0.04 ^a (-8.6%)	0.51 ± 0.07 ^a (121.7%)	0.3 ± 0.05 ^a (30.4%)	1.5 ± 0.16 ^{a*} (552%)	0.31 ± 0.04 ^{b*} (-79.3%)	0.46 ± 0.08 ^{b*} (-69.3%)	0.85 ± 0.04 ^{b*} (-43.3%)

The data were analyzed by One-Way ANOVA followed by Tukey's *post-hoc* test. **p*<0.05, ^aIndicates the comparison with control rats, ^bIndicates the comparison with CCl₄ control rats.

Data were expressed in means ± standard deviation (n= 6). The values in parenthesis represent percentage (%) increased or decreased as compared to their respective control. CCl₄: Carbon tetrachloride, WE: Water extract

Table 3. Effect of water extract of *Padina pavonia* and *Caulerpa racemosa* on renal and lipid profile in normal and CCl₄-intoxicated rats

Treatments	Normal rats model				Fibrotic rats model			
	Normal control	<i>P. padina</i> (WE)	<i>C. racemosa</i> (WE)	Silymarin	CCl ₄ control	<i>P. padina</i> (WE) + CCl ₄	<i>C. racemosa</i> (WE) + CCl ₄	Silymarin + CCl ₄
Urea (mg/dL)	27.6 ± 6.8	23.3 ± 4.0 ^a (-15.5%)	25.6 ± 5.4 ^a (-7.2%)	22.0 ± 1.00 ^a (-20.2%)	69.5 ± 10 ^{a*} (151.8%)	28.3 ± 5.4 ^{b*} (-59.2%)	30 ± 3.07 ^{b*} (-56.8%)	39 ± 0.57 ^{b*} (-43.8%)
Creatinine (mg/dL)	0.2 ± 0.04	0.2 ± 0.05 ^a (0%)	0.43 ± 0.05 ^a (115%)	0.7 ± 0.05 ^a (250%)	1.8 ± 0.14 ^{a*} (816%)	0.2 ± 0.02 ^{b*} (-88.88%)	0.25 ± 0.039 ^{b*} (-86.1%)	0.75 ± 0.05 ^{b*} (-58.3%)
Cholesterol (mg/dL)	107 ± 9.6	79 ± 7.6 ^a (-26.1%)	137.5 ± 10.6 ^a (28.03%)	80.3 ± 0.5 ^a (-24.9%)	26.6 ± 8.6 ^{a*} (-75.1%)	64 ± 5.5 ^{b*} (140.6%)	46.4 ± 4.3 ^{b*} (74.4%)	70.3 ± 11.5 ^{b*} (164.2%)
TGs (mg/dL)	103.1 ± 16.7	84.16 ± 5.8 ^a (-18.4%)	126 ± 3.8 ^a (-22.3%)	90 ± 6.00 ^a (-12.6%)	38.6 ± 3.2 ^{a*} (-62.5%)	94 ± 6.3 ^{b*} (143.5%)	58.1 ± 6.6 ^{b*} (50.5%)	50.3 ± 3.5 ^{b*} (30.3%)

The data were analyzed by One-Way ANOVA followed by Tukey's *post-hoc* test, **p*<0.05, ^aIndicates the comparison with control rats, ^bIndicates the comparison with CCl₄ control rats.

Data were expressed in means ± standard deviation (n= 6). The values in parenthesis represent percentage (%) increased or decreased as compared to their respective control. CCl₄: Carbon tetrachloride, WE: Water extracts

Rats treated with WE of *P. pavonia* significantly ($p \leq 0.05$) reciprocated the elevation of serum urea (-59.2%) and creatinine (-88.8%) with remarkable elevation in serum lipid levels *i.e.* cholesterol (140.6%) and TGs (143.5%). WE of *C. racemosa* showed significant ($p \leq 0.05$) reduction in serum urea (-56.8%) and creatinine (-86.1%). It also produced elevation in serum lipid levels *i.e.* cholesterol (74.4%) and TGs (50.5%) against CCl_4 -induced liver fibrosis in rats. Silymarin also showed a reduction in serum urea and creatinine levels *i.e.* (-43.8% and -58.3%, respectively, and increased the serum cholesterol and TGs levels *i.e.*, (164.2%, 30.3%). Conclusively, both seaweed extracts have the potential to maintain the renal and lipid metabolites, which are enhanced in response to CCl_4 administration.

Effect of water extracts of *P. pavonia* and *C. racemosa* on liver antioxidant profile

CCl_4 administration significantly damaged the liver tissue, which ultimately depleted the GSH (-76%) and elevated the MDA (551%) concentrations. The reduction in Gpx (-49%) and CAT (-31%) activity were also observed after administration of CCl_4 , when compared with normal rats. The CCl_4 intoxicated rats concomitantly treated with WE of *P. pavonia* showed increased hepatic antioxidant enzymes activities *viz*; Gpx (32.2), CAT (18.5%) along with improvement in hepatic GSH concentration (141.5%), and decreased MDA (-57.4%) respectively. The same trend was observed for WE of *C. racemosa*, which significantly ($p \leq 0.05$) combated the adverse effect of CCl_4 -induced oxidative stress indices by enhancing the activities of CAT (52.6%), Gpx (23%), and improved GSH (89.2%) concentration, whereas reduced the MDA (-55.8%) level. Silymarin-treated group showed a significant ($p \leq 0.05$) improvement in oxidative stress indices *i.e.* GSH (115.3%), Gpx (87.7%), CAT (23.8%), and MDA (-41.7%) (Figures 1, 2). These results validated the antioxidant capability of WE of the seaweeds, as they have the potential to attenuate the oxidative stress indices in response to CCl_4 administration.

Histological changes in liver tissue of normal and fibrotic rats

treated with water extract of *P. pavonia* and *C. racemosa*

Normal control rats showed stabilized hepatic lobules, consisted of normal central vein and peripheral 4 to 5 portal triads along with no evidence of portal expansion or necrosis (Figures 3A, B). CCl_4 intoxicated rats showed portal fibrosis with evidence of expansion in the portal tract (grade I) with massive acidophilic bodies (Figures 3C, D). Additionally, they also showed macrophage infiltration, evidence of hepatic lobular and portal inflammation (grade II & I) along with lipid deposition evident by clear vacuoles, abundance of loosely aggregated collagen fibers also seen around the portal tract. Intoxicated rats treated with WE of *C. racemosa* did not show any presence of collagen fibers, with no evidence of lobular inflammation or piecemeal necrosis (Figure 3E, F). Whereas *P. pavonia* demonstrated mild portal expansion with no evidence of lobular inflammation or piecemeal necrosis, they also showed the deposition of collagen fibers around the portal tract in lesser intensity (Figure 3G, H). The WE of both seaweeds have the potential to stabilize the normal cellular morphology. However, further investigations must unveil the potent component(s) of seaweed, which may play a role in reciprocating the toxic effect induced by CCl_4 administration.

DISCUSSION

Liver fibrosis is one of the serious health problems around the globe and it causes apoptosis or necrosis, inflammation, tissue remodeling and repair processes.^{6,31} Excessive deposition of ECM, particularly deposition of collagen type (I & III) are major cause of liver fibrosis.³²

In this study, animal model of liver fibrosis have been developed *via* repeated administration of CCl_4 . Chronic exposure of CCl_4 promotes degeneration of hepatocytes, which results in excessive secretion of aminotransferases (ALAT & ASAT).³³ In the harmony of previous findings, current data demonstrated significant ($p \leq 0.05$) elevation in serum levels of transaminases (ALAT & ASAT) in CCl_4 -intoxicated model. ALP is usually distributed in microvilli of liver sinusoids and bile duct capillary.

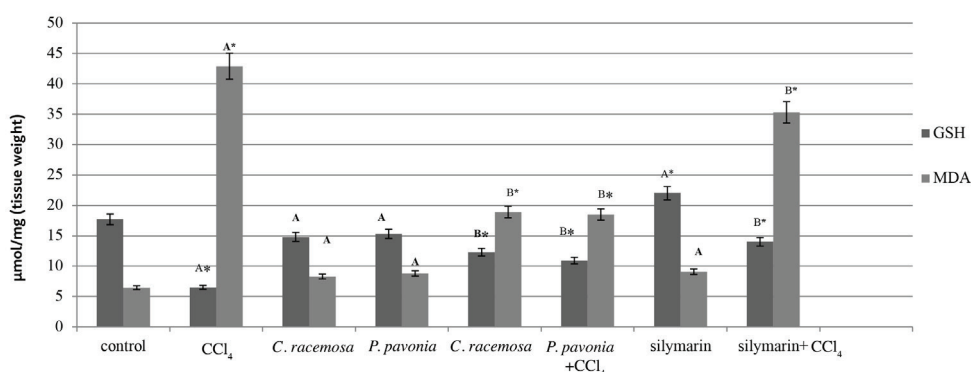


Figure 1. Effect of water extracts of *Padina pavonia* and *Caulerpa racemosa* on liver total glutathione and lipid peroxidation activities in normal and CCl_4 -intoxicated rats. The data were analyzed by One-Way ANOVA followed by Tukey's *post-hoc* test. Each bar expressed means \pm standard deviation ($n = 6$).

* $p < 0.05$, ^AIndicates the comparison with control rats while the, ^BIndicates the comparison with CCl_4 control rats, CCl_4 : Carbon tetrachloride, GSH: Glutathione, MDA: Malondialdehyde

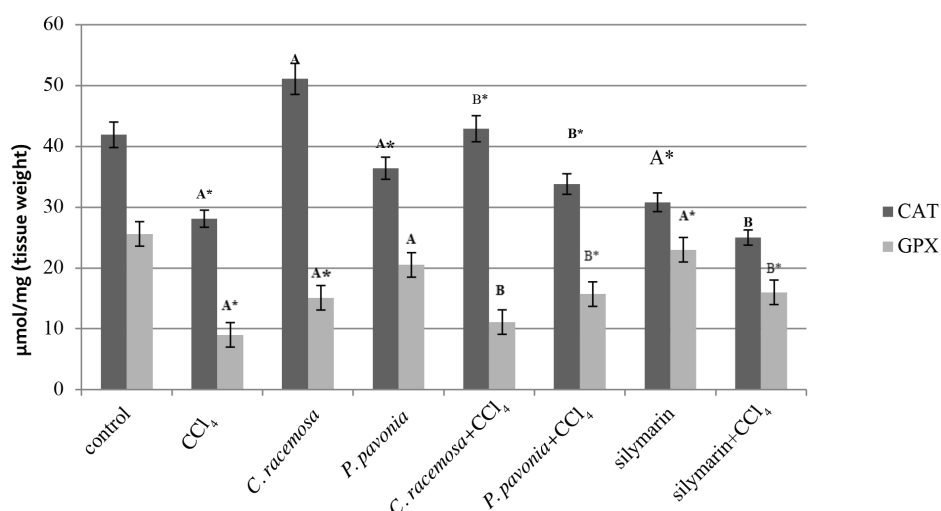


Figure 2. Effect of water extracts of *Padina pavonia* and *Caulerpa racemosa* on liver glutathione peroxidase and catalase activity in normal and CCl₄-intoxicated rats. The data were analyzed by One-Way ANOVA followed by Tukey's *post-hoc* test. Each bar expressed means \pm standard deviation ($n=6$).

* $p<0.05$, ^AIndicates the comparison with control rats while the, ^BIndicates the comparison with CCl₄ control rats, CCl₄: Carbon tetrachloride, CAT: Catalase, GPX: Glutathione peroxidase

CCl₄ administration induces hepatocyte degradation, which is responsible for exerting pressure on bile duct capillaries and promotes excessive release of ALP in serum.³⁴ Persistent liver insults by CCl₄ administration significantly ($p\leq 0.05$) elevated the serum ALP level. Moreover, the CCl₄-intoxicated model showed a significant ($p\leq 0.05$) increase in serum LDH levels. It is usually released under hypoxic conditions, responsible for to shift metabolic cellular dependency on the anaerobic glycolytic pathway. Persistent exposure of toxicants (CCl₄) induces hepatocyte stress and promotes necrosis, which results in leakage of LDH into the serum. CCl₄ responsible for the activation of HSCs (stored retinoid) may contribute to excessive bile secretion in blood along with disturbance in redox mechanism, impaired mitochondrial integrity, and promotes apoptosis.³⁵ In the present work, CCl₄-intoxicated model also showed a remarkable elevation in serum total bilirubin and direct bilirubin besides increasing liver enzymes. A previous study also revealed that CCl₄ induced liver fibrosis increased serum liver markers; aspartate transaminase, alanine transaminase, and total bilirubin. The current study showed that supplementation of WE of both seaweeds *C. racemosa* and *P. pavonia* caused a significant ($p\leq 0.05$) alleviation in serum levels of ALAT, ASAT, ALP, and LDH along with bilirubin in CCl₄-induced liver fibrotic rats. Further, both seaweeds have the potential to reduce the degradation of hepatocytes and might play a role in the deactivation of activated HSC, evident by a remarkable reduction in serum aminotransferases, dehydrogenases, and phosphatase.

Among the tested seaweeds herein, *Caulerpa* species have been used around the globe due to their high nutritive value, whereas brown seaweeds have been recognized by researchers due to their medicinal importance.^{15,18} Marine macroalgae are reported to have antioxidant activity and a tendency to reciprocate the

effect induced through various toxicants.^{1,15} *P. pavonia* also demonstrated a significant effect on thioacetamide-induced hepatic fibrosis.³⁶ The hepatoprotective effect of *C. racemosa* has not been reported, yet. Repeated episodes of liver insult by CCl₄ administration caused generation of ROS, usually they are short span molecules generated by partial reduction of oxygen.³⁷ Chronic exposure of toxicants disrupts the balance between ROS and cellular antioxidant defense results in induction in oxidative stress. Further elevated levels of ROS caused depletion in antioxidants molecules and parameters *i.e.* GSH, Gpx, and CAT and increased LPO in terms of MDA. Nevertheless, ROS activates HSCs, which promotes the production of collagen and contributes in the progression of liver fibrosis. The present study showed a marked increase in MDA levels in CCl₄ control rats compared to normal rats. The following findings support our results that liver fibrosis promotes the generation of ROS, which ultimately caused a reduction in GSH, Gpx and CAT activities.³⁸ CCl₄-treated rats administered with WE of both algal species significantly attenuated LPO by decreasing the formation of MDA and improved hepatic GSH levels and elevated the Gpx and CAT activities compared to CCl₄ control rats. *P. pavonia* improves the activities of superoxide dismutase and Gpx induced by azoxymethane intoxication.²¹ However, these results showed that seaweeds might affect down-regulation of ROS induced by repeated administration of CCl₄ as they showed decreased levels of MDA and improved GSH concentration and enhanced Gpx and CAT activity.

Previous findings suggested that fibrotic liver tissue showed significant morphological destruction characterized by expansion of the central vein, portal vein, and necrosis in CCl₄ treated rats.^{32,33} The current findings validate the previous findings, as repeated episodes of CCl₄-treated rats showed expansion of the central vein, portal vein, and necrosis, whereas

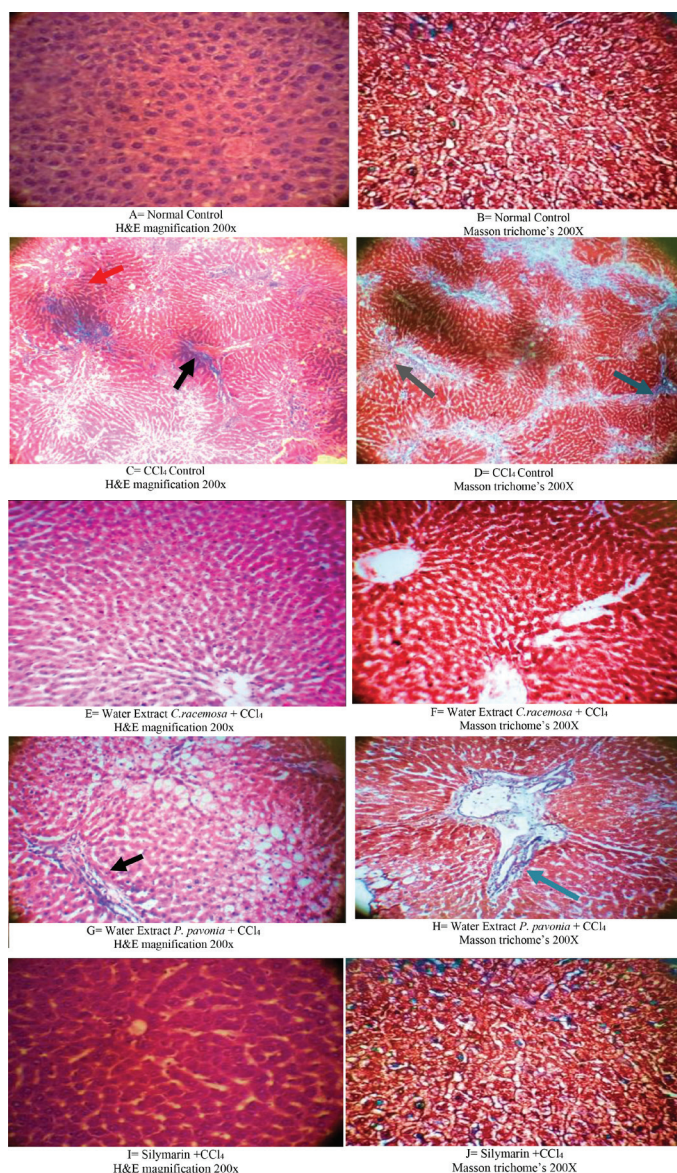


Figure 3. Light microscopy of liver tissue (200x), black arrow represent portal expansion, red arrow represent macrophages infiltration, blue arrow represent collagen deposition. Grey arrow represent necrotic cells. (A, B) Normal architecture of cellular organization along with stabilized hepatocytes, (C, D) hepatocytes damage, cellular atrophy is visible, sinusoidal cells become dilated, portal track destruction and ulcerative lesion, (E, F) stabilization of cellular morphology and attenuation of lobular destruction, foamy cells formation and lowering of intensity of highly fused cells, (G, H) stabilization of cellular morphology and attenuation of lobular destruction, foamy cells formation and lowering of intensity of highly fused cells, (I, J) stabilization of cellular morphology and lowering of lobular destruction and intensity of fused cells

CCl₄: Carbon tetrachloride, H&E: Hematoxylin and eosin

there were no changes found in normal liver tissue. In addition, intoxicated rats showed an abundance of collagen fibers, which can clearly be visualized by Masson's staining. The current study was designed to elucidate the efficacy of WEs of *C. racemosa* and *P. pavonia* against liver fibrosis. Furthermore, WEs of *C. racemosa* and *P. pavonia* showed a reciprocal effect on CCl₄ intoxication and improved the abnormal cellular

architecture of liver tissue. Both extracts showed notable reduction in the collagen fibers. Overall, results showed that these seaweeds tend to attenuate the liver fibrosis. Moreover, several reports showed that *P. pavonia* has potential to down regulate anti-apoptotic and pro-apoptotic pathways, which may relate to morphological repairs of cellular architecture.²⁰ The hepatoprotective activity of seaweeds was found to be comparable to the silymarin, in improving the cellular architecture distorted by CCl₄ intoxication.

Previous studies showed that liver-associated problems are not localized and it also affect the activity of nearby organs such as impairment in renal, lipid, and glucose metabolism.¹ Liver damage also affects renal function by increasing the concentrations of urea and creatinine. In this study, CCl₄ administration showed remarkable increases in kidney markers *i.e.*, urea and creatinine compared to normal control rats. Sohail et al.¹⁵ reported that drug induced hepatotoxicity and nephrotoxicity has been suppressed by supplementation of marine macroalgae. Another report also showed that *P. pavonia* reversed renal dysfunction induced by azoxymethane.³⁸ The current findings show that both algal species (*C. racemosa* and *P. pavonia*) extracts have the potential to attenuate the elevated levels of serum urea and creatinine. WE of both seaweeds have the potential to reciprocate the renal toxicity induced as a consequence of repeated administration of CCl₄.

The present study showed that CCl₄ administration disturbed the lipid metabolism by decreasing the cholesterol and TG levels. Ishikawa et al.³⁹ reported that CCl₄-induced liver fibrosis caused alteration in lipid metabolism evident by decreased levels of cholesterol and TGs. The distortion of hepatic parenchymal cells is responsible for impaired lipid metabolism.⁴⁰ However, the extracts of both seaweeds significantly elevated the cholesterol and TG levels toward the normal range. CCl₄ toxicity also affects the glucose metabolism, resulting in hyperglycemia in CCl₄ control rats, which was reduced in seaweed-treated groups. The ability of seaweed extracts to abrogate the elevated concentration of glucose in serum may be due to the protection of hepatocytes from toxic substances and their hypoglycemic potential.¹

CONCLUSION

The present study showed that both seaweeds (*C. racemosa* and *P. pavonia*) can reciprocate the cellular damages and associated complications produced by repeated administration of CCl₄. Both algal species showed significant positive effects on fibrotic rats. The efficacy of seaweed was compared with commonly known herbal medicine silymarin showed almost similar effect on serum enzymes and hepatic antioxidant enzymes. Generally, WE of *C. racemosa* has great potential to attenuate the liver fibrosis induced by CCl₄. Hepatoprotective activity of *C. racemosa* may be due to the presence of polysaccharides, which have been reported from other seaweeds. *C. racemosa* is an edible seaweed and its use as a diet supplement may be supportive for liver health.

ACKNOWLEDGMENTS

The help of Dr. Aisha Begum, Department of Botany, the University of Karachi for seaweed identification is acknowledged.

Ethics

Ethics Committee Approval: The approval has been received from Institutional Bioethical Committee of University of Karachi (IBC-KU-132/2020).

Informed Consent: Not applicable.

Peer-review: Externally peer-reviewed.

Authorship Contributions

Concept: M.A., K.H., S.A.Q., N.K., J.A., S.E.H., Design: M.A., K.H., S.A.Q., N.K., J.A., S.E.H., Data Collection or Processing: M.A., K.H., S.A.Q., N.K., J.A., S.E.H., Analysis or Interpretation: M.A., K.H., S.A.Q., N.K., J.A., S.E.H., Literature Search: M.A., K.H., S.A.Q., N.K., J.A., S.E.H., Writing: M.A., K.H., S.A.Q., N.K., J.A., S.E.H.

Conflict of Interest: No conflict of interest was declared by the authors.

Financial Disclosure: Financial assistance provided by the Higher Education Commission, Pakistan (Grant # nrpu-4505) is sincerely acknowledged.

REFERENCES

- Hira K, Sultana V, Ara J, Ehteshamul-Haque S. Protective role of *Sargassum* species in liver and kidney dysfunctions and associated disorders in rats intoxicated with carbon tetrachloride and acetaminophen. *Pak J Pharm Sci.* 2017;30:721-728.
- Blaner WS, O'Byrne SM, Wongsiriroj N, Kluwe J, D'Ambrosio DM, Jiang H, Schwabe RF, Hillman EM, Piantadosi R, Libien J. Hepatic stellate cell lipid droplets: a specialized lipid droplet for retinoid storage. *Biochim Biophys Acta.* 2009;1791:467-473.
- Laskin DL, Sunil VR, Gardner CR, Laskin JD. Macrophages and tissue injury: agents of defense or destruction? *Annu Rev Pharmacol Toxicol.* 2011;51:267-288.
- Baiocchi A, Montaldo C, Conigliaro A, Grimaldi A, Correani V, Mura F, Ciccocanti F, Rotiroli N, Brenna A, Montalbano M, D'Offizi G, Capobianchi MR, Alessandro R, Piacentini M, Schininà ME, Maras B, Del Nonno F, Tripodi M, Mancone C. Extracellular matrix molecular remodeling in human liver fibrosis evolution. *PLoS One.* 2016;11:e0151736.
- Lee UE, Friedman SL. Mechanisms of hepatic fibrogenesis. *Best Pract Res Clin Gastroenterol.* 2011;25:195-206.
- Byass P. The global burden of liver disease: a challenge for methods and for public health. *BMC Med.* 2014;12:159.
- Yoo S, Wang W, Wang Q, Fiel MI, Lee E, Hiotis SP, Zhu J. A pilot systematic genomic comparison of recurrence risks of hepatitis B virus-associated hepatocellular carcinoma with low-and high-degree liver fibrosis. *BMC Med.* 2017;15:214.
- Schiff ER, Maddrey WC, Sorrell MF. Schiff's Diseases of the Liver. (11th ed). West Sussex: John Wiley & Sons; 2011.
- Marcellin P, Gane E, Buti M, Afdhal N, Sievert W, Jacobson IM, Washington MK, Germanidis G, Flaherty JF, Aguilar Schall R, Bornstein JD, Kitisinos KM, Subramanian GM, McHutchison JG, Heathcote EJ. Regression of cirrhosis during treatment with tenofovir disoproxil fumarate for chronic hepatitis B: a 5-year open-label follow-up study. *Lancet.* 2013;381:468-475.
- Dong S, Chen QL, Song YN, Sun Y, Wei B, Li XY, Hu YY, Liu P, Su SB. Mechanisms of CCl₄-induced liver fibrosis with combined transcriptomic and proteomic analysis. *J Toxicol Sci.* 2016;41:561-572.
- Halliwell B, Gutteridge JM. Free radicals in biology and medicine. (5th ed). New York, USA: Oxford University Press; 2015.
- Klaas M, Kangur T, Viil J, Mäemets-Allas K, Minajeva A, Vadi K, Antsov M, Lapidus N, Järvekülg M, Jaks V. The alterations in the extracellular matrix composition guide the repair of damaged liver tissue. *Sci Rep.* 2016;6:27398.
- Barkia I, Saari N, Manning SR. Microalgae for high-value products towards human health and nutrition. *Mar Drugs.* 2019;17:304.
- Dore CM, das C Faustino Alves MG, Will LS, Costa TG, Sabry DA, de Souza Rêgo LA, Accardo CM, Rocha HA, Filgueira LG, Leite EL. A sulfated polysaccharide, fucans, isolated from brown algae *Sargassum vulgare* with anticoagulant, antithrombotic, antioxidant and anti-inflammatory effects. *Carbohydr Polym.* 2013;91:467-475.
- Sohail N, Hira K, Kori JA, Farhat H, Urooj F, Khan W, Sultana V, Ali MS, Ehteshamul-Haque S. Nephroprotective effect of ethanol extract and fractions of a sea lettuce, *Ulva fasciata* against cisplatin-induced kidney injury in rats. *Environ Sci Pollut Res Int.* 2020;28:9448-9461.
- Costa LS, Fidelis GP, Cordeiro SL, Oliveira RM, Sabry DA, Câmara RB, Nobre LT, Costa MS, Almeida-Lima J, Farias EH, Leite EL, Rocha HA. Biological activities of sulfated polysaccharides from tropical seaweeds. *Biomed Pharmacother.* 2010;64:21-28.
- Wang L, Wang X, Wu H, Liu R. Overview on biological activities and molecular characteristics of sulfated polysaccharides from marine green algae in recent years. *Mar Drugs.* 2014;12:4984-5020.
- Ara J, Sultana V, Qasim R, Ahmad VU. Hypolipidaemic activity of seaweed from Karachi coast. *Phytother Res.* 2002;16:479-483.
- de Gaillande C, Payri C, Remoissenet G, Zubia M. *Caulerpa* consumption, nutritional value and farming in the Indo-Pacific region. *J Appl Phycol.* 2017;29:2249-2266.
- Bernardini G, Minetti M, Polizzotto G, Biazio M, Santucci A. Pro-apoptotic activity of French Polynesian *Padina pavonica* extract on human osteosarcoma cells. *Mar Drugs.* 2018;16:504.
- Abdella EM, Mahmoud AM, El-Derby AM. Brown seaweeds protect against azoxymethane-induced hepatic repercussions through up-regulation of peroxisome proliferator-activated receptor gamma and attenuation of oxidative stress. *Pharm Biol.* 2016;54:2496-2504.
- Ismail A Jr, Tan S. Antioxidant activity of selected commercial seaweeds. *Malays J Nutr.* 2002;8:167-177.
- Iredale JP, Benyon RC, Pickering J, McCullen M, Northrop M, Pawley S, Hovell C, Arthur MJ. Mechanisms of spontaneous resolution of rat liver fibrosis. Hepatic stellate cell apoptosis and reduced hepatic expression of metalloproteinase inhibitors. *J Clin Invest.* 1998;102:538-549.
- Wang L, Huang QH, Li YX, Huang YF, Xie JH, Xu LQ, Dou YX, Su ZR, Zeng HF, Chen JN. Protective effects of silymarin on triptolide-induced acute hepatotoxicity in rats. *Mol Med Rep.* 2018;17:789-800.
- Moron MS, Depierre JW, Mannervik B. Levels of glutathione, glutathione reductase and glutathione S-transferase activities in rat lung and liver. *Biochim Biophys Acta.* 1979;582:67-78.

26. Flohé L, Günzler WA. Assays of glutathione peroxidase. *Methods Enzymol.* 1984;105:114-121.
27. Sinha AK. Colorimetric assay of catalase. *Anal Biochem.* 1972;47:389-394.
28. Ohkawa H, Ohishi N, Yagi K. Assay for lipid peroxides in animal tissues by thiobarbituric acid reaction. *Anal Biochem.* 1979;95:351-358.
29. Qiao JB, Fan QQ, Zhang CL, Lee J, Byun J, Xing L, Gao XD, Oh YK, Jiang HL. Hyperbranched lipid-based lipid nanoparticles for bidirectional regulation of collagen accumulation in liver fibrosis. *J Control Release.* 2020;321:629-640.
30. Batts KP, Ludwig J. Chronic hepatitis. An update on terminology and reporting. *Am J Surg Pathol.* 1995;19:1409-1417.
31. Ribeiro PS, Cortez-Pinto H, Solá S, Castro RE, Ramalho RM, Baptista A, Moura MC, Camilo ME, Rodrigues CM. Hepatocyte apoptosis, expression of death receptors, and activation of NF- κ B in the liver of nonalcoholic and alcoholic steatohepatitis patients. *Am J Gastroenterol.* 2004;99:1708-1717.
32. Du WD, Zhang YE, Zhai WR, Zhou XM. Dynamic changes of type I, III and IV collagen synthesis and distribution of collagen-producing cells in carbon tetrachloride-induced rat liver fibrosis. *World J Gastroenterol.* 1999;5:397-403.
33. Yu C, Wang F, Jin C, Wu X, Chan WK, McKeehan WL. Increased carbon tetrachloride-induced liver injury and fibrosis in FGFR4-deficient mice. *Am J Pathol.* 2002;161:2003-2010.
34. Hu J, Zhang X, Gu J, Yang M, Zhang X, Zhao H, Li L. Serum alkaline phosphatase levels as a simple and useful test in screening for significant fibrosis in treatment-naïve patients with hepatitis B e-antigen negative chronic hepatitis B. *Eur J Gastroenterol Hepatol.* 2019;31:817-823.
35. Qaisiya M, Coda Zabetta CD, Bellarosa C, Tiribelli C. Bilirubin mediated oxidative stress involves antioxidant response activation *via* Nrf2 pathway. *Cell Signal.* 2014;26:512-520.
36. Hamza AH, Hegazi MM, Youness ER, Ahmed HH. Brown algae as a golden mine for treatment of liver fibrosis: a proposal based on experimental animal study. *Int J Curr Pharm Rev Res.* 2015;6:225-236.
37. Lambeth JD. NOX enzymes and the biology of reactive oxygen. *Nat Rev Immunol.* 2004;4:181-189.
38. Mahmoud AM, El-Derby AM, Elsayed KN, Abdella EM. Brown seaweeds ameliorate renal alterations in mice treated with the carcinogen azoxymethane. *Int J Pharm Pharm Sci.* 2014;6:365-369.
39. Ishikawa M, Saito K, Yamada H, Nakatsu N, Maekawa K, Saito Y. Plasma lipid profiling of different types of hepatic fibrosis induced by carbon tetrachloride and lomustine in rats. *Lipids Health Dis.* 2016;15:74.
40. Havel RJ. Functional activities of hepatic lipoprotein receptors. *Annu Rev Physiol.* 1986;48:119-134.



Design, Development, Optimization and Evaluation of Ranolazine Extended Release Tablets

✉ Raghavendra Kumar GUNDA^{1*}, ✉ Prasada Rao MANCHINENI², ✉ Dhachinamoorthi DURAI SWAMY³, ✉ Koteswara Rao GSN⁴

¹Vignan's Foundation for Science, Technology and Research (Deemed to be University), Faculty of Pharmacy, Department of Pharmaceutical Sciences, Andhra Pradesh, India

²M.A.M College of Pharmacy, Department of Pharmaceutical Analysis, Andhra Pradesh, India

³QIS College of Pharmacy, Department of Pharmaceutics, Andhra Pradesh, India

⁴KL College of Pharmacy, Koneru Lakshmaiah Education Foundation (Deemed to be University), Department of Pharmaceutics, Andhra Pradesh, India

ABSTRACT

Objectives: The objective of the current study was to develop an extended release (XR) tablet formulation for ranolazine using Eudragit L 100-55 and hydroxypropylmethylcellulose (HPMC) K100M in an appropriate composition. Ranolazine, an anti-anginal agent, is mainly used for treating chronic stable angina pectoris. The main advantage of this drug that it exhibits anti-ischemic effect, which was not influenced by either blood pressure or heart rate.

Materials and Methods: XR tablets of ranolazine were prepared using variable amounts of Eudragit L 100-55 and HPMC K100M in various proportions as *per* 3² factorial design by direct compression technique. The amount of polymers with desired sustained drug release was labeled as factors. On other hand, time taken for drug dissolution was labeled as responses ($t_{10\%}$, $t_{50\%}$, $t_{75\%}$, $t_{90\%}$).

Results: Nine formulations were obtained as *per* design, developed, and evaluated for quality control parameters. The obtained results clear that all formulations pass the compendial limits. Data obtained from the dissolution study fitted well to kinetic modeling and kinetic parameters were determined. Polynomial equations were derived for responses and checked for validity.

Conclusion: RF₅ composed of 31.25 mg of Eudragit L 100-55 and 31.25 mg of HPMC K100M, is the best formulation showing similarity f_2 : 85.78, f_1 : 2.32 with the marketed product (RANEXA). Formulation RF₅ follows zero order, whereas the release mechanism was found to be non-fickian type ($n=0.65$).

Key words: Ranolazine, extended release, Eudragit L 100-55, HPMC K100M, 3² factorial design, non-fickian diffusion

INTRODUCTION

Extended release (XR) formulations deliver effective plasma concentrations of the drug for desired prolonged period. They improve patient compliance by reducing the repeated administration of dosage regime. They also offer improved *in vivo* clinical performance (good clinical outcome).^{1,2}

The popularly used symbols for extended release are extra long/extra large; long acting; XR. They show a 2-fold reduction in the dosing frequency and maintains steady state plasma profile.³ There are many challenges for formulation of prolonged release dosage forms in a controlled manner for obtaining absorption and improved bioavailability.^{4,5}

Ranolazine is an anti-anginal agent, which is a piperazine acetamide derivative. It acts by partial inhibition of fatty acid oxidase that increases the adenosine triphosphate production from glucose, thereby improves the functionality of the myocardium. Hence, it exhibits anti-ischemic action, independent of hemodynamics such as blood pressure and heart rate. There will be no significant effect of its effectiveness by the above-mentioned factors and other co-morbidities. Due to this advantage, it is employed as effective anti-ischemic or antiangina agents for treating unstable chronic angina pectoris (exercise induced variant), myocardial infarction, and cardiac arrhythmias.⁶⁻⁸

*Correspondence: raghav.gunda@gmail.com, Phone: +91-9666705894, ORCID-ID: orcid.org/0000-0002-4271-8614

Received: 06.05.2021, Accepted: 26.07.2021

©Turk J Pharm Sci, Published by Galenos Publishing House.

Ranolazine belongs to biopharmaceutical classification system class-II agent. It shows an erratic (variant) and extensive first pass effect. Solubility was found to be relatively high at acidic pH (stomach). The half-life is around 2.5 h (2.5 ± 0.5). Hence, selection of release rate modifiers is a challenging task for researchers.⁹⁻¹⁴

The current study focuses on, development of XR tablets for ranolazine with the help of polymers Eudragit L 100-55 (partially neutralized pH dependent polymer) along with hydroxypropylmethylcellulose (HPMC) K100M (pH independent polymer).

The application of polynomial based response surface morphology (RSM) occupies a major volume in case of pharmaceutical product development. The most widely used methods in the above-mentioned category as follows factorial design (2^3 , 3^2 , 3^3), central composite design, Box-Behnken design.^{15,16}

The manufacture of tablets processed using direct compression technique is a frequent method, observed in many pharmaceutical industries.¹⁷

A two factors, 3-levels study (3^2 factorial design) was used to observe the combination effect of both polymers (Eudragit L 100-55; HPMC K100M) on the drug release from the formulation (to see the effect of factors on the responses),¹⁸ which may improve patient compliance by using enhanced clinical efficiency.

MATERIALS AND METHODS

Materials

A gift sample of ranolazine was procured from Mahys Pharma, Solan, India. Eudragit L 100-55 was obtained from KU Pharma Pvt Ltd., while bartoli HPMC K100M was gifted from QIM Chemicals, Guntur. All other excipients were obtained from S.D. Fine Chem., Ltd. Mumbai, India.

Design and development of extended release tablets for ranolazine

Quantities required for the Eudragit L 100-55 and HPMC K100M for developing ranolazine XR tablets were chosen as factors (X_1 , X_2 respectively). Time to obtain dissolution was chosen as responses ($t_{10\%}$, $t_{50\%}$, $t_{75\%}$, $t_{90\%}$). RSM prediction equations (polynomial) were derived for responses according to linear stepwise backward regression technique.¹⁹

The 3 levels of X_1 (Eudragit L 100-55) were 3.75%, 6.25%, 8.75%. Three levels of X_2 (HPMC K100M) were 3.75%, 6.25%, 8.75% (% with respect to weight of active ingredient). Nine ranolazine XR tablet formulations were designed using selected combinations of X_1 , X_2 and checked for selecting optimum composition required to meet the primary objective of the study.

Preparation of ranolazine extended release tablets

A 3 level, 2-factor design was used for this research work. The amount of Eudragit L 100-55 chosen as X_1 and amount of HPMC K100M chosen as X_2 shown in Table 1. Three levels of both factors chosen indicated as -1=3.75%; 0=6.25%; +1=8.75%.

XR tablets for ranolazine were obtained using the direct compression method. Each tablet contained 500 mg of ranolazine. The formulae for the preparation of tablets are presented in Table 2. All ingredients were collected and weighed accurately as *per* the formula. All were subjected to sifting to achieve good compression properties. After sifting, they were mixed in polybag for obtaining uniform blend. The obtained blend was subjected to lubrication and processed for applying force to get desired tablet press. Resultant tablets were subjected to pharmaceutical product performance tests.

Evaluation of ranolazine extended release tablets

Crushing strength

It was determined using tablet hardness tester on the basis of diametric breakage of tablets.

Friability

This test was performed using a friability test apparatus (Roche). The selected number of tablets (20) were weighed accurately weight was noted (W_0), tablets were subjected to rotations (25 rpm for 4 min) again weight was noted (W). % weight loss was determined using the following formula.

$$\text{Weight loss (\%)} = [(W_0 - W) / W_0] \times 100$$

Drug content

It was carried out as *per* the standard procedure, take 20 tablets and triturated to obtain fine powder, a quantity equivalent to 100 mg of ranolazine was calculated and was dissolved in 0.1 N HCl. The sample was subjected to sonication and clarified by passing the solution *via* 0.45 μ filter press. After preparing the aliquots, their absorbances were measured at 272 nm using ultraviolet-visible (UV) spectrophotometer.

Thickness

It was obtained using vernier calipers on the principal longitudinal basis.

Drug dissolution

This test was performed using USP tablet dissolution test apparatus (type 2) as per the standard conditions, such as 900 mL of pH 1.2 buffer as the dissolution medium for the first 2 h followed by phosphate buffer pH 6.8. The temperature was maintained at $37 \pm 0.5^\circ\text{C}$ and paddle was rotated at a rate of 50 revolutions per minute. The samples were collected as *per* the protocol and analyzed for drug release using spectrometry at 272 nm. Analysis is done in triplicate manner.¹⁴

Statistical analysis

The data obtained were fit to kinetic modeling to ascertain the mechanism of drug release. The statistical parameters (a , b , r) were determined as kinetic parameters.^{20,21} The dissolution parameters were also determined using polynomial equations.

RESULTS AND DISCUSSION

XR tablets of ranolazine were developed as *per* 3-level, 2-factor design for optimizing the combination of drug release modifiers (Eudragit L 100-55, HPMC K100M). The formulation design is

presented in Table 1. The quantity of Eudragit L 100-55 (X_1) and HPMC K100M (X_2) chosen as factors and time for obtaining dissolution chosen as responses ($t_{10\%}$, $t_{50\%}$, $t_{75\%}$, $t_{90\%}$). Nine trials were developed as *per* the formula given in Table 2.

All trials have ranolazine (500 mg) as an XR formulation, obtained as tablet using direct compression technique. The

Table 1. Experimental design layout

Formulation code	X_1	X_2
RF ₁	1	1
RF ₂	1	0
RF ₃	1	-1
RF ₄	0	1
RF ₅	0	0
RF ₆	0	-1
RF ₇	-1	1
RF ₈	-1	0
RF ₉	-1	-1
CR ₁	-0.5	-0.5
CR ₂	+0.5	+0.5

developed formulations were evaluated for pharmaceutical product performance tests. The data are presented in Table 3. All formulations have sufficient mechanical strength. All formulations found to be less friable, as within the limits. All batches passed the drug content uniformity test. All formulation batches passed the weight variation test. Dissolution rate test was carried as *per* standard procedure, the dissolution specifications such as 900 mL of simulated gastric fluid for the first 2 h followed by simulated intestinal fluid; paddle was rotated at a speed of 50 rpm, the temperature maintained as $37 \pm 0.5^\circ\text{C}$ throughout the test period. The dissolution profile was well fit to kinetic modeling, results are presented in Table 4 and the same was presented as plots from Figure 1-4. From the results, observed that there was a clear relation existed between the quantities of polymers in combination with the drug release rate (both were inversely proportional to each other). Predicted sustained release of drug was obtained by appropriate composition of factors (X_1 , X_2).

Based on the desirability factor, RF₅ is considered the best formulation among all batches. RF₅ composed of both Eudragit L 100-55 and HPMC K100M in equal quantity *i.e.* 31.25 mg each, produced promising dissolution characteristics, which help in meeting the purpose of research by extended period of drug release (optimum delivery of drug) from dosage form.

Table 2. Formulae for ranolazine extended release tablets

Name of ingredients	Quantity of ingredients <i>per</i> each tablet (mg)								
	RF ₁	RF ₂	RF ₃	RF ₄	RF ₅	RF ₆	RF ₇	RF ₈	RF ₉
Ranolazine	500	500	500	500	500	500	500	500	500
Avicel pH 101	36.5	49	61.5	49	61.5	74	61.5	74	86.5
Eudragit L 100-55	43.75	43.75	43.75	31.25	31.25	31.25	18.75	18.75	18.75
HPMC K100M	43.75	31.25	18.75	43.75	31.25	18.75	43.75	31.25	18.75
Magnesium stearate	8	8	8	8	8	8	8	8	8
Talc	8	8	8	8	8	8	8	8	8
Total weight	640	640	640	640	640	640	640	640	640

HPMC: Hydroxypropylmethylcellulose

Table 3. Post-compression parameters for the formulations (n= 3)

Batch code	Hardness (kg/cm ²)	Thickness (mm)	Friability (%)	Average weight (mg)	Drug content (%)
RF ₁	8.47 \pm 0.27	4.06 \pm 0.08	0.10 \pm 0.001	641.09 \pm 0.01	99.94 \pm 0.49
RF ₂	8.2 \pm 0.28	3.98 \pm 0.085	0.11 \pm 0.001	641.11 \pm 0.01	99.45 \pm 0.50
RF ₃	7.93 \pm 0.27	3.9 \pm 0.08	0.09 \pm 0.001	641.10 \pm 0.01	99.11 \pm 0.51
RF ₄	8.52 \pm 0.42	4.1 \pm 0.06	0.06 \pm 0.001	641.14 \pm 0.02	99.74 \pm 0.32
RF ₅	8.10 \pm 0.41	4.05 \pm 0.06	0.07 \pm 0.001	642.2 \pm 0.02	99.43 \pm 0.33
RF ₆	7.7 \pm 0.41	3.99 \pm 0.05	0.07 \pm 0.001	641.31 \pm 0.02	99.11 \pm 0.34
RF ₇	8.35 \pm 0.42	4.18 \pm 0.05	0.05 \pm 0.001	640.66 \pm 0.02	99.70 \pm 0.43
RF ₈	7.91 \pm 0.42	4.05 \pm 0.06	0.04 \pm 0.001	641.2 \pm 0.01	99.23 \pm 0.47
RF ₉	7.49 \pm 0.41	4.02 \pm 0.06	0.05 \pm 0.001	640.65 \pm 0.01	98.77 \pm 0.35

Table 4. Regression analysis for factorial trials

Formulation code	Kinetic parameters											
	Zero order			First order			Higuchi			Korsmeyer-Peppas		
	a	b	r	a	b	r	a	b	r	a	b	r
RF ₁	14.410	3.284	0.982	1.988	0.034	0.986	1.685	17.614	0.995	1.089	0.629	0.962
RF ₂	14.857	3.285	0.981	1.986	0.034	0.986	1.308	17.641	0.995	1.098	0.625	0.959
RF ₃	15.304	3.285	0.979	1.985	0.034	0.986	0.930	17.667	0.995	1.107	0.621	0.957
RF ₄	15.946	3.819	0.982	2.110	0.065	0.931	2.738	20.473	0.995	1.125	0.651	0.960
RF ₅	16.302	3.834	0.982	2.171	0.077	0.877	2.481	20.560	0.995	1.132	0.649	0.958
RF ₆	16.657	3.848	0.981	2.117	0.068	0.931	2.224	20.646	0.995	1.138	0.647	0.956
RF ₇	23.404	3.915	0.948	2.112	0.093	0.964	2.240	21.685	0.992	1.199	0.641	0.950
RF ₈	23.778	3.923	0.948	2.185	0.110	0.949	2.539	21.742	0.993	1.204	0.638	0.948
RF ₉	24.304	3.883	0.946	2.286	0.124	0.915	3.157	21.565	0.993	1.210	0.634	0.945
Marketed product	17.313	3.884	0.979	2.201	0.086	0.897	1.910	20.897	0.995	1.148	0.644	0.955

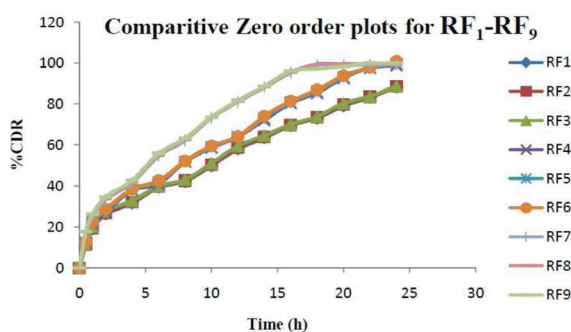


Figure 1. Comparative zero order plots

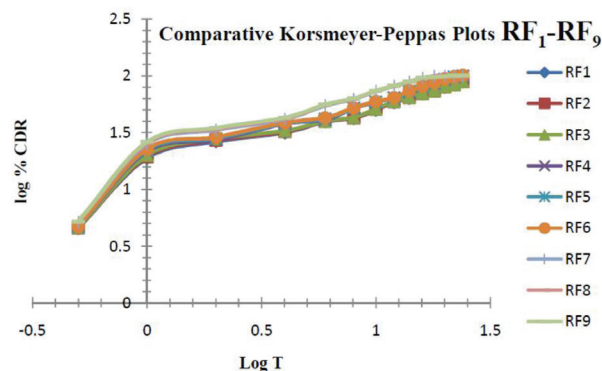


Figure 4. Comparative Korsmeyer-Peppas plots

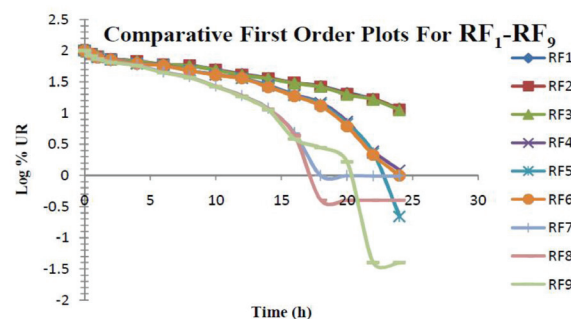


Figure 2. Comparative first order plots

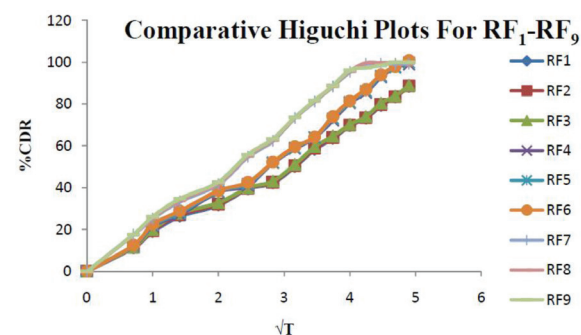
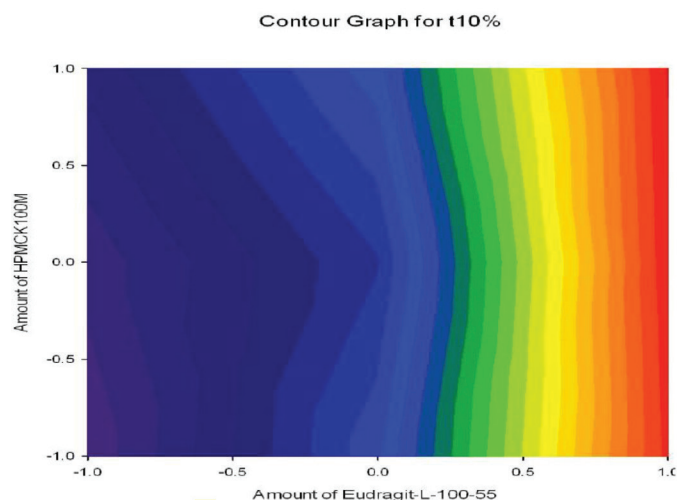
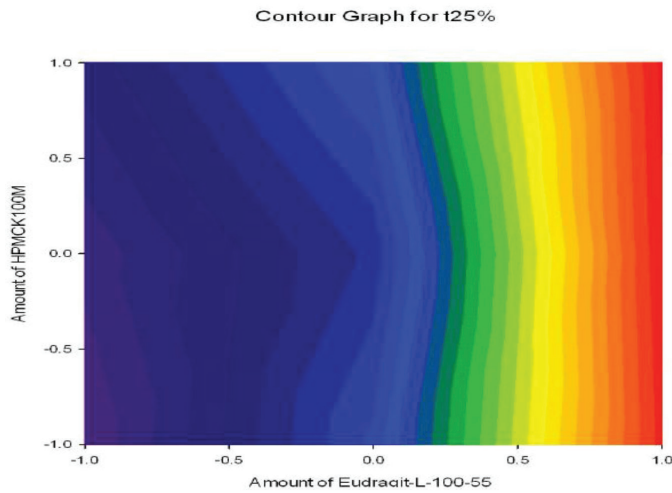
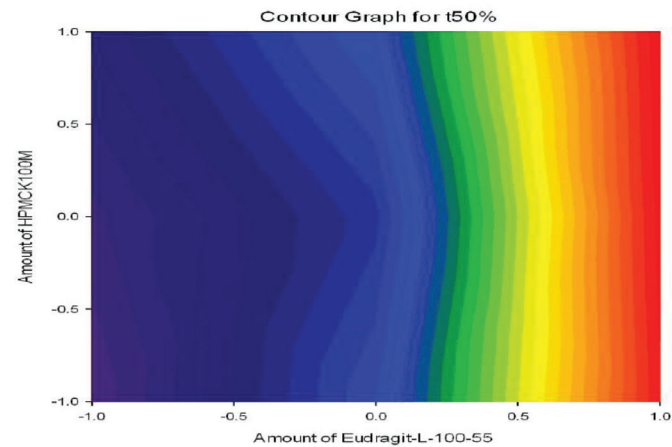
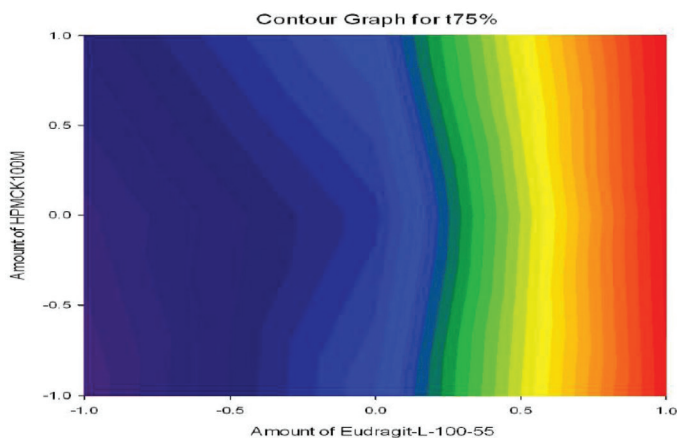


Figure 3. Comparative Higuchi plots

Figure 5. Contour plots for $t_{10\%}$

RSM equations (polynomial) were derived for all responses using PCP Disso and RSM plots were obtained with the help of Design-Expert 7.0. The response morphological plots were presented as Figure 5-9. The dissolution parameters for RF₁-RF₉ were summarized as Table 5.

Figure 6. Contour plots for $t_{25\%}$ Figure 7. Contour plots for $t_{50\%}$ Figure 8. Contour plots for $t_{75\%}$

RSM equations for the determination of predicted kinetic parameters as follows;

$$Y_1 = 0.810 + 0.461X_1 + 0.038X_2 - 0.024X_1X_2 + 0.232X_1^2 + 0.035X_2^2 \quad (t_{10\%})$$

$$Y_2 = 2.210 + 1.23X_1 + 0.084X_2 - 0.065X_1X_2 + 0.632X_1^2 + 0.096X_2^2 \quad (t_{25\%})$$

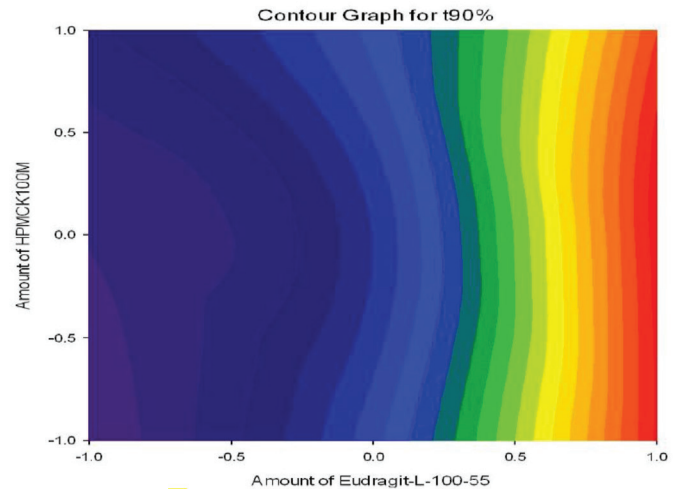
Figure 9. Contour plots for $t_{90\%}$

Table 5. Dissolution parameters for factorial formulations

Formulation code	Dissolution parameters				
	$t_{10\%}$ (h)	$t_{25\%}$ (h)	$t_{1/2}$ (h)	$t_{75\%}$ (h)	$t_{90\%}$ (h)
RF ₁	1.362	3.719	8.962	17.923	29.779
RF ₂	1.348	3.679	8.865	17.731	29.460
RF ₃	1.333	3.639	8.769	17.537	29.139
RF ₄	0.701	1.913	4.611	9.221	15.321
RF ₅	0.596	1.627	3.921	7.843	13.030
RF ₆	0.669	1.827	4.401	8.803	14.626
RF ₇	0.493	1.345	3.242	6.484	10.773
RF ₈	0.415	1.132	2.728	5.456	9.065
RF ₉	0.369	1.007	2.426	4.852	8.061
Marketed product	1.362	1.447	3.487	17.923	11.589

$$Y_3 = 5.33 + 3.04X_1 + 0.21X_2 - 0.156X_1X_2 + 1.52X_1^2 + 0.23X_2^2 \quad (t_{50\%})$$

$$Y_4 = 10.65 + 6.07X_1 + 0.41X_2 - 0.31X_1X_2 + 3.04X_1^2 + 0.46X_2^2 \quad (t_{75\%})$$

$$Y_5 = 17.695 + 10.08X_1 + 0.675X_2 - 0.518X_1X_2 + 5.05X_1^2 + 0.765X_2^2 \quad (t_{90\%})$$

Results for the predicted responses vs actual responses are presented in Table 6. Not much deviation was observed in the predicted vs actual responses. It indicates the validity of the developed equation. RF₅ was considered as ideal, it shows similarity factor (f₂) 85.78, difference factor (f₁) tcl, $t_{cal} < 0.05$ compared with the marketed product (RANEXA). Comparative dissolution plots for best formulation (RF₅) and marketed product are shown in Figure 10.

CONCLUSION

On the basis of the current study, the use of macromolecules (polymers) in combination had its own advantages of maintaining integrity and extended drug release form of the formulation. The combination of a partially neutralized pH-dependent polymer and pH-independent polymer at an appropriate proportion will yield desired extended drug release,

Table 6. Dissolution parameters for check point formulations

Formulation code	Predicted value					Actual observed value				
	t _{10%} (h)	t _{25%} (h)	t _{50%} (h)	t _{75%} (h)	t _{90%} (h)	t _{10%} (h)	t _{25%} (h)	t _{50%} (h)	t _{75%} (h)	t _{90%} (h)
CR ₁	0.624	1.704	4.106	8.22	13.643	0.62	1.69	4.31	8.19	13.71
CR ₂	1.116	3.047	7.342	14.684	24.397	1.12	3.11	7.54	14.55	23.99

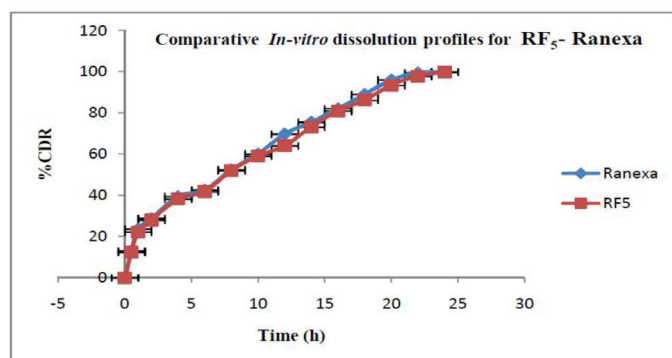


Figure 10. Comparative dissolution plots for RF5-Ranexa

which ultimately 2-fold reduction in the dosing frequency of ranolazine. This is achieved by preparing the ranolazine with combination polymers like Eudragit L 100-55 and HPMC K100M employing along with other excipients using 3² factorial design approaches. Among the various ER formulations studied, the formulation (RF₅) showed the best result in all aspects of objective, which was considered as the ideal formulation. The best formulation RF₅ follows zero order release, non-fickian diffusion, it may improve patient compliance by reducing the dosing frequency to 2 fold or more, which will ultimately improve the clinical response.

ACKNOWLEDGMENTS

Authors acknowledge sincere thanks to the Management and Staff of M.A.M College of Pharmacy, India for the facilities granted and constant encouragement for completing current research investigation.

Ethics

Ethics Committee Approval: There is no requirement for ethical approval.

Informed Consent: Not applicable.

Peer-review: Externally peer-reviewed.

Authorship Contributions

Concept: R.K.G., D.D., **Design:** K.R.G., **Data Collection or Processing:** R.K.G., **Analysis or Interpretation:** P.R.M., D.D., **Literature Search:** R.K.G., **Writing:** R.K.G., K.R.G.

Conflict of Interest: No conflict of interest was declared by the authors.

Financial Disclosure: The authors declared that this study received no financial support.

REFERENCES

- Remington. The science and practice of pharmacy. (21st ed). USA; Lippincott, Williams and Wilkins Publications; 2005:939-964.
- Tegk M, Mukkala BVP, Babu VV S. Formulation and evaluation of ranolazine extended release tablets: influence of polymers. Asian J Pharm. 2011;5:162-166.
- Adepu H, Srilatha S, Reddy MR. Formulation and evaluation of film coated ranolazine extended release tablets. Int J Inn Pharm Sci Res. 2014;2:2283-2294.
- Uddin NM, Ahmed I, Roni MA, Islam MR, Rahman MH, Ul Jalil R. *In vitro* release kinetics study of ranolazine from swellable hydrophilic matrix tablets. Dhaka Univ J Pharm Sci. 2009;8:31-38.
- Gunda RK, Vijayalakshmi A. Formulation development and evaluation of gastro retentive bioadhesive drug delivery system for moxifloxacin. HCl. Ind J Pharm Edu Res. 2019;53:724-732.
- Jitendra G, Govind M, Prabakaran L, Reena G. Formulation development and characterization of modified release microspheres of antianginal. Drug Int J Drug Dev Res. 2014;6:252-265.
- Bawankar DL, Deshmame SV, More SM, Channawar MA, Chandewar AV, Shreekanth J. Design and characterization of extended release ranolazine matrix tablet. Res J Pharm Tech. 2009;2:756-761.
- Kumar CB, Aparna C, Srinivas P. Formulation and evaluation of solid self emulsifying drug delivery sytem of ranolazine. J Glob Tren Pharm Sci. 2014;5:2238-2247.
- Bidada J, Gonjari I, Bhusari A, Raut C, Dhule A. Development of extended release matrix tablets of ranolazine containing polyacrylic and ethylcellulose polymers. Der Pharm Let. 2011;3:215-226.
- Kuchekar SB, Mohite SK. Design and evaluation of extended release ranolazine liquisoloid tablets using placket burman screening design. Asian J Pharm Clin Res. 2015;8:292-300.
- Rahman M, Hasan S, Alam A, Roy S, Kumar Jha M, Ahsan Q, Rahman H. Formulation and evaluation of ranolazine sustained release matrix tablets using Eudragit and HPMC. Int J Pharm Biomed Res. 2011;1:172-177.
- Pittala B, Bommagani NK, Vasudeva Murthy S, Basani M, Nagavalli P. Formulation and evaluation of ranolazine extended release tablets by using pH dependent and independent polymers. Int J Pharm Bio Arc. 2013;4:1164-1171.
- Asaduzzaman, Rahman R, Khan SR, Islam SMA. Development of sustain release matrix tablet of ranolazine based on methocel K4M CR: *in vitro* drug release and kinetic approach. J App Pharm Sci. 2011;1:131-136.
- Priya MR, Natarajan R, Rajendran NN. Design and *in vitro* evaluation of sustained release tablets of ranolazine. Int J Pharm Sci Res. 2011;2:922-928.
- Gunda RK. Formulation development and evaluation of rosiglitazone maleate sustained release tablets using 3² factorial design. Int J Pharm Tech Res. 2015;8:713-724.

16. Gunda RK, Manchineni PR. Statistical design and optimization of sustained release formulations of pravastatin. *Turk J Pharm Sci.* 2020;17:221-227.
17. Kumar GR, Vijayalakshmi A. Formulation and evaluation of gastro retentive floating drug delivery system for novel fluoroquinolone using natural and semisynthetic polymers. *Iran J Pharm Sci.* 2020;16:49-60.
18. Gunda RK, Vijayalakshmi A. Development and evaluation of gastroretentive formulations for moxifloxacin. hydrochloride. *Thai J Pharm Sci.* 2020;44:30-39.
19. Gunda Kumar R, Kumar JNS. Formulation development and evaluation of doxofylline sustained release tablets. *FABAD J Pharm Sci.* 2017;42:199-208.
20. Babu AK, Ramana MV. *In vitro* and *in vivo* evaluation of quetiapine fumarate controlled gastroretentive floating drug delivery system. *Int J Drug Del.* 2016;8:12-22.
21. Ramana M, Babu A, Thadanki M. Formulation development and evaluation of omeprazole microspheres by using the pH sensitive enteric polymers. *The FASEB Journal*, 28: LB590. doi.org/10.1096/fasebj.28.1_supplement.lb590



Protective Role of *Diospyros lotus* L. in Cisplatin-Induced Cardiotoxicity: Cardiac Damage and Oxidative Stress in Rats

Neşe BAŞAK TÜRKMEN^{1*}, Dilan AŞKIN ÖZEK², Aslı TAŞLIDERE³, Osman ÇİFTÇİ⁴, Özlem SARAL⁵, Cemile Ceren GÜL³

¹Inonu University, Faculty of Pharmacy, Department of Pharmaceutical Toxicology, Malatya, Turkey

²Firat University, Kovancılar Vocational School, Department of Pharmacy Services, Elazığ, Turkey

³Inonu University, Faculty of Medicine, Department of Histology and Embryology, Malatya, Turkey

⁴Pamukkale University, Faculty of Medicine, Department of Medical Pharmacology, Denizli, Turkey

⁵Recep Tayyip Erdoğan University, Faculty of Health Sciences, Department of Nutrition and Dietetics, Rize, Turkey

ABSTRACT

Objectives: Cisplatin is a powerful chemotherapeutic drug that is used to treatment a wide variety of cancers. Despite clinical data demonstrating the cardiotoxic effect of cisplatin, few studies have been carried to improve the cardiotoxicity of cisplatin. In cisplatin-induced toxicity, oxidative stress plays a critical role. This study determined the effect of *Diospyros lotus* L. fruit (DL), a powerful antioxidant plant, on heart damage caused by cisplatin through histological examination and oxidative stress parameters.

Materials and Methods: Twenty eight male rats were randomly divided into four groups. An isotonic solution was given to the control group. A single dose of 7 mg/kg cisplatin was administered intraperitoneally to the cisplatin group. 1.000 mg/kg DL was given by gavage for 10 days to the DL group. Cisplatin and DL were administered together in the same doses to the treatment group. Thiobarbituric acid reactive substances (TBARS) levels, superoxide dismutase (SOD), catalase (CAT), glutathione peroxidase (GPx) activities, and total glutathione (GSH) level were measured in the heart tissue of the experimental rats. Histological examination was also performed to determine any damage to the hearts of the experimental rats.

Results: While TBARS levels in the cisplatin group increased significantly, SOD, CAT, GPx activities, and total GSH level decreased significantly. TBARS levels decreased significantly and SOD, CAT, GPx activities and GSH levels increased with DL treatment. According to the histological examination, histopathological differences were observed in the cisplatin group. Histopathological findings were either absent or decreased in the DL-treated group.

Conclusion: Results of the study showed that DL therapy reduced oxidative stress and histological changes caused by cisplatin. DL could be a potential candidate for reducing cardiac damage caused by cisplatin.

Key words: *Diospyros lotus*, cisplatin, cardiotoxicity, oxidative stress

INTRODUCTION

Cisplatin, an extremely effective chemotherapeutic drug, is a platinum-based drug with strong activity against ovarian, cervical, testicular, bladder, lung cancers, and solid tumors, which are resistant to other treatments.^{1,2} Cisplatin shows a cytotoxic effect by cross-linking on DNA with purine bases, causing DNA damage and apoptosis in cancer cells. Notwithstanding the effect stated above, cisplatin provides more than 90% recovery in testicular cancer.³

The serious side effects of cisplatin such as neurotoxicity, nephrotoxicity, gastrointestinal disorders, reproductive toxicity, and bone marrow suppression limit its use in therapy.⁴ Some studies have suggested that cisplatin treatment may cause cardiotoxicity.⁵⁻⁷ Heart failure, arrhythmias, myocardial infarction, pericarditis, myocarditis, and congestive cardiomyopathy have been defined as cardiotoxic symptoms caused by cisplatin chemotherapy.^{6,7} Cardiotoxicity by cisplatin limits its clinical use. Cisplatin's cardiotoxic mechanism is fully

*Correspondence: nese.basak@inonu.edu.tr, Phone: +90 534 222 95 72, ORCID-ID: orcid.org/0000-0001-5566-8321

Received: 25.03.2021, Accepted: 26.07.2021

©Turk J Pharm Sci, Published by Galenos Publishing House.

unknown, but it was proposed that cardiotoxicity can result from cisplatin's direct toxic impact on cardiac myocytes and the formation of reactive oxygen species (ROS).⁸ Cisplatin reduces the activity of antioxidant enzymes in cardiac tissue, while increasing tissue total oxidant potential and lipid hydroperoxide levels.⁹

The presence of cisplatin in the blood even years after treatment may cause cardiotoxicity later in life. This situation poses a significant risk of cancer patients treated with cisplatin.^{6,7,10} The treatment to cisplatin-induced cardiotoxicity is important. Although some cardioprotective strategies are available today, they are insufficient in preventing or reducing cardiotoxicity, especially in clinical practice.¹¹ According to some studies, cisplatin-induced toxicity is exacerbated by elevated oxidative stress. However, it has been suggested that various antioxidant treatments show beneficial effects by reducing oxidative stress.^{5,9,12}

The date palm tree is a member of Ebenaceae family, which is grown in many regions such as Asia, Southern Europe, and Turkey. It has a nutritious fruit used in traditional Chinese medicine.^{12,13} *Diospyros lotus* L. fruits (DL) have significant antioxidant activity due to their phenolic content. Therefore, it is an effective source of natural antioxidants. DL is thought to be an important food product and its ingredients have health benefits.^{13,14} A previous study suggested that sperm toxicity caused by cisplatin can be reduced with DL fruits.¹²

The purpose of this study was to investigate the easing effect of DL, which is thought to have high antioxidant potential, on the cardiotoxic effects of cisplatin. Hence, histopathological and biochemical changes caused by cisplatin in the heart were examined and the effects of DL treatment were investigated in this study. In this study, a single extract was prepared from the plant. Since the amount of phenolic substances in the extracts prepared with water, acetone, and methanol was higher in the water part, the aqueous extract was used in our study. Phenolic substance measurement was not performed.¹²

MATERIALS AND METHODS

Chemicals

Cisplatin (10 mg/10 mL, code 1876A) was purchased from Faulding Pharmaceuticals Plc (Warwickshire, UK). DL fruits were obtained from Kumludere village (Trabzon, Turkey) in autumn of 2020. All other chemicals were purchased from Sigma Chemical Co. (St. Louis, MO, USA).

Plant material and preparation of the extract

DL was collected in autumn in 2020 around Trabzon. The DL was dried at 38°C for 5 days in an oven and milled to 2-3 mm in size. Extract was obtained using distilled water for 24 h using the percolation method. The extract was filtered through filter paper. The filtrated part was freeze-dried until a crude solid extract was obtained.¹⁵ Identification of the plant was performed by Assoc. Dr. Mustafa Karaköse from Department of Medicinal and Aromatic Plants, Espiye Vocational School, Giresun University (Turkey).

Twenty-eight adult male Sprague Dawley rats, 2-3 month-old and weighing 250-300 g, were used for the experiments. Rats were obtained from the Institute of Experimental Animals in Pamukkale, Turkey and maintenance was performed in these centers.

The rats were housed in a 12-hour daylight/12-hour dark cycle, ventilated, constant temperature ($21 \pm 1^\circ\text{C}$) rooms and sterile cages according to the standards. Their feeding was provided by standard rat pellet feed and tap water. No special diet was applied. All experimental applications were performed according to the "Guidelines for the Care and Use of Laboratory Animals published by the US National Institutes of Health". The experimental protocol was approved by the Ethical Committee on Animal Research of Pamukkale University (PAUHDEK -2021/09).

Drug administration

The 28 rats were divided into 4 groups. A single dose of cisplatin at 7 mg/kg was administered intraperitoneally (*i.p.*). Previous studies showed that a single dose of 7 mg/kg injection of cisplatin causes testicular damage in rats.^{16,17}

The phenol content of the extract of DL in water is higher than that of extracts from methanol or acetone. Because of the antioxidant effect of the aqueous extract, DL was suspended in distilled water in this experiment. 1.000 mg/kg DL extract was administered for 10 days. The effective dose was determined by reference to the study of Rashed et al.¹⁸ A control group was accepted as the negative control. Isotonic saline *i.p.* and distilled water was administered gavage. 7 mg/kg of cisplatin was given once to the cisplatin group. DL extract was given to DL group without cisplatin by gavage for 10 days. Cisplatin and DL were administered to the treatment group with the specified protocol. Because of the procedure, tissue and blood samples were taken. The heart tissue, which was quickly removed, was sliced on cold glass. Blood samples were centrifuged at 3000 rpm for 20 min at 4°C and blood serum was obtained. Tissue and serum samples were stored at -80°C.

Biochemical analysis

Care was taken to protect the cold chain in all homogenization processes. 1:10 (w/v) dilution was made by adding 150 mM KCl (pH 7.4) to homogenize the heart tissue. Homogenization was done in a teflon glass homogenizer. The examples were centrifuged for 40 min at 3500 rpm at +4°C using a refrigerated centrifuge. Catalase (CAT), thiobarbituric acid reactive substances (TBARS), and total glutathione (GSH) activities were analyzed in the homogenate. Superoxide dismutase (SOD) and glutathione peroxidase (GPx) activities were determined in the supernatant obtained after centrifugation.

Determination of thiobarbituric acid reactive substances activity

TBARS activity in homogenized tissue as a lipid peroxidation marker was determined by the Yagi¹⁹ method. Under aerobic conditions and pH: 3.5, the tissue homogenate was precipitated with 10% trichloroacetic acid (TCA) and kept in a water bath for 15 min, then cooled and centrifuged at 3000 rpm for 10 min. The

supernatant obtained was incubated with TBA in a 95°C water bath for 50 min and cooled. The absorbances of the pink-colored complex formed because of the reaction of malondialdehyde, the secondary product of lipid peroxidation, with TBA were measured at 532 nm using a spectrophotometer.

Determination of total glutathione levels

The supernatant was obtained from the homogenates centrifuged at 3500 rpm for 10 min with 10% TCA (0.2 M, pH: 8.9). Tris-ethylenediamine tetraacetic acid (EDTA) buffer solution and 0.01 M 5,5'-Dithiobis(2-nitrobenzoic acid) (DTNB) were added to the supernatants. DTNB is reduced by sulfhydryl compounds and forms a yellow complex, which is a disulfide compound. The optical density of this yellow compound was determined at 412 nm with a spectrophotometer using the Sedlak and Lindsay²⁰ method.

Determination of SOD activity

SOD enzyme activity was determined as described by Sun et al.²¹ SOD determination method is based on nitroblue tetrazolium (NBT) reduction of superoxide produced by xanthine/xanthine oxidase system. This reaction was stopped by adding copper (II) chloride. The colored formazan product formed by the reduction of NBT by superoxide radicals was measured using a spectrophotometer at 560 nm.

Determination of CAT activity

The CAT activity of the heart tissue was analyzed using the Aebi²² method. The catalytic activity of CAT decomposed H_2O_2 was added to the sample into water and oxygen. In the CAT determination, hydrogen peroxide showed maximum absorbance at 240 nm as measured by a spectrophotometer. The breakdown of H_2O_2 by CAT was followed by an absorbance reduction. This decrease in absorbance is directly proportional to the enzyme activity. CAT activity was determined by the absorbance difference *per unit time*.

Determination of GPx activity

GPx activity was analyzed according to the method of Paglia and Valentina.²³ GPx is an enzyme that converts H_2O_2 to water using reduced glutathione. GPx catalyzes the conversion of GSH to oxidized glutathione disulfide (GSSG) in the presence of H_2O_2 . GSSG formed by GPx in the presence of H_2O_2 is converted back to GSH with the help of glutathione reductase and nicotinamide adenine dinucleotide phosphate (NADPH). For this purpose, NADPH, GSH reductase, and sodium azide were prepared separately in buffered EDTA solution. The prepared solutions were added to the supernatant maintained and kept at room temperature for 30 min. GSH-Px activity was measured using a spectrophotometer at 340 nm, the absorbance difference that occurred in the optical density with the conversion of NADPH in the experimental environment to $NADP^+$.

Determination of total protein amount

The amount of protein in heart tissue was measured using $CuSO_4$, Folin-Ciocalteu reagent, and bovine serum albumin according to the Lowry et al.²⁴ Analysis procedure is as follows; alkaline copper (Cu^{+2}) forms a complex with peptide bonds

and each 7 or 8 amino acid residues bind 1 atom of copper. When the Folin-Ciocalteu reagent is added to the copper-treated mixture, a violet-blue color is formed, which is measured by a spectrophotometer at 700 nm.

Histological analysis

Heart tissue samples were fixed in 10% formaldehyde solution. Then, the samples embedded in paraffin were cut into sections of 5 μm thickness. Sections were stained with hematoxylin-eosin on a coverslip. Tissue samples were examined for necrosis, mononuclear cell infiltration, bleeding, vascular occlusion using a "Leica DFC280 light microscope" and a "Leica Q Win Image Analysis system (Leica Micros Imaging Solutions Ltd., Cambridge, UK)". The histopathological damage score was calculated according to the findings.

Statistical analysis

Biochemical and histological data are presented as mean \pm standard deviation. The normal distribution of biochemical data was analyzed using the Shapiro-Wilk test. One-Way ANOVA and Tukey tests were used for biochemical statistical analysis. Kruskal-Wallis were used for histological results. For statistical significance, $p < 0.001$ was accepted. "SPSS 13.0 (SPSS Inc., Chicago, Ill., USA)" and "MedCalc 11.0 (Belgium)" statistical programs were used for analysis.

RESULTS

Biochemical evaluation

TBARS levels, SOD, CAT, GPx activities, and total GSH levels in heart tissue was measured by spectrophotometric methods. The results showed that cisplatin administration significantly ($p < 0.01$) increased TBARS levels and decreased SOD, GPx, CAT activities, and total GSH levels compared to all groups. There was no statistically significant difference between the control group and the DL-only groups in terms of biochemical parameters. TBARS levels increased with cisplatin in the treatment group and decreased significantly ($p < 0.01$) with DL treatment. SOD, GPx, CAT activities, and total GSH levels decreased with cisplatin but increased again with DL treatment. DL treatment reduced the negative effects of cisplatin on biochemical parameters, as shown in (Table 1).

Histological evaluation

In the control (Figure 1A) and DL (Figure 1B) groups, the heart tissue was in normal histological appearance. Necrosis (Figure 2A), mononuclear cell infiltration (Figures 2B and E), hemorrhage (Figures 2C and D), vascular occlusion (Figure 2F) were determined in the cisplatin group. The damage score calculated according to histopathological findings increased significantly in the cisplatin group (2.29 ± 0.10) compared to the control (0.49 ± 0.08) (Table 2). Although histological changes decreased in the treatment group compared with the cisplatin group, small-vessel occlusion (Figure 3A) and mononuclear cell infiltration (Figure 3B) were observed. The level of damage decreased significantly in the treatment group (0.86 ± 0.10) (Table 2).

Table 1. The activities of TBARS, total GSH, CAT, SOD and GPx and in rat heart tissue (mean \pm SD)

Groups	TBARS (nmol/g tissue)	Total GSH (nmol/mL)	CAT (U/mg protein)	SOD (U/mg protein)	GPx (U/mg protein)
Control	9.28 \pm 0.92 ^a	92.7 \pm 3.41 ^a	0.035 \pm 0.0007 ^a	34.8 \pm 2.14 ^a	256.5 \pm 23.9 ^a
CIS	15.5 \pm 1.12 ^b	71.1 \pm 3.59 ^b	0.022 \pm 0.0005 ^b	22.4 \pm 2.48 ^b	158.9 \pm 25.2 ^b
DL	8.92 \pm 0.89 ^a	97.3 \pm 4.19 ^a	0.036 \pm 0.0005 ^a	35.2 \pm 3.61 ^a	265.3 \pm 23.6 ^a
CIS + DL	12.4 \pm 1.06 ^c	85.1 \pm 3.16 ^c	0.029 \pm 0.0008 ^c	28.7 \pm 2.47 ^c	204.2 \pm 28.1 ^c

Values with different superscripts in the same column are statistically significantly different from each other ($p \leq 0.01$). a: Indicates that the control and DL group is different from the other groups, b: Indicates that the CIS group is different from the other groups, c: Indicates that the CIS + DL group is different from the other groups. TBARS: Thiobarbituric acid reactive substances, GSH: Glutathione, CAT: Catalase, SOD: Superoxide dismutase, GPx: Glutathione peroxidase, CIS: Cisplatin, DL: *Diospyros lotus*, SD: Standard deviation (n= 7)

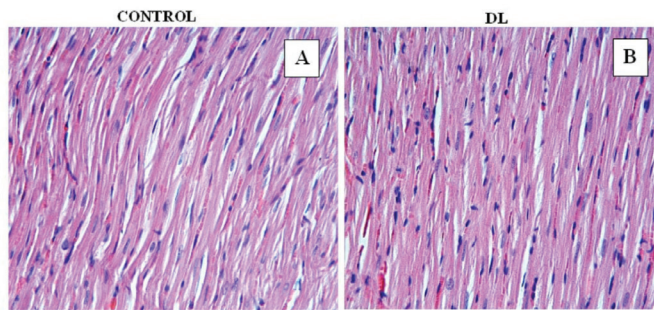


Figure 1. Control and DL group. In control and DL groups, heart tissue showed a normal histological appearance. (A) H-E; X40, (B) H-E; X40, DL: *Diospyros lotus* group, H-E: Hematoxylin-eosin

Table 2. Comparison of histopathological heart damage score between groups

Groups	Histopathological heart damage score (mean \pm SD)
Control	0.49 \pm 0.08 ^a
CIS	2.29 \pm 0.10 ^b
CIS + DL	1.41 \pm 0.12 ^c
DL	0.86 \pm 0.10 ^a

a: Indicates that the control and DL group is different from the other groups, b: Indicates that the CIS group is different from the other groups, c: Indicates that the CIS+DL group is different from the other groups. The mean differences of values with different superscript letters in the same column are statistically significant ($p \leq 0.001$). CIS: Cisplatin, DL: *Diospyros lotus*, SD: Standard deviation (n= 7)

DISCUSSION

Cisplatin is a very potent chemotherapeutic drug. However, its adverse effects on the heart, kidneys, liver, and other organs limit its use in cancer treatment.^{4,6} Approaches to reduce the toxic effects of cisplatin will contribute positively to increase the quality of life of cancer patients and to extending drug-dose limits. The toxicity caused by cisplatin is directly related to oxidative stress.²⁵ In this study, the easing role of DL, which has high antioxidant potential, against cisplatin-induced cardiotoxicity in rats was investigated. Although lipid peroxidation levels in heart tissue increased significantly in the cisplatin group, the antioxidant enzyme activities and total GSH levels decreased. In the group treated with DL, cisplatin-induced reductions in antioxidant enzyme activities and total

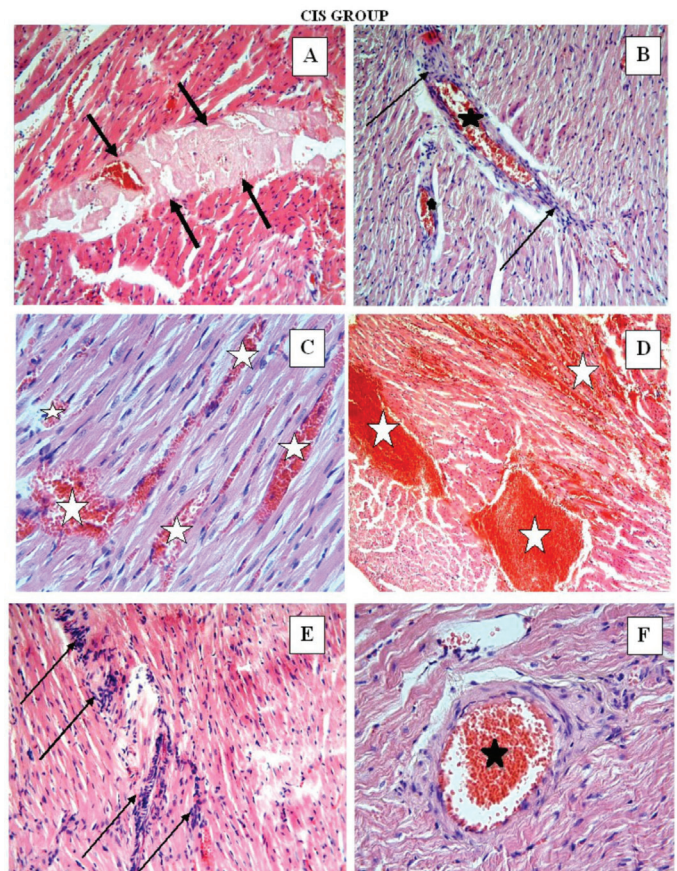


Figure 2. CIS group. Necrosis (black arrows) (A), mononuclear cell infiltration (thin black arrows) (B, E), hemorrhage (white asterisks) (C, D), vascular congestion (black asterisks) (F) were observed in CIS group. (A, B, E): H-E; X20, (D, F): H-E; X10, (C): H-E; X40. CIS: Cisplatin, H-E: Hematoxylin-eosin

GSH levels were improved. Lipid peroxidation levels decreased. According to the findings, DL showed a protective effect by reducing cisplatin cardiotoxicity. histopathological examination confirmed this suggestion.

Impairment of the balance between free radical levels and the antioxidant defense system causes oxidative stress. The increase in free radicals causes increased lipid peroxidation and decreased antioxidant enzymes because of impaired GSH metabolism. SOD, GPx, and CAT enzymes affect the endogenous defense mechanism. These enzymes can reduce

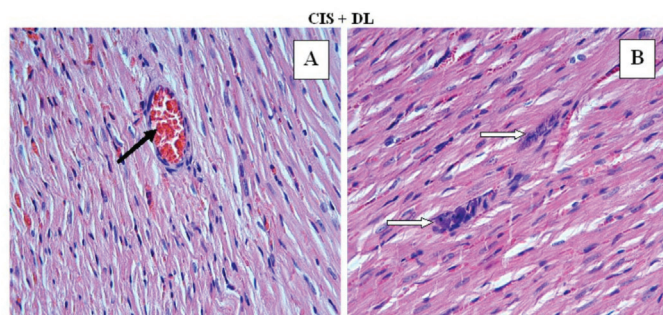


Figure 3. CIS + DL group. Histological changes were decreased in CIS + DL group compared with CIS group. Little vascular congestion (black arrow) (A), mononuclear cell infiltration (white arrow) (B) were observed in CIS + DL group. (A, B): H-E; X40. CIS: Cisplatin, DL: *Diospyros lotus*, H-E: Hematoxylin-eosin

oxidative stress by removing superoxide, hydrogen peroxide, and hydroxyl radicals.²⁶ Due to lipid peroxidation, TBARS are produced and are considered indicators of oxidative stress.²⁷ In this study, cisplatin was shown to increase TBARS levels in heart tissues of rats and cause lipid peroxidation. Similarly, different studies have suggested that cisplatin treatment causes cardiotoxicity with increased lipid peroxidation.^{5,7,9} Lipid peroxidation causes cell and organ damage. Cardiotoxicity caused by cisplatin therapy has generally been associated with increased oxidative stress.²⁵ The glutathione mechanism converts cisplatin into a reactive form that can react rapidly with thiol molecules. Cisplatin reduces glutathione and other antioxidant enzymes, causing ROS accumulation in cells by disrupting the cell's redox mechanism.⁵ Increased TBARS levels and decreased endogenous antioxidant enzyme activities are evidence that cisplatin causes oxidative stress. Increased oxidative stress caused damage and histopathological changes in the heart tissue. Previous studies have shown that reducing oxidative stress with antioxidant therapy attenuates cisplatin-induced organ damage.^{1,25,28}

DL is a good natural source of antioxidants.^{13,14} DL extracts can protect against oxidative stress by eliminating free radicals.¹³ Its content of phenolic compounds and flavonoids act as a reducing agent and chelator against free radicals.^{14,29} Azadbakhta et al.³⁰ showed that 1000 mg/kg DL reduced liver, kidney, and heart damage and improved organ morphology in streptozotocin-induced diabetic rats. Saral et al.¹² showed that 1000 mg/kg DL given reduced cisplatin-induced testicular damage. According to the data, in the group treated with DL, TBARS levels decreased significantly while total GSH, CAT, GPx, and SOD activities increased significantly. Observations of this study agree with the results of other previous studies.

Some histological changes such as vascular congestion, hemorrhage, vacuolization in the interstitial area, eosinophilic stained and pyknotic nuclei cells, mononuclear cell infiltration, and necrosis were observed in the cisplatin group. These results are consistent with the histopathological findings of previous cisplatin studies.¹² Histopathological findings were absent or decreased in the groups treated with DL, which alone did not cause any histological changes. Oxidative stress, which

decreased with DL treatment, contributed to the recovery of heart tissue.

The results of this study showed that DL antioxidant potential reduces oxidative stress and histological changes caused by cisplatin-induced cardiotoxicity. Increased SOD, CAT, total GSH, and GPx activity as well as decreased TBARS levels suggested that the cardioprotective effect of DL is mediated by its antioxidant content.

CONCLUSION

Oxidative stress caused by cisplatin causes increased lipid peroxidation, decreased antioxidant enzyme activity, and histopathological changes in the heart. The results of this study showed that DL, which has strong antioxidant properties, reduces oxidative stress and histological changes caused by cisplatin treatments. The use of DL may help reduce the cardiotoxic side effects of cisplatin therapy in cancer, thereby increasing the effectiveness of the treatment. These ameliorative effects of DL are attributable to its antioxidant and radical scavenging properties. Therefore, we suggest that DL treatment may be used against CP-induced cardiotoxic toxicity.

ACKNOWLEDGMENTS

We would like to thank Assoc. Dr. Mustafa Karaköse for his contributions to the diagnosis and identification of the plant species used in the study.

Ethics

Ethics Committee Approval: The experimental protocol was approved by the Ethical Committee on Animal Research of Pamukkale University (PAUHDEK -2021/09).

Informed Consent: There is no need.

Peer-review: Externally and internally peer-reviewed.

Authorship Contributions

Surgical and Medical Practices: N.B.T., D.A.Ö., Concept: Ö.S., Design: O.Ç., Data Collection or Processing: N.B.T., A.T., C.C.G., Analysis or Interpretation: N.B.T., A.T., Literature Search: N.B.T., D.A.Ö., Writing: N.B.T.

Conflict of Interest: No conflict of interest was declared by the authors.

Financial Disclosure: The authors declared that this study received no financial support.

REFERENCES

1. Yousef MI, Saad AA, El-Shennawy LK. Protective effect of grape seed proanthocyanidin extract against oxidative stress induced by cisplatin in rats. *Food Chem Toxicol.* 2009;47:1176-1183.
2. Wang D, Lippard SJ. Cellular processing of platinum anticancer drugs. *Nat Rev Drug Discov.* 2005;4:307-320.
3. Dasari S, Tchounwou PB. Cisplatin in cancer therapy: molecular mechanisms of action. *Eur J Pharmacol.* 2014;740:364-378.
4. Rabik CA, Dolan ME. Molecular mechanisms of resistance and toxicity associated with platinating agents. *Cancer Treat Rev.* 2007;33:9-23.

5. El-Awady el-SE, Moustafa YM, Abo-Elmatty DM, Radwan A. Cisplatin-induced cardiotoxicity: mechanisms and cardioprotective strategies. *Eur J Pharmacol.* 2011;650:335-341.
6. Bano N, Najam R, Qazi F. Adverse cardiac manifestations of cisplatin-a review. *Int J Pharm Sci Rev Res.* 2013;18:80-85.
7. Patanè S. Cardiotoxicity: cisplatin and long-term cancer survivors. *Int J Cardiol.* 2014;175:201-202.
8. Dugbartey GJ, Peppone LJ, de Graaf IA. An integrative view of cisplatin-induced renal and cardiac toxicities: molecular mechanisms, current treatment challenges and potential protective measures. *Toxicology.* 2016;371:58-66.
9. Gunturk EE, Yucel B, Gunturk I, Yazici C, Yay A, Kose K. The effects of *N*-acetylcysteine on cisplatin induced cardiotoxicity. *Bratisl Lek Listy.* 2019;120:423-428.
10. Feldman DR, Schaffer WL, Steingart RM. Late cardiovascular toxicity following chemotherapy for germ cell tumors. *J Natl Compr Canc Netw.* 2012;10:537-544.
11. Kalam K, Marwick TH. Role of cardioprotective therapy for prevention of cardiotoxicity with chemotherapy: a systematic review and meta-analysis. *Eur J Cancer.* 2013;49:2900-2909.
12. Saral S, Ozelcik E, Cetin A, Saral O, Basak N, Aydin M, Cifci O. Protective role of *Diospyros lotus* on cisplatin-induced changes in sperm characteristics, testicular damage and oxidative stress in rats. *Andrologia.* 2016;48:308-317.
13. Gao H, Cheng N, Zhou J, Wang B, Deng J, Cao W. Antioxidant activities and phenolic compounds of date plum persimmon (*Diospyros lotus* L.) fruits. *J Food Sci Technol.* 2014;51:950-956.
14. Ayaz FA, Kadioğlu A, Reunanen M. Changes in phenolic acid contents of *Diospyros lotus* L. during fruit development. *J Agric Food Chem.* 1997;45:2539-2541.
15. Moghaddam AH, Nabavi SM, Nabai SF, Bigdellou R, Mohammadzadeh S, Ebrahimzadeh MA. Antioxidant, antihemolytic and nephroprotective activity of aqueous extract of *Diospyros lotus* seeds. *Acta Pol Pharm.* 2012;69:687-692.
16. Beytur A, Ciftci O, Oguz F, Oguzturk H, Yilmaz F. Montelukast attenuates side effects of cisplatin including testicular, spermatological, and hormonal damage in male rats. *Cancer Chemother Pharmacol.* 2012;69:207-213.
17. Ciftci O, Cetin A, Aydin M, Kaya K, Oguz F. Fish oil, contained in eicosapentaenoic acid and docosahexaenoic acid, attenuates testicular and spermatological damage induced by cisplatin in rats. *Andrologia.* 2014;46:1161-1168.
18. Rashed KN, Chang CW, Wu LY, Peng WH. Hepatoprotective activity of *Diospyros lotus* fruits on acute liver injury induced by carbon tetrachloride and phytochemical analysis. *Topcls J Herb Med.* 2013;2:75-83.
19. Yagi K. Simple assay for the level of total lipid peroxides in serum or plasma. *Methods Mol Biol.* 1998;108:101-106.
20. Sedlak J, Lindsay RH. Estimation of total, protein-bound, and nonprotein sulfhydryl groups in tissue with Ellman's reagent. *Anal Biochem.* 1968;25:192-205.
21. Sun Y, Oberley LW, Li Y. A simple method for clinical assay of superoxide dismutase. *Clin Chem.* 1988;34:497-500.
22. Aebi H. Catalase. In: methods of enzymatic analysis. Bergmeyer HU (ed). Academic Press, New York; 1974, pp. 673-677.
23. Paglia DE, Valentine WN. Studies on the quantitative and qualitative characterization of erythrocyte glutathione peroxidase. *J Lab Clin Med.* 1967;70:158-169.
24. Lowry OH, Rosebrough NJ, Farr AL, Randall RJ. Protein measurement with folin phenol reagent. *J Biol Chem.* 1951;193:265-275.
25. Yüce A, Ateşşahin A, Çeribaşı AO, Aksakal M. Ellagic acid prevents cisplatin-induced oxidative stress in liver and heart tissue of rats. *Basic Clin Pharmacol Toxicol.* 2007;101:345-349.
26. Yildirim NC, Kandemir FM, Ceribasi S, Ozkaraca M, Benzer F. Pomegranate seed extract attenuates chemotherapy-induced liver damage in an experimental model of rabbits. *Cell Mol Biol (Noisy-le-grand).* 2013;59 Suppl:OL1842-1847.
27. Karthikeyan K, Bai BR, Devaraj SN. Cardioprotective effect of grape seed proanthocyanidins on isoproterenol-induced myocardial injury in rats. *Int J Cardiol.* 2007;115:326-333.
28. Ateşşahin A, Çeribaşı AO, Yuce A, Bulmus O, Cikim G. Role of ellagic acid against cisplatin-induced nephrotoxicity and oxidative stress in rats. *Basic Clin Pharmacol Toxicol.* 2007;100:121-126.
29. Loizzo MR, Said A, Tundis R, Hawas UW, Rashed K, Menichini F, Ferega NG, Menichini F. Antioxidant and antiproliferative activity of *Diospyros lotus* L. extract and isolated compounds. *Plant Foods Hum Nutr.* 2009;64:264-270.
30. Azadbakhta M, Safapour S, Ahmadi A, Ghasemi M, Shokrzadeh M. Anti-diabetic effects of aqueous fruits extract of *Diospyros lotus* L. on streptozotocin-induced diabetic rats and the possible morphologic changes in the liver, kidney and heart. *J Pharmacognosy Phytother.* 2010;2:10-16.



A Combination of Virgin Coconut Oil and Extra Virgin Olive Oil Elicits Superior Protection Against Doxorubicin Cardiotoxicity in Rats

Andi Ulfiana UTARI¹, Yulia Yusrini DJABIR^{1*}, Bogie Putra PALINGGI²

¹Hasanuddin University, Faculty of Pharmacy, Department of Pharmacy, Makassar, Indonesia

²Labuang Baji Province General Hospital, Clinic of Cardiology and Vascular Medicine, Makassar, Indonesia

ABSTRACT

Objectives: The use of the chemotherapy agent doxorubicin (DOX) is associated with free radical formation that may lead to cardiotoxicity. Virgin coconut oil (VCO) and extra virgin olive oil (EVOO) are plant-based oil that is rich in antioxidants. This study examined the protective effects of VCO and EVOO combination to reduce DOX acute cardiotoxicity in rats.

Materials and Methods: Twenty-five male rats (180-200 g) were divided into the following groups: Group I as a control, group II was given DOX *i.p.* injection of 25 mg/kg body weight (b.w.), group III to V received peroral administration of either VCO, EVOO or VCO-EVOO (1:1) combination at a dose of 10 mL/kg b.w. for 6 days before receiving DOX *i.p.* injection. After 24 hours from DOX injection, blood samples and organs were collected. Cardiac biomarkers, such as serum glutamic-oxaloacetic transaminase (SGOT), lactate dehydrogenase (LDH), and creatine kinase-MB (CKMB) were analyzed followed by histopathological examination.

Results: The administration of EVOO alone was found to reduce the marked elevation of SGOT, LDH, and CKMB levels in DOX-treated rats ($p < 0.05$), while VCO administration only significantly reduced LDH and CKMB levels. However, when both oils were used in combination, the protective effect was shown to be more powerful since all cardiac biomarker levels were maintained at near-normal levels ($p < 0.05$). Histopathological analysis showed a significant improvement in the myocardial tissue structures after pre-treatment with VCO-EVOO combination.

Conclusion: The administration of VCO and EVOO in combination was superior to elicit protection against DOX-induced cardiotoxicity compared to their individual application in rats.

Key words: Doxorubicin, cardiac toxicity, virgin coconut oil, extra virgin olive oil

INTRODUCTION

Doxorubicin (DOX) is an anthracycline isolated from *Streptomyces peucetius* var. *caesius* in the 1970s.¹ DOX has been widely used for treating various malignancies, including breast and lung cancers, lymphomas, myeloma, and sarcomas.² However, clinical studies have reported approximately 3-33% of patients, who received DOX developed subclinical cardiomyopathy and some progress to congestive heart failure, even with an average cumulative dose of 300 mg/m².^{3,4}

The mechanism of DOX toxicity is mediated by the metabolic conversion of DOX to its secondary alcohol doxorubicinol.⁵ This metabolite then interacts with iron and initiates the formation

of reactive oxygen species (ROS) that subsequently damage cellular macromolecules.⁶ DOX can also form semiquinone radical intermediates that react with oxygen to produce superoxide anion radicals, which in turn produce hydrogen peroxide and hydroxyl radicals that mostly attack lipids, proteins, and DNA molecules.⁷ As a result, DOX-treated patients are at high risks of experiencing cardiotoxicity.

Bioactive compounds that can protect the heart against cardiotoxicity have been continuously pursued over the past few decades. Virgin coconut oil (VCO) and extra virgin olive oil (EVOO) are two different plant-based oils that provide health benefits to cardiac tissue and function. VCO contains

*Correspondence: yulia.yusrini@unhas.ac.id, Phone: +6282237792614, ORCID-ID: orcid.org/0000-0002-5891-7247

Received: 05.06.2021, Accepted: 26.07.2021

©Turk J Pharm Sci, Published by Galenos Publishing House.

antioxidants mostly in the form of polyphenols, which have the capability to inhibit low-density lipoprotein (LDL) oxidation in rats.⁸ In separate studies, VCO or EVOO administration increases antioxidant enzyme activities and improve the body's defense system against oxidative stress.^{9,10} Moreover, the hydroxytyrosol and oleuropein content of EVOO can act as free radical scavengers and inhibit the oxidation of LDL.¹¹ Accordingly, this study compared the cardioprotective effects of VCO, EVOO, and their combination (1:1) on DOX-induced cardiotoxicity in rats.

MATERIALS AND METHODS

Materials

VCO (Avcol®, Indonesia) and EVOO (CV. Asy Syifa, Indonesia) used in this study are registered in the Indonesian Food and Drug Administration and were purchased from a registered pharmacy. DOX HCl 50 mg/25 mL (Kalbe Farma, Indonesia) and sodium chloride (NaCl) 0.9% were obtained from a local hospital.

Animals

Male Wistar rats weighed at 180–200 g (n= 25) were procured from a laboratory animal breeder in Makassar, Indonesia. The animals were cared for in a laboratory with a 12 hour dark/light cycle and provided with food and drink daily. The animals were acclimatized to laboratory environmental conditions for 14 days before the experiment was carried out. All animal protocols were performed based on institutional guidelines for animal laboratory handling and registered under an institutional ethical clearance number of UH21020059 from the Ministry of National Education, University of Hasanuddin Faculty of Medicine, Health Research Ethics Committee.

Experimental design

A simplified scheme of the experimental protocol is illustrated in Figure 1. The rats were divided into 5 groups where each group consisted of 5 rats. Rats' blood samples (3 mL) were withdrawn before treatment initiation to provide serum biomarker baseline levels. Group I as a control group was intraperitoneally (*i.p.*) injected with 0.9% NaCl solution as a placebo, while group II was *i.p.* injected with 25 mg/kg b.w. of DOX on the 7th day of the experiment. Group III to V received pre-treatments of either VCO (10 mL/kg), EVOO (10 mL/kg), or VCO-EVOO (1:1 at 10 mL/kg dose), respectively. The oil treatment was administered using an oral cannula for 6 days, before receiving DOX *i.p.* injection on the next day. After 24 h from DOX injection, rats were anesthetized with diethyl ether, and 3 mL of blood samples were obtained from lateral veins using vacutainer tubes containing ethylenediaminetetraacetic acid. Blood samples were centrifuged (Hettich®) at a speed of 2000 rpm for 25 min. The serum was collected immediately and stored at -20°C until biomarker analysis was performed. The experimental protocols used in this study was based on Djabir et al.¹² study which also delivered a short-term pre-treatment to protect against cardiotoxicity induced by a single *i.p.* injection of DOX (25 mg/kg). A short-term pre-treatment with VCO (10 mL/kg/day) for 7 days was shown to significantly reduce paracetamol-induced hepatotoxicity.¹³ Meanwhile, pre-treatments with EVOO phytochemicals, such as oleuropein or hydroxytyrosol, for up to 7 days sufficiently elicit protection against a range of drug-induced cardiotoxicities.^{14–16}

Biomarker analysis

The levels of serum glutamic oxaloacetic transaminase (SGOT), lactate dehydrogenase (LDH), and plasma biomarker creatine kinase-MB (CKMB) were analyzed using diagnostic

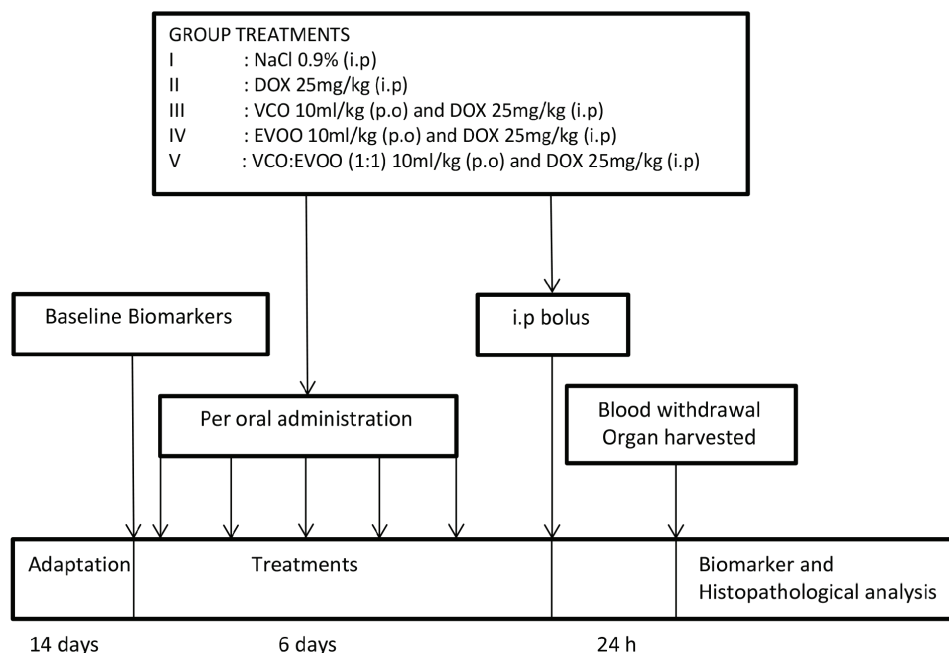


Figure 1. The scheme of experimental protocols

kits obtained from Human Diagnostic World (Germany). All analytical procedures were carried out according to the kits' instructions. The absorbance was measured using Humalyzer 3500 (Human Diagnostic World) instrumentation.

Histopathological examination

Following a blood sample collection, rats were euthanized using a cervical dislocation method. The heart was carefully removed and fixated in 10% formalin in phosphate buffer saline and embedded in paraffin blocks. Sections of 5 μ m thick were serially sliced with a microtome and stained with hematoxylin and eosin. The microscopic observation of the longitudinal section of the heart tissue was performed by a veterinary pathologist, especially in the area of the ventricles, using a light microscope (Olympus®) at 40X magnification.

Statistical analysis

The numerical data were presented as mean \pm standard error of the mean. The distribution of data normality was tested using a Shapiro-Wilk normal distribution analysis. Normally distributed data were then analyzed with One-Way ANOVA followed by a *post-hoc* Tukey's honestly significant difference test. Statistical analysis was declared significant if the *p* value was below 0.05 ($p < 0.05$).

RESULTS

Biomarker analysis

The result of cardiac biomarker analysis is illustrated in Figure 2. The healthy control did not show significant changes in the CKMB, LDH, and SGOT levels after receiving 0.9% NaCl injection as a placebo (Figure 2). However, in the DOX group, marked increases in CKMB, LDH, and SGOT levels were experienced in all rats. The CKMB, LDH, and SGOT levels of the DOX group were at least three times their baseline values, and this biomarker upsurge was detected as soon as 24 hours from DOX *i.p.* injection at a dose of 25 mg/kg b.w. ($p < 0.01$).

Apart from the DOX group, the VCO treatment group also experienced an increase in SGOT value after receiving DOX injection, which was significantly higher than the control group ($p < 0.01$). The other cardiac biomarkers, such as LDH and CKMB levels, also rose about 50% above the normal control; nevertheless, the statistical analysis did not reach a significant difference compared to the control group.

The administration of EVOO at 10 mL/kg resulted in a near-normal level of CKMB similar to the control group (298 ± 33 vs. 214 ± 40 mg/dL). However, the LDH level of the EVOO group increased twice as much as that of the normal controls (597 ± 98 vs. 218 ± 98 mg/dL); yet, it was found not statistically significant. The SGOT level also significantly increased in the EVOO group, but it was still significantly lower than that of the DOX-treated animals ($p < 0.05$). In contrast, the administration of VCO-EVOO combination prevented the increase in CKMB and LDH, resulting in normal biomarker levels. Even though the elevation of SGOT level was still experienced by the VCO-EVOO group, it was significantly attenuated compared to the DOX group ($p < 0.05$).

Histopathological examination

The normal control that was not subjected to the DOX injection showed regular cardiac myocyte shapes and structures (Figure 3A1). The bands and nucleus of cardiac myocytes and the myofibrils were clearly clear. There were barely inflammatory cells or necrotic damage found in the area of myocytes. In contrast, the DOX group experienced mild-to-moderate histopathological injuries. Histopathological changes in the heart muscle cells were evident and profound in the area of myocytes. Moderate damage was observed in most DOX-treated rats, which was characterized by hyper-eosinophilic cytoplasm and necrotic cell nuclei, myocardial cell atrophy, loss of nuclei, myolysis, infiltration of inflammatory cells, and hemorrhagic area (Figure 3B1-B3).

Figure 4 shows the representative microscopic images of cardiomyocyte histopathological changes found in rats treated with VCO, EVOO, or their combination. In the VCO-treated rats (Figure 4C1, C2), most cardiac sections showed necrotic cells

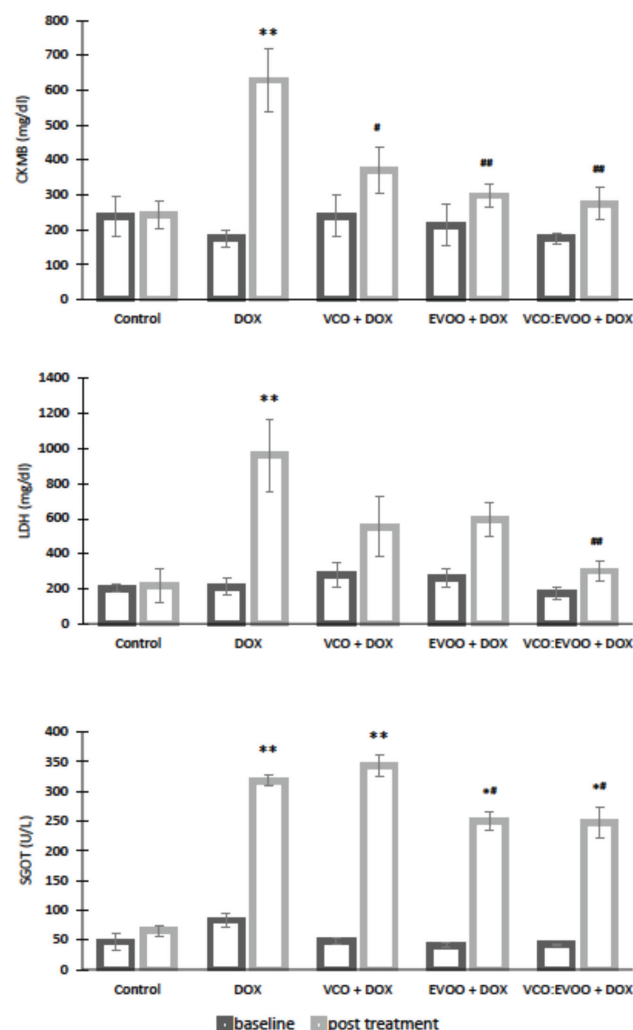


Figure 2. Comparison of creatine kinase-MB, lactate dehydrogenase, and serum glutamic-oxaloacetic transaminase levels between treatment groups at baseline and post-treatment

DOX: Doxorubicin, VCO: Virgin coconut oil, EVOO: Extra virgin olive oil

* $p = 0.05$ compared to control. $p = 0.05$ compared to DOX group

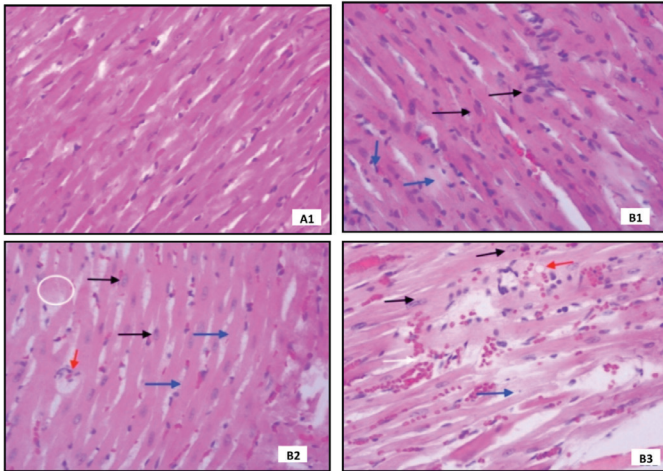


Figure 3. Representative of microscopic images of cardiac tissues in the control and DOX-treated rats. The control (A1) showed normal architecture of myocytes. cells with a normal structure with a magnification of 40X. The DOX group (B1, B2, and B3) showed necrotic cells (black arrow), myocardial muscle atrophy (blue arrow), vacuolar degeneration and hemorrhage (red arrow), and myolysis (white)

DOX: Doxorubicin

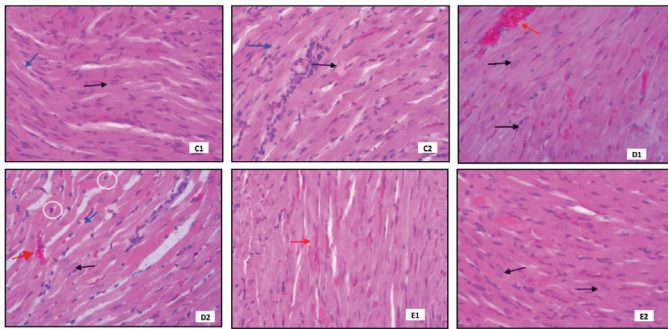


Figure 4. Representative of microscopic images of cardiac tissues in DOX treated rats that received pre-treatment with VCO (C1-2), EVOO (D1-2), and VCO-EVOO (E1-2). Necrotic myocardial cells (black arrow), muscle atrophy (blue arrow), inflammatory cells (white circle), and hemorrhagic area (red arrow)

DOX: Doxorubicin, VCO: Virgin coconut oil, EVOO: Extra virgin olive oil

and cardiomyocyte atrophy. The degree of myocardial injury was found mild to moderate (Table 1). With EVOO pre-treatment, the injection of DOX still resulted in mild-to-moderate damage, shown by the presence of necrotic cells, atrophy of cardiomyocytes, and inflammatory cells in cardiac tissue of rats (Figure 4D1, D2). Conversely, the administration of VCO and EVOO combination could reduce the presence of myocardial pathological damage. In this group, some histopathological changes were found, including hemorrhage and necrotic cells, but the degree was minimal (Figure 4E1, E2). Only two of five animals in this group had minimal myocardial damage, while the three others did not elicit myocardial injury similar to that observed in the normal controls (Table 1).

DISCUSSION

In spite of its chemotherapy benefit, the use of the DOX regimen is closely related to increased incidence of cardiotoxicity in

Table 1. Histopathological changes and scores found in each animal in the treatment groups

Groups	Rat	Histopathological changes (score)
Control	A1	None (0)
	A2	None (0)
	A3	None (0)
	A4	None (0)
	A5	None (0)
DOX	B1	Necrotic cells and atrophy of cardiomyocytes (2)
	B2	Necrotic cells, vacuolization, atrophy of cardiomyocytes, and myolysis (3)
	B3	Necrotic cells, atrophy of cardiomyocytes, vacuolar degeneration, and hemorrhage (3)
	B4	Necrotic cells, atrophy of cardiomyocytes and inflammatory cells (2)
	B5	Necrotic cells and atrophy of cardiomyocytes (2)
VCO + DOX	C1	Necrotic cells and atrophy of cardiomyocytes (2)
	C2	Necrotic cells and atrophy of cardiomyocytes (2)
	C3	Necrotic myocardial cells (1)
	C4	Cardiomyocyte degeneration and inflammatory cells (1)
	C5	Cardiomyocyte degeneration (1)
EVOO + DOX	D1	Cardiomyocyte degeneration and hemorrhage (1)
	D2	Necrotic cells, atrophy of cardiomyocytes and inflammatory cells (2)
	D3	Necrotic cells and atrophy of cardiomyocytes (2)
	D4	Cardiomyocyte degeneration and hemorrhage (1)
	D5	Necrotic cells, atrophy of cardiomyocytes and inflammatory cells (1)
VCO: EVOO + DOX	E1	Mild hemorrhage (1)
	E2	Degenerative cells (1)
	E3	None (0)
	E4	None (0)
	E5	None (0)

The level of damage was none to minimal (0), mild (1), moderate (2), and intense (3). DOX: Doxorubicin, VCO: Virgin coconut oil, EVOO: Extra virgin olive oil

cancer patients.¹⁷ Consequently, various research is imposed in the pursuit of cardioprotective agents that can impede DOX-induced toxicity, including olive oil,¹⁸ taurine,¹⁹ vitamin E,²⁰ and vitamin C.^{21,22} The progression of DOX cardiotoxicity is instigated by the formation of free radicals in the metabolic process of the chemotherapy agent, leading to impaired calcium transport in the sarcolemma, increased production of lipid peroxides, and the release of TNF-, interleukin-2, and free cytokines.²³ In this study, the administration of DOX was employed to trigger cardiotoxicity in rats. A previous study has shown that DOX *i.p.* injection (25 mg/kg) in rats was associated with increased ROS formation, myocyte necrosis, cardiomyocyte atrophy, vacuolar degeneration, and hemorrhage.¹²

In this present study, a single injection of DOX (25 mg/kg) was shown to trigger a significant elevation of cardiac injury biomarkers, demonstrating its deleterious effects on cardiac cells. Additionally, the toxic effect of DOX manifests in histopathological lesions, mostly portrayed by the presence of necrosis and atrophy of cardiomyocytes. The pre-treatment with either EVOO or VCO-EVOO combination in DOX-treated rats caused an attenuation of SGOT, LDH, and CKMB elevations. However, we found that the combination of VCO and EVOO was more effective to restore cardiac biomarkers to normal levels compared to the administration of EVOO as single preparation. Interestingly, in this study, although VCO could ease the increase of CKMB and LDH levels, it failed to improve the SGOT level in DOX-treated rats. A similar result was also depicted in the histopathological examination. It is shown that DOX-induced histological alteration was mostly improved with VCO and EVOO combination compared to VCO or EVOO alone. Indeed, the application of the oil combination before DOX injection apparently capable of preserving the normal features of cardiac muscle cells.

The health benefit of EVOO consumption has long been recognized due to the high concentration of monounsaturated fatty acids (MUFAs) content, especially oleic acid. Oleic acid increases plasma high density lipoprotein and reduce LDL cholesterol levels.²⁴ For this reason, oleic acid is expected to prevent cardiovascular disease, which is the leading cause of death in industrialized countries. Previously, several studies have shown the cardioprotective effect of olive oil on DOX-induced cardiotoxicity.^{18,25} This effect was bestowed by the antioxidative compounds contained in olive oil,¹⁰ including oleuropein and hydroxytyrosol.^{11,26} Instead of hindering anticancer activity of DOX, the antioxidant activity of EVOO was found to synergistically improve DOX effect as chemotherapy.²⁷

VCO has also been known to provide benefits in eliminating stress, weight loss, lowering cholesterol and LDL levels, maintaining blood pressures, circulatory disorders, as an immunomodulator and anti-inflammatory agent.^{28,29} Indeed, VCO's benefits on endogenous antioxidant and defense mechanism have been known for years.^{30,31} These promising effects have placed VCO as one of the virtuous candidates for cardioprotective agents. Nonetheless, apart from studies focusing on VCO's hepatoprotective, antioxidant, and

immunomodulatory effects,³²⁻³⁴ there is lack of studies that focus on VCO's cardioprotection against DOX toxicity.

In our study, it is demonstrated that VCO's cardioprotection against DOX toxicity was inferior compared to EVOO. Various studies have shown that the health benefits of EVOO are far beyond MUFA effects since EVOO is also rich in phenolic contents, tocopherol, squalene, phytosterols, triterpenoids, and β -carotene.³⁵ Compared to coconut oil, olive oil was found to be superior in reducing atherosclerotic plaque in hamsters fed with a high-fat diet.³⁶ Another study has also confirmed this result by showing better prevention of hepatic steatosis, insulin sensitivity, inflammation, and fatty acid oxidation in mice treated with olive oil compared to coconut oil.³⁷ Having said that the important finding in this present study is that EVOO's protective effects were augmented when it was combined with VCO. The combination could significantly improve cardiac injury biomarkers as well as histological features of cardiac tissues compared to EVOO alone. It is believed that by combining VCO and EVOO, the antioxidant compounds contained in both oils may work synergistically to restrain the formation of free radicals and restore the antioxidant balance. This finding necessitates future studies to further investigate the enhanced benefit of EVOO by combining it with VCO as nutraceutical, especially to provide protection against DOX-induced cardiotoxicity.

CONCLUSION

The combination of VCO and EVOO (1:1) at 10 mL/kg of rat body weight was superior to either VCO or EVOO alone in preventing the elevation of cardiac biomarker injury in DOX-treated rats. VCO and EVOO combination was found capable of recovering cardiac histopathological alteration due to acute toxicity of DOX.

ACKNOWLEDGMENTS

The authors want to thank Professor Elly Wahyudin, Professor Natsir Djide, and Yusnita Rifai, Ph.D for their valuable advice during the study.

Ethics

Ethics Committee Approval: All animal protocols were performed based on institutional guidelines for animal laboratory handling and registered under an institutional ethical clearance number of UH21020059 from the Ministry of National Education, University of Hasanuddin Faculty of Medicine, Health Research Ethics Committee.

Informed Consent: Not applicable.

Peer-review: Externally peer-reviewed.

Authorship Contributions

Concept: Y.Y.D., Design: Y.Y.D., B.P.P., Data Collection or Processing: A.U.U., Analysis or Interpretation: Y.Y.D., A.U.U., Literature Search: A.U.U., Writing: A.U.U., Y.Y.D., B.P.P.

Conflict of Interest: No conflict of interest was declared by the authors.

Financial Disclosure: The authors declared that this study received no financial support.

REFERENCES

- Thorn CF, Oshiro C, Marsh S, Hernandez-Boussard T, McLeod H, Klein TE, Altman RB. Doxorubicin pathways: pharmacodynamics and adverse effects. *Pharmacogenet Genomics*. 2011;21:440-446.
- Borgatti A. Chemotherapy, in canine and feline gastroenterology, RJ Washabau, MJ Day, Editors. 2013, WB Saunders: Saint Louis:494-499.
- Khattry N, Malhotra P, Grover A, Sharma SC, Varma S. Doxorubicin-induced cardiotoxicity in adult Indian patients on chemotherapy. *Indian J Med Paediat Oncol*. 2009;30:9-13.
- Sandamali JAN, Hewawasam RP, Fernando MACSS, Jayatilaka KAPW, Madurawe RD, Sathananthan PP, Ekanayake U, Horadugoda J. Anthracycline-induced cardiotoxicity in breast cancer patients from Southern Sri Lanka: an echocardiographic analysis. *BioMed Res Int*. 2020;2020:1847159.
- Scully R, Miller A, Grant Y, and Lipshultz SE, Anthracycline, herceptin, and cv toxicity, in comprehensive toxicology (second edition), CA McQueen, Editor. Elsevier: Oxford. 2010;413-427.
- Schaupp CM, White CC, Merrill GF, Kavanagh TJ. Metabolism of doxorubicin to the cardiotoxic metabolite doxorubicinol is increased in a mouse model of chronic glutathione deficiency: a potential role for carbonyl reductase 3. *Chem Biol Interact*. 2015;234:154-161.
- Siraki AG, Klotz LO, and Kehrer JP, Free radicals and reactive oxygen species, in Comprehensive toxicology 3rd edition, CA McQueen, Editor. Elsevier: Oxford. 2018;262-294.
- Nurul-Iman BS, Kamisah Y, Jaarin K, Qodriyah HM. Virgin coconut oil prevents blood pressure elevation and improves endothelial functions in rats fed with repeatedly heated palm oil. *Evid Based Complement Alternat Med*. 2013;2013:629329.
- Arunima S, Rajamohan T. Effect of virgin coconut oil enriched diet on the antioxidant status and paraoxonase 1 activity in ameliorating the oxidative stress in rats - a comparative study. *Food Funct*. 2013;4:1402-1409.
- Rus A, Molina F, Ramos MM, Martínez-Ramírez MJ, Del Moral ML. Extra virgin olive oil improves oxidative stress, functional capacity, and health-related psychological status in patients with fibromyalgia: a preliminary study. *Biol Res Nurs*. 2017;19:106-115.
- Umeno A, Takashima M, Murotomi K, Nakajima Y, Koike T, Matsuo T, Yoshida Y. Radical-scavenging activity and antioxidative effects of olive leaf components oleuropein and hydroxytyrosol in comparison with homovanillic alcohol. *J Oleo Sci*. 2015;64:793-800.
- Djabir YY, Arsyad MA, Sartini S, Lallo S. Potential roles of *Kleinhovia hospita* L. leaf extract in reducing doxorubicin acute hepatic, cardiac and renal toxicities in rats. *Pharmacogn Res*. 2017;9:168-173.
- Zakaria ZA, Rofiee MS, Somchit MN, Zuraini A, Sulaiman MR, Teh LK, Salleh MZ, Long K. Hepatoprotective activity of dried- and fermented-processed virgin coconut oil. *Evid Based Complement Alternat Med*. 2011;2011:142739.
- Çömez MS, Cellat M, Özkan H, Borazan Y, Aydın T, Gökçek İ, Türk E, Güvenç M, Çakır A, Özsoy ŞY. Protective effect of oleuropein on ketamine-induced cardiotoxicity in rats. *Naunyn Schmiedeberg's Arch Pharmacol*. 2020;393:1691-1699.
- Mnafgui K, Hajji R, Derbali F, Khelif I, Kraiem F, Ellefi H, Elfeki A, Allouche N, Gharsallah N. Protective effect of hydroxytyrosol against cardiac remodeling after isoproterenol-induced myocardial infarction in rat. *Cardiovasc Toxicol*. 2016;16:147-155.
- Andreadou I, Sigala F, Iliodromitis EK, Papaefthimiou M, Sigalas C, Aligiannis N, Savvari P, Gorgoulis V, Papalabros E, Kremastinos DT. Acute doxorubicin cardiotoxicity is successfully treated with the phytochemical oleuropein through suppression of oxidative and nitrosative stress. *J Mol Cell Cardiol*. 2007;42:549-558.
- Nagy AC, GulAcsi-BARDOS P, CserEp Z, Hangody L, Forster T. Late cardiac effect of anthracycline therapy in physically active breast cancer survivors - a prospective study. *Neoplasma*. 2017;64:92-100.
- Kumral A, Giriş M, Soluk-Tekkeşin M, Olgaç V, Doğru-Abbasoğlu S, Türkoğlu Ü, Uysal M. Effect of olive leaf extract treatment on doxorubicin-induced cardiac, hepatic and renal toxicity in rats. *Pathophysiology*. 2015;22:117-123.
- Samadi M, Haghi-Aminjan H, Sattari M, Hooshangi Shayesteh MR, Bameri B, Armandeh M, Naddafi M, Eghbal MA, Abdollahi M. The role of taurine on chemotherapy-induced cardiotoxicity: a systematic review of non-clinical study. *Life Sci*. 2021;265:118813.
- Kumral A, Giriş M, Soluk-Tekkeşin M, Olgaç V, Doğru-Abbasoğlu S, Türkoğlu Ü, Uysal M. Beneficial effects of carnosine and carnosine plus vitamin E treatments on doxorubicin-induced oxidative stress and cardiac, hepatic, and renal toxicity in rats. *Hum Exp Toxicol*. 2016;35:635-643.
- Ludke A, Sharma AK, Bagchi AK, Singal PK. Subcellular basis of vitamin C protection against doxorubicin-induced changes in rat cardiomyocytes. *Mol Cell Biochem*. 2012;360:215-224.
- Djabir YY, Usmar U, Wahyudin E, Mamada SS, Hamka IRN, Putri DPS, Amalia I. Roles of vitamin C and vitamin E on doxorubicin-induced renal and liver toxicity in rats. *Nusantara Med Sci J*. 2016;1:16-23.
- Angsutararux P, Luanpitpong S, Issaragrisil S. Chemotherapy-induced cardiotoxicity: overview of the roles of oxidative stress. *Oxid Med Cell Longev*. 2015;2015:795602.
- Jimenez-Lopez C, Carpena M, Lourenço-Lopes C, Gallardo-Gomez M, Lorenzo JM, Barba FJ, Prieto MA, Simal-Gandara J. Bioactive compounds and quality of extra virgin olive oil. *Foods*. 2020;9:1014.
- AlMalki WH, Shahid I. Characterization of antihypertensive and cardioprotective effects of extra virgin olive oil against doxorubicin induced cardiomyopathy in rats. *J Pharm Pharmacogn Res*. 2020;8:316-326.
- Omar SH. Oleuropein in olive and its pharmacological effects. *Sci Pharm*. 2010;78:133-154.
- El-Kammar H, Ghazy SE. Synergistic effect of combined treatment with extra virgin olive oil and doxorubicin on squamous cell carcinoma cell line. *Egypt Dent J*. 2018;64:3407-3416.
- Ma ZF, Lee YY. Virgin coconut oil and its cardiovascular health benefits. *Nat Prod Commun*. 2016;11:1151-1152.
- Babu AS, Veluswamy SK, Arena R, Guazzi M, Lavie CJ. Virgin coconut oil and its potential cardioprotective effects. *Postgrad Med*. 2014;126:76-83.
- Famurewa AC, Ekeleme-Egedigwe CA, Nwali SC, Agbo NN, Obi JN, Ezechukwu GC. Dietary supplementation with virgin coconut oil improves lipid profile and hepatic antioxidant status and has potential benefits on cardiovascular risk indices in normal rats. *J Diet Suppl*. 2018;15:330-342.
- Nevin KG, Rajamohan T. Beneficial effects of virgin coconut oil on lipid parameters and *in vitro* LDL oxidation. *Clin Biochem*. 2004;37:830-835.

32. Silalahi J, Rosidah Y, Satria D. Virgin coconut oil modulates tCD4+ and tCD8+ cell profile of doxorubicin-induced immune-suppressed rats. *Biomed Pharmacother.* 2010;64:579-581.
33. Mustika M, Fachrial E, Girsang E, Lister INE. Effect of virgin coconut oil toward antioxidant endogen and stress oxidative on rats induced doxorubicin. In 2020 3rd International Conference on Mechanical, Electronics, Computer, and Industrial Technology (MECnIT). 2020. IEEE.
34. Girsang E, Nasution AN, Lister INE. Comparison hepatoprotective effect of virgin coconut oil and *Curcuma longa* Linn against doxorubicin induced hepatotoxicity in wistar rat. In 2020 3rd International Conference on Mechanical, Electronics, Computer, and Industrial Technology (MECnIT). 2020. IEEE.
35. Silenzi A, Giovannini C, Scazzocchio B, Vari R, D'Archivio M, Santangelo C, Masella R. Extra virgin olive oil polyphenols: biological properties and antioxidant activity, in Pathology, VR Preedy, Editor. Academic Press. 2020;225-233.
36. Mangiapane EH, McAteer MA, Benson GM, White DA, Salter AM. Modulation of the regression of atherosclerosis in the hamster by dietary lipids: comparison of coconut oil and olive oil. *Br J Nutr.* 1999;82:401-409.
37. López-Salazar V, Tapia MS, Tobón-Cornejo S, Díaz D, Alemán-Escondrillas G, Granados-Portillo O, Noriega L, Tovar AR, Torres N. Consumption of soybean or olive oil at recommended concentrations increased the intestinal microbiota diversity and insulin sensitivity and prevented fatty liver compared to the effects of coconut oil. *J Nutr Biochem.* 2021;94:108751.



Phytochemical, Histochemical and *In Vitro* Antimicrobial Study of Various Solvent Extracts of *Costus speciosus* (J. Koenig) Sm. and *Costus pictus* D. Don

✉ Sana Saffiruddin SHAIKH*, ✉ Abubakar Salam BAWAZIR, ✉ Barrawaz Aateka YAHYA

Y.B. Chavan College of Pharmacy, Dr. Rafiq Zakaria Campus, Department of Quality Assurance, Aurangabad, India

ABSTRACT

Objectives: Costaceae family comprises many ornamental and medicinal plants used for different diseases. This investigation includes the phytochemical, histochemical, and *in vitro* antimicrobial study of *Costus speciosus* (J. Koenig) Sm. and *C. pictus* D. Don.

Materials and Methods: Solvents such as methanol, ethyl acetate, and hexane were used to extract the leaves and rhizomes of both plants. The antibacterial study was executed using the agar well diffusion technique.

Results: Phytochemical study confirmed that alkaloids, flavonoids, quinones, and saponins were present in solvent extracts of both plants. The macromorphological studies including size, shape, texture, surface characters, and color, were analyzed. *Salmonella typhi*, *Bacillus subtilis*, *Escherichia coli*, *Pseudomonas aeruginosa*, and *Staphylococcus aureus* were used for the antibacterial study. Agar well diffusion and agar disk diffusion methods were performed to determine the susceptibility of bacterial strains to various extracts of these plants.

Conclusion: Histochemical analysis revealed alkaloids, proteins, and phenols in the vascular bundles, the cortex, and epidermis of stem, root, and leaves of the plants. Inhibition zones caused by the methanol and hexane extracts showed better antibacterial activity compared to those of other extracts. Future work on the isolation, purification, and characterization of the active constituents and the elucidation of possible mechanisms can be executed.

Key words: Costaceae, *Costus pictus*, *Costus speciosus*, histochemical, antibacterial activity

INTRODUCTION

Plants have been used as medicine since the start of the human race.¹ These medicines were initially used as poultices, tinctures, teas, powders, etc.² Medicinal plants are familiar sources of medicine. Substantial evidence can be cited favoring herbs being used to treat diseases and restoring and fortifying body systems in the ancient systems of medicines such as Ayurvedic, Unani, and Chinese traditional medicine.³ Antimicrobial activity is one of the most eyed usefulness in the field of herbal medicines. A measurement of determination of antibacterial activity is zone of inhibition. There is a proportionate relationship between the zone of inhibition and antibacterial activity.⁴ Many plants have shown a profound antimicrobial activity. The family of Zingiberaceae comprises about 1300 species and 52 genera spread all over Asia, tropical Africa, and the Americas.⁵ In a

country like India, the plant propagates in the sub-Himalayan region, central India, Maharashtra, Karnataka, and Kerala.⁶ The *Costus* spp. from the family Costaceae are commonly grown as medicinal and ornamental plants.^{7,8} The *Costus* spp. additionally used as a dietary supplement to manage many diseases throughout the world.⁹ *Costus speciosus* (CS), commonly known as crepe ginger,¹⁰ is an essential plant grown in India.¹¹ The name CS was changed recently to *Hellenia speciosa* (J. Koenig ex Smith) S. Dutta.^{12,13} The pharmacological activities reported for CS are antioxidant, antibacterial, analgesic, anti-cholinergic activity, antidiabetic, anti-inflammatory, antidiuretic, antifungal, larvicidal, estrogenic activities, and anti-stress.^{14,15} *Costus pictus* (CP) is another ornamental plant from the family of Costaceae. CP is also known as fiery *Costus*, insulin plant, spiral flag, and step ladder.^{16,17} The rhizome and leaves show antidiuretic,

*Correspondence: sana.shaikh310194@gmail.com, Phone: +7769898161, ORCID-ID: orcid.org/0000-0001-8517-7531

Received: 21.05.2021, Accepted: 31.07.2021

©Turk J Pharm Sci, Published by Galenos Publishing House.

bacterial, anti-anthelmintic, and antitumor activities.¹⁸ It also possesses hypoglycemic and anti-inflammatory action.^{19,20} The main purpose of the current study was to conduct phytochemical and histochemical analysis and evaluate the antibacterial activity of various solvent extracts of CS and CP on selected bacterial pathogens.

MATERIALS AND METHODS

Analytical-grade chemicals such as hexane, methanol, ethyl acetate, and nutrient agar were procured from Sigma-Aldrich, Germany. Other chemicals such as phloroglucinol, safranin were obtained from Loba Chemie, Sudan red III and iodine from Qualigens Fine Chemicals. Other chemicals such as sulfuric acid, hydrochloric acid, sodium hydroxide, ferric chloride, ammonium hydroxide, and acetic acid were also used.

Collection, identification, and authentication of plant materials

Healthy plants of CS and CP were collected from Usha nursery, Mallapuram district, Kerala. Both the plants have deposited video accession number 722 and 723 in the Herbarium, Department of Botany Dr. Babasaheb Ambedkar Marathwada University, Aurangabad, Maharashtra, India. The fresh leaves²¹ from the plant's CP while the rhizome of CS²² was collected, washed thoroughly, and shade dried. The sample was powdered using a laboratory mixer grinder at high speed for 5 min and was stored in a tightly-closed container for one day before being used for analysis.

Preparation of the plant extracts

Aqueous extraction: Preparation of the extracts was done by the following method. 2 g of powdered material was extracted with 50 mL of water by the maceration process. The mixture was filtered with Whatman filter paper. The filtered solution was reduced to one-fourth of its original volume (50 mL) by vacuum in a rota-evaporator at 40°C to a constant weight until the volume reached a concentration of 160 mg/mL. The solution obtained was autoclaved at 121°C and 15lb pressure and stored at 4°C for further studies.²³

Solvent extraction (cold maceration)

The dried and powdered materials from the rhizome and leaves (2 g) were weighed accurately. The powder was macerated separately with ethyl acetate, hexane, and methanol sequentially with occasional stirring for 48 h.²⁴ The mixture was filtered and then reduced to one-fourth volume at 40°C with rota-evaporator and stored for further studies.^{25,26}

Macro-morphological study

Macroscopic observation of the plant was carried out.^{27,28} Qualitative analysis was performed on the basis of morphological and sensory properties such as size, shape, texture, surface characteristics, taste, color, odor, etc., was recorded.²⁹⁻³¹

Histochemical study

Freehand sections of leaves, stem, rhizome and root materials were taken and treated with the respective reagent to localize the chemical constituents in the tissues. The stained sections were compared with the fresh unstained sections. The sections

were mounted on a slide to be observed under a compound microscope. The mounted sections were observed under the compound microscope and were studied for various phytochemicals such as alkaloids, phenols, tannins, proteins, etc.³²⁻³⁴

Physicochemical tests

Various parameters such as total ash value, acid insoluble ash, water-soluble ash, sulfated ash, moisture content (loss on drying), water content, foreign organic matter, and extractive values (methanol, hexane, ethyl acetate, and water) were studied.³⁵⁻³⁷

Phytochemical screening:

a. Test for tannins: To about 2-3 mL extract, 2-3 drops of 5% FeCl₃ solution. With the formation of green or bluish-black color, the presence of tannins is indicated.³⁸

b. Test for saponins (Foam formation test): To about 2 to 3 mL extract, 5 mL de-ionized water was added. Vigorous shaking resulted in persistent foam formation. It was allowed to stand for 15 min and kept for honeycomb froth, which shows saponins.³⁹

c. Test for flavonoids (Shinoda test): To 1 mL extract, a few magnesium ribbon fragments and 4-5 drops of conc. HCl was added. The presence of flavonoids is confirmed by the formation of the pink or red.⁴⁰

d. Test for terpenoids (Salkowski test): In 0.5 mL extract, 2 mL chloroform along with conc. H₂SO₄ was added. The red-brown color at the interface indicates terpenoids.⁴¹

e. Test for carbohydrates (Molisch's test): 1 mL extract in addition to 1 mL of conc. H₂SO₄, gives a red to violet zone, which is visible at the interphase of the oil-water layers. The presence of carbohydrates and glycosides is indicated.⁴²

f. The test for anthraquinone (Bontrager's test): To 1 mL of extract, 5 mL benzene was added. Further, it was shaken and filtered. 5 mL of ammonium hydroxide (10%) was added, followed by shaking the contents. A red, pink, or violet in the lower ammoniacal phase confirms the presence of anthraquinones.⁴³

g. Test for cardiac glycosides (Keller-Kiliani test): A mixture of 2 mL of acetic acid added with 1-2 drops of 2% ferric chloride solution was mixed with 1 mL extract. This mixture was then introduced into another test tube that had 2 mL conc. H₂SO₄. The appearance of a brownish-colored ring at the interphase and cardiac glycosides are indicated in the sample.⁴⁴

h. Test for coumarins: A test tube was made with filter paper moistened in dilute NaOH, about 1 mL of sample extract was taken. The sample was heated for 3-5 min. Further, the filter paper was examined under ultraviolet (365 nm) for yellow-colored fluorescence, which confirms the test for coumarins.⁴⁵

i. Test for steroids (Liebermann-Burchard test): About 2 mL of acetic acid was added to 1 mL extract. After cooling the solution on an ice bath, conc. H₂SO₄ was added carefully. The development of violet to blue or bluish-green color confirms the test for steroids.⁴⁶

j. Test for alkaloids: In 1 mL extract, 2 mL of 1% HCl was added, and the solution was heated. Further, 4 to 5 drops of Mayer's

reagent was added. A precipitate white or cream in color formation confirms the test for alkaloids.⁴⁷

Antimicrobial activity studies

Microorganisms

Reference bacterial strains were obtained from the Master of Science Department of Maulana Azad College, Dr. Rafiq Zakaria Campus, Aurangabad (MS.), India. The strains comprise of *Bacillus subtilis* (ATCC 19659), *Staphylococcus aureus* (ATCC 6538), *Pseudomonas aeruginosa* (ATCC 9027), *Escherichia coli* (ATCC 8739), and *Salmonella typhi* (ATCC 14028). The bacterial isolates were kept at 4°C on an agar slant. The sample was sub-cultured for 24 h in nutrient agar at 37°C before any susceptibility test.⁴⁸

Media preparation

About 23 g of nutrient agar was dissolved in distilled water (1000 mL). The mixture was autoclaved for 15 min at 121°C. Further, it was left to cool at room temperature. After cooling (about 45°C), it was transferred into petri dishes. Each petri dish was left to cool for about 30-35 min until completely set.⁴⁹⁻⁵¹

Agar disk diffusion method

Each bacterial sample was spread on sterile agar plates using a clean and pre-sterilized cotton swab. Pre-calibrated Whatman filter paper disks of about 5 mm in diameter and 2.5 µL infused capacity was prepared and sterilized. Each disk was infused with different crude extracts of concentration 40 mg/disk and then sited on bacterial pre-swabbed agar plates. Streptomycin was used as a positive control. The samples were allowed to diffuse at RT for 30 min. The diffused petri plates were kept for incubation at 35 ± 0.5°C for 24 h. After incubation, the microbial growth was determined by measuring the diameter (mm) for inhibition zones.⁵²⁻⁵⁴

Agar well diffusion test

Each bacterial inoculum was swabbed on the sterile agar plate using a clean and a sterilized cotton swab. Wells of about 7 mm in diameter with 50 µL capacity were made into the agar plates. The initial concentration of crude extract used for the agar well diffusion method was 40 mg/mL. Due to the higher concentration of the crude extract, it was found that the zones of inhibition merged with each other. Henceforth, the concentration of the crude extracts was reduced to 20 mg/mL. Positive control (PC) (streptomycin) 30 µg/µL, negative control (various solvent extracts), and sample solution (all crude extracts) were added to each well and allowed to diffuse for 30 min at RT. Plates were incubated for 24 h at 35 ± 0.5°C to determine the inhibition zones (mm) as a measure of antibacterial activity.^{55,56} No statistical analysis was carried out in this study.

RESULTS

Macro-morphological study

Costus speciosus: CS is an erect succulent herb up to 3 m in height. The leaves are elliptical to oblong-lanceolate silky beneath, subsessile, thick spirally arranged with stem-clasping

sheaths up to 4 cm. The rhizome of CS is tuberous, having 10-15 cm length and 1-3 cm diameter. Rhizomes are usually sub-cylindrical unbranched and covered with a brownish epidermis or cork. Small circular scars of about 2 - 4 mm in diameter are present on the upper and lower surfaces at specific intervals. Flowers are white, large, thick, cone-like terminal spikes, with bright red stripes, lips with the yellowish throat; red capsules, fruits globose trigonous, the diameter of about 2 cm, black colored seeds, with white aril. The upper surface was marked with nodal scars circular with a residue of leaf bases, lower and lateral surfaces exhibited small circular spots of roots, or few thin rootlets fractured fibrous and fractured yellowish-brown surface. Stems nearly woody at base, unbranched, spirally twisted in the upper part. No characteristics of taste or odor (Figure 1).

CP is a perennial herb. Typically, multi-trunked or clumping stems. The stems hirsute and green near the apex, glabrous and purple toward the base, with spiral light green leaves and airy, the tissue paper-like flowers are yellow with orange-red stripes. The leaves are alternate, simple, entire, smooth surface, pinnate parallel venation, conspicuously ligulate (red-colored) large fresh-looking spirally arranged, and oblong-lanceolate being dark green above when mature, and lighter green below. The leaf's shape is narrowly elliptical with a length of 10 to 25 cm and a width up to 6 cm. The leaves have a characteristic taste and odor (Figure 2).

Histochemical study

Histochemical studies help in the determination of chemical constituents in the cells and tissues. The method can identify cellular components such as carbohydrates, proteins, nucleic acids, lipids, etc.^{57,58} Thin sections of leaves, roots, rhizomes, and stem were taken. Further, the sections were stained using various stains, such as Sudan red III, iodine, phloroglucinol, and ferric chloride. The transverse section of rhizome leaves and stems of the plants show fibrovascular bundles. Plants are monocot commends (Figure 3). The leaves and stem show epidermis bearing simple, unignified, thick-walled trichome unicellular, simple, and multicellular glandular with pointed apex; central vascular bundles closed system with collenchyma on both sides. Leaves are dorsiventral on the upper epidermis. Parenchymatous cells encircle the vascular bundles in the presence of starch grains. Phytochemicals such as phenols, alkaloids, and proteins were found to be present in the epidermal tissue, the cortex, and vascular bundles of the root, stem, and leaves. The stem shows scattered lignified vascular bundles, thin-walled unignified collenchyma, uniseriate multicellular trichome central vascular pith primary xylem. Rhizomes are monocot with cortex showing scattered vascular bundle, thin-walled parenchymatous cells. The roots show wide vessel parenchymatous thin corks with thin-walled medulla. Central cork/pith in the epidermal region brownish with the presence of fibrous vascular bundles scattered. The primary xylem toward the center shows brownish content in the cell. The cortex is occupied in 2/3 portion surrounded by the thin-walled parenchymatous cell (Figure 4).

Physiochemical and phytochemical tests

As there is an increase in antibiotic resistance in various diseases, the alternative system medicine can be of interest. Many plants contain phytochemicals with antimicrobial properties, which could play a crucial role in therapeutic treatments.⁵⁹ The physiochemical properties such as organoleptic properties, ash value, extractive values, moisture content, foreign organic matter, and swelling index are given (Table 1). The aqueous, methanolic, ethyl acetate, and hexane extracts (HE) (Table 2) show various compounds identified. The different tests indicated alkaloids, flavonoids, quinones, and saponins. The crude extracts from leaf and rhizome samples of CP and CS did show a positive test for terpenoids and steroids. The methanolic crude extract showed a positive test for tannins. HE from both plants show chemicals like steroids, alkaloids, flavonoids, and triterpenoids, while saponins and tannins were absent. Ethyl acetate crude extract from both plants showed a negative test for saponins, while CP ethyl acetate extract indicated the presence of alkaloids.

Antimicrobial activity studies

The investigational study for antibacterial activity against various pathogenic bacterial strains using the agar disk diffusion technique was conducted. The disk diffusion method was used only for qualitative evaluation of antibacterial activity for respective crude extracts. Optimization of the

antibacterial activity was carried out by using the agar well diffusion test.

Table 2. Phytochemical constituent of plants *Costus speciosus* and *Costus pictus*

Chemical constituent	<i>Costus speciosus</i>				<i>Costus pictus</i>			
	AE	ME	EAE	HE	AE	ME	EAE	HE
Tannins	-	+	-	-	-	-	-	-
Saponins	+	+	-	-	+	+	-	-
Flavonoids	+	-	-	-	+	+	+	+
Quinones	+	+	+	+	+	+	+	+
Glycosides	-	+	+	+	+	+	+	+
Cardiac glycosides	+	+	+	+	+	+	+	+
Carbohydrates	-	+	+	+	-	+	+	+
Terpenoids	-	+	+	+	+	+	+	+
Phenols	+	+	-	-	+	+	+	+
Coumarins	+	+	-	-	+	+	+	+
Steroids	+	+	-	-	+	+	+	+
Alkaloids	-	+	-	-	+	+	+	+

AE: Aqueous extract, ME: Methanolic extract, HE: Hexane extract, EAE: Ethyl acetate extract

Table 1. Physiochemical test results for *Costus speciosus* and *Costus pictus*

Tests	Results	
	<i>Costus speciosus</i> (rhizome)	<i>Costus pictus</i> (leaves)
1- Organoleptic properties		
a) Appearance	Buff colored powder	Light green powder
b) Color	Buff brown	Light green
c) Odor	No characteristic odor	Characteristic odor
d) Taste	No taste	Sour in taste
e) pH	7.4 ± 0.06	6.5 ± 0.08
2- Moisture content (%)	4.5 ± 0.32	10.155 ± 0.032
3- Ash value (%)	-	-
a) Total ash value	4.5 ± 0.5	14.29 ± 0.15
b) Acid insoluble ash value	0.932 ± 0.03	3.20 ± 0.060
c) Water soluble ash value	1.58 ± 0.07	8.70 ± 0.012
4- Foreign organic matter (%)	0.7 ± 0.04	0.07 ± 0.063
5- Extractive values (%)	-	-
a) Methanol	8.74 ± 0.99	17 ± 0.03
b) Ethyl acetate	5.32 ± 0.63	7.60 ± 0.02
c) Hexane	2.06 ± 0.02	6.50 ± 0.03
d) Aqueous	7.34 ± 0.63	10.25 ± 0.07
6- Swelling index	Initial (mL) 3.5 ± 0.32 Final (mL) 5.6 ± 0.13	Initial (mL) 2.5 ± 0.20 Final (mL) 6.5 ± 0.130

Agar disk diffusion method

The different solvent extracts for CS had a lower to negligible effect based on the agar disk diffusion method. However, the marketed extract of CS was highly effective against various bacterial strains. The solvent extracts of CP had an efficient antibacterial activity; however, the marketed extract shows a lesser activity comparatively. Concluding the overall results, the marketed extract of CS and different solvent crude extracts of CP was used for the agar well diffusion method. The zone of inhibition obtained for the agar disk diffusion technique is shown in (Table 3). The graphical representation of the zone of inhibition achieved using the agar disk diffusion technique is shown (Figure 5).

Agar well diffusion test

The methanolic extract (ME) showed the highest inhibition against *E. coli*. In contrast, the hexane and ethyl acetate extracts displayed comparatively low activity. A potential antibacterial activity was exerted by the hexane extract and ME against *S. aureus* with inhibition zones of 38 and 17 mm, respectively (Figure 6). However, the ethyl acetate extract showed comparatively lower activity (9 mm). The standard extract showed maximum activity against *B. subtilis*. While the hexane, ethyl acetate, and methanolic extracts, caused comparatively lower activity. Against *P. aeruginosa*, the HE shows the highest activity, while the ME, reference and ethyl acetate extract show comparatively lesser activity. The best antibacterial activity against *S. typhi* was observed with the ME comparatively with other extracts (Table 4). The aqueous extract indicated a mild activity against *S. typhi*, while no activity was recorded against other bacterial pathogens tested. The graphical representation of the inhibition zones achieved using the agar well diffusion method is shown at Figure 7.



Figure 1. *Costus speciosus* (A) flowers (B) rhizomes (C) whole plant of *C. speciosus*

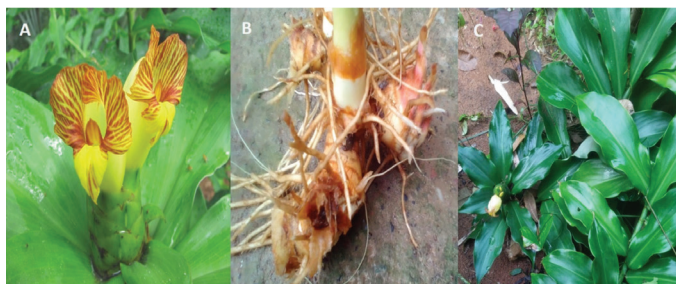


Figure 2. *Costus pictus* (A) flowers (B) roots (C) whole plant of *C. pictus*

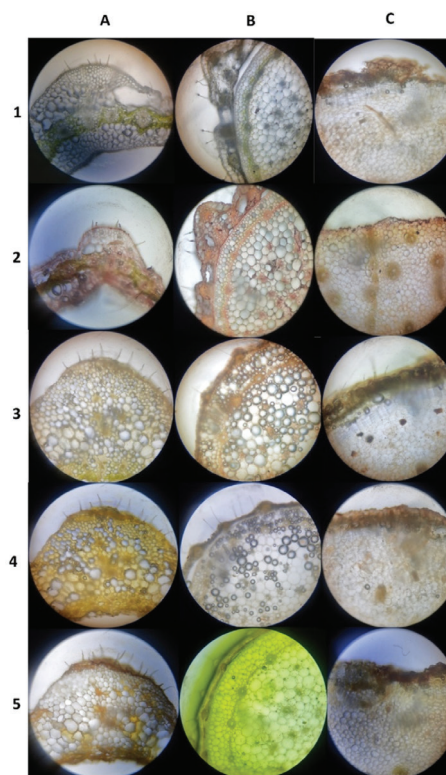


Figure 3. Histochemical studies on (A) leaves (B) stem (C) rhizome of *Costus speciosus* (1) unstained section (2) test for fixed oils, volatile oils (3) test for lignified tissues (4) test for proteins (5) test for phenols

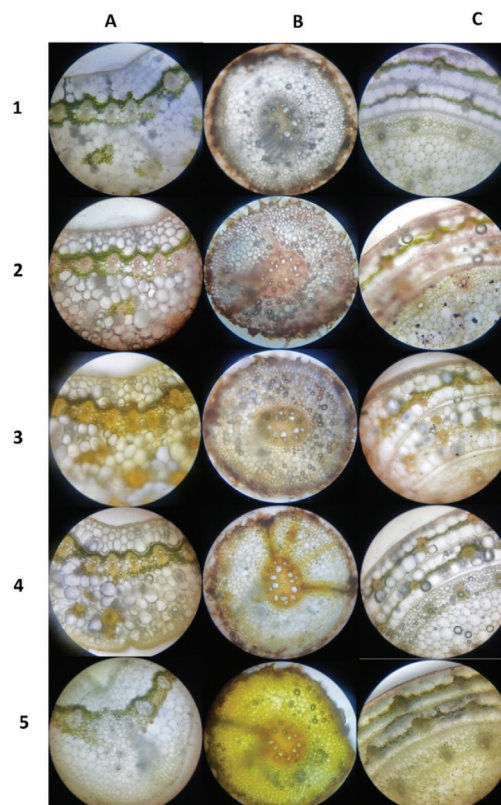


Figure 4. Histochemical studies on (A) leaves (B) roots (C) stem of *Costus pictus* (1) unstained section (2) test for fixed oils, volatile oils (3) test for lignified tissues (4) test for proteins (5) test for phenols

Table 3. Disc diffusion method results

Microorganism	Zone of inhibition (in mm)											
	<i>Costus speciosus</i>						<i>Costus pictus</i>					
	PC ^a	AE ^b	ME ^c	HE ^d	EAE ^e	SE ^f	PC	AE	ME	HE	EAE	SE
<i>Staphylococcus aureus</i>	33	-	-	5	-	12	33	-	-	-	11	12
<i>Bacillus subtilis</i>	30	-	-	-	-	15	3	-	80	-	12	13
<i>Pseudomonas aeruginosa</i>	28	-	-	-	-	18	25	-	70	-	10	1
<i>Escherichia coli</i>	26	-	-	-	-	9	26	-	80	-	80	9
<i>Salmonella typhi</i>	-	-	-	-	-	9	-	-	14	60	60	9

^aPC: Positive control, ^bAE: Aqueous extract, ^cME: Methanolic extract, ^dHE: Hexane extract, ^eEAE: Ethyl acetate extract, ^fSE: Standard extract

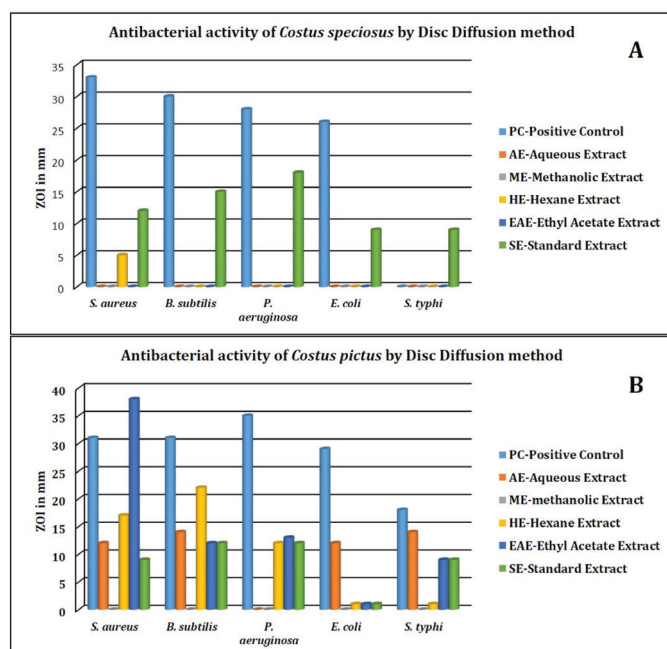
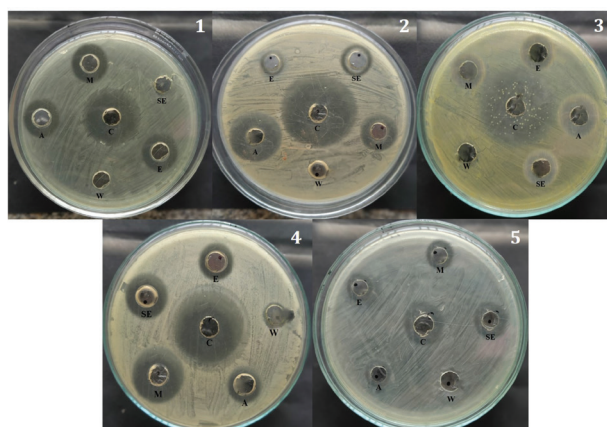


Figure 5. Graphical representation of the zone of inhibition achieved by disc diffusion method

Figure 6. Zone of inhibition for agar well diffusion (1) *Escherichia coli* (2) *Pseudomonas aeruginosa* (3) *Staphylococcus aureus* (4) *Salmonella typhi* (5) *Bacillus subtilis*

A: Hexane extract, C: Positive control, E: Ethyl acetate extract, M: Methanolic extract, SE: Standard extract, W: Aqueous extract

Table 4. Agar well diffusion method results

Microorganism	Zone of inhibition (mm)					
	PC ^a	<i>Costus speciosus</i> (SE ^f)	<i>Costus pictus</i>			
			AE ^b	ME ^c	HE ^d	EAE ^e
<i>Staphylococcus aureus</i>	31	12	-	17	38	9
<i>Bacillus subtilis</i>	31	14	-	22	12	12
<i>Pseudomonas aeruginosa</i>	35	12	-	12	13	12
<i>Escherichia coli</i>	29	-	-	11	10	10
<i>Salmonella typhi</i>	18	14	-	10	9	9

^aPC: Positive control, ^bAE: Aqueous extract, ^cME: Methanolic extract, ^dHE: Hexane extract, ^eEAE: Ethyl acetate extract, ^fSE: Standard extract

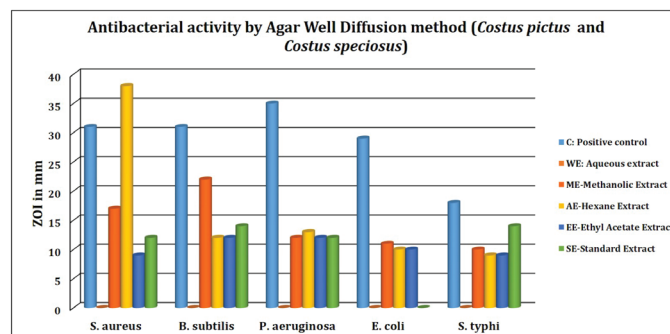


Figure 7. Graphical representation of the zone of inhibition achieved by agar well diffusion method

DISCUSSION

The histochemical and phytochemicals investigation of CS and CP reveals alkaloids, phenols, proteins, saponins, tannins, anthraquinones, and flavonoids. The literature⁶⁰⁻⁶² reveals that presence of these phytochemicals is responsible for having curative activity against several microbes. Therefore, CS and CP extracts were evaluated for antimicrobial activity and ensuring promising results as antimicrobial agents (Tables 3, 4). The comparative study carried out gives an idea about the antibacterial potential of the plant crude extracts. The standard and crude extracts show inhibitory activity against the examined

bacterial strains. *B. subtilis* was found to be more resistant compared with other bacterial strains, while *P. aeruginosa* and *S. typhi* were found to be more susceptible toward the crude and standard extracts. The negative control used in the study does not show any markable antibacterial activity against the selected pathogenic strains. Extracts of both plants that showed inhibition zone diameters of >10 mm were considered active. In according to this, both extracts are better antibacterial agents and, therefore, using these plants as antibacterial agents has been validated.

CONCLUSION

The pharmacognostic study of CS and CP gave important information concerning the morphology of crude drugs. They can be used for the authentication of CS and CP among all *Costus* spp. The adulteration and purity of these drugs can also be determined. The microscopic character, physicochemical, and phytochemical screening parameter studies help set standards for these crude drugs. Significantly, fewer data was available on the histochemical study of both the plants CS and CP; henceforth, it was carried out elaboratively. Histochemical studies revealed alkaloids, flavonoids, carbohydrates, and terpenoids in the leaf, stem, and roots. The phytochemical screening study also confirmed chemical components such as alkaloids, flavonoids, carbohydrates, phenols, glycosides, and terpenoids. Up to date, the antibacterial potential and comparative study against specified bacterial pathogens were not reported. Besides this, the novelty of the current work is to differentiate the activity between Gram-positive and Gram-negative bacterial strains. The potential increase of 2 folds in the antibacterial activity for HE (CP) against *S. aureus* was observed, however, ME (CP) shows an equivalent activity as PC. The result indicates that both plants show potential antibacterial activity ensuring bioactive compounds useful in primary healthcare. Further work is needed on the isolation, characterization, and purification of the active constituents and understanding the possible mechanism of action as an antibacterial agent.

Ethics

Ethics Committee Approval: No Ethics Committee approval required.

Informed Consent: Not applicable.

Peer-review: Externally peer-reviewed.

Authorship Contributions

Concept: A.S.B., Design: A.S.B., Data Collection or Processing: S.S.S., Analysis or Interpretation: B.A.Y., Literature Search: S.S.S., B.A.Y., Writing: S.S.S.

Conflict of Interest: No conflict of interest was declared by the authors.

Financial Disclosure: The authors declared that this study received no financial support.

REFERENCES

- Samuelsson G, Drugs of Natural Origin: A Textbook of Pharmacognosy, 5th Swedish Pharmaceutical Press, Stockholm. ISBN:91-9743-184-2. 2004 DOI: <https://doi.org/10.1021/np0582291>.
- Balunas MJ, Kinghorn AD. Drug discovery from medicinal plants. *Life Sci*. 2005;78:431-441.
- Shahzad Aslam M, Syarhabil Ahmad M. Worldwide importance of medicinal plants: current and historical perspectives. *Rec Adv Biol Med*. 2016;2:88-93.
- Cowan MM. Plant products as antimicrobial agents. *Clin Microbiol Rev*. 1999;12:564-582.
- Jiang K, Delin W, Larsen K. Zingiberaceae. *Flora China*. 2000;24:322377.
- Katoriya VS, Deokar G, Kshirsagar S, Rupvate S. A review on medicinal boon: *Costus* species. *Int J Inst Pharm Life Sci*. 2016;6:60-77.
- Rani Sabitha A, Sulakshana G, Patna S. *Costus speciosus*, an antidiabetic plant-review. *FS J Pharm Res*. 2012;1:52-53.
- Kala C, Salman Ali S, Chaudhary S. Comparative pharmacognostical evaluation of *Costus speciosus* (wild ginger) and *Zingiber officinale* (ginger) rhizome. *Int J Curr Pharm Res*. 2016;819-823.
- Sheikh BY. The role of prophetic medicine in the management of diabetes mellitus: a review of literature. *J Taibah Univ Med Sci*. 2016;11:339-352.
- El-Far AH, Shaheen HM, Alsenosy AW, El-Sayed YS, Al Jaouni SK, Mousa SA. *Costus speciosus*: traditional uses, phytochemistry, and therapeutic potentials. *Pharmacognosy Rev*. 2018;12:120-127.
- Pawar VA, Pawar PR. *Costus speciosus*: an important medicinal plant. *Int J Sci Res*. 2014;3:28-33.
- Govaerts R, Hellenia Retz. The correct name for *Cheilocostus* C.D. specht (Costaceae). *Phytotaxa*. 2013;151:63-64.
- Randall RP. A global compendium of weeds. (3rd ed). Perth, Western Australia; 2017. <https://www.cabi.org/isc/FullTextPDF/2017/20173071957.pdf>
- Waisundara VY, Watawana MI, Jayawardena SN. *Costus speciosus* and *Coccinia grandis*: traditional medicinal remedies for diabetes. *S Afr J Bot*. 2015;98:1-5.
- Malabadi RB, Meti NT, Mulgund G, Nataraja K. Synthesis of silver nanoparticles from *in vitro* derived plants and callus cultures of *Costus speciosus* (Koen); assessment of antibacterial activity. *Res Plant Biol*. 2012;2:32-42.
- Radha Devi GM. A comprehensive review on *Costus pictus* D. Don. *Int J Pharm Sci Res*. 2019;10:3187-3195.
- Shiny CT, Palni LMS. Taxonomic, molecular and physiological evaluation of *Costus pictus* D. Don plants originally obtained from different parts of Kerala, India. *J Appl Fund Sci*. 2016.
- Saju T, Devi BS. Phytochemical and *in vitro* anthelmintic studies of hydro-alcoholic extract of *Costus pictus* D. DON. *Int J Pharmacy Pharm Sci*. 2013;494:639-641.
- Remya R, Daniel M. Phytochemical and pharmacognostic investigation of anti-diabetic *Costus pictus*. D. Don. *Int J Phar Biomed Res*. 2012;3:30-39.
- Srivastava S, Singh P, Mishra G, Jha KK. *Costus speciosus* (Keukand): a review. *Der Pharm Sin*. 2011;2:118-128.
- Shiny CT, Saxena A, Gupta SP. Phytochemical and hypoglycaemic activity investigation of *Costus pictus* plants from Kerala and Tamilnadu. *Int J Pharm Sci Invent*. 2013;2:11-18.
- Chen U, Hussani S, Mazumder T, Uddin SMN, Banik S. Neuropharmacological evaluation of methanolic extract of *Costus speciosus* Linn. rhizome in Swiss Albino mice. *Asian Pac J Trop Biomed*. 2019;9:217-221.
- Parekh J, Chanda S. Antibacterial and phytochemical studies on twelve species of Indian medicinal plants. *Afr J Biomed Res*. 2007;10:175-181.
- Harborne AJ. Phytochemical methods a guide to modern techniques of plant analysis, (3rd ed). Chapman and Hall; 1998.

25. Shiny CT, Saxena A, Gupta SP. Phytochemical investigation of the insulin plant "*Costus pictus*" D. Don. *Int J Pharm Biomed Res.* 2013;4:97-104.
26. Behera A, Supriya Devi R, Pradhan S, Biswal S, Kumar Jena P, Biswal SK, Kumar S. Phytochemical analysis and antioxidant potential of *Costus speciosus* L. *Eur J Med Plants.* 2020;31:64-72.
27. Aruna A, Nandhini R, Karthikeyan V, Bose P, Jegadeesh S, Vijayalakshmi K. Insulin plant (*Costus pictus*) leaves: pharmacognostical standardization and phytochemical evaluation. *Am J Pharm Health Res.* 2014;2:106-119.
28. Bhogonkar PY, Devarkar VD, Lande SK. Physical characterization of *Costus speciosus* (Koenig ex Retz.) Smith - a well known ayurvedic drug plant. *Life Sci Leaflets.* 2012;11:1-9.
29. Khandelwal KR. Practical pharmacognosy, technique and experiments. (19th ed). Nirali Prakashan; 2008:259.
30. Kumar D, Gupta J, Kumar S, Arya R, Kumar T, Gupta A. Pharmacognostic evaluation of *Cayratia trifolia* (Linn.) leaf. *Asian Pac J Trop Biomed.* 2012;2:6-10.
31. Naik A, Krishnamurthy R, Janardan P. Comparative physicochemical and phytochemical evaluation for insulin plant-*Costus pictus* D. Don accessions. *Int J Appl Ayurved Res.* 2017;3:420-426.
32. Matias LJ, Mercadante-Simões MO, Royo VA, Ribeiro LM, Santos AC, Fonseca JMS. Structure and histochemistry of medicinal species of *Solanum*. *Rev Bras Farmacogn.* 2016;26:147-160.
33. Sushma BK, Ashalatha KS, Ray P, Raveesha HR. Histochemical and phytochemical analysis of medicinally important plants. *Eur J Med Plants.* 2019;30:1-13.
34. Souza DMF, Sá RD, Araújo EL, Randau KP. Anatomical, phytochemical and histochemical study of *Solidago chilensis* Meyen. *An Acad Bras Cienc.* 2018;90(Suppl 1):2107-2120.
35. Musila MF, Dossaji SF, Nguta JM, Lukhoba CW, Munyao JM. *In vivo* antimalarial activity, toxicity and phytochemical screening of selected antimalarial plants. *J Ethnopharmacol.* 2013;146:557-561.
36. Al-Daihan S, Al-Faham M, Al-shawi N, Almayman R, Brnawi A, Zargar S, Shafi Bhat R. Antibacterial activity and phytochemical screening of some medicinal plants commonly used in Saudi Arabia against selected pathogenic microorganisms. *J King Saud Univ Sci.* 2013;25:115-120.
37. Tuama AA, Mohammed AA. Phytochemical screening and *in vitro* antibacterial and anticancer activities of the aqueous extract of *Cucumis sativus*. *Saudi J Biol Sci.* 2019;26:600-604.
38. Ciulei I. Practical manual on the industrial utilization of medicinal and aromatic plants. Romania; Bucharest; 1982:1-62.
39. Auwal MS, Saka S, Mairiga IA, Sanda KA, Shuaibu A, Ibrahim A. Preliminary phytochemical and elemental analysis of aqueous and fractionated pod extracts of *Acacia nilotica* (Thorn mimosa). *Vet Res Forum.* 2014;5:95-100.
40. Yadav RNS, Agarwala M. Phytochemical analysis of some medicinal plants. *J Phytol.* 2011;3:10-14.
41. Khodja NK, Makhlof LB, Madani K. Phytochemical screening of antioxidant and antibacterial activities of methanolic extracts of some Lamiaceae. *Ind Crops Prod.* 2014;61:41-48.
42. Maggi F, Ferretti G, Pocceschi N, Menghini L, Ricciuti M. Morphological, histochemical and phytochemical investigation of the genus *Hypericum* of the Central Italy. *Fitoterapia* 2004;75:702-711.
43. Usman H, Abdulrahman F, Usman A. Qualitative phytochemical screening and *in vitro* antimicrobial effects of methanol stem bark extract of *Ficus thonningii* (Moraceae). *Afr J Tradit Complement Altern Med.* 2009;6:289-295.
44. Naz R, Bano A. Phytochemical screening, antioxidants and antimicrobial potential of *Lantana camara* in different solvents. *Asian Pac J Trop Dis.* 2013;3:480-486.
45. Pathan RK, Gali PR, Pathan P, Gowtham T, Pasupuleti S. *In vitro* antimicrobial activity of *Citrus aurantifolia* and its phytochemical screening. *Asian Pac J Trop Dis.* 2012;(Suppl 1):328-331.
46. Ali Alabri TH, Al Musalami AHS, Hossain MA, Afaf MW, Al-Riyami Q. Comparative study of phytochemical screening, antioxidant and antimicrobial capacities of fresh and dry leaves crude plant extracts of *Datura metel* L. *J King Saud Univ Sci.* 2014;26:237-243.
47. Saraf A. Phytochemical and antimicrobial studies of medicinal plant *Costus speciosus* (Koen.). *EJ Chemistry.* 2010;7:405-413.
48. Mahasneh AM, El-Oqlah AA. Antimicrobial activity of extracts of herbal plants used in the traditional medicine of Jordan. *J Ethnopharmacol.* 1999;64:271-276.
49. Arunprasad A, Gomathinayagam M. Qualitative study of *Costus speciosus* (Koen ex. Retz.) Sm. and its potentiality against human pathogenic microbes. *Int J Pharm Biol Sci Arch.* 2014;5:93-98.
50. Kaur GJ, Arora DS. Antibacterial and phytochemical screening of *Anethum graveolens*, *Foeniculum vulgare* and *Trachyspermum ammi*. *BMC Complement Altern Med.* 2009;9:30.
51. Asfere Y, Kebede A, Zinabu D. *In-vitro* antimicrobial activities and phytochemical screening of selected plant extracts against some medically and agriculturally important pathogens. *European J Med Plants.* 2020;31:167-189.
52. Singha PK, Roy S, Dey S. Antimicrobial activity of *Andrographis paniculata*. *Fitoterapia.* 2003;74:692-694.
53. Duraipandian V, Al-Harbi NA, Ignacimuthu S, Muthukumar C. Antimicrobial activity of sesquiterpene lactones isolated from traditional medicinal plant, *Costus speciosus* (Koen ex.Retz.) Sm. *BMC Complement Altern Med.* 2012;12:13.
54. Pochapski MT, Fosquiera EC, Esmerino LA, Dos Santos EB, Farago PV, Santos FA, Groppo FC. Phytochemical screening, antioxidant, and antimicrobial activities of the crude leaves' extract from *Ipomoea batatas* (L.) Lam. *Pharmacogn Mag.* 2011;7:165-170.
55. Khayyat S, Al-Kattan MO. Phytochemical screening and antimicrobial activities of *Costus speciosus* and Sea Qust. *Biomed Res.* 2017;28:389-393.
56. Vinicius CK, Vale FHA. Leaf histochemistry analysis of four medicinal species from Cerrado. *Rev Bras Farmacogn.* 2016;26:673-678. doi: <http://dx.doi.org/10.1016/j.bjp.2016.05.015>.
57. Dhale DA. Histochemical investigation of some medicinal plants. *Adv Res Pharm Biol.* 2011;1:147-154.
58. El Amine Dib M, Allali H, Bendiabdellah A, Meliani N, Tabti B. Antimicrobial activity and phytochemical screening of *Arbutus unedo* L. *J Saudi Chemical Society* 2013;17:381-385.
59. Vaidya M, Shingadia H. Antimicrobial activity of *Costus speciosus* (J. Koieng) Sm. *World J Pharm Res.* 2020;9:959-963.
60. Prabhu S, Puneeth, Rao Priyadarshini, Narayana SKK, Basaviah R. Comparative phytochemical and antioxidant properties of *Costus pictus* and *C. speciosus*, *J Ayu Med Sci.* 2017;2:121-128.
61. Meshram PV, Moregaonkar SD, Gatne MM, Gaikwad RV, Zende RJ, Ingole SD, Vanage GR. Physicochemical and phytochemical screening of aqueous and ethanolic extracts of *Costus pictus* D. Don and *Enicostema littorale* Blum. *Chem Sci Rev Lett.* 2017;6:426-434.



Formulation and Development of Aqueous Film Coating for Moisture Protection of Hygroscopic *Herniaria glabra* L. Tablets

✉ Hakim EL MABROUKI*, ✉ Irina Evgenievna KAUKHOVA

Saint-Petersburg State Chemical Pharmaceutical University, Department of Industrial Technology of Drugs, Saint-Petersburg, Russia

ABSTRACT

Objectives: The present study aims to develop a moisture-protective coating solution and use it to film coat hygroscopic *Herniaria glabra* L. tablets.

Materials and Methods: Five coating formulations were developed and applied on *H. glabra* core tablets in a fluidized-bed coating. The film-coated tablets were evaluated by appearance, percentage of moisture gain, disintegration time, and percent of drug release. Physicochemical properties and stability during storage of the best obtained coated tablets were studied.

Results: The results of this study showed that the film coating F5 containing 25% hydroxypropyl methyl cellulose (HPMC), 20% shellac, 10% polyethylene glycol (PEG) 1500, 29.6% PEG 4000, 5% tween 80, 10% titanium dioxide, and 0.4% acid red 2 offered good protection for coated tablets against moisture. Coated tablets showed physical and dissolution stability during storage.

Conclusion: A combination of hydrophilic polymer HPMC and hydrophobic polymer shellac is suitable for balancing moisture-protective properties and attaining the fast release of drugs. This study could make it worthwhile to develop a pharmaceutical moisture barrier film coating system for immediate release tablets. However, more studies will be needed to evaluate the moisture-resistant film further.

Key words: HPMC, shellac, moisture protection, coating, *Herniaria glabra* tablets

INTRODUCTION

Tablets are the most popular dosage form of the drugs in use today. However, tablets may contain moisture-sensitive active pharmaceutical ingredients (APIs). The stability of API in tablets during their shelf life is necessary to ensure its effectiveness. Thus, absorbing moisture can cause hydrolysis and oxidation, which conduct to the degradation of the active substances and consequently decrease in therapeutic efficiency of the medicine.¹ Therefore, the most suitable is to protect the core tablets with a moisture protective film that could efficiently prevent water vapor from attaining the cores and hence prevent the hydrolytic degradation of API.^{2,3}

Moisture protective films are used for protection from moisture and improve physical appearance, mechanical resistance, and masking unpleasant odors and tastes.⁴

A perfect coating film should exhibit various qualities to attain the function of the moisture barrier. Thus, the coating film

should be uniform and smooth and guarantee the stability of the drug during the shelf life. Such a coating film should also possess an adequate thickness and low permeability to water vapor.⁵

The use of the coating film with water-soluble polymers has seen great success in recent years due to the drawbacks of organic solvents (toxicity, pollution, and explosion hazards) utilized in water-insoluble polymers.^{6,7} Therefore, water-soluble polymers, including hydroxypropyl methyl cellulose (HPMC), hydroxyethyl cellulose, and polyvinyl alcohol, are widely used in moisture barrier coating.⁸

A coating film formed with entero-soluble polymers, such as shellac polymer, could efficiently provide moisture protection and enteric functionalities due to their insolubility at acidic and neutral pH.^{9,10} Shellac polymer can be used in coating film to achieve enteric applications, immediate-release properties, taste masking, and seal coating.

*Correspondence: hakimelmabrouki@yahoo.fr, Phone: +7 (812) 234 57 20/+7 (812) 234 60 41, ORCID-ID: orcid.org/0000-0002-2826-3609

Received: 19.03.2021, Accepted: 02.08.2021

©Turk J Pharm Sci, Published by Galenos Publishing House.

Different methods have been developed to test the moisture uptake of drugs. The most common method is to measure the weight increase of the dosages at various constant temperature and humidity conditions. Therefore, both uncoated and coated pharmaceutical dosages are investigated for their moisture uptake at these various humidity conditions created by a saturated salt.

Tablets containing *Herniaria glabra* L. extract, potassium citrate, and sodium citrate were developed in a laboratory to study their diuretic and antilithiasic effect.¹¹⁻¹³ However, studies have shown that obtained tablets are moisture sensitives. Thus, absorbing moisture can cause degradation of the active substances and consequently reduce their therapeutic efficacy.

The objective of this study was to develop moisture barrier films based on HPMC and shellac polymers, to film coat hygroscopic *H. glabra* core tablets, and evaluate the moisture barrier properties of the films at different humidity conditions. Drug release of the coated tablets was investigated. In addition, the stability of the coated tablets during storage was also evaluated.

MATERIALS AND METHODS

Chemicals and reagents

H. glabra was supplied by herbs Morocco (Rabat, Morocco); potassium citrate, sodium citrate, shellac, lactose monohydrate, calcium stearate, tween 80, and titanium dioxide were provided by Merck (Darmstadt, Germany); HPMC 6FC was obtained from Dow Chemical Company (Midland, MI, USA); polyethylene glycol (PEG) 1500 and PEG 4000 was provided by Stepan Company (Northfield, USA), while stearic acid was received from Tianjin Damao Chemical Reagent Factory (Tianjin, China); acid red 2 was supplied by Spectrum Chemical (New Brunswick, USA).

Preparation of film-coated Herniaria glabra tablets

Preparation of saponin-rich extract of Herniaria glabra

H. glabra herb was initially defatted with petroleum ether in the Soxhlet apparatus and then extracted with ethanol 70% for 7 days by maceration.¹⁴ The obtained extract was purified from ballast and accompanying substances using the selective liquid-liquid extraction method with organic solvents (cyclohexane, chloroform, and ethyl acetate) and then precipitated in cold acetone, obtaining purified saponin-rich extract.¹⁵ The obtained extract was dried at 60°C.

Preparation of core tablet

The core tablet contains 50 mg saponin-rich extract *H. glabra*, 100 mg potassium citrate, 100 mg sodium citrate, 245 mg lactose, and 5 mg calcium stearate was obtained by wet granulation method. All the ingredients were weighed correctly and sieved through a 20 mesh sieve. Saponin-rich extract *H. glabra*, potassium citrate, and sodium citrate as drug substances and lactose monohydrate as a diluent was loaded into a Laboratory High Shear Mixer Granulator (STE Techpharm, Spain) and mixed for 5 min.¹⁶ The powder blend was granulated using purified water as granulating fluid. Purified water was sprayed

onto the powders with 3 g/min and 0.11 MPa spray air pressure. During the spraying, the impeller speed was 600 rpm. The wet granules were air-dried in the Lab Fluid Bed Dryer (STREA-1, Aeromatic Fielder, Switzerland) at an inlet temperature of 60°C for 10 min.¹⁷ The dried granules were milled through an 850 µm sieve and lubricated for 5 min with calcium stearate, and stored for compression into tablets. The tablets were compressed with a single punch machine (Korsch EK0, Germany). The average weight of the tablets was 500.0 mg.

Preparation of film-coating suspensions

Five coating formulations were developed using HPMC and shellac as film-forming agents, stearic acid, PEG 1500 and 4000 as plasticizers, tween 80 as the surfactant, titanium dioxide as a pigment, and acid red 2 as colorant; detailed compositions were shown in the Tables 1 and 2.

Formulation F1 contained 8% shellac, 0.6% stearic acid, 6% PEG 4000, 0.4% tween 80, 1.5% TiO₂, 0.05% acid red 2 dye, 10% ammonia 25% and 73.45% distilled water. Polymeric shellac solution was obtained by dissolving 40 g shellac polymer in a mixture of 200 mL water and 50 g 25% ammoniated aqueous solution under stirring and heating at a temperature between 50-60°C.¹⁸ The obtained polymer shellac solution was cooled to room temperature. 30 g PEG 4000, 2.0 g tween 80, and 3.0 g stearic acid were added progressively and mixed to the polymeric shellac solution until evenly dispersed. Titanium dioxide (7.5 g) was dispersed in 100 mL purified water using a magnetic stirrer for 2 hours in a separate container. The obtained shellac mixture was thoroughly mixed with titanium dioxide suspension, 0.25 g acid red 2 dye, and remaining water under stirring for 60 minutes to obtain a homogenized distribution.

Formulation F2 contained 7.5% shellac, 7.5% PEG 4000, 0.5% tween 80, 1.5% TiO₂, 0.05% acid red 2 dye, 10% ammonia 25% and 72.95% distilled water. Formulation F2 (not containing stearic acid) was prepared in the same way as F1.

Formulation F3 contained 6% HPMC, 6% PEG 4000, 0.3% tween 80, 1% TiO₂, 0.05% acid red 2 dye and 86.65% distilled water. Polymeric HPMC solution was obtained by dissolving 30.0 g HPMC polymer in 300.0 mL purified water with magnetic stirring at 80°C for 60 minutes. The obtained polymeric HPMC solution was cooled to room temperature (RT) and mixed with 30.0 g PEG 4000 and 1.5 g tween 80. In a separate container, 5.0 g titanium dioxide was dispersed in 100 mL purified water using a magnetic stirrer for 2 hours. The obtained HPMC mixture was mixed with titanium dioxide suspension, 0.25 g acid red 2 dye, and remaining water under stirring for 60 minutes to obtain a homogenized distribution.

Formulation F4 contained 2.4% shellac, 3% HPMC, 2.8% PEG 4000, 1% PEG 1500, 0.6% tween 80, 1.2% TiO₂, 0.05% acid red 2 dye, 4% ammonia 25% and 84.95% distilled water. Polymeric shellac solution (12.0 g shellac prepared in the same way as F1) was mixed with 14.0 g PEG 4000, 5.0 g PEG 1500, and 3.0 g tween 80 to obtain a homogenized shellac mixture. Polymeric HPMC solution (15.0 g HPMC prepared similarly to F3) was mixed with the shellac mixture, titanium dioxide suspension

(6.0 g TiO₂), 0.25 g acid red 2 dye, and remaining water under stirring for 60 minutes in order to obtain a homogenized distribution.

Formulation 5 contained 2.4% shellac, 3% HPMC, 3.6% PEG 4000, 1.2% PEG 1500, 0.6% tween 80, 1.2% TiO₂, 0.05% acid red 2 dye, 4% ammonia 25% and 83.95% distilled water. Formulation F5 was prepared in the same way as F4.

The coating solutions were filtered through sieve number 140, equivalent to 160 µm (ASTM E-11, Cole Parmer, USA), and stored in an airtight container.

Preparation of free films

Free films were prepared by casting polymer solution onto glass petri dishes and placed in an oven at 50°C for 24 h. Dried films were removed and cut carefully into strips with an average thickness of 200–300 µm, a width of 10 mm, and a length of 50 mm. The free film was kept in a desiccator with 50% RH

Table 1. Composition of coating solutions (w/w%)

Component	F1	F2	F3	F4	F5
Shellac	8.0	7.5	-	2.4	2.4
Stearic acid	0.6	- ^a	-	-	-
HPMC ^b 6FC	-	-	6.0	3.0	3.0
PEG ^c 4000	6.0	7.5	6.0	2.8	3.6
PEG 1500	-	-	-	1.0	1.2
Tween 80	0.4	0.5	0.3	0.6	0.6
TiO ₂	1.5	1.5	1.0	1.2	1.2
Acid red 2	0.05	0.05	0.05	0.05	0.05
Ammonia 25%	10.0	10.0	-	4.0	4.0
Distilled water	73.45	72.95	86.65	84.95	83.95

^aNone, ^bHPMC: Hydroxypropyl methyl cellulose, ^cPEG: Polyethylene glycol

at RT until mechanical analyses were performed. Mechanical properties of the films, including tensile strength and elongation at break, were evaluated by a texture analyzer (TA-XT plus, UK) using a 50 N load cell and crosshead speed of 5 mm/min.

Coating process

The coating of the tablets was carried out in a fluid bed coater (Strea-1 Aeromatic Fielder, Switzerland) and the coating parameters were as follows: Batch size 500.0 g, inlet air temperature 60°C, outlet air temperature 45°C, airflow 90 m³/h, atomizing air pressure 2.0 bar, spray rate 3 g/min, drying temperature 50°C and drying time 15 min. The tablets were coated until a weight gain of 6% w/w. The coating solution was stirred continuously during the overcoating process.

Evaluation of tablets core and coated tablets

The thickness, friability, hardness, and disintegration time of the core tablets and coated tablets were studied according to the methods described in the Russian Pharmacopoeia 14.¹⁹ The thickness was determined with a micrometer (moore and right 1965B, UK), the friability was determined with a friabilator (Erweka TA 100, Germany), the hardness was measured using a hardness tester (Erweka TBH 125, Germany) and the disintegration time was studied in distilled water (disintegration medium) at 37 ± 0.5°C using disintegration tester (Erweka ZT 120, Germany).

Dissolution test of tablets

The dissolution test was performed using the Russian Pharmacopoeia 14 paddle method.²⁰ Drug release was measured in Erweka dissolution tester (DT 720, Germany) using distilled water as the dissolution medium, maintained at 37 ± 0.5°C and agitated at 50 rpm (n= 6). The samples were withdrawn at 5, 10, 15, 20, 30, 45, and 60 min.

Drug release of saponins was determined spectrophotometrically based on the method of Hiai et al.²¹ To 0.5 mL of sample and

Table 2. Compositions of film-coating (%)

Component	F1 (%)	F2 (%)	F3 (%)	F4 (%)	F5 (%)
Shellac	48.3	44.0	- ^a	21.7	20.0
Stearic acid	3.7	-	-	-	-
HPMC ^b 6FC	-	-	45.0	27.1	25.0
PEG ^c 4000	36.3	44.0	45.0	25.3	29.6
PEG 1500	-	-	-	9.1	10.0
Tween 80	2.4	2.9	2.2	5.5	5.0
TiO ₂	9.0	8.8	7.4	10.9	10.0
Acid red 2	0.3	0.3	0.4	0.4	0.4
Ammonia 25%	* ^d	*	*	*	*
Distilled water	*	*	*	*	*
Total	100.0%	100.0%	100.0%	100.0%	100.0%

^aNone, ^bHPMC: Hydroxypropyl methyl cellulose, ^cPEG: Polyethylene glycol, ^dDistilled water and ammonia 25% are volatile components, which do not remain in the film coating

standard (escin), 0.5 mL of 8% vanillin solution. Then 5.0 mL of 72% sulfuric acid were added and mixed well in an ice water bath. The mixture was warmed in a bath at 60°C for 10 min, then cooled in water at the ambient temperature for 5 min. The absorbance of the standard and samples was measured at 560 nm using a ultraviolet 1240 spectrophotometer from Shimadzu, Japan.

Preparation of reagents: 8% (w/v) vanillin solution: 800 mg of vanillin was dissolved in 10 mL of 99.5% ethanol. Prepared freshly for each determination.

72% (v/v) sulfuric acid: To 28 mL of deionized water, 72 mL of sulfuric acid was added.

Drug release of citrates was determined using the non-aqueous acid-base titrimetry method described in European Pharmacopeia 8.²² 20 mL of sample was evaporated gently on a hot plate until dryness, then dissolved in 20 mL of anhydrous acetic acid, heating to about 50°C. It allowed cooling. 0.25 mL of naphtholbenzein solution as an indicator was added, and the solution was titrated with 0.1 N perchloric acid until a green color was obtained.

Preparation of reagents: Preparation of anhydrous acetic acid: 104 mL of acetic anhydride poured into glacial acetic acid in small portions with stirring. The acid container was left to stand for about a day.

Preparation of 0.1 N titrated perchloric acid solution in anhydrous acetic acid: Approximately 8.5 mL of 72% perchloric acid was dissolved in 100 mL of anhydrous acetic acid, about 30 mL of acetic anhydride was added in small portions with constant cooling of the solution to bind water. The bottle was closed with a cork and left for a day in a dark place, then the volume of the solution was brought to 1 liter.

Moisture uptake of tablets

Moisture uptake of the tablets was determined by placing the tablets in desiccators of 25°C/75% RH, saturated sodium chloride solution, and 25°C/91% RH, saturated potassium nitrate solution.²³ Weight gain was measured at predetermined time points.

Stability test of coated tablets

The samples of coated tablets were blister packed in aluminum using the packing machine DP-210 (Wenzhou T&D Packaging Machinery Factory, China). Stability studies were realized according to ICH guidelines.²⁴ Tests were conducted under RT

and accelerated stability conditions. The samples designed for RT were kept at 30 ± 2°C and 65 ± 5% relative humidity, while the accelerated stability samples were kept at 40 ± 2°C and 75 ± 5% RH in a humidity chamber (Binder KBF 115, Germany). The RT samples were tested at 0, 3, 6, 9, and 12 months. The accelerated stability samples were tested at 0, 1, 2, 3, and 6 months. The coated tablets were tested for their physical appearance, hardness, friability, disintegration, and dissolution during storage.

Ethics committee approval

In this study, ethics committee approval is not required.

Statistical analysis

In this study, statistical data was not used.

RESULTS AND DISCUSSION

It has been shown that coatings affect the physicochemical properties of the tablet to varying degrees and these changes are suggestive of the effect of the coating materials.^{25,26} The moisture uptake behavior of coated tablets exposed to different relative humidity conditions can be utilized to measure the ability of a film coating to protect the core tablet against moisture.²⁷ Thus, core tablets of *H. glabra* were coated using the prepared coating solutions (Tables 1, 2). The results of the tested parameters are presented in Table 3 and Figures 1-3.

For formulations F1 and F2

Tablets coated with formulation F1 (TCF1) showed an excellent physical appearance with a smooth surface. The coated tablets exhibited the best moisture protection compared to other coated tablets (moisture gain of 5.1% at 75% RH and 6.4 at 90% RH). Coated tablets' disintegration time was increased compared to core tablets (from 3 min in core tablets to 25 min in coated tablets). The dissolution profile of TCF1 showed a decrease in drug release (80.2% of saponins and 84.4% of citrates).

TCF2 also showed an excellent physical appearance and good moisture protection. Removing stearic acid from F2 has slightly decreased disintegration time (22 min) and increased dissolution of coated tablets (82.3% of saponins and 87.2% of citrates).

Free shellac films F1 and F2 presented lower tensile strength and higher elongation (Figure 1).

Interestingly, shellac-coated tablets showed the lowest moisture uptake at 75% and 90% relative humidity (Figure 2). However,

Table 3. Physicochemical properties of uncoated and coated *Herniaria glabra* tablets

Formulation	Disintegration (min)	Saponin release (%)	Citrate release (%)	Physical appearance
Tablet cores	3 ± 1	94.1 ± 1.2	96.0 ± 1.3	-
CTF1	25 ± 1	80.2 ± 1.5	84.4 ± 0.5	Smooth shiny surface
CTF2	22 ± 1	82.3 ± 0.7	87.2 ± 1.2	Smooth shiny surface
CTF3	7 ± 1	90.2 ± 1.2	93.2 ± 0.9	Signs of cracking
CTF4	15 ± 1	86.1 ± 0.9	89.3 ± 1.1	Signs of cracking
CTF5	15 ± 1	88.0 ± 1.6	90.6 ± 0.8	Smooth shiny surface

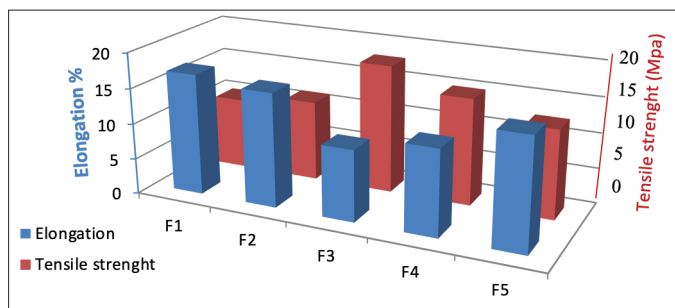


Figure 1. Tensile strength and percentage elongation of free films

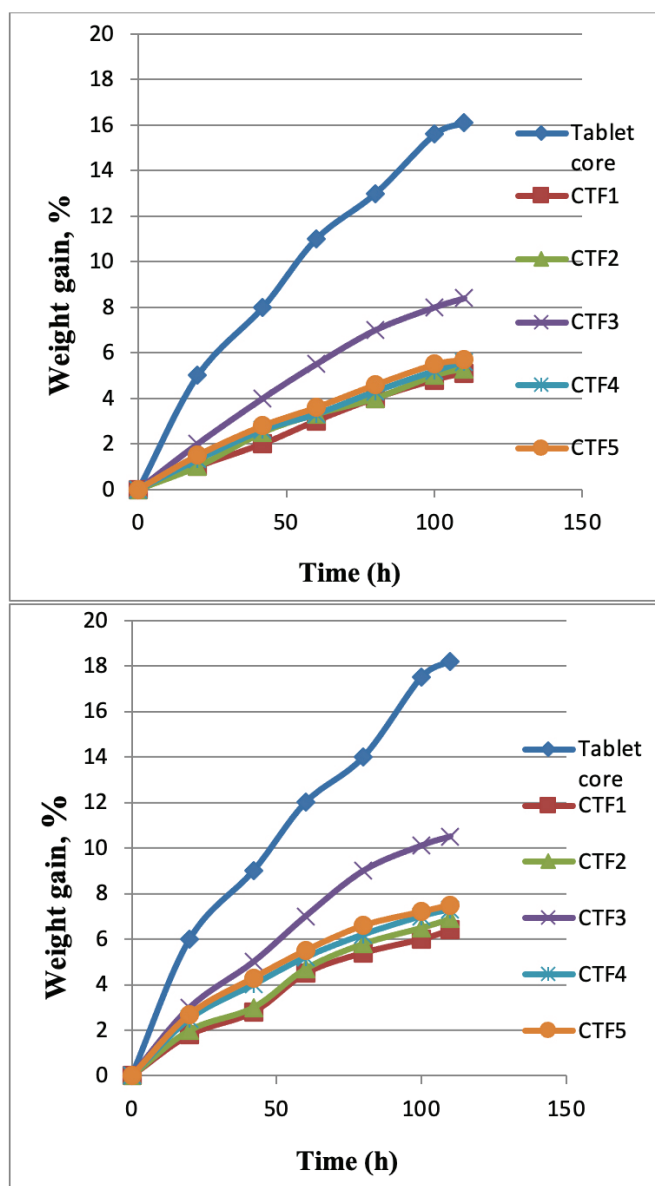


Figure 2. Percent moisture (weight) gain of coated tablets at 25°/75% RH and at 25°/90% RH

shellac coating led to a long disintegration time and reduced the resulting drug release rate considerably. Therefore, it is convincing to suggest that these findings can be attributed to shellac's poor water solubility and the hydrophobic character of

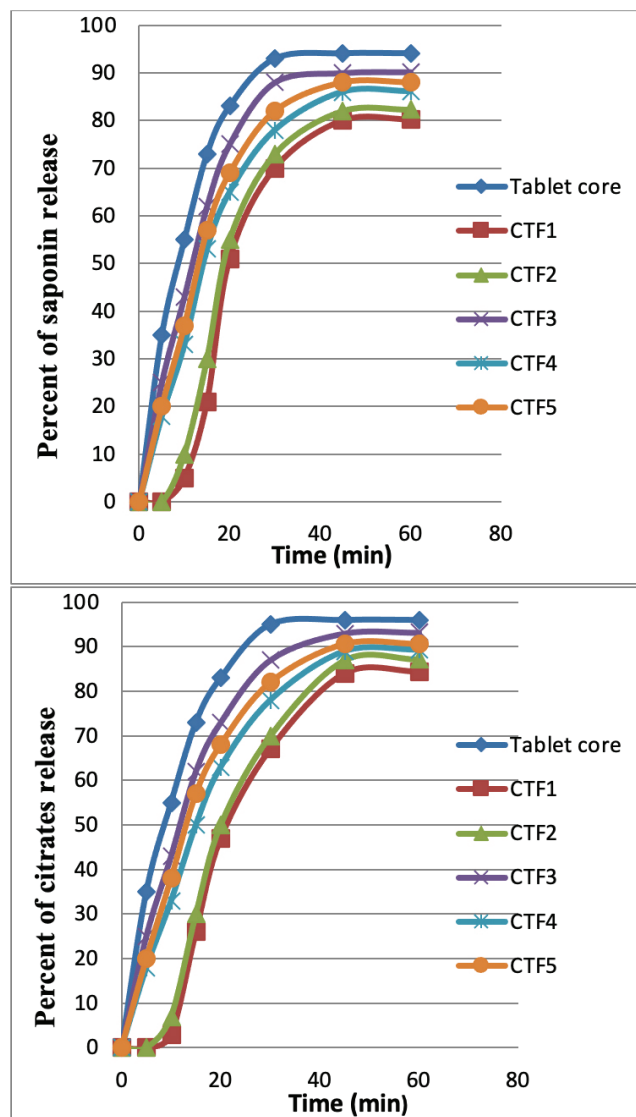


Figure 3. Drug release of *H. glabra*-coated tablets with different coating solutions (F1, F2, F3, F4, and F5)

the stearic acid (in F1), which have led to the form of a coating film with low permeability.²⁸⁻³⁰

For formulation F3

TCF3 showed the shortest disintegration time (7 min) and exhibited the best drug release (90.2% of saponins and 93.1% of citrates) in comparison to other coated tablets. However, coated tablets manifested high moisture uptake (moisture gain of 8.4% at 75% RH and 10.5% at 90% RH) and showed signs of cracking.

Therefore, the tablets coated with HPMC film showed higher moisture uptake than tablets coated with shellac film, indicating that HPMC has a lower potential for moisture protection than shellac. This is a result of the hydrophilic nature of the HPMC film. Then, the HPMC polymer, a hydrocolloid, absorbs water molecules due to hydrogen bonding with water molecules and itself. As a result, when the film is exposed to water/moisture, it tends to allow a water vapor permeability.³¹

For formulations F4 and F5

TCF4 showed lower water uptake rates than HPMC-coated tablets (moisture gain 5.6% at 75% RH and 7.3% at 90% RH). The disintegration time of TCF4 was reduced (15 min) in comparison to HPMC-coated tablets. The dissolution profile of TCF4 showed an increase in drug release (86.1% of saponins and 89.3% of citrates) in comparison to HPMC-coated tablets. However, TCF4 has shown signs of cracking attributed to a lack of plasticizer concentration in film.

Increasing concentrations of plasticizers, 1.2% PEG 1500 and 3.6% PEG 4000 in coating solution F5 (10% PEG 1500 and 29.6% PEG 4000 in film coating F5), have disappeared and well-coated tablets (TCF5) with smooth surfaces were obtained. Increasing the number of plasticizers has also led to a decrease in tensile strength and increased percent elongation (Figure 1). TCF5 showed a low moisture uptake. Thus, the weight gain was decreased from 16.1% of core tablets to 5.7% of TCF5 at 75% RH and from 18.2% of core tablets to 7.5% of TCF5 at 90% RH.

In the shellac-HPMC composite film, shellac is a hydrophobic component that repels water molecules from forming a bond

due to its hydrophobicity and hence reduces the permeability of water vapor through the composite film.^{32,33}

TCF5 showed a satisfactory disintegration time within 15 min, and drug release achieved 88% of saponins and 90.6% of citrates which complied with the Russian dissolution requirements.

Therefore, the combination of 3% HPMC and 2.4% shellac in coating solution (25% HPMC and 29.6% shellac in film coating) has led to good protection for coated tablets against moisture and provided satisfactory dissolution.

According to these findings, the formulation F5 showed the most satisfactory results and was selected as an optimized formulation after comparative evaluation.

The properties of uncoated and coated tablets can be seen in Table 4. TCF5 showed a slight increase in hardness and a decrease in friability. The tablets' weight variation also decreased, which is indicative of the excellent coating uniformity provided by the fluid bed process. The disintegration time was increased from 3 min (core) to 15 min. From the results, uncoated and coated tablets showed suitable characteristics which complied with the Russian Pharmacopoeia 14.

Stability studies

TCF5 was stored in a stability chamber with controlled temperature and humidity to study their stability. Thus, physicochemical properties were studied. The results are shown in Table 5.

Long-term and accelerated stability studies showed no major change in physical characteristics, hardness, friability, and disintegration of coated tablets. Drug release was within acceptable limits and complied with the Russian dissolution requirements. Thus, TCF5 was stable under stability testing conditions.

CONCLUSION

Hydrophilic polymer HPMC and hydrophobic polymer shellac are suitable for balancing moisture-protective properties and

Table 4. Physicochemical properties of uncoated and film-coating *Herniaria glabra* tablets CTF5

	Uncoated	CTF5
Average weight of tablet (mg)	500.0 ± 1.7	530.0 ± 0.8
Diameter (mm)	11.0 ± 0.4	11.5 ± 0.5
Thickness (mm)	3.11 ± 0.12	3.35 ± 0.14
Hardness (n)	12.1 ± 0.8	12.4 ± 0.7
Friability (%)	0.15	0.12
Disintegration time (min)	3 ± 1	15 ± 1
Saponin content (%)	94.1 ± 1.2	88.0 ± 1.6
Citrate content (%)	96.0 ± 1.3	90.6 ± 0.8

Table 5. Stability testing of *Herniaria glabra* coated tablets at room temperature and under accelerated conditions

	Period (month)	Physical characteristics (pink tablet)	Hardness (n)	Friability (%)	Disintegration (min)	Saponin release (%)	Citrate release (%)
CTF5 at room temperature	0	Appropriate	12.4 ± 0.8	0.10 ± 0.12	15 ± 1	88.0 ± 1.6	90.6 ± 0.8
	3	Appropriate	12.4 ± 0.6	0.10 ± 0.11	15 ± 1	88.0 ± 1.0	90.6 ± 1.2
	6	Appropriate	12.3 ± 0.4	0.11 ± 0.09	15 ± 1	87.9 ± 1.1	90.5 ± 1.3
	9	Appropriate	12.2 ± 0.3	0.13 ± 0.08	15 ± 1	87.8 ± 1.5	90.3 ± 0.9
	12	Appropriate	12.2 ± 0.9	0.14 ± 0.14	15 ± 1	87.6 ± 0.9	90.1 ± 1.1
CTF5 under accelerated conditions	0	Appropriate	12.4 ± 0.8	0.10 ± 0.12	15 ± 1	88.0 ± 1.6	90.6 ± 0.8
	1	Appropriate	12.3 ± 0.5	0.11 ± 0.13	15 ± 1	87.9 ± 1.2	90.4 ± 1.4
	2	Appropriate	12.3 ± 0.7	0.12 ± 0.07	15 ± 1	87.8 ± 1.5	90.2 ± 1.2
	3	Appropriate	12.2 ± 0.6	0.12 ± 0.12	15 ± 1	87.6 ± 1.4	90.1 ± 0.8
	6	Appropriate	12.1 ± 0.9	0.14 ± 0.15	15 ± 1	87.3 ± 0.7	89.9 ± 1.5

attaining fast-release drugs. The results of this study showed that formulation of film coating containing 25% HPMC and 20% shellac as film-forming agent, 10% PEG 1500 and 29.6% PEG 4000 as plasticizers, 5% tween 80 as a surfactant, 10% titanium dioxide as pigment and 0.4% acid red 2 as colorant offered good protection for coated *H. glabra* tablets against moisture. Moreover, coated tablets showed physical and dissolution stability during storage. This study could make it worthwhile to develop a pharmaceutical moisture barrier film coating system for immediate release tablets. However, more studies will be needed to evaluate the moisture-resistant film further.

Ethics

Ethics Committee Approval: Approval is not required for this study.

Informed Consent: Informed consent is not required for this study.

Peer-review: Externally peer-reviewed.

Authorship Contributions

Concept: H.E.M., I.E.K., Design: H.E.M., Data Collection or Processing: H.E.M., Analysis or Interpretation: H.E.M., I.E.K., Literature Search: H.E.M., Writing: H.E.M.

Conflict of Interest: No conflict of interest was declared by the authors.

Financial Disclosure: The authors declared that this study received no financial support.

REFERENCES

- Joshi S, Petereit HU. Film coatings for taste masking and moisture protection. *Int J Pharm*. 2013;457:395-406.
- Haleblian JK, Goodhart FW. Pharmaceutical sciences-1974: literature review of pharmaceuticals. *J Pharm Sci*. 1975;64:1085-1148.
- Du J, Hoag SW. The influence of excipients on the stability of the moisture sensitive drugs aspirin and niacinamide: comparison of tablets containing lactose monohydrate with tablets containing anhydrous lactose. *Pharm Dev Technol*. 2001;6:159-166.
- Gong Y, Zha Q, Li L, Liu Y, Yang B, Liu L, Lu A, Lin Y, Jiang M. Efficacy and safety of fufangkushen colon-coated capsule in the treatment of ulcerative colitis compared with mesalazine: a double-blinded and randomized study. *J Ethnopharmacol*. 2012;141:592-598.
- Guo JH, Robertson RE, Amidon GL. Influence of physical aging on mechanical properties of polymer free films: the prediction of long-term aging effects on the water permeability and dissolution rate of polymer film-coated tablets. *Pharm Res*. 1991;8:1500-1504.
- Uzma N, Salar BM, Kumar BS, Aziz N, David MA, Reddy VD. Impact of organic solvents and environmental pollutants on the physiological function in petrol filling workers. *Int J Environ Res Public Health*. 2008;5:139-146.
- Joshi D, Adhikari N. An overview on common organic solvents and their toxicity. *J Pharm Res Int*. 2019;28:1-18.
- Yang Q, Yuan F, Xu L, Yan Q, Yang Y, Wu D, Guo F, Yang G. An update of moisture barrier coating for drug delivery. *Pharmaceutics*. 2019;11:436.
- Al-Gousous J, Penning M, Langguth P. Molecular insights into shellac film coats from different aqueous shellac salt solutions and effect on disintegration of enteric-coated soft gelatin capsules. *Int J Pharm*. 2015;484:283-291.
- De Leo V, Milano F, Mancini E, Comparelli R, Giotta L, Nacci A, Longobardi F, Garbetta A, Agostiano A, Catucci L. Encapsulation of curcumin-loaded liposomes for colonic drug delivery in a pH-responsive polymer cluster using a pH-driven and organic solvent-free process. *Molecules*. 2018;23:739.
- Bellakhdar J. *Plantes Médicinales au Maghreb et soins de base*. Précis de phytothérapie moderne. Editions le Fennec Casablanca; 2006:180.
- Rhiouani H, El-Hilaly J, Israili ZH, Lyoussi B. Acute and sub-chronic toxicity of an aqueous extract of the leaves of *Herniaria glabra* in rodents. *J Ethnopharmacol*. 2008;118:378-386.
- Phillips R, Hanchanale VS, Myatt A, Somani B, Nabi G, Biyani CS. Citrate salts for preventing and treating calcium containing kidney stones in adults. *Cochrane Database Syst Rev*. 2015;10:CD010057.
- Hostettmann K, Marston A. *Chemistry and Pharmacology of Natural Products- Saponins*. Cambridge University Press; 1995:146.
- Chua LS, Lau CH, Chew CY, Dawood DAS. Solvent fractionation and acetone precipitation for crude saponins from *Eurycoma longifolia* extract. *Molecules*. 2019;24:1416.
- Parikh DM, Gokhale R, Sun Y, Shukla AJ. High-shear granulation. *Handbook of pharmaceutical granulation technology*. (2nd ed). Taylor & Francis; North Carolina; 2005:195-224.
- Parikh DM, Mogavero M. Fluid bed drying. *Handbook of Pharmaceutical Granulation Technology*. (2nd ed). Taylor & Francis; North Carolina; 2005:265-268.
- Redlick AB, Cherry Hill, Michael NJ. Secora. Pharmaceutical tablets coated with wax-free ammonia solubilized water soluble shellac, U.S. Pat. 3,390,049, 25 Jun 1964.
- Russian Pharmacopoeia, 14th edition, 2018; 2: 2111-2163.
- Russian Pharmacopoeia, 14th edition, 2018; 2: 2164-2174.
- Hiai S, Oura H, Nakajima T. Color reaction of some saponins and saponins with vanillin and sulfuric acid. *Planta Med*. 1976;29:116-122.
- European Pharmacopeia, 8th edition, 2014; 3066.
- Vertucci CW, Roos EE. Theoretical basis of protocols for seed storage II. The influence of temperature on optimal moisture levels. *Seed Sci Res*. 1993;3:201-213.
- International Conference on Harmonisation of Technical Requirements for Registration of Pharmaceuticals for Human Use. ICH Harmonised Tripartite Guideline, Stability testing of new drug substances and products Q1A (R2). 2003. <https://database.ich.org/sites/default/files/Q1A%28R2%29%20Guideline.pdf>
- Rhodes CT, Porter SC. Coatings for controlled-release drug delivery systems. *Drug Dev Ind Pharm*. 1998;24:1139-1154.
- Wheatley TA. Water soluble cellulose acetate: a versatile polymer for film coating. *Drug Dev Ind Pharm*. 2007;33:281-290.
- Pearnchob N, Siepmann J, Bodmeier R. Pharmaceutical applications of shellac: moisture-protective and taste-masking coatings and extended-release matrix tablets. *Drug Dev Ind Pharm*. 2003;29:925-938.
- Farag Y, Leopold CS. Physicochemical properties of various shellac types. *Dissolution technologies*. 2007;16:33-39. http://dissolutiontech.com/DTresour/200905Articles/DT200905_A04.pdf

29. Limmatvapirat S, Limmatvapirat C, Puttipatkhachorn S, Nuntanid, J, Luandana-Anan M. Enhanced enteric properties and stability of shellac films through composite salts formation. *Eur J Pharm Biopharm.* 2007;67:690-698.
30. Schindler WD, Hauser PJ. Repellent finishes. *Chemical Finishing of Textiles.* 2004:74-86. <https://www.elsevier.com/books/chemical-finishing-of-textiles/schindler/978-1-85573-905-5>
31. Asrar S. Development and characterization of shellac-hydroxypropyl methyl cellulose composite films with acid catalyst. *All Theses.* 2012:1438.https://tigerprints.clemson.edu/cgi/viewcontent.cgi?article=2438&context=all_theses
32. Nelson KL, Fennema OR. Methylcellulose films to prevent lipid migration in confectionery products. *J Food Sci.* 1991;56:504-509.
33. Kester J, Fennema O. Edible films and coatings - a review. *Food Technol.* 1986;40:47-59.



Vitamin D with Calcium Supplementation Managing Glycemic Control with HbA1c and Improve Quality of Life in Patients with Diabetes

Sanjana MEHTA¹, Parminder NAIN^{1*}, Bimal K. AGRAWAL², Rajinder Pal SINGH³

¹Maharishi Markandeshwar College of Pharmacy (Deemed to be University), Department of Pharmacy Practice, Haryana, India

²Maharishi Markandeshwar Institute of Medical Science and Research (Deemed to be University), Department of Medicine, Haryana, India

³Pancham Multi Speciality Hospital, Department of Medicine, Ludhiana, India

ABSTRACT

Objectives: This study evaluates the effect of vitamin D with calcium supplementation on glycemic control and quality of life (QoL) in patients with diabetes.

Materials and Methods: A prospective, observational, open-label randomized, controlled study was conducted on 150 type-2 patients with diabetes. A total number of patients were divided into three groups (n= 50 in each group) i.e. group 1 (patient on oral hypoglycemic agents), group 2 (oral hypoglycemic agents with vitamin D 60.000 IU/week), and group 3 (oral hypoglycemic agents, vitamin D 60.000 IU/week along with daily calcium of 1.000 mg/day). Biochemical estimation of fasting/random blood glucose (RBG), hemoglobin A1c (HbA1c), serum insulin and patient's QoL were analyzed using modified diabetes QoL (MDQoL)-17 questionnaire after 12 weeks of treatment. Data were analyzed using a student *t*-test (paired *t*-test)

Results: The majority of the patients were male (more than 50%) with an average age of 50 ± 6 years having a diabetic history of more than 10 years and HbA1c level >10% in all three groups. After 12 weeks supplementation, the mean value of vitamin D was 25.73 ± 6.2 ng/mL, 29.98 ± 5.3 ng/mL and 62.71 ± 7.8* ng/mL in groups 1, 2, and 3, respectively (*p*<0.05) compared to baseline. A change in the mean value of HbA1c, in group 2 (14.64 ± 3.48 to 13.99 ± 3.16%) and group 3 (14.05 ± 2.65 to 12.04 ± 2.21%) was also seen at the end of the study. Moreover, patients showed a positive effect of vitamin D with calcium in group 3 with increased MDQoL, 30% of patients were in more than 70 score range.

Conclusion: The result of the study indicates that vitamin D supplementation with calcium significantly controlled or reduced HbA1c; fasting and RBG levels moreover improve QoL in type-2 patients with diabetes. It suggests that this combination can be considered a therapeutic supplement along with a primarily used anti-diabetic regimen.

Key words: *Diabetes mellitus* type-2, glycemic control, quality of life, vitamin D, calcium

INTRODUCTION

Diabetes mellitus is a chronic, serious, and growing metabolic disorder of the pancreatic gland, caused by relative or absolute insulin deficiency. It develops frequently after the age of 40, therefore, it is known as "Adult - Onset Diabetes".¹ More than 62 million patients with diabetes have been currently diagnosed with the disease and it is the third leading cause of death. Worldwide the number will keep on increasing due to aging, population growth, and increasing prevalence of obesity or physical inactivity because of a sedentary lifestyle.² Diabetes

is considered a potential epidemic and India is also called "The Diabetes Capital of the World".³ According to the World Health Organization, the number of diabetic patients has risen from 108 million in 1980 to 422 million in 2014.⁴ International Diabetes Federation is expecting that there will be 578 million diabetics by 2030 and estimates to raise 700 million by 2045.⁵ Over the past few decades, an interesting angle to the pathophysiology of diabetes suggested a strong link of vitamin D concentrations in the body with diabetes etiopathogenesis and vitamin D deficiency is considered as a leading cause of this disease.⁶

*Correspondence: parminder.nain26@gmail.com, Phone: +08168693619, ORCID-ID: orcid.org/0000-0003-4571-3306

Received: 30.05.2021, Accepted: 09.08.2021

©Turk J Pharm Sci, Published by Galenos Publishing House.

Vitamin D is required for normal insulin secretion and glucose tolerance.⁷ In various prospective observational studies, it has been found that low serum vitamin D levels increase the risk of developing insulin resistance in diabetes.⁷ Moreover vitamin D deficiency or insufficient calcium intake may modify the balance between the intracellular and extracellular β -cell calcium pools, resulting in disturbing normal insulin secretion.⁸ According to the pathogenesis of type-2 diabetes, the presence of vitamin D receptors on the β -cells is responsible for insulin resistance by affecting calcium metabolism or β -cell function.^{9,10} In addition, vitamin D improves insulin sensitivity by attenuating the expression of pro-inflammatory cytokines.¹¹ Vitamin D deficiency is prevailing in epidemic proportions worldwide and specifically all over the Asian and European continent with a prevalence of 70-100% in the general population.¹² Thus, we found it important to elucidate the level of vitamin D and the potential role of vitamin D supplementation with or without calcium in improving glycemic control and quality of life (QoL) in type-2 patients with diabetes.¹³

MATERIALS AND METHODS

This study was a prospective, observational; open-label randomized controlled study of 12 weeks duration, to evaluate the effect of vitamin D supplementation with or without calcium on the glycemic profile in 150 patients of type-2 diabetes mellitus. Patients were selected from outpatient and inpatient departments of medicine in a tertiary care hospital for the period from November 2020 to March 2021 (including 2 months of recruitment). The Institutional Ethics Committee (IEC) Maharishi Markandeshwar Institute of Medical Science and Research approval was obtained (project no: IEC-1565) before the conduct of the study. Written informed consent was signed from all patients before participation in the study. All biochemical test parameters were assessed after one day of the last administered dose of supplements. Patients were selected based on inclusion and exclusion criteria.

Inclusion criteria

Adult patients (40-60 years) having type-2 diabetes for at least 10 years, who were taking one or two oral hypoglycemic agents regularly, hemoglobin A1c (HbA1c) $>10\%$ and low vitamin D levels (≤ 24 ng/mL)

Exclusion criteria

Patients with other types of diabetes, current or previous use of vitamin D or multivitamins, pregnant women, patients with chronic kidney disease stage 5; diabetic ketoacidosis, liver cirrhosis, hypothyroidism/hyperthyroidism, osteoporosis and patients with a body mass index (BMI) more than 30 kg/m^2 were excluded from the study.

Study design

The sample size was calculated based on the data obtained from previous studies using power and precision software. A total of 150 patients were identified according to inclusion and exclusion criteria and were divided into three groups ($n=50$ per group) by simple randomization.

At the baseline of the study, after detailed patient history and clinical examination, routine investigations were done to exclude any comorbidity. The baseline values of fasting blood glucose (FBG), random blood glucose (RBG), HbA1c, fasting serum insulin, serum calcium, serum phosphate and vitamin D levels were obtained on the day of enrollment to the study and follow-up of these patients were up to 12 weeks. FBG/RBG levels were observed every 4th week, whereas HbA1c, serum vitamin D, and serum calcium levels were recorded at the end of the study (Figure 1). During the study, the drugs were prescribed by guidelines, and patients were instructed not to change their oral anti-diabetic medicines, diet and lifestyle. The QoL of selected patients with diabetes were assessed by the validated questionnaire modified diabetes QoL (MDQoL)-17, which consists of 17 questions comprising seven domains including role limitations due to physical health problems, physical functioning, social functioning, and emotional well-being, role limitations due to personal or emotional problems, general health perceptions and energy or fatigue (Table 1).¹⁴ The information was obtained and entered in a case report form after obtaining their consent. The patients were scored in the range between 0 and 100, where 0 is the minimum and 100 is the maximum score. For comparison and analysis, the QoL score of MDQoL-17 was expressed as the percentage of the total possible score achieved. The patients with having an MDQoL score of less than 50 had a poor QoL, a score between 50-70 had a moderate QoL and a more than 70 score had a better QoL.

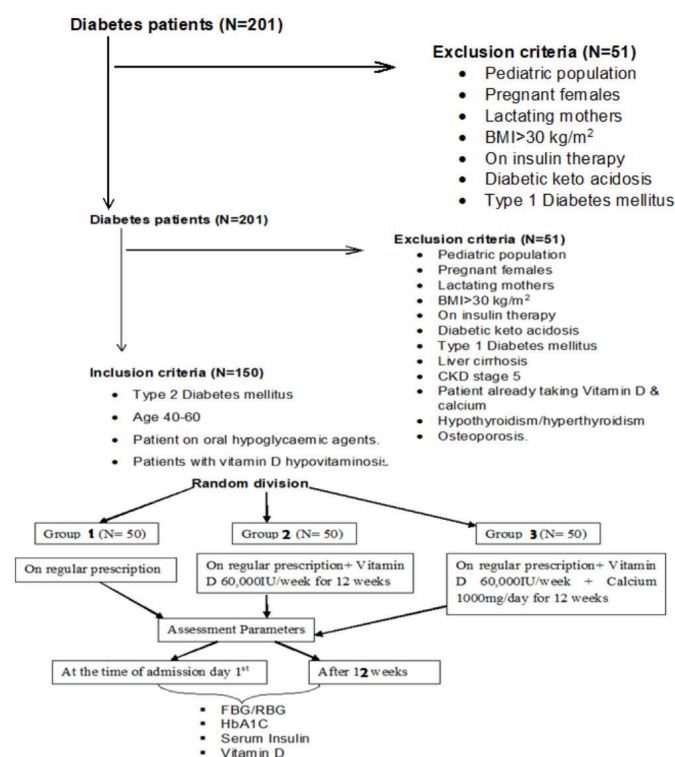


Figure 1. Plan of work

FBG: Fasting blood glucose, RBG: Random blood glucose, HbA1c: Hemoglobin A1c

Statistical analysis

The data were normally distributed according to Kolmogorov-Smirnov normality test.

Statistical methods were used to determine the differences among the variables under study. The parametric data were analyzed using paired Student *t*-test followed by Dunnett's test into consideration for the special structure of comparing

treatment against control, yielding narrower confidence intervals. *Statistical analysis* was done using *SPSS software* version 23 with $p < 0.05$ considered statistically significant.

RESULTS

Demographic data of 150 type-2 diabetic patients who were divided into three groups based on the study protocol revealed

Table 1. Modified diabetes quality of life -17 questionnaire

Domains		Response category and scores					
General health		1 (100)	2 (75)	3 (50)	4 (25)	5 (0)	-
1	How is your overall health after being diagnosed as diabetic?	Excellent	Very good	Good	Fair	Poor	-
2	Diabetes has worsened your quality of life?	Not at all	Slightly	Moderately	Quite a bit	Extremely	-
3	You get sick quite often compared to others?	Definitely false	Mostly false	Don't know	Mostly true	Definitely true	-
Physical functioning		1 (100)	2 (50)	3 (0)	-	-	-
4	Walking for normal daily chores (like going to work or market?)	No not limited at all	Yes limited a little	Yes limited a lot	-	-	-
5	Climbing several flights of stairs?	No not limited at all	Yes limited a little	Yes limited a lot	-	-	-
6	Climbing one flight of stairs?	No not limited at all	Yes limited a little	Yes limited a lot	-	-	-
Role limitations due to physical health		1 (100)	2 (75)	3 (50)	4 (25)	5 (0)	-
7	Diabetes is affecting your work life?	Not at all	Slightly	Moderately	Quite a bit	Extremely	-
Emotional well being		1 (100)	2 (80)	3 (60)	4 (45)	5 (20)	6 (0)
8	Do you feel downhearted or depressed?	None of the time	A little of time	Some of time	A good bit of time	Most of the time	All of the time
9	Is diabetes affecting your peace of mind?	None of the time	A little of time	Some of time	A good bit of time	Most of the time	All of the time
10	Do you feel scared when you think about living with diabetes?	None of the time	A little of time	Some of time	A good bit of time	Most of the time	All of the time
Role limitations due to emotional wellbeing		1 (100)	2 (80)	3 (60)	4 (45)	5 (20)	6 (0)
11	Whether diabetes made you feel lost since it restricts the food items you like?	None of the time	A little of time	Some of time	A good bit of time	Most of the time	All of the time
12	Is diabetes making you lose your confidence in your abilities?	None of the time	A little of time	Some of time	A good bit of time	Most of the time	All of the time
Social functioning		1 (100)	2 (75)	3 (50)	4 (25)	5 (0)	-
13	Is diabetes is affecting your family life?	Not at all	Slightly	Moderately	Quite a bit	Extremely	-
14	Do you feel embarrassed managing your Diabetes in public (like taking tablets/ injecting the medicine?)	None of the time	A little of time	Some of time	A good bit of time	Most of the time	All of the time
15	Whether diabetes is a hindrance when you are planning for any travel	None of the time	A little of time	Some of time	A good bit of time	Most of the time	All of the time
16	Is diabetes bringing up economic burden to you?	None of the time	A little of time	Some of time	A good bit of time	Most of the time	All of the time
Energy fatigue		1 (100)	2 (80)	3 (60)	4 (45)	5 (20)	6 (0)
17	Do you feel energetic?	None of the time	A little of time	Some of time	A good bit of time	Most of the time	All of the time

that most patients affected by diabetes were male (more than 50%) compared to females in all three groups. The mean age of the patient found in this study was 50 ± 6.2 years and BMI was (27.7 ± 0.6 kg/m²). All the patients were having type-2 diabetes mellitus for more than 10 years and were taken from both in patient ($14 \pm 2\%$) and out-patient ($84 \pm 4\%$) departments in all three groups. No statistical difference was found in all three groups of patients. The patient with diabetes was admitted to the hospital, not due to diabetes or its complication. They were admitted to the hospital due to other illnesses and diabetes was found as a comorbid condition (Table 2). Drug prescribing patterns in recruited patients were studied and analyzed on the basis of symptoms and existing comorbid conditions. The major categories of drugs prescribed were oral hypoglycemic agents (monotherapy or dual therapy) with anti-hypertensive, anti-platelets, statins, and antibiotics.

The mean FBG decreased (170 ± 13.11 mg/dL to 162 ± 26.23 mg/dL) with oral hypoglycemic agents such as sulfonylureas and biguanides in group 1, whereas in group 2 when oral hypoglycemic agents were given with vitamin D supplementation FBG levels decreased (176 ± 09.54 mg/dL to 169 ± 11.72 mg/dL) and in group 3 the level of FBG was at maximum decline *i.e.* (167 ± 17.22 mg/dL to 139 ± 11.59 mg/dL) with calcium and vitamin D supplementation.

The RBG post supplementation was decreased non-significantly (328.45 ± 19.49 mg/dL to 249.45 ± 18.43 mg/dL) in group 2, whereas a statistically significant ($p < 0.05$) decrease was seen in group 3 (305.10 ± 17.45 mg/dL to $202.10 \pm 12.37^*$ mg/dL).

The serum insulin levels were also found to be on the lower side (30 ± 11.27 μ U/mL to 29 ± 16.75 μ U/mL) in group 1, whereas in group 2 after supplementation of vitamin D without calcium the serum insulin levels were (28 ± 9.65 μ U/mL to 24.67 ± 11.95 μ U/mL) but statistically significant ($p < 0.05$) decrease (29 ± 7.39 μ U/mL to $20.76 \pm 6.23^*$ μ U/mL) was seen in group 3 post supplementation (Table 3).

The mean baseline serum vitamin D levels for group 1, group 2, and group 3 were 25.78 ± 5.3 ng/mL, 28 ± 4.1 ng/mL and 28 ± 5.3 ng/mL, respectively. The levels of vitamin D were significantly ($p < 0.05$) increased $62.71 \pm 7.8^*$ ng/mL in group 3, after giving vitamin D with calcium supplementation for three months. However, a non-significant increase in mean serum vitamin D level was observed in group 1 and group 2 compared to baseline after three months *i.e.* 25.73 ± 6.2 ng/mL and 29.98 ± 5.3 ng/mL, respectively (Figure 2).

When calcium was given with vitamin D (group 3), a decrease in HbA1c levels from baseline *i.e.* $14.05 \pm 2.65\%$ to $12.04 \pm 2.21\%$ was observed after three months of supplementation. However, there was a slight increase in HbA1c levels ($14.64 \pm 3.2\%$) in group 1 and a non-significant decrease in levels of HbA1C ($13.99 \pm 3.16\%$) was observed in group 2 with respect to baseline parameters ($14.93 \pm 2.4\%$) and ($14.64 \pm 3.48\%$), respectively (Figure 3).

The mean calcium levels among individuals of group 2 revealed a non-significant increase (9.06 ± 0.63 mg/dL to 9.1 ± 0.49 mg/dL) from the baseline level among type-2 patients with diabetes. In group 3, the levels of serum calcium after supplementation for 3 months were found significantly ($p < 0.05$) increase ($10.1 \pm 0.71^*$ mg/dL) compared to baseline (8.7 ± 0.54 mg/dL), while no change was observed in mean serum calcium levels in group 1 from (8.3 ± 0.42 mg/dL to 8.41 ± 0.51 mg/dL) (Table 3). Vitamin D supplementation gradually increased phosphate levels (3.7 ± 0.25 mg/dL) and (3.4 ± 0.51 mg/dL) compared to their respective mean baseline levels (3.3 ± 0.43 mg/dL) and (3.1 ± 0.33 mg/dL) in group 2 and 3 (Table 3).

After supplementation for 3 months, only 2% of patients in group-1 and 5% patients of group-2 experienced a better QoL, but nearly 20% of the patients from group 3 scored more than 70 in MDQoL scoring. Moreover, the number of patients scoring less than 50 score remains unchanged in group 1, whereas compared to baseline scores of poor QoL class a decrease of

Table 2. Demographic data of study population

Serial no	Parameters	Population (n= 150)		
		Group 1 (n= 50)	Group 2 (n= 50)	Group 3 (n= 50)
1	Age			
	- 41-50	46% (n= 23)	48% (n= 24)	56% (n= 28)
	- 51-60	54% (n= 27)	52% (n= 26)	44% (n= 22)
2	Gender			
	- Male	58% (n= 29)	62% (n= 31)	54% (n= 27)
	- Female	42% (n= 21)	38% (n= 19)	46% (n= 23)
3	BMI (kg/m ²)	26.9 ± 0.5	28.9 ± 0.7	27.2 ± 0.8
4	Duration of type-2 DM			
	- 10-15 years	44% (n= 22)	42% (n= 21)	46% (n= 23)
	- 15-20 years	56% (n= 28)	58% (n= 29)	54% (n= 27)
5	Type of patient			
	- In patient	12% (n= 6)	16% (n= 8)	14% (n= 7)
	- Out patient	88% (n= 44)	84% (n= 42)	86% (n= 43)

BMI: Body mass index, DM: Diabetes mellitus

5% and 18% was seen in groups 2 and 3, respectively, post supplementation. However, gradual changes have been seen in moderate QoL score *i.e.* 2% of patients experienced an improvement in their QoL in groups 1 and 3, respectively, after 3 months of supplementation. This improvement is due to proper adherence to oral hypoglycemic agents and vitamin D with or without calcium supplementation (Table 4).

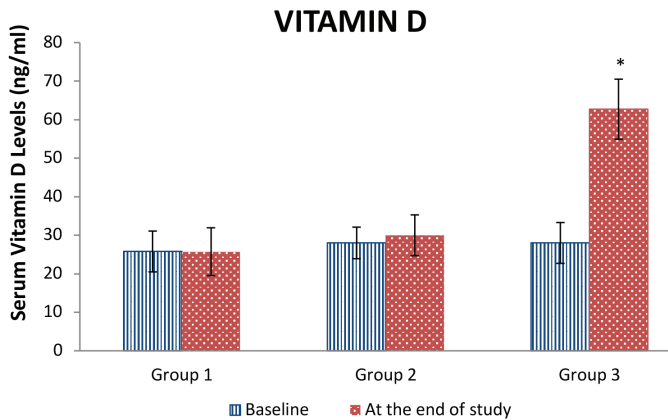


Figure 2. Serum vitamin D concentrations at baseline and at the end of the study

* $p < 0.05$ was significant when compared with baseline value

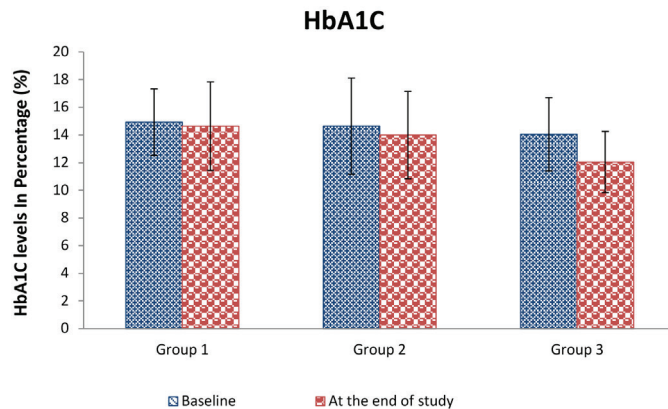


Figure 3. Serum HbA1c concentrations at baseline and at the end of the study

HbA1c: Hemoglobin A1c

DISCUSSION

In this study, we investigated the relationship of diabetes with respect to glycemic profile. Our study results revealed that males are most frequently affected by type-2 diabetes compared to females. Our study results are similar to the previous study by Bahendeka et al.¹⁴ has shown the prevalence of diabetes among males (1.6%) is more dominant than in females (1.1%). Sedentary lifestyle is considered as a reason for increased body fat, increased BMI, and increasing the probability of occurrence of metabolic diseases like type-2 diabetes mellitus, dyslipidemia, and hypertension.¹⁵ Because of our study patients having BMI-25-29 kg/m² and this lead to the progression of diabetes. Another major reason behind the increasing trend of diabetes type-2 is vitamin D deficiency. Various studies have shown that vitamin D stimulates the absorption of intestinal calcium by increasing the reabsorption of calcium from the distal tubule and by stimulating calcium mobilization from bone, whereas vitamin D also helps in phosphorous absorption by stimulating bone mobilization.¹⁶ Asian and European populations are found to be vitamin D-deficient.^{12,17} Thus, prescribing vitamin D and calcium supplementation to diabetes patients perhaps helps manage glycemic control in patients with diabetes. Therefore, we evaluated the patients to measure the effect of vitamin D and calcium after oral vitamin D supplementation of 60,000 IU/week without and with calcium supplementation of 1000 mg/day for 12 weeks. However, calcium supplementation alone did not find any therapeutic effect on glucose levels, insulin secretion or HbA1c levels.¹⁸ Vitamin D controls insulin secretion indirectly and normalizes the extracellular calcium by ensuring normal calcium flux through cell membranes.¹⁹ Therefore, combination therapy of vitamin D and calcium was found to be significantly more effective in managing the glycemic profile of study participants than vitamin D or calcium as monotherapy. We also found decreased mean baseline serum vitamin D levels in patients with diabetes and our results are similar to Scragg et al.²⁰, who also stated that there was a strong inverse association between diabetes and low levels of vitamin D, whereas normalizing these levels will result in 55% relative reduction in the risk of developing type-2 diabetes mellitus. Numerous studies have also confirmed the effects of vitamin D supplementation on glucose metabolism.^{19,21} Present study results follow previous studies. Reduction of FBG,

Table 3. Blood biochemical parameters before and after the supplementation of vitamin D and serum calcium

Serial no	Biochemical parameters and units	Group 1 (n= 50)		Group 2 (n= 50)		Group 3 (n= 50)	
		Baseline values	Values after 3 months (mean \pm SD)	Baseline values	Values after 3 months (mean \pm SD)	Baseline values	Values after 3 months (mean \pm SD)
1	Fasting blood glucose (mg/dL)	170 \pm 13.11	162 \pm 26.23	176 \pm 09.54	169 \pm 11.72	167 \pm 17.22	139 \pm 11.59
2	Random blood glucose (mg/dL)	308.36 \pm 18.26	287.36 \pm 13.65	328.45 \pm 19.49	249.45 \pm 18.43	305.10 \pm 17.45	202.10 \pm 12.37*
3	Fasting serum insulin (μ U/mL)	30 \pm 11.27	29 \pm 16.75	28 \pm 9.65	24.67 \pm 11.95	29 \pm 7.39	20.76 \pm 6.23*
4	Serum calcium (mg/dL)	8.3 \pm 0.42	8.41 \pm 0.51	9.06 \pm 0.63	9.1 \pm 0.49	8.7 \pm 0.54	10.1 \pm 0.71*
5	Serum phosphate (mg/dL)	2.9 \pm 0.47	3.1 \pm 0.39	3.3 \pm 0.43	3.7 \pm 0.25	3.1 \pm 0.33	3.4 \pm 0.51

$p < 0.05$ was significant when compared with baseline value. SD: Standard deviation

Table 4. Quality of life on basis of MDQoL scoring

QoL score	Classification on basis of MDQoL scoring	Group 1 (n= 50)		Group 2 (n= 50)		Group 3 (n= 50)	
		(Baseline)	(After 3 months)	(Baseline)	(After 3 months)	(Baseline)	(After 3 months)
Less than 50	Poor QoL	54%	54%	56%	51%	60%	42%
50-70	Moderate QoL	28%	26%	32%	32%	30%	28%
More than 70	Better QoL	18%	20%	12%	17%	10%	30%

MDQoL: Modified diabetes quality of life

RBG, and HbA1c after administration of vitamin D along with calcium; thus, managing glycemic control.^{21,22} Initially, serum calcium levels were tested to rule out hypercalcemia due to supplementation but the concentration of serum calcium was lower in patients with diabetes. Previous studies have also shown an inverse correlation between calcium and disease progression.²³ These levels gradually began to increase after supplementation. However, the mean levels of calcium remained within the normal range at the end of the study, no hypercalcemia was found because of supplementation and our study results followed previous studies.²² Results of this study also suggest that the mean level of phosphate was in the normal range yet they were slightly increased from baseline parameters, which are similar to previous studies.²⁴ The reason behind this increase irrespective of the medication and supplementation, is usually caused by a kidney problem associated with natural diabetes progression.^{24,25} The present study also assessed the QoL in patients with diabetes on the basis of various domains including physical and emotional wellbeing, mental state, and social functioning. We observed an inverse correlation between QoL and disease progression, it is suggesting that progression in diabetes has a negative impact on QoL. Results were supported by previous studies which stated that QoL was way better in patients at a younger age without complications, with a BMI of <18.4 kg/m² and HbA1c level between 7.1-8.0%.^{26,27} Diabetic patients with a diabetic history of more than 10 years were found to have a poor QoL in this study, whereas, the MDQoL score for the patients on vitamin D with calcium supplementation along with diabetic therapy was improved than the patients on oral hypoglycemic agents only. This may be attributed to the fact that using vitamin D with calcium as an adjuvant therapy gives better glycemic control and improves the QoL and decreases the rate of disease progression along with other diabetic complications.²⁸

Study limitations

The small sample size and time constraints were the limitations of our study that impacted our results.

CONCLUSION

The study indicates that the administration of vitamin D with calcium supplementation in type-2 patients with diabetes significantly improved QoL by controlling or reducing HbA1C, fasting, and RBG levels improved in patients with diabetes. Therefore the study suggests that vitamin D and calcium can be considered add-on therapeutic supplements along with

other anti-diabetic regimens for managing diabetic-related consequences and other diabetic complications.

ACKNOWLEDGEMENTS

We would like to acknowledge the staff of Pancham Multi-Specialty hospitals for their kind support and cooperation. We are thankful for the management of Maharishi Markandeshwar (Deemed to be University), Mullana (Ambala), India for encouragement and providing necessary facilities and support.

Ethics

Ethics Committee Approval: The Institutional Ethics Committee (IEC) Maharishi Markandeshwar Institute of Medical Science and Research approval was obtained (project no: IEC-1565) before the conduct of the study.

Informed Consent: Written informed consent was signed from all patients before participation in the study.

Peer-review: Externally peer-reviewed.

Authorship Contributions

Surgical and Medical Practices: B.K.A., R.P.S., Concept: S.M., P.N., B.A.K., Design: S.M., P.N., B.A.K., Data Collection or Processing: S.M., P.N., Analysis or Interpretation: S.M., P.N., Literature Search: S.M., P.N., Writing: S.M., P.N., B.K.A.

REFERENCES

1. Kaveeshwar SA, Cornwall J. The current state of *diabetes mellitus* in India. *Australas Med J*. 2014;7:45-48.
2. Batra HS, Sampath S, Kumar SA, Kumar AVSA, Mayar N. Study of vitamin D supplementation in type 2 *diabetes mellitus*. *Int J Contemp Med Res*. 2019;6:H5-H9.
3. Rajhans PA, Kulkarni PY, Kelkar DS, Jog SA, Ranade G, Utpat S, Hande V. Effect of diabetes on severity of illness, length of hospital stay and mortality among patients brought by emergency medical system (EMS). *Int J Med Public Health*. 2017;7:156-161.
4. Sandhu RK, Sharma G, Nayyar SB, Gupta M. To study the efficacy and safety of vitamin D as an add-on therapy in patients of type 2 *diabetes mellitus* on oral antidiabetic drugs. *Int J Basic Clin Pharmacol*. 2015;4:1276-1280.
5. Williams R, Colagiuri S, Almutairi R, Montoya P, Basit A, Beran D. *IDF Diabetes Atlas*, 9th edition 2019. International Diabetes Federation; 2019.
6. Mezza T, Muscogiuri G, Sorice GP, Prioletta A, Salomone E, Pontecorvi A, Giaccari A. Vitamin D deficiency: a new risk factor for type 2 diabetes? *Ann Nutr Metab*. 2012;61:337-348.

7. Amirasgari F, Torkfar S, Rezazadeh S, Farzaneh M, Tajik E. Effect of vitamin D on glucose homeostasis, sensitivity and insulin resistance in type 2 diabetes. *Curr Res Diabetes Obes J*. 2019;11:555810.
8. Norman AW, Frankel JB, Heldt AM, Grodsky GM. Vitamin D deficiency inhibits pancreatic secretion of insulin. *Science*. 1980;209:823-825.
9. Chertow BS, Sivitz WI, Baranetsky NG, Clark SA, Waite A, Deluca HF. Cellular mechanisms of insulin release: the effects of vitamin D deficiency and repletion on rat insulin secretion. *Endocrinology*. 1983;113:1511-1518.
10. Kadowaki S, Norman AW. Dietary vitamin D is essential for normal insulin secretion from the perfused rat pancreas. *J Clin Invest*. 1984;73:759-766.
11. Tanaka Y, Seino Y, Ishida M, Yamaoka K, Yabuuchi H, Ishida H, Seino S, Seino Y, Imura H. Effect of vitamin D3 on the pancreatic secretion of insulin and somatostatin. *Acta Endocrinol (Copenh)*. 1984;105:528-533.
12. Alpdemir M, Alpdemir MF. Vitamin D deficiency status in Turkey: a meta-analysis. *Int J Med Biochem*. 2019;2:118-131.
13. Bhanubhai PV, Raushan B, Acharya LD, Shubha S. Assessment of quality of life in type II diabetic patients using the modified diabetes quality of life (MDQoL)-17 questionnaire. *Braz J Pharm Sci*. 2017;53:e17144.
14. Bahendeka S, Wesonga R, Mutungi G, Muwonge J, Neema S, Guwatudde D. Prevalence and correlates of *diabetes mellitus* in Uganda: a population-based national survey. *Trop Med Int Health*. 2016;21:405-416.
15. Park JH, Moon JH, Kim HJ, Kong MH, Oh YH. Sedentary lifestyle: overview of updated evidence of potential health risks. *Korean J Fam Med*. 2020;41:365-373.
16. DeLuca HF. The metabolism and functions of vitamin D. *Adv Exp Med Biol*. 1986;196:361-375.
17. Cashman KD, Dowling KG, Škrabáková Z, Gonzalez-Gross M, Valtueña J, De Henauw S, Moreno L, Damsgaard CT, Michaelsen KF, Mølgaard C, Jorde R, Grimnes G, Moschonis G, Mavrogianni C, Manios Y, Thamm M, Mensink GB, Rabenberg M, Busch MA, Cox L, Meadows S, Goldberg G, Prentice A, Dekker JM, Nijpels G, Pilz S, Swart KM, van Schoor NM, Lips P, Eiriksdottir G, Gudnason V, Cotch MF, Koskinen S, Lamberg-Allardt C, Durazo-Arvizu RA, Sempos CT, Kiely M. Vitamin D deficiency in Europe: pandemic? *Am J Clin Nutr*. 2016;103:1033-1044.
18. Pittas AG, Lau J, Hu FB, Dawson-Hughes B. The role of vitamin D and calcium in type 2 diabetes. A systematic review and meta-analysis. *J Clin Endocrinol Metab*. 2007;92:2017-2029.
19. Moharir G, Naikawadi AA, Patil J, Bhixavatimath P, Bharatha A. Effect of vitamin D on blood sugar, HbA1c and serum insulin levels in streptozotocin-induced diabetic rats. *Maedica (Bucur)*. 2020;15:327-331.
20. Scragg R, Sowers M, Bell C; Third National Health and Nutrition Examination Survey. Serum 25-hydroxyvitamin D, diabetes, and ethnicity in the third National Health and Nutrition Examination Survey. *Diabetes Care*. 2004;27:2813-2818.
21. Shah IU, Sameen A, Manzoor MF, Ahmed Z, Gao J, Farooq U, Siddiqi SM, Siddique R, Habib A, Sun C, Siddeeq A. Association of dietary calcium, magnesium, and vitamin D with type 2 diabetes among US adults: National Health and Nutrition Examination Survey 2007-2014-A cross-sectional study. *Food Sci Nutr*. 2021;9:1480-1490.
22. Al-Daghri NM, Alkharfy KM, Al-Othman A, El-Kholie E, Moharram O, Alokail MS, Al-Saleh Y, Sabico S, Kumar S, Chrousos GP. Vitamin D supplementation as an adjuvant therapy for patients with T2DM: an 18-month prospective interventional study. *Cardiovasc Diabetol*. 2012;11:85.
23. Rigo J, Pieltain C, Viellevoe R, Bagnoli F. Calcium and Phosphorus Homeostasis: Pathophysiology. In: Buonocore G, Bracci R, Weindling M. *Neonatology*. Springer, Cham, 2018.
24. Ditzel J, Lervang HH. Disturbance of inorganic phosphate metabolism in diabetes mellitus: temporary therapeutic intervention trials. *Diabetes Metab Syndr Obes*. 2009;2:173-177.
25. Winiarska A, Filipka I, Knysak M, Stompór T. Dietary phosphorus as a marker of mineral metabolism and progression of diabetic kidney disease. *Nutrients*. 2021;13:789.
26. Manjunath K, Christopher P, Gopichandran V, Rakesh PS, George K, Prasad JH. Quality of life of a patient with type 2 diabetes: a cross-sectional study in rural South India. *J Family Med Prim Care*. 2014;3:396-399.
27. Bosić-Zivanović D, Medić-Stojanoska M, Kovacev-Zavisić B. [The quality of life in patients with *diabetes mellitus* type 2]. *Vojnosanit Pregl*. 2012;69:858-863.
28. Thommasen HT, Zhang W. Health-related quality of life and type 2 diabetes: a study of people living in the Bella Coola Valley. *BC Med J*. 2006;48:272-278.



Preparation and Characterization of Orlistat Bionanocomposites Using Natural Carriers

✉ Santosh PAYGHAN^{1*}, ✉ Vaishali PAYGHAN¹, ✉ Kavita NANGARE¹, ✉ Lalita DAHIWADE¹, ✉ Karna KHAVANE², ✉ Ram PHALKE³

¹Vasantidevi Patil Institute of Pharmacy, Kodoli, Department of Pharmaceutics, Kolhapur, India

²Gurunank Institute of Pharmacy, Department of Pharmaceutics, Beed, India

³Tatyasaheb Kore College of Pharmacy, Department of Pharmaceutics, Kolhapur, India

ABSTRACT

Objectives: Bionanocomposites (BNCs) are biopolymers or a natural polymers embedded in a combination of two or more different chemicals using natural carriers or bio. BNCs are widely used in drug formulation and in the development of new drugs for various therapeutic drugs, new dosage forms and in pharmacological medicine.

Materials and Methods: Useful and improved melting was achieved by converting selected Biopharmaceutics Classification System (BCS) class II drug into BNCs using natural carriers such as the gums of *Moringa oleifera* Lam. and *Aegle marmelos* (L.) Correa, respectively. The current work focuses on the enhancement of the novel natural polymers such as *M. oleifera* and *A. marmelos*, used to prepare BNC for BCS class II orlistat using a microwave system designed for the distribution method. The natural polymer helps improve the melting of the dispersion when it converts them into BNC. Definitions of orlistat, natural carriers, and prepared BNCs were developed and studied comparatively. The fourier transform infrared spectroscopy (FTIR), differential scanning calorimetry (DSC) study revealed that there was no communication between drug associations and environmental carriers.

Results: Crowd reduction studies were conducted to investigate the material that enhances the melting of BNC compounds dissolving and *in vitro* disposal of BNCs prepared by DSC, scanning electron microscopy, X-ray diffraction studies, and FTIR. BNCs affect orlistat: *M. oleifera* (OSMO-BNC-1: 3), orlistat: *A. marmelos* (OSAM-BNC- 1: 4) is well developed.

Conclusion: Ornat BNCs developed with *M. oleifera* and *A. marmelos* provide significant improvements in dissolve and highlight their use in reducing fortification. Additionally, land melting limits were applied and determined for the melting of BNCs prepared using the Hansen Solubility parameters in particular, Hoy's, Fedor and Van Krevelen system and it was found that this report there was a significant increase in the melting of batches prepared for BNCs.

Key words: Bionanocomposite, BCS class II, orlistat, *Moringa oleifera*, *Aegle marmelos*, microwave-assisted fusion method, Hansen parameters parameter

INTRODUCTION

The therapeutic efficacy of a drug depends on its availability and ultimately in the formulation of chemicals hydrophilic compounds of the compound and the dissolution of drug molecules. It is a great deal of difficulty in preparing and developing the most effective form of improper water solubility of many drugs. Innocence is a parameter for achieving the desired combination of drugs in the distribution of the system so that the therapeutic response is shown. It is estimated that 40% or more of the drug molecules identified during the experiment of compounds do not dissolve well in water. There

is a need for systematic and simple preparation and structural methods to make less-soluble drugs available. Making these drugs unavailable means that they show enough absorption after oral administration or they may be injected with 3-4 injections.¹⁻⁵

The main purpose of this work is to prepare, mark the structural requirements of the hydrophilic environment, to construct and test the bionanocomposite (BNC) of orlistat with its low water content, reducing its drug absorption, which reflects the Biopharmaceutics Classification System (BCS) class-II drug

*Correspondence: sapayghan.tkcp@gmail.com, Phone: +912328223341, ORCID-ID: orcid.org/0000-0002-0653-6784

Received: 18.03.2021, Accepted: 10.08.2021

©Turk J Pharm Sci, Published by Galenos Publishing House.

profile. Current work is being done to provide alternative drug delivery with improved solubility and a level of detoxification in the form of nanocrystal drugs that will overcome the problems in the existing dosage form.⁶ Many methods have been used to stabilize moisture, such as salt formation, co-crystallization, co-solvency, hydrotropic, solvating agent and nanotechnology by chemical modification. Under the body modification to reduce particle size, crystal behavior modification, gravity, mixing with surfactants and drug distribution to carriers.

Nanocomposite is a combination of two or more different chemicals that have different properties and blends, to combine these two beautiful structures. The combination has two elements of different textures and the combination of those displays is enhanced in its larger structures.⁷ The body composition of the drug and its natural or bio-carrier compounds are nanotechnology and their experimental parameters, such as *in vivo* and *in vitro* profiles and biological detection, are therefore called BNC.⁸ BNC for microwave irradiation can be used in various ways such as improved melting, melting and the availability of drug-soluble drugs.⁹ Microwave radiation contains frequent frequencies between infrared and radio waves, in the range of 0.3-300 GHz. It passes through objects and causes their molecules to glide, releasing heat. Microwaves, which can penetrate into anything, allow heat to be produced at any time in the sample at a specific time.¹⁰

Orlistat is a lipase inhibitor for managing obesity, which functions by inhibiting the absorption of saturated fats. Orlistat is a modified inhibitor of gastric and pancreatic lipase. The orlistat falls under category II according to BCS, which means it exhibits poor oral discretion due to low melting. In this study, the microwave-induced diffusion (MIND) process was used to increase the melting and oral availability of orlistat using *Moringa oleifera* and *Aegle marmelos* gum as the leads. Performance tests of the method, physicochemical composition, and *in vitro* dissolution are presented in this report. The promotion and use of new polymers such as *M. oleifera* and *A. marmelos* gum to improve the melting of orlistat and its converted form through its combination of nano-composition using a microwave-assisted process and the drug spread into a natural gum carrier. Gum carriers, orlistat and integrated BNC were tested for solubility, drug content, solubility, *in vitro* and spectral readings, and thermal and nanoscale temperatures for BNCs prepared by fourier transform infrared spectroscopy (FTIR), differential scanning calorimetry (DSC), and scanning electron microscopy (SEM).¹¹ The rate of melting of the drug and the reduction of the drug for the desired liquid soluble drug does not only reflect the availability of the drug. Additionally, melting was determined using the parameters of Hansen solubility and hildebrand solubility by bringing them closer to various systems such as Hoy's system, Fedor's constant, and Van Krevelen equation. The use of this method in determining the melting of BNC prepared in pharmaceuticals highlights the best systematic approach to obtain the need for the study reported here to ensure the melting of prepared BNCs.

Hansen solubility parameters (HSPs)

Hildebrand and Scott introduced the concept of solubility parameter (δ), which suggested that objects with similar values could be felt (Hildebrand and Scott, 1964) HSP model 1967 predicting liquid reactions, incompatibility of polymer mixtures, soil moisture and pigmentation on HSP surface. After predicting the ineffectiveness of active substances/carriers in the strong distribution of HSPs in medical science. Guessing the compatibility of pharmaceutical materials, and their use is recommended as a tool in pre-construction and tablet development is recommended by HSPs. The study found that drug and substance abuse disorders, as predicted by deceptive tools that could be used, could be used to predict the co-crystal formation, orlistat was selected as an active drug ingredient (API). The group donation methods used to calculate HSPs for conformers and orlistat were used.¹²⁻¹⁵ The three-component tools used were used to predict the orlistat and conformer irregularities laboratory tests for co-crystals were performed using thermal and fluid-assisted methods in the prediction of inaccuracies. Heat exchangers and powder X-ray diffraction (XRD) were used for co-crystal precision.

$$\Delta H = V_T \sqrt{(\Delta E_{v1}/V_{m1})} - \sqrt{(\Delta E_{v2}/V_{m2})}^2 \quad 01.02 \quad (1)$$

ΔH is the heat of mixing, V_T is the total volume, ΔE_v is the energy of vaporization, V_m is the molar volume, φ is the volume fraction, and 1 and 2 stands for the solute and solvent. The energy of vaporization per unit volume as the cohesion energy density (CED) explained.

$$\delta = (CED)^{0.5} = (\Delta E/V)^{0.5} \quad (2)$$

Here, V is the molar volume.

Hansen determined that total cohesion energy is the sum of dispersion E_D , polar E_P , and hydrogen bond energy E_H .

$$E_T = E_D + E_P + E_H \quad (3)$$

The total HSP or Hildebrand solubility parameter δ_T by dividing both sides of the equation by molar volume V .

$$\delta_T^2 = \delta_D^2 + \delta_P^2 + \delta_H^2$$

Where:

δ : Total solubility parameters

δ : Dispersion interactive (London) force

δ : Permanent dipoles in interacting molecules, called dipole - dipole interactive forces

δ : Hydrogen bonding force

According to equation (1) if δ_T of both solute and solvent are a like, this will allow predicting solubility. (J/m^3) 0.5, MPa 0.5 or (cal/cm^3) 0.5, where one (cal/cm^3) 0.5 is equivalent to 2.0421 MPa 0.5 or (J/m^3) 0.5 are commonly used units for δ in literature. δ calculation methods were different between practical and theoretical ones according to either direct/indirect

measurement of essential properties of material as evaporation temperature, viscosity, solubility in preset solvents, etc.¹⁶⁻¹⁹

Orlistat testing/prediction for co-crystallization

Group donation methods are applied to the limits of melting of soluble solvents using Hoys molar attraction constants, Fedor's substants, and Van Kreevalen which are currently used methods. In this study, these methods were used to reach the melting point parameters. The resulting structure has an open combination of chains and open rings are the basic steps of Fedor's method. Then, using the potential possible lumps. This is summarized and the melting point is calculated as the square root of the total energy mixing of the variable elements separated by the number of times the volume of molar substituent constants. The rate of constant molar attraction to the molar volume is expressed by the Hoys process. Drug effects and compounds are compared and their durability status is expressed. The selection of drug-related conformer, group donation method is used in the calculation of the doctrine. HSPs determine whether the drug and conformer are compatible and form the molecular structure of the drug and the conformer. Fedor's, Hoys', and Van Kreevlens's methods of calculation are derived from atomic or molecular attachments to form a structure. These methods are used in the calculations of melting theory.

MATERIALS AND METHODS

Orlistat was received as a gift sample at INTAS Pharmaceuticals Ltd., (Ahmadabad, and Gujarat, India). The drug was stored in an amber glass container wrapped in aluminum foil and stored in a refrigerator at 5-7°C. *M. oleifera* and *A. marmelos* gum were collected from a local garden, Waranananagar. *M. oleifera* gum was collected by making a hole in the trees (an area damaged by trees). Gum was collected in a suitable air-tight container followed by air drying. Another natural gum, *A. marmelos* was collected as beal fruit contains a lot of gum, and after breaking, the beal fruit gum was carefully collected in a suitable air container followed by sun and wind suspension.²⁰⁻²³

No need to ethical committee approval.

*Extraction and purification of natural gum*²⁴⁻²⁸

Gums *M. oleifera* and marmelos collected are dried on the ground under the sun. Dry gum was passed through Sieve no: 80. Dry gum (10 g) was stirred in distilled water (250 mL) for 6-8 h at room temperature. Through centrifugation, supernatant was obtained and the remains were washed with distilled water. The process was repeated four times. Finally, a precipitant with a strength of more than 500 mL was twice treated with acetone volume for continuous movement. The products were burned and washed with distilled water and the same products were dried at 50-60°C under a machine.

Swelling characteristics

Measured 10 g of natural carrier is placed in a measuring cylinder of 100 mL. The first dose of powdered gums was noted, and the cylinder was filled with refined water up to 100 mL. The cylinder was kept aside for 24 h, and the volume of the swollen powder was noted. The inflammation index is

expressed as a percentage and is calculated according to the following equation:

$$\% \text{ inflammation} = (X_t - X_0) / X_0 \times 100 \dots (3)$$

There, X_0 is the first height of the powder on the graduated cylinder and X_t refers to the constant height of the swollen gums after 24 h.

Viscosity determination^{29,30}

The viscosity of the cleaned gums was determined by taking 1 g each *M. oleifera* and *A. marmelos* gum, respectively and dispersed in 100 mL (1% w/v) water. The estimated distribution viscosity was measured by Rheometer (Spindle 3, Brookfield DV-E, Brookfield Engineering Laboratories, Inc., Middleboro, MA, USA).

Foaming index

The dynamic index of the carrier term is measured to determine the functional properties. One gram of carrier was dispensed in 100 mL of distilled water and stirred vigorously for 2 min. The overflow index of network company is measured to establish its operational structures. The foam index is calculated using the following equation:

$$\text{Foam guide} = V_f - V_i \dots (4)$$

There, V_f is a 1% w/v solution for network company after a shake and V_i is a 1% w/v solution for a network company solution before shaking.

Ash value

Three samples of purified gum were placed on pre-measured crucibles and measured. These are then placed in a preheated oven at 300°C for 3 h. The temperature of the furnace then rose to 600°C until the hot metal samples were white to ash. Samples were then extracted using lumps and allowed to cool in the desiccators. After cooling, crosses containing the samples were weighed again. The amount of ash obtained by subtracting the combined weight of ash samples and crosses from the combined weight of new samples and crucibles.

Total ash value: 5 g of purified gum powder was ignited in an electric furnace at 600°C in a silica crucible until the sample reached a constant weight.

Water-soluble ash value: Total ash obtained was heated up to 600°C with the addition of 25 mL water for 10 min. It was filtered through whatman paper no. 41 and the residue was ignited in the furnace to get a constant weight.

Acid-insoluble ash value: Total ash obtained was heated with the addition of 25 mL of 0.1 N HCL for 10 min. It was filtered through whatman paper no. 41 and the residue was ignited in the furnace to get a constant weight.

Physical mixtures

A portable combination of drugs containing natural doses extracted from the gums was prepared in sequence with a simple drug mix with natural carriers in the required dosage (1:1 to 1:10 drug:carriers) for 10 min.

Bionanocomposites by microwave-induced diffusion³¹⁻³⁴

The preparation of BNC by two groups such as orlistat and *M. oleifera* gum (OSMONC) and *A. marmelos* gum (OSAMNC) was performed. The clear combination of the drug and the natural agent is made by mixing similar to each sample. Weight loss (w/w) dose of the drug in the manager is taken as required by the values that maintain the constant value of the combination. After that 4 mL of water was added to each gram of the drug carrier mixture to form a consistent slurry (water is added to the carrier hydration). The prescribed amount of slurry (5 g) was placed on a glass board with a teflon stirrer (exposed to microwaves) and treated with microwave radiation at various times with a power of 560 W. The temperature of the compound was recorded at the end of the treatment using a built-in temperature test. The samples were then milled in a glass mortar and the same sample was filtered to obtain a particle size of 80-250 μm .

BNCs were prepared by incorporating the weight-bearing drug orlistat and the *M. oleifera* and *A. marmelos* gum carrier at 1:1 to 1:10 w/w size (Table 1). The same physical combination of OS and network compound was prepared using mud and a pestle. The slurry was prepared by adding 4 mL of distilled water to each gram of the drug-carrying compound. A limited amount of slurry (5 g) was placed in a glass beaker and radiated by microwave radiation at 700 W (IFB Microwave Oven, Model 17 PM-MEC1, Kolkata, India) for continuous operation. Temperature was noted using a temperature measurement built-in within the end of treatment. BNCs were laid using mud and pestle to obtain the required size of 80-250 μm . The synthetic BNCs of natural-containing orlistat (*M. oleifera* and *A. marmelos*) vary in the appropriate process for preparing OSMONC and OSAMNC.

Evaluation of bionanocomposite

Solubility

The melting study of BNCs (OSMONC and OSAMNC) was conducted by adding a higher dose of orlistat (equivalent to 30 mg) and BNCs to 150 mL of distilled bottled water. The resulting mixture was stirred 24 h at a temperature of 25°C using an orbital shaker incubator. The excess liquid was collected and filtered through 0.2 membrane filters and analyzed by a ultraviolet (UV)-visible spectrophotometer of 203 nm wavelength at 28 sequences. The optimization ratio (drug:carrier) is done on the basis of the best melted detection.

Drug content

The amount of orlistat added to BNCs such as OSMONC and OSAMNC, was determined by extracting 100 mg of the drug from BNC by diluting it into 25 mL enough methanol. The resulting solution was filtered through a 0.2 and membrane

filter and analyzed by a UV-visible spectrophotometer (UV-Carry 60, Agilent) at a wavelength of 215 nm, respectively, against methanol as a blank 8.

Powder dissolution

Powdered extraction tests performed on BNCs followed the USP XXIV Apparatus 6 (paddle) method in 900 mL of dissolved media stored in $37 \pm 0.5^\circ\text{C}$ powder containing 5 mg API added to dehydration sources. 1 mL sample was withdrawn periodically and the resulting solution was filtered through a 0.2 μm membrane filter and analyzed by a UV-visible spectrophotometer (UV-Carry 60, Agilent) at a wavelength of 215 nm, respectively, against methanol as empty 8. All tests are made in 3 steps. BNC dispersion profiles were compared with the pure drug under similar experimental conditions.

Characterization of bionanocomposites

A well-defined BNC standardization was performed by FTIR, DSC, XRD, and SEM to ensure the best results of the current drug and polymer study.

Fourier-transform infrared spectroscopy

FTIR spectra of impure drug (orlistat), pure polymers (*M. oleifera* and *A. marmelos* gum), and BNCs of individual polymers (*M. oleifera* and *A. marmelos* gum) were developed to monitor drug compatibility polymer. Drug BNCs with each polymer (OSMOM, OSAMM, were stored directly in the sample holder and scanned using the FTIR spectrophotometer (Cary 60, Agilent Corp., Germany) in terms of drug interactions with the polymer. The materials were scanned in the range from 400 to 4000 cm^{-1} with 1 at a resolution of 4 cm^{-1} . The peak properties of orlistat, *M. oleifera* and *A. marmelos* were compared to BNCs designed to test drug compatibility-polymer. IR detectors were used to determine and predict BNC melting by the HSP.

Differential scanning calorimetry

DSC studies of orlistat, *M. oleifera* and *A. marmelos* gum, and BNCs of drugs with individual polymers (*M. oleifera* and *A. marmelos* gum) were conducted to detect improved drug availability. The DSC thermogram was obtained using a scanning calorimeter (DSC 60; Shimadzu) at a temperature of 11°C/min from a temperature of 0°C to 250°C in an inert state and the physical, chemical interaction between the drug and the polymer that helps determine and predict the melting of BNCs with Hansen parameter.

X-ray diffraction studies

XRD studies of drugs (orlistat), pure polymers (*M. oleifera* and *A. marmelos* gum), and BNCs of individual polymer drugs (*M. oleifera* and *A. marmelos* gum) were intended to test changes in crystallinity the drug is mixed with gums. The crystallinity

Table 1. Formulation design for bionanocomposites batches

Drug + carrier	1:1	1:2	1:3	1:4	1:5	1:6	1:7	1:8	1:9	1:10
OS ^a - MO ^b gum	1:1	1:2	1:3	1:4	1:5	1:6	1:7	1:8	1:9	1:10
OS - AM ^c gum	1:1	1:2	1:3	1:4	1:5	1:6	1:7	1:8	1:9	1:10

^aOS: Orlistat, ^bMO: *Moringa oleifera* gum, ^cAM: *Aegle marmelos* Gum

property is associated with the physicochemical properties of the material. XRD patterns of orlistat, gums and BNCs were recorded using (Bruker, D8) and Cu-k α radiation.

Scanning electron microscopy

The surface morphology of orlistat BNCs was detected by SEM. Samples were placed directly on a two-dimensional SEM adhesive sample and the images were recorded at the required amplification of 15 kV power and 8 mm working distance on XL30-SFEG Philips (Lab exchange, Burladingen, Germany).

Theoretical prediction of solubility

Fedor's substituent constants

$$\delta = \sqrt{\frac{\sum \Delta \Delta U}{\sum \Delta V}} \quad (4)$$

Where,

* $\Delta \Delta U$ is constant for energy mixing

** ΔV is constant for molar volume

Hoys method/Hoys molar attractions

According to [(cal cc) 1/2 mol⁻¹] unit

$$\delta = \frac{\sum \text{molar attraction}}{V} \quad (5)$$

Van Kreevalen's solubility parameters

The given calculation of solubility parameter and molar volume by Van Kreevalen's method is based on experimental molar volume and measured cm³ mol⁻¹.

$$\delta d = \sum F_d / V \quad (6)$$

$$\delta p = \sqrt{\sum F_p^2} / V \quad (7)$$

$$\delta h = \sqrt{\sum U_h} / V \quad (8)$$

$$\delta^2 T = \sqrt{\delta d^2 + \delta p^2 + \delta h^2} \quad (9)$$

RESULT AND DISCUSSION

Physical characterization of carriers

The inflammatory properties and viscosity of *M. oleifera* and *A. marmelos* gum were low (Table 2). Due to the low viscosity of *M. oleifera* and *A. marmelos* gum, they were considered for the melting and elimination of selected BCS class-II drugs. Both gums were therefore more efficient and easily exploited in improving the melting and degradation rate of orlistat.

Rheological characterization of gums

Rheological description of *M. oleifera* L. *A. marmelos* was performed using a rheometer R/S-CPS + rheometer with the calibration system: C75-2. Viscosity and thixotropic analysis were performed (Table 3 and Figure 1), low viscosity was obtained. As shown in Figure 2, thixotropic analysis obtained 13.23 Pa/s of *A. marmelos* and 17.63 Pa/s of *M. oleifera* gum. Therefore, both gums exhibit stability and help increase the solubility of BCS class-II drugs by preparing its BNCs and can withstand the microwave radiation.

Table 2. Organoleptic and physical characterization of natural gums

Sr. no.	Parameters/particulars	<i>Moringa oleifera</i>	<i>Aegle marmelos</i>
	Colour	Brownish black	Yellowish white
	Odour	Characteristic	Characteristic
	Taste	Mucilaginous	Mucilaginous
	Swelling index \pm SD ^a	19.7 \pm 2.21	20.3 \pm 1.01
	Foaming index \pm SD	17 \pm 0.92	16 \pm 0.65
	Angle of repose	33°	31°
	Bulk density (gm/mL)	0.71 gm/mL	0.67 gm/mL
	Tapped density (gm/mL)	1.23 gm/mL	1.25 gm/mL
	Compressibility index (%)	47.27%	52.71%
	Hygroscopicity	17%	16%
	Swelling Index (mL/gm)	19.7	20.3
	Loss on drying	11% w/w	9% w/w
	Total ash	2.6%	3.3%
	Insoluble matter	0.03% w/w	0.02% w/w
	pH	5.5	6.5

^aAll values are represented as means \pm SD (n= 3), SD: Standard deviation

Table 3. Rheological characterization of *Aegle marmelos* and *Moringa oleifera* gum

Parameter	<i>Aegle marmelos</i>	<i>Moringa oleifera</i>
Viscosity (Pa.s)	0.5740	1.5442
Torque (mNm)	0.6772	4.1996
Speed (1/min)	16.8300	16.8302
Shear stress (Pa)	6.1317	38.0230
Shear rate (1/s)	50.4901	50.4907
Density (g/cm ³)	1.0000	1.0000
Angular velocity	0.0000	0.0000

Characterization of the bionanocomposites

Solubility

Melting is mainly focused on the use of *M. oleifera* and *A. marmelos*, which are used to stabilize the moisture content of water-soluble drugs. Melting was performed and expressed in mg/mL by the clear combination of the selected BCS class-II drug. It was noted that the melting of a more visible compound than that of orlistat (Figure 3).

The orlistat insoluble study, conducted by comparisons similar to their body composition with BNCs prepared, found that there was a significant increase in the solubility as the polymer drug dose increased. After the OSMO-BNC ratio of 1:3 and the OSAM-BNC ratio of 1:4, there was no clear improvement in melting as shown in Figure 3.

The solubility (mg/mL) of the prepared BNCS of orlistat with *M. oleifera* and *A. marmelos* was observed to be a well-developed dose of OSMO-BNC (1:03) and OSAM-BNC (1:04) selected after practice melting research. This well-performed measure was then confirmed by the removal of the powder and found to be increasing in melting. Soluble reinforcement of OSMO-BNC (1:03) and OSAM-BNC (1:04) is widely available and this is due to the foam index and viscosity profile of *M. oleifera* and *A. marmelos* gum, a drug spread in gum form I. Its BNC has a structural modification that is made of a type of hydrophilic drug

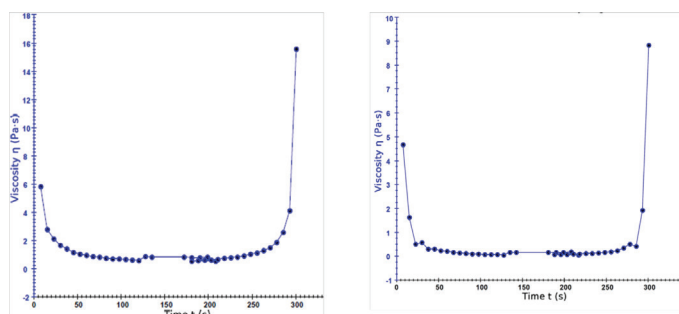


Figure 1. Viscosity diagrams of (A) *Aegle marmelos* (B) *Moringa oleifera*

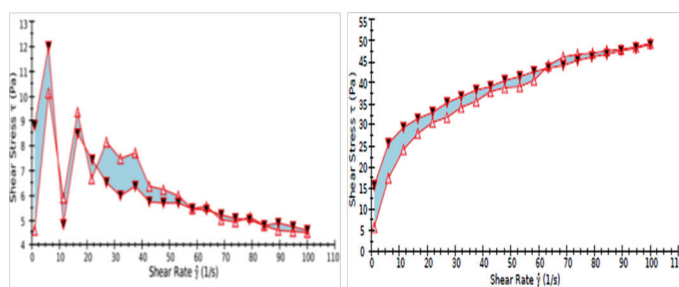


Figure 2. Thixotropic analysis of *Aegle marmelos* and *Moringa oleifera*

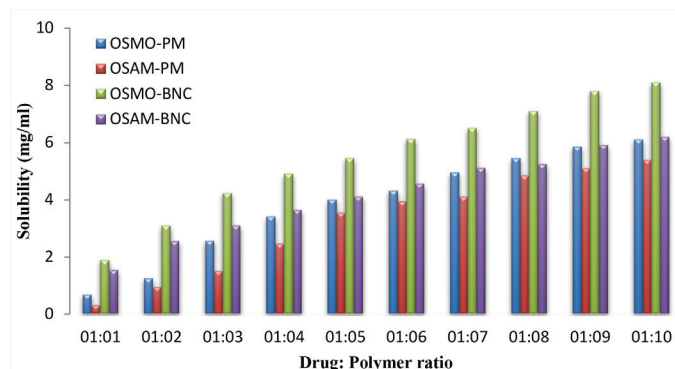


Figure 3. Solubility of orlistat in physical mixture and bionanocomposite with *Moringa oleifera* and *Aegle marmelos* (OSMO-PM; OSAM-PM and OSMO-BNC, OSAM-BNC)

OSMO: Orlistat, *Moringa oleifera* gum, BNC: Bionanocomposite, OSAM: Orlistat, *Aegle marmelos*

enriched with hydrogen bonding and this hydrogen compound helps the molecule disperse and open the rings by producing molar volume without affecting its parental function. This type of hydrophilic has apparently been used to stabilize improper water solubility.

Drug content

The differential distribution of orlistat in BNCs is determined by the drug content analysis. It was found that 95% - 98% of the drugs were trapped in BNCs, showing the same prevalence.

Powder dissolution

Powder dispersion tests are performed to check the stability of the enhancement components. The degradation profile of the clear compound showed a surprising improvement in the degradation rate compared to orlistat and their clear combination with natural carriers. The combination of orlistat with both gums showed good results. As reported in Figure 4, the dosage of prescription drugs in % of the pure drug orlistat was found to be 54.69 ± 4.5 . The combined drug release of OSMO-PM body composition was observed $70.2 \pm 7.5\%$, of OSAM-PM 3 was 61.1 ± 7.5 after 60 min.

BNC orlistat with both gums showed good results. As reported, the cumulative drug release in % of the orlistat was found to be 54.69 ± 4.5 . The cumulative drug release of BNCS, such as OSMO-BNC was $97.22 \pm 1.1\%$, for OSAM-BNC was $70.21 \pm 1.9\%$ after 60 min (Figure 5). From the observed results, it was clearly shown that the ornate BNCs the orlistat (suggested batches) showed better drug release compared to their pure form and body composition form, it was concluded in the study that a natural polymer was used for microwave BNC included in the separation the dispersion rate is improved in the prepared BNCs.

Characterization of bionanocomposites

Fourier transform infrared spectroscopy analysis

FTIR spectroscopy of orlistat shows a high values of 3301.30 (OH simple hydrogen bond), 2918.302 (simple CH alkanes group), 2853.553 (CH stretching alkanes group), 1721.653 (C=O carboxylic expansion group), 1665.0 (C=C amide extraction amide), 1201.904 (CO to dilute alcohol), and 1841.144 (C= Extension

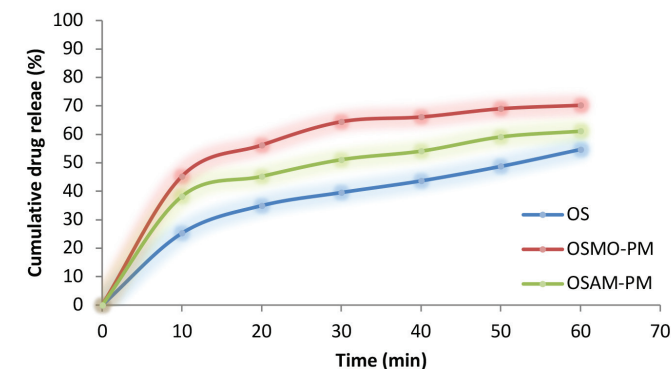


Figure 4. Powder dissolution of physical mixture of orlistat with *Moringa oleifera* and *Aegle marmelos*

OS: Orlistat, OSMO: Orlistat, *Moringa oleifera* gum, OSAM: Orlistat, *Aegle marmelos*

of anhydrides) respectively (Figure 6). Whole-gum exudates from *M. oleifera* was found to contain L-arabinose, galactose, glucuronic acid, and L-rhamnose, -mannose, and xylose, while a single polysaccharide, with a gum polysaccharide containing G-galactose, -glucuronic acid and iron; certain metals such as sodium, potassium, calcium and magnesium; and L-mannose have been found in mild hydrolysis of all acids. For the most part, the gum has frames with large branches that contain different units of sugar with many possible variations in terms of branch level, branch length and type of connection. The IR spectrum (Figure 6) shows a height of 3301 and 3263 cm^{-1} due to the OH of the main alcohol extraction. The absorption height of 2928 cm^{-1} indicates that -CH extends vibration of the methyl group. 1603 cm^{-1} bands are a C=O element of aldehyde. The height at 1310 cm^{-1} is due to the variability of the CH_2 equation with the C-OH group. Weak bond at 770 cm^{-1} because r contributes to

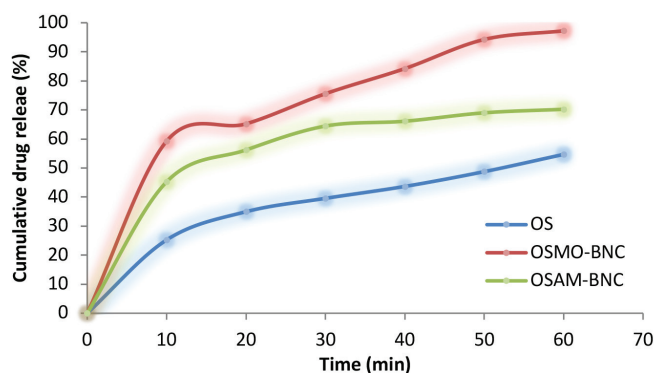


Figure 5. Powder dissolution study of bionanocomposite of orlistat with *Moringa oleifera* and *Aegle marmelos*

OS: Orlistat, OSMO: Orlistat, *Moringa oleifera* gum, OSAM: Orlistat, *Aegle marmelos*, BNC: Bionanocomposite

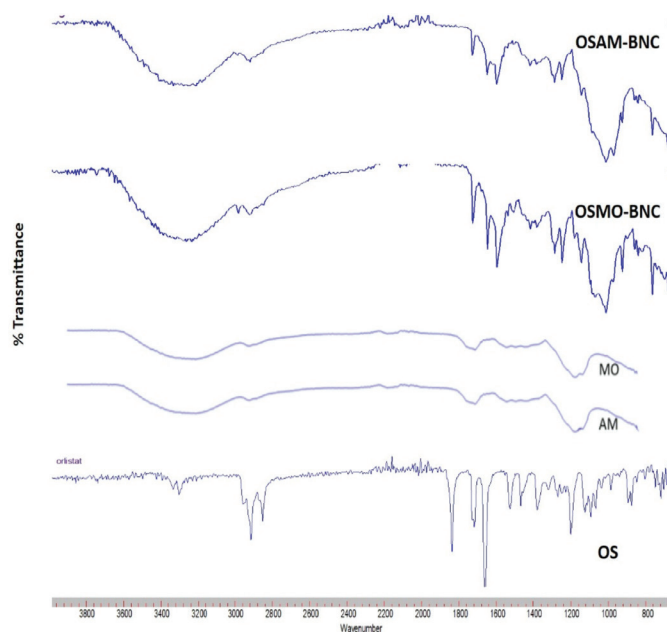


Figure 6. FTIR studies of pure *Moringa oleifera* (MO), *Aegle marmelos* (AM), orlistat (OS) and BNCs such as OSMO-BNC, OSAM-BNC

FTIR: Fourier transform infrared spectroscopy, OSMO: Orlistat, *Moringa oleifera* gum, OSAM: Orlistat, *Aegle marmelos*, BNC: Bionanocomposite

ringing binding and ring flexion of α -D- (1-4) and α -D- (1-6). All of this in conjunction with the polysaccharide structure indicates that, either starch or cellulose, but there were certain peptide cross links and other amino sugars.

Active data of the *A. marmelos* group showed that the major neutral sugars are α -D-glucose, β -D-glucose, and galactose as shown in the composition of osazone. The IR spectrum, shown in Figure 7, indicated to rises to 3296.65 cm^{-1} due to -OH to extend the main alcohol. The absorption height at 2977 cm^{-1} indicated that -CH extends the vibration of the methyl group. The absence of a large fragrant stretch in the region of 1838 cm^{-1} and the weakness of the fibers means that there is a limited number of cross-linked peptides. Belts at 1633 cm^{-1} element C=O aldehyde. The height at 1315 cm^{-1} is due to the variability of the CH_2 equation with the C-OH group. A weak bond at 821 cm^{-1} because r contributes to ringing binding and ring conversion of α -D-(1-4) and α -D-(1-6).

Scanning electron microscopy

SEM research was conducted to look at the surface morphology of the drug particles. Orlistat particles were made of a smooth surface, while OSMO and OSAM particles had unequal shape and size. From this study and writing 7, it is clearly shown that the crystal structure of orlistat was completely changed in OSMO-BNC and OSAM-BNC showing orlistat crystals embedded in the matrix.

Differential scanning calorimetry analysis

Pharmaceutical DSC thermograms (OS), polymers (*M. oleifera* and *A. marmelos*) and BNCs for each drug with each polymer are shown in Figure 8. Orlistat DSC showed high endothermic intensity at 51°C indicating melting of orlistat. Dimethyl sulfoxide OSMO-BNC and OSAM-BNC showed the same endothermic intensity as that of the pure drugs but with less energy, which may be due to a decrease in the crystal type of drug. A slight change in the melting point showed a reduction of the drug to a nanocrystalline form. The high rate of exposure showed that most of the drug was converted to the nanocrystalline form. No chemical interactions between the drug and the polymer were observed. The physical interaction is the way a drug is bound to a polymer. These studies have confirmed that as the crystalline nanoparticle size of the crystal decreases; its melting point decreases slightly. A slight change in the melting point showed a reduction of the drug to a nanocrystalline form. The high rate

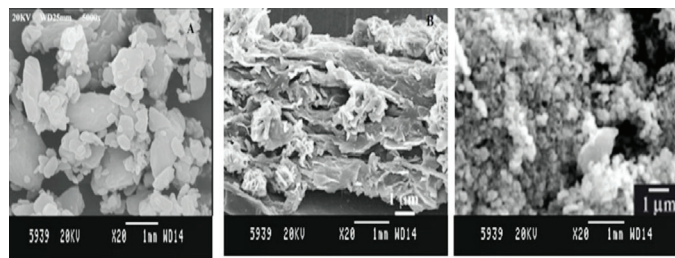


Figure 7. SEM images of orlistat and its BNCs i.e. OSMO-BNC and OSAM-BNC with *Moringa oleifera* and *Aegle marmelos*²⁶

SEM: Scanning electron microscopy, BNCs: Bionanocomposites, OSMO: Orlistat, *Moringa oleifera* gum, OSAM: Orlistat, *Aegle marmelos*

of exposure showed that most of the drug was converted to the nanocrystalline form.

No chemical interactions between the drug and the polymer were observed. The physical interaction is the way a drug is bound to a polymer. These studies have confirmed that as the crystalline nanoparticle size of the crystal decreases; its melting point decreases slightly (Figure 8).

X-ray diffraction

XRD was performed to assess the physical condition of the body and its BNCs. XRD patterns of impure drug (OS), pure polymer (*M. oleifera* and *A. marmelos*) and its BNCs are shown

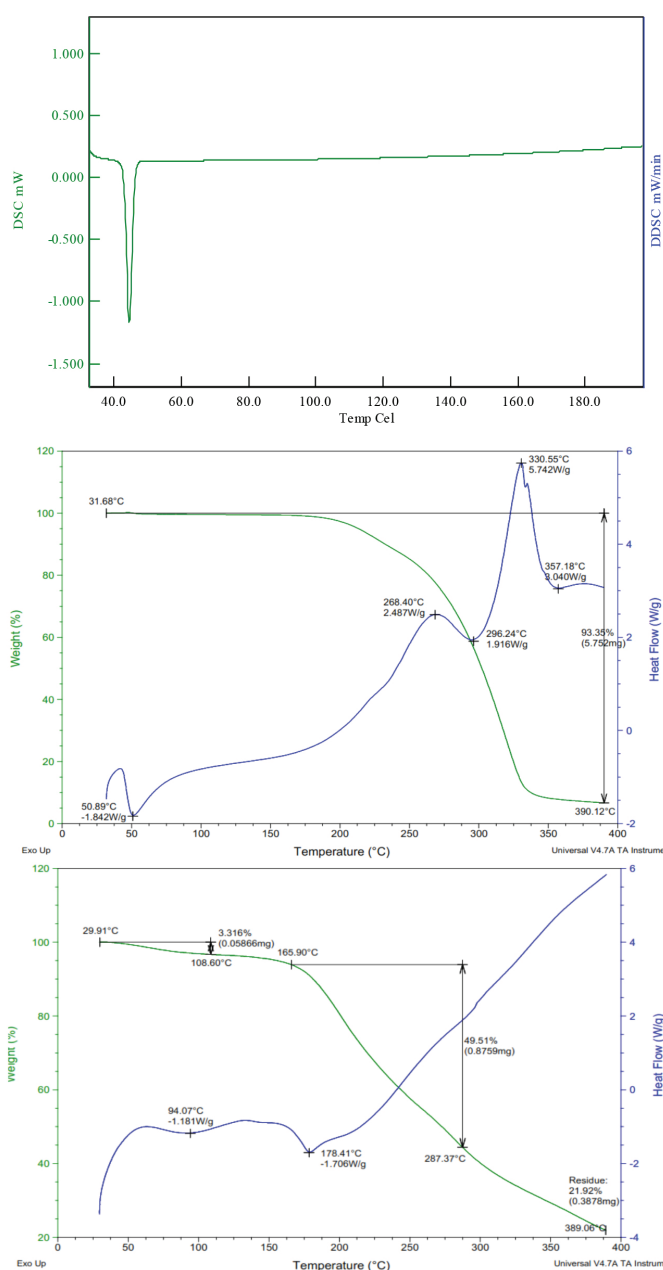


Figure 8. Differential scanning calorimetry of (A) orlistat and its BNCs *i.e.* (B) OSMO-BNC (C) OSAM-BNC with *Moringa oleifera*, and *Aegle marmelos* BNCs: Bionanocomposites, OSMO: Orlistat, *Moringa oleifera* gum, OSAM: Orlistat, *Aegle marmelos*

in Figure 9. The XRD pattern of pure orlistat showed a high crystalline value between 100 and 600, 14.50, 17.50, 19, 21, 24, 25.50, 28, 30, 32 and 35 with a very high value of 24 indicating the crystalline form of orlistat. The XRD patterns of OSMONC and OSAMNC showed a significant decrease in elevation due to the decrease in crystallinity. Decreased levels of BNCs may be due to a decrease in drug size to nanolevel.

Theoretical prediction of solubility

Fedor's method

Fedor has proposed a method for determining the melting parameter without using the compound density. The contribution of the largest number of active groups has been tested, and the method only requires knowledge of the formula formulation of the combination.

Based on Fedor's succession

$$\delta = \sqrt{(\Delta\Delta U/AV)}; = (32700)/37.44 = 29.55 \text{ H}$$

*U always meets a combination of forces

** ΔV retains the molar volume

The result obtained from the above calculation of Fedor's stable orlistat was found to be 29.55 H. The hydrogen concentration is determined after the opening of the ring in the orlistat structure. The total strength must determine the molecular weight in relation to the molar volume (Table 4).

Orlistat bionanocomposite (OSMO-BNC)

A modified BNC *i.e.* OSMO-BNC (orlistat with *M. oleifera*), where it was considered to dissolve, was found at the time of cracking and in the amount observed in FTIR. There was hydrogen binding possible and the melting parameter helped determine it. Fedor's permanent effect was 11.08 H, due to the strong hydrogen bonding in the molecule and the conversion of the other two bonds into bonds that bind together Fedor's BNC orlistat bond also increases and this number of hydrogen bonding increases eventually increases the melting of molecules *i.e.* smearing constantly in Fedor. Additionally, the molar volume is less representative of their numbers.

Orlistat bionanocomposite (OSAM-BNC)

The BNCs prepared namely OSAM-BNC (orlistat with *A. marmelos*), when considered for its detection was found at the time cracking and in the amount observed in FTIR. There was a high hydrogen binding and the melting was determined by a parameter, Fedor's continuous effect δ was 11.56 H. Due to excess hydrogen molecular bonding and the conversion of other double bonds to its binding bonds Fedor's constant of BNC, orlistat also increases and this increase in hydrogen bonding ultimately leads to increased molecular melting, which means an increase in Fedor's consistency.

Hoy's method

The small scheme provided an easy way to measure the amount of solubility parameter in most solvents and polymers. However, the list of constants is not complete. Hoy has published many

jaw-dropping features found in the pressure points of various groups (Table 5).

According to [(cal/cc) 1/2 mol⁻¹] unit

$$\delta = \frac{\sum \text{molar attraction}}{V} = \frac{3110.4}{317.958} = 9.78 \text{H}$$

By using Hoy's formula, the molar attraction for pure orlistat

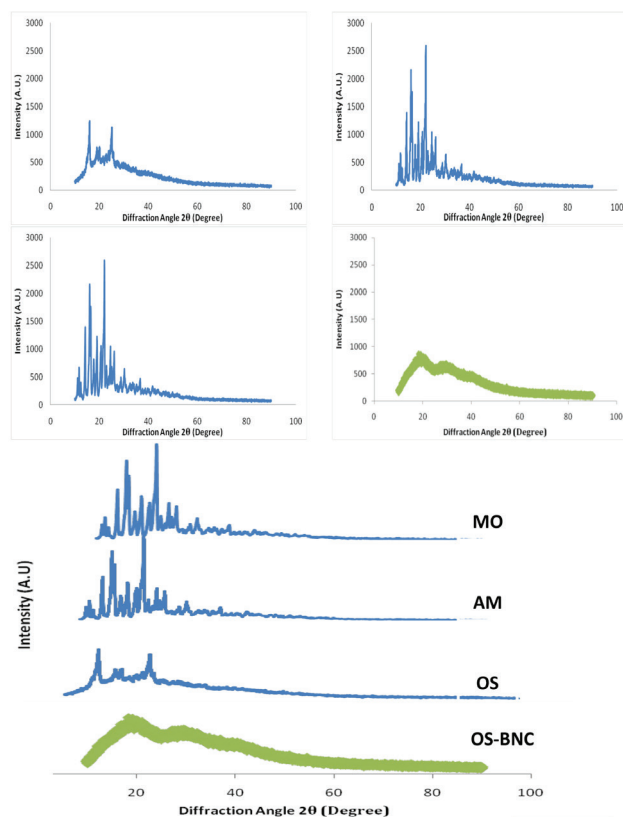


Figure 9. XRD studies of orlistat and its BNCs i.e. OSMO-BNC and OSAM-BNC with *Moringa oleifera* and *Aegle marmelos*

XRD: X-ray diffraction, BNCs: Bionanocomposites, OSMO: Orlistat, *Moringa oleifera* gum, OSAM: Orlistat, *Aegle marmelos*

was calculated and it was found 9.78 H, where is the sum of the group molar attraction constants of the compound Hoftyzer and Van Kreevalen published a series of group molar attraction constants similar to those of small and Hoy.

Orlistat bionanocomposite (OSMO-BNC)

By using Hoy's formula, the molar embrace for OSMO-BNC (orlistat with *M. oleifera*) was calculated and found 23.59 H and which more than that of the pure orlistat that was 9.78 H.

Orlistat bionanocomposite (OSAMNC)

By using Hoy's formula, the molar magnetism for OSAMNC (orlistat with *A. marmelos*) was calculated and found 22.86 H, which was more than that of pure orlistat which was 9.78 H.

Van Kreevalen's solubility parameters

Van Kreevalen derived F_i values for the assistance of atoms i.e., C, H, N, O, halogens, and statutory effects (such as double or tribal bonds, etc.) solubility parameter (δ) can be calculated using the following equation:

$$\delta = \frac{\sum F_i}{V_m}$$

where $\sum F_i$ is the sum of the atomic contributions and V_m is the molar volume (Table 6).

Calculation of solubility parameter and molar volume of pure orlistat by Van Kreevalen's solubility parameter was obtained 7.71 H.

Orlistat bionanocomposite (OSMO-BNC)

Calculation of solubility parameter and molar volume of OSMONC (orlistat with *M. oleifera*) by Van Kreevalen's solubility parameter was obtained 8.02 H which is more than the pure form of orlistat i.e. 7.71 H.

Orlistat bionanocomposite (OSAM-BNC)

The calculation of the melting point and molar volume of OSAMNC (orlistat with *A. marmelos*) by Van Kreevalen's melting

Table 4. Calculation of δ value of orlistat by F, G, and C methods

Fragments/groups	No of groups	$\Delta\Delta U^*$ for each (cal.mol ⁻¹)	Total $\Delta\Delta U$	ΔV^{**} for each (m ⁻¹ mol ⁻¹)	Total ΔV
-CH ₃	4	1125	4500	33.5	134
-CH ₂	18	1180	21240	16.1	289.8
-C	2	350	700	19.2	-38.4
-CH	3	820	2460	-1.0	-3
-NH	1	1000	1000	-9.0	-9.0
-O	2	800	1600	3.8	7.6
Ring closer	-	-	-	-	-
Conjugate bond	3	400	1200	-2.2	-6.6
-	-	-	$\Sigma = 32700$	-	$\Sigma = 37.44$

parameter was obtained at 9.9 H, which indicates more than the purest form of the drug *i.e.*, 7.71 H.

It was noted that the combination of hydrogen with the orlistat molecule was proposed to potentially improve solubility. As the formation of the impact on the established BNCs will be in line with the need to study. A greater number of covalent and hydrogen bonds were formed, when drugs were incorporated into their BNCs and natural carriers.

From the structure obtained, -O -OH bond to indicate hydrogen bond and CH-OH meaning bond covalent bond and due to such an interaction between selected drugs and gums held in covalent bonds and stated that hydrogen bonding between low energies must break such bond. Additionally, the weak Vander Waals strength found in the prepared BNCs is why the molecular meltdown is enhanced in the proposed way.

CONCLUSION

Application of natural polymers such as *M. oleifera* and *A. marmelos* for the generation BNC of orlistat by MIND simple, convenient and cost effective method. Further, use of natural carriers influences the physicochemical properties of drug. MIND shows promising approach for enhancing the solubility and dissolution rate of prepared BNCs. The characterization approach using FTIR, XRD, DSC, and SEM explores that orlistat generated into the BNCs showed significant liability to enhance the solubility and increase the dissolution rate. The application of the HSP and hildebrand solubility parameters including Fedor's constant, Hoy's molar attraction, and Van Kreevalen system in prediction and determination of the solubility of prepared BNCs were revealed its utilization in pharmaceutical formulation. It was found that there was significant enhanced solubility of optimized ratios compared with pure entities. Hence, it was concluded here HSP provides acceptable determination of solubility in pharmaceutical science.

Table 5. Calculation of solubility parameter of orlistat based on Hoy's molar attractions

Fragments/groups	No of groups	$\Delta\Delta U^*$ for each (cal.mol ⁻¹)	Total $\Delta\Delta U$	ΔV^{**} for each (m ⁻¹ mol ⁻¹)	Total ΔV
-CH ₃	4	148.36	593.44	21.548	86.192
-CH ₂	18	131.5	2.367	15.553	279.954
-C=O	2	262.96	525.62	17.265	34.53
-CH	1	85.99	85.99	9.557	9.557
-NH	1	180	180	8.774	8.774
-O	2	114.98	229.96	6.46	12.92
CH=O	1	117.12	117.12	13.417	13.417
Six membered ring	1	-23.44	-23.44	0	0
Conjugated bond	3	23.26	69.78	0	0
Ortho	2	9.69	19.38	0	0
Meta	2	6.6	13.2	0	0
Base value	0	0	0	0	0
-	-	-	$\Sigma = 4178$	-	$\Sigma = 431.97$

Table 6. Calculation of solubility parameter and molar volume of orlistat by Van Kreevalen's solubility parameter

Fragments/groups	No of groups	Fd	Total Fd	Fp	Total Fp	Fp2	Uh	Total Uh
-CH ₃	4	420	1680	0	0	0	0	0
-CH ₂	18	270	4860	0	0	0	0	0
-C=O	2	0	0	0	0	0	0	0
-CH ₂	1	80	80	0	0	0	0	0
-NH	1	280	280	610	610	372100	8400	8400
-O	2	100	200	410	820	672400	3000	3000
-CH=O	1	200	1800	0	0	0	0	0
6/5 member ring	1	190	190	0	0	0	0	0
-	-	-	$\Sigma = 8890$	-	$\Sigma = 1044$	-	-	$\Sigma = 14400$

Ethics

Ethics Committee Approval: Not required.

Informed Consent: Not required.

Peer-review: Externally peer-reviewed.

Authorship Contributions

Surgical and Medical Practices: S.P., Concept: S.P., Design: S.P., Data Collection or Processing: K.K., L.D., K.N., Analysis or Interpretation: V.P., Literature Search: V.P., R.P., Writing: V.P.

Conflict of Interest: No conflict of interest was declared by the authors.

Financial Disclosure: The authors declared that this study received no financial support.

REFERENCES

- Shinde SM, Jadhav CM, Kate VK, Payghan SA, D'souza JL. Physicochemical assessment of pharmaceutical salt forms: a quality attribute. *Int J Pharm Sci Invent*. 2014;2:46-53.
- Pathak CD, Savjani KT, Gajjar AK, Savjani JK. Cocrystal formation of paracetamol with indomethacin and mefenamic acid: an efficient approach to enhance solubility. *Int J Pharm Pharma Sci*. 2013;5:414-419.
- Payghan SA, Shrivastava DN. Potential of solubility in drug discovery and development. *Pharm Rev*. www.pharmainfo.net
- Neha O, Bala P. Advances in solubility enhancement techniques. *Int J Pharm Sci Rev Res*. 2013;21:351-358.
- Patwekar SL, Jamkhane P, Gattani SG, Payghan SA. Nanobiocomposite a new approach to drug delivery system. *Asian J Pharm*. 2016;10(Suppl):646-656.
- Bhat MR, Sharma S, Derkar GK, Chimkode RM, Payghan SA. Microwave-generated bionanocomposite for solubility enhancement of nifedipine. *Asian J Pharm*. 2016;10(Suppl):741-749.
- Shewale S, Shete AS, Doijad RC, Kadam SS, Patil VA, Yadav AV. Formulation and solid state characterization of nicotinamide-based cocrystals of fenofibrate. *Indian J Pharm Sci*. 2015;77:328-334.
- Khabade SS, Chopade SS, Gaikwad ER, Payghan SA. Potential screening of spray dried solid dispersion of orlistat using three dimensional solubility parameter. *Asian J Pharm*. 2017;11(Suppl):760-772.
- Payghan SA, Patwekar S, Kate VK, Khavane K, Purohit SS. Pharmaceutical solid polymorphism: approach in regulatory consideration. *J Glob Pharma Technol*. 2010;1:45-53.
- Vo CL, Park C, Lee BJ. Current trends and future perspectives of solid dispersions containing poorly water-soluble drugs. *Eur J Pharm Biopharm*. 2013;85:799-813.
- Mounika P, Raj SV, Divya G, Gowramma A, Vijayamma G. Preparation and characterization of novel co-crystal forms of fexofenadine. *Int J Innov Pharm*. 2015;6:458-463.
- Mohammad MA, Alhalaweh A, Velaga SP. Hansen solubility parameter as a tool to predict cocrystal formation. *Int J Pharma*. 2011;407:63-71.
- Belmares M, Blanco M, Goddard WA 3rd, Ross RB, Caldwell G, Chou SH, Pham J, Olofson PM, Thomas C. Hildebrand and hansen solubility parameters from molecular dynamics with applications to electronic nose polymer sensors. *J Comput Chem*. 2004;25:1814-1826.
- Savova M, Kolusheva T, Stourza A, Seikova I. The use of group contribution method for predicting the solubility of seed polyphenols of *Vitis vinifera* L. within a wide polarity range in solvent mixtures. *J Chem Technol Metall*. 2007;42:295-300.
- Martin A, Newburger J, Adjei A. Extended hildebrand solubility approach: solubility of theophylline in polar binary solvents. *J Pharm Sci*. 1980;69:487-491.
- Thimmasetty J, Subrahmanyam CVS, Vishwanath BA, Babu S. Solubility parameter estimation of celecoxib by current methods. *Asian J Research Chem*. 2009;2:188-195.
- Kopparam M, Subrahmanyam C. V. S, Juturu T, Kumar S. N. Solubility parameter of gatifloxacin and its correlation with antibacterial activity. *J Solution Chem*. 2012;41:381-391.
- Gaikwad ER, Khabade SS, Sutar TB, Payghan SA. Preparation and characterization of molecular complexes of fenofibrate cocrystal. *Asian J Pharm*. 2017;11(Suppl):745-759.
- Fedors RF. A method for estimating both the solubility parameters and molar volumes of liquids. *Polym Eng Sci*. 1974;14:147-154.
- Rathi PB, Mourya VK. Extended hildebrand solubility approach: satranidazole in mixtures of dioxane and water. *Indian J Pharm Sci*. 2011;73:315-319.
- Schultheiss N, Newman A. Pharmaceutical cocrystals and their physicochemical properties. *Cryst Growth Des*. 2009;9:2950-2967.
- Fukte SR, Wagh MP, Rawat S. Coformer selection: an important tool in cocrystal formation review article. *Int J Pharm Pharm Sci*. 2014;6:9-14.
- Shaikh K, Patwekar S, Payghan S, Souza JD. Dissolution and stability enhancement of poorly water soluble drug - lovastatin by preparing solid dispersions. *Asian j Biomed Pharm Sci*. 2011;1:24-31.
- Payghan SA, Purohit SS, Shrivastava DN. Non-aqueous emulsion: versatile vehicle for drug delivery. *Pharm Rev*. 2008. www.pharmainfo.net
- Nangare KA, Powar SD, Kate VK, Khavane KK, Payghan SA. Nanosuspension: potential applications of nano therapeutics in ocular delivery. *Mod Appl Bioequiv Availab*. 2018;3:1-10.
- Nangare KA, Powar SD, Kate VK, Patwekar SR, Payghan SA. Therapeutics applications of nanosuspension in topical/ mucosal delivery drug delivery. *J Nanomed Res*. 2018;7:26-36.
- Yadav AV, Shete AS, Dabke AP, Kulkarni PV, Sakhare SS. Co-crystals: a novel approach to modify physicochemical properties of active pharmaceutical ingredients. *Indian J Pharm Sci*. 2009;71:359-370.
- Sarda A, Powar S, Nangare KA, Payghan SA. Formulation and characterization of sublingual tablet for rapid absorption and taste masking of tenoxicam. *Inventi Rapid: Pharm Tech*. 2018:29-42.
- Alexandre M, Dubois P. Polymer-layered silicate nanocomposites: preparation, properties and uses of a new class of materials. *Mater Sci Eng*. 2000;28:1-63.
- Sonawane AR, Rawat SS, Bhagyashree K, Marathe R. Crystal engineering of nabumetone by cocrystallization. *Int J Pharm Pharm Sci*. 2014;3:22-29.
- Sanjay AN, Manohar D, Bhanudas SR. Pharmaceutical cocrystallization: a review. *J Adv Pharm Education Res*. 2014;4:388-396.

-
32. Gaikwad ER, Khabade SS, Sutar TB, Bhat MR, Payghan SA. Three dimensional Hansen solubility parameters as predictors of miscibility in cocrystal formation. *Asian J Pharm.* 2017;11:302-318.
 33. Patel JR, Carlton RA, Needham TE, Chichester CO, Vogt FG. Preparation, structural analysis, and properties of tenoxicam cocrystals. *Int J Pharm.* 2012;436:685-706.
 34. Laszlo F. Cambridge structural database analysis of molecular complementary in cocrystals. *Cryst Growth Des.* 2009;9:1436-1443.



13, 14-Epoxyoleanan-3-ol-acetate: A Male Fertility-Enhancing Constituent from Hexane Fraction of *Momordica charantia* L. (Cucurbitaceae)

✉ Oluwasegun ADEDOKUN^{1*}, ✉ Adebayo GBOLADE¹, ✉ Bunyaminu AYINDE²

¹Igbinedion University, College of Pharmacy, Department of Pharmacognosy, Okada, Nigeria

²University of Benin, Faculty of Pharmacy, Department of Pharmacognosy, Benin City, Nigeria

ABSTRACT

Objectives: Male infertility has been associated with oxidative stress-induced and/or microbial induced in some men. The use of medicinal plants to overcome oxidative stress-induced infertility cannot be over emphasized. Hence, the aim of this research was to isolate the antilipid peroxidation (an index of usage for treating oxidative stress-induced male infertility) bioactive principle from *Momordica charantia* using bioactivity-guided isolation.

Materials and Methods: *n*-Hexane fraction from the crude ethanol extract obtained by Soxhlet extraction of aerial parts (without fruit) of bitter melon, *M. charantia*, was assessed for *in vitro* lipid peroxidation, followed by bioactivity-guided isolation of bioactive principles using *in vitro* lipid peroxidation as an index of aphrodisiac and male fertility enhancer.

Results: Fractionation of the active *n*-hexane fraction using vacuum liquid chromatography (VLC) gave five pooled fractions on the basis of their thin layer chromatography (TLC) characteristics (*n*-hexane: EtOAc, 2:3, sulphuric acid spray). *In vitro* activity of the most active VLC fraction C was less than that of the positive control, vitamin E. Further fractionation of VLC-C by open column chromatography on silica gel led to the isolation of a compound which was purified by preparative-TLC. The purified compound, 10 mg/mL (*R*_f 0.54, TLC silica gel, *n*-hexane: ethyl acetate; 2:3) was equipotent with vitamin E (25 mg/mL) in reducing peroxidation of polyunsaturated fatty acids *in vitro*. Structural elucidation by NMR (¹H, ¹³C) and mean mass spectroscopy confirmed the identity of the new bioactive compound as 13, 14-epoxyoleanan-3-ol-acetate.

Conclusion: This study scientifically validates the traditional claim of *M. charantia* as an aphrodisiac or male fertility enhancer and suggests that 13, 14-epoxyoleanan-3-ol-acetate might be responsible for the observed activity.

Key words: *Momordica charantia*, *n*-hexane fraction, *in vitro* lipid peroxidation assay, 13, 14-epoxyoleanan-3-ol-acetate, vitamin E, VLC

INTRODUCTION

Sexual dysfunction is a serious medical and social problem that occurs in 10-25% of men and 25-63% of women.^{1,2} Among men aged 40-70 years, estimated 34.8% have moderate to complete erectile dysfunction.² This condition can be managed *via* psychotherapeutic and pharmacotherapeutic approaches.^{1,3}

Free radicals are present in seminal plasma, some of the most prevalent reactive oxygen species (ROS) are hydroxyl,

superoxide, and hydrogen peroxide radicals. During oxidative stress, excessive production of the ROS or free radicals in seminal plasma tends to have a destructive effect of the sperm cells and in turn induce oxidative stress induced male infertility. Moreover, antioxidants in seminal plasma aid in scavenging the harmful effect of the ROS *via* the donation of electrons to the electron-impaired radicals, thereby reduce their influence.⁴ Spermatozoa in mammals are rich in polyunsaturated fatty acids (PUFA) as a result of that they are very prone to membrane lipid

*Correspondence: adedokun.oluwasegun@iuokada.edu.ng, Phone: +2348035485083, ORCID-ID: orcid.org/0000-0001-7264-3695

Received: 09.07.2020, Accepted: 10.08.2021

©Turk J Pharm Sci, Published by Galenos Publishing House.

peroxide ion and ROS attack. Moreover, a balance is maintained between the amount of ROS produced and that scavenged arises, when this disturbed equilibrium toward pro-oxidants in semen and vaginal secretions can induce an oxidative stress on spermatozoa, which in turn can cause its damage and cause infertility.⁴

Theoretically, oxidative stress-induced sperm cells results in decreased sperm motility, presumably by a rapid loss of intracellular adenosine triphosphate leading to axonemal damage, decreased sperm viability and increased midpiece morphology defects, with deleterious effects on sperm capacitation and acrosome reaction.⁵ However, the key mechanism of ROS-induced sperm damage leading to infertility is principally induced by the effect peroxidation of sperm membrane lipid.⁶ Among the medicinal plants used in treating numerous diseases including male sexual dysfunction and infertility is *Momordica charantia* L. (Cucurbitaceae).⁶⁻¹⁰ It is a climbing vine commonly found in the tropics and subtropics. It is also a tropical vegetable employed in ethnomedicine for the treatment of various diseases including diabetes, malaria and dysentery, and as a stomachic, stimulant, emetic, antibilious, and laxative.¹¹

Previously, *M. charantia* has been investigated for analgesic and antipyretic,^{7,8} antimicrobial,⁹ and anti-HIV activities. Bioactive compounds responsible for the widely investigated antidiabetic and hypoglycemic activities have been linked to cucurbitanetriterpenoids.¹¹⁻¹³ The cucurbitane-type triterpenoids have been extensively isolated from various parts of *M. charantia*.¹¹⁻¹⁵

Until date, literature information is unavailable on male fertility enhancing the potential of *M. charantia*, and only a mention of traditional use of the Nigerian plant as an aphrodisiac is known.^{7,9,16} We therefore investigated *in vitro* fertility activity (using lipid peroxidation as index) of the most active hexane fraction of the aerial parts (it contain no fruit) by lipid peroxidation assay, and isolated the bioactive constituent to rationalize the traditional claim of the plant as an aphrodisiac plant by the people of Esan community in Edo State, Nigeria.

MATERIALS AND METHODS

Plant collection and authentication

M. charantia used in the research was collected from wild in the Ewu community of Esan-Central Local Government Area of Edo state (Nigeria) in January 2012 and authenticated at the herbaria in Paxherbal Laboratories, Ewu (Nigeria) by Professor J. C. Okafor and the Federal Forestry Research Institute of Nigeria, Ibadan, Oyo State (FHI 109577). Voucher specimens were also deposited in these herbaria and at the herbarium of Department of Pharmacognosy, Faculty of Pharmacy, University of Benin, Nigeria.

Extraction and solvent partitioning

1.2 kg of the dried aerial part of the plant was extracted to exhaustion with absolute ethanol in a Soxhlet apparatus. The extract was reduced *in vacuo* to yield a residue that was

refrigerated at 4°C until needed. The crude ethanol extract was partitioned into *n*-hexane, chloroform, and water using a separatory funnel and total yield of the fractions was determined.

Chromatographic studies

Vacuum liquid chromatography (VLC): *n*-Hexane fraction (21.00 g) was packed onto a sintered glass Buchner filter funnel, loaded with silica gel for analytical thin layer chromatography (TLC) without binder and eluted with *n*-hexane, chloroform, and methanol mixtures to yield 17 fractions (x 200 mL each). The fractions were bulked according to their TLC profile (*n*-hexane: EtOAc, 2:3; H₂SO₄ spray reagent) into 5 main fractions (A-E), weighed and bio-assayed *in vitro*.

Bottom of form

Column chromatography (CC)/preparative-TLC: Conventional open CC (30 cm long and 5 cm diameter) of the most active VLC fraction C was done. The silica gel used was 70-230 mesh size (0.063-0.200 mm) particle size. The silica gel was loaded on top of the column and allowed to settle. VLC fraction C (3 g) was diluted, adsorbed onto silica gel and poured on top of the column which was eluted with *n*-hexane, chloroform, ethyl acetate, and methanol mixtures. Eluates (151 fractions x 10 mL) were collected into test tubes and bulked according to their TLC characteristics (silica gel, *n*-hexane: ethylacetate, 2:3; H₂SO₄ spray reagent) into 5 main fractions CC (A-E), dried, and weighed. The most active fraction, *i.e.* CC-D (0.63 g), was subjected to prep-TLC (commercial type) with *n*-hexane: ethyl acetate (4:6). The bands were scrapped, eluted with methanol, filtered, and evaporated in a fume closet to yield needle-shaped crystals.

Spectroscopic studies

1D NMR (¹H and ¹³C NMR) as well as 2D NMR (DEPT, HMBC) experiments were performed on the isolated compound. Mean mass spectroscopy (MS) was recorded on an Agilent Technologies S973 network mass selective detector and the spectrum was compared with database NIST02 reference spectra library.

In vitro lipid peroxidation assay

Fresh but frozen Titus fish (*Scomber japonicum*) were purchased from the Ekpoma market in Benin City, washed, and fleshy muscular parts will be used. The tissue homogenate was prepared as described earlier as the modified method of Luotola and Luotola.¹⁷ Twenty grams of raw fish muscle tissue was turned into a paste in a mortar. 200 mL distilled water was added and the mixture was cooked at a temperature of 100°C for 15 min followed by thoroughly blending in an electric blender (10% w/v). This, in turn, was filtered and unbroken cells along with cell debris were removed by centrifugation at 1500 rpm for 15 min. The supernatant thus obtained was termed as a homogenate and used for the *in vitro* lipid peroxidation study. A lipid peroxidation study was conducted almost immediately after the homogenate preparation. 1 mL of each VLC fraction (100 mg) was added to 1 mL of the fish homogenate and mixed together. Thiobarbituric (TBA) reactivity in the homogenate

was determined by following a modified method of Luotola and Luotola.¹⁷ 3 mL of 20% trichloroacetic acid was added, mixed, and centrifuged for 15 min. Then, TBA (0.67% w/v, 1 mL) was added to 2 mL supernatant, mixed, and kept in a boiling water bath for 10 min, which, after, cooled down to room temperature. TBA chromogen (intensity of the pink coloured complex) was measured at 532 nm against blanks using a ultraviolet spectrophotometer (Thermo spectronic, Genesys 20 model). Vitamin E was used as the reference. A graph of absorbance against concentration will be plotted using the data obtained for pure vitamin E. Thiobarbituric acid reactive substances (TBARS) of the extract were evaluated from the standard curve and expressed as nmol TBARS *per* mg of tissue. This procedure was repeated for the positive control (vitamin E, 25 mg/mL), negative control (5% Tween 80, 1 mL), column fractions, and the isolated compound (10 mg/mL). All results were replicated three times and the mean was determined.

Statistical analysis

All data collected from the entire study was analyzed using Microsoft excel and Statistical Package for Social Sciences (SPSS) version 17 (when needed). All values in the test were presented as mean \pm standard error of mean (SEM). Statistical differences between the means of the various groups were evaluated by One-Way ANOVA and tested at 0.05 level of significance. The results were considered statistically significant if the *p* values were 0.05 or less.

RESULTS

Lipid peroxidation of bulked VLC fractions of the hexane fraction

From an earlier study described by Adedokun et al.¹⁸, the *n*-hexane fraction was the most active aphrodisiac agent, *in vivo* and *in vitro* of the three fractions from the crude ethanol extract of *M. charantia*. The result of lipid peroxidation of the entire bulked VLC fractions (VLC-A to VLC-E) is shown in Table 1.

The values above represent the mean \pm SEM of 5 replicates. Values with superscripts indicate significant different relative to the negative control (5% Tween 80) at *p* \leq 0.05 across the

column for each time using One-Way ANOVA (non-parametric). From Table 1, VLC-C showed the highest degree of inhibition of polyunsaturated fatty acids in the fish tissue over time with lowest and highest amounts of malondialdehyde observed at 0 min and 240 min as 98.00 ± 0.01 and 171.00 ± 0.08 respectively, significantly different from negative control at *p* \leq 0.05 at a similar time interval as shown in Table 1.

Lipid peroxidation of isolated compound and vitamin E

The result of comparative lipid peroxidation study of isolated compound X (10 mg/mL) with both vitamin E (26 mg/mL) as well as the negative control (5% Tween 80) is shown in Figure 1. No significant difference was observed in the activity of compound X (10 mg/mL) and positive control (vitamin E) 26 mg/mL using an *in vitro* model.

Spectroscopic analysis of compound X

Compound X was subjected to spectroscopic analysis to identify the nomenclature of the unknown bioactive compound, NMR studies (¹H, ¹³C, DEPT, and HMBC) and MS, as shown in Figures 2-6.

DISCUSSION

Bioactivity-guided studies by VLC with the *n*-hexane, chloroform, and methanol mixtures gave five bulked VLC fractions: -VLC-A (2.8 g, 13.4%), VLC-B (2.6 g, 12.5%), VLC-C (3.1 g, 14.7%), VLC-D (11.6 g, 55.2%), and VLC-E (0.8 g, 4.0%). In *in vitro* aphrodisiac screening of the VLC fractions (100 mg/mL each), ability of the fractions to reduce lipid peroxidation significantly increased with time (Table 1).

The potency of the fractions can be ranked as the following: VLC-C > VLC-D > VLC-A > VLC-B > VLC-E. Of all five VLC fractions, VLC-C had the highest potential in reducing the destruction of sperm, giving 171 nmoles malondialdehyde *per* gram of fish tissue in 240 min, which is less than 28 nmoles malondialdehyde *per* gram of fish tissue produced by the positive control, vitamin E, implying 16% potency.

VLC-C, upon open CC and elution with *n*-hexane, ethyl acetate, methanol mixtures gave six bulked fractions CC (A-E) of which

Table 1. *In vitro* lipid peroxidation of bulked VLC fractions of hexane fraction

Sample	n moles of malondialdehyde/gm tissue/time				
	0 min	60 min	120 min	180 min	240 min
VLC-A (100 mg/mL)	300.00 \pm 0.01	324.00 \pm 0.03	334.00 \pm 0.01	335.00 \pm 0.11	330.00 \pm 0.13
VLC-B (100 mg/mL)	327.00 \pm 0.21	448.00 \pm 0.14	500.00 \pm 0.16	548.00 \pm 0.22	523.00 \pm 0.20
VLC-C (100 mg/mL)	98.00 \pm 0.01*	124.00 \pm 0.07*	137.00 \pm 0.09*	161.00 \pm 0.09*	171.00 \pm 0.08*
VLC-D (100 mg/mL)	206.00 \pm 0.08	334.00 \pm 0.04	224.00 \pm 0.09	241.00 \pm 0.05	290.00 \pm 0.05
VLC-E (100 mg/mL)	647.00 \pm 0.01	635.00 \pm 0.03	633.00 \pm 0.02	610.00 \pm 0.04	614.00 \pm 0.05
Vitamin E (positive control, 25 mg/mL)	25.17 \pm 0.02*	40.67 \pm 0.23*	27.92 \pm 0.05*	28.33 \pm 0.07*	28.08 \pm 0.09*
5% Tween 80 (negative control, 1 mL)	275 \pm 0.05	282 \pm 0.03	295 \pm 0.01	299 \pm 0.06	302 \pm 0.02

The values above are mean of three replicates. n= 3. n \pm SEM. Samples with superscript * indicate significant difference at *p* < 0.05 relative to negative control using One-Way ANOVA (Kruskal-Wallis test) while samples with no superscript * indicate no significant difference at *p* < 0.05 relative to negative control using One-Way ANOVA (Kruskal-Wallis test). VLC: Vacuum liquid chromatography

CC-D (1 g) was the most active *in vitro*. A bioactive compound (50 mg) was finally isolated from CC-D by prep-TLC (hexane: ethyl acetate, 6:4). It gave R_f 0.54 (TLC silica gel, *n*-hexane: ethyl acetate; 2:3, brown on spraying with concentrated H_2SO_4). *In vitro* antilipid peroxidation bioassay of this compound showed a high degree of reduction of the peroxidation of PUFA that was stable over the experimentation period and parallel that of 25 mg of vitamin E (α -tocopherol) producing 30 nmoles malondialdehyde *per gram fish tissue* in 240 min (Figure 1).

Spectroscopic information from NMR studies (1H , ^{13}C , DEPT, and HMBC) and MS suggested the bioactive compound to be a pentacyclic triterpene, 13, 14-epoxyoleanan-3-ol-acetate (M^+ 470, $C_{31}H_{50}O_3$) as shown in Figures 2-7 below.

This is the first time this compound has been reported in *M. charantia* and according to the literature, no direct pharmacological property has been associated with this compound.

To date, only the structurally-related oleanan compounds, soyasaponins I-III have been isolated from the Japanese *M. charantia*.¹⁹ However, Venkatesh et al.²⁰ recently reported the isolation of 3-hydroxy-21-normethyl-19-vinylidenylursane, an *in*

vivo aphrodisiac compound, from a Bombacaceae plant, *Durio zibenthinus* fruit. A wide variety of cucurbita triterpenes and triterpene saponins have been isolated from *M. charantia*. Notable among these triterpenes are di- and tri-hydroxycucurbitadienes with antidiabetic activity, momordicolide (10E)-3-hydroxyl-dodeca-10-en-9-olide and momordicophenolide A, cucurbitane-type triterpenoid saponins such as momordicosides M, N, O, L, F1, F2, G, L, A, K, U, V, and W.²¹⁻²³ However, none of these triterpenes is associated with aphrodisiac activity.

According to Kumar et al.¹⁰ *M. charantia* has been reported to negatively affect fertility in both male and female animals, without mention of any active constituent. The present study has established improvement in sexual activity of normal male rats by *M. charantia*. Apart from *M. charantia*, other Nigerian medicinal plants with reported *in vitro* lipid peroxidation activity are *Syzygium aromaticum* flower bud and *Fadogia agrestis* stem and *Terminalia catappa* seeds from elsewhere.^{17,24-27} Reviews on aphrodisiac and male fertility enhancing plants have been published.^{2,3,7,8} antioxidant activity of *M. charantia* might be connected with its ability to reduce lipid peroxidation, and hence protect sperm.^{26,27} It therefore has potential for treating sperm-related male infertility. *M. charantia* is one of a traditional aphrodisiac plant that has not yet been fully explored. This study is a continuation of our investigation into the aphrodisiac activity of *M. charantia*.

CONCLUSION

This investigation establishes *in vitro* male fertility enhancing activity for the aerial part of *M. charantia* and suggested bioactivity to be due to a pentacyclic triterpene 13, 14-epoxyoleanan-3-ol-acetate isolate from the most active *n*-hexane fraction for the first time. It has not been previously isolated from Cucurbitaceae or elsewhere. The *in vitro* aphrodisiac activity of the compound compared with that of vitamin E. Its structure was confirmed by NMR, MS, and by comparison with a computer database. The study further lends credence to the ethnopharmacological claim

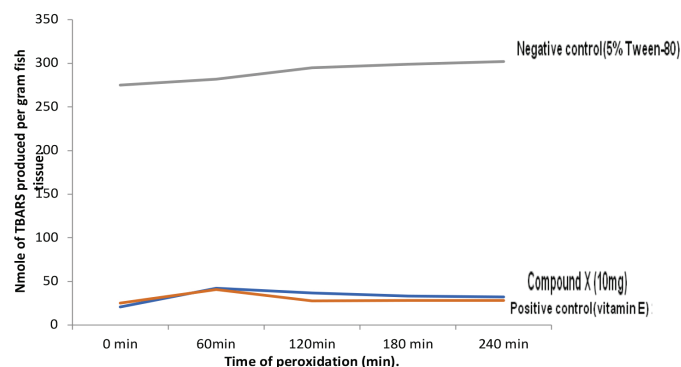


Figure 1. *In vitro* lipid peroxidation of bioactive compound and vitamin E (25 mg/mL)

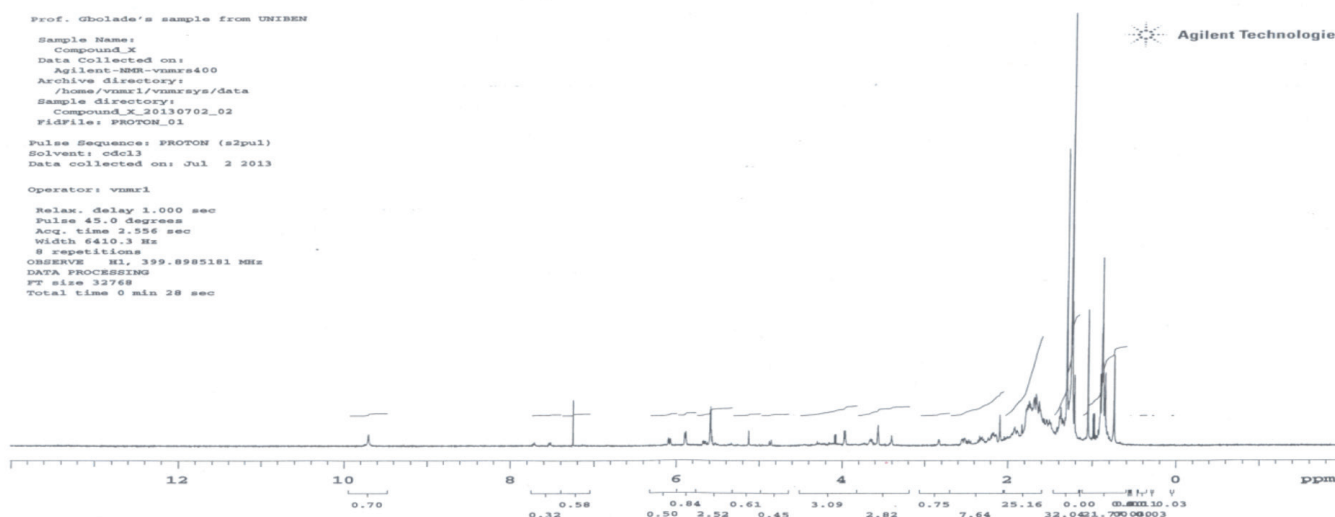


Figure 2. 1H NMR of isolated compound X

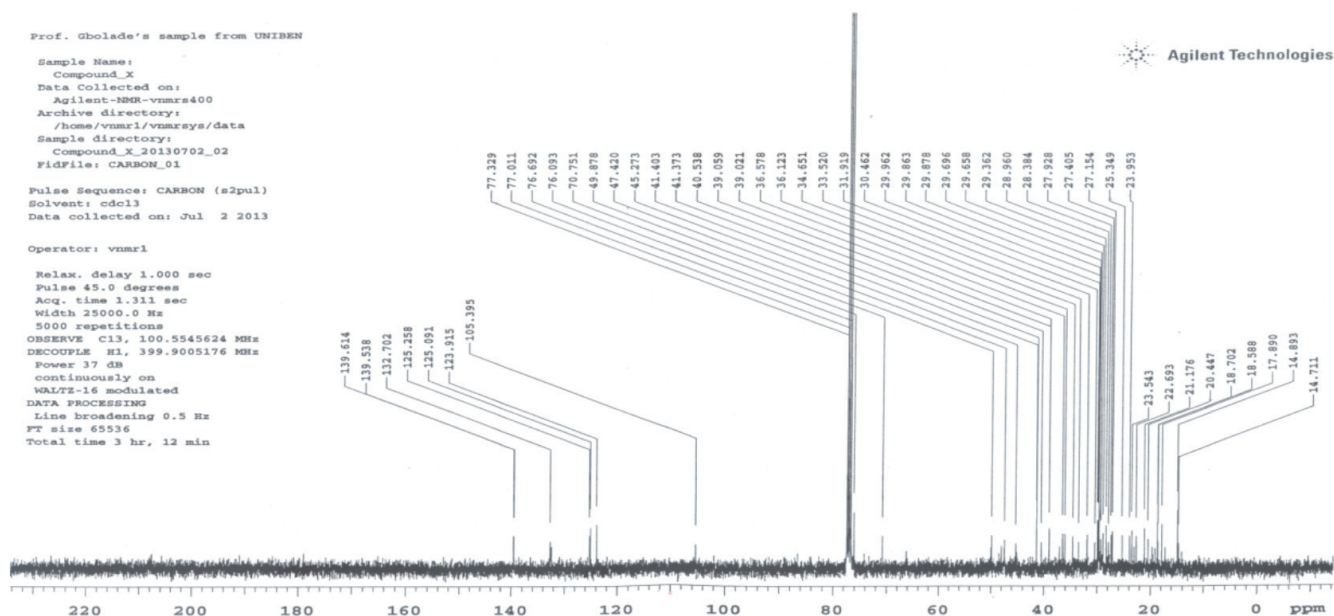
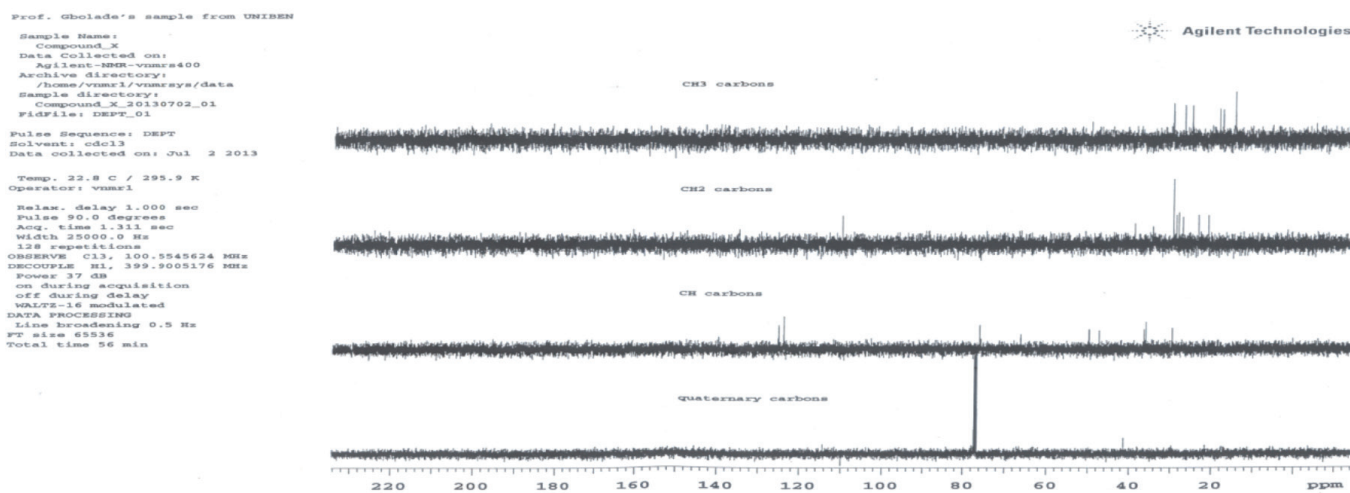
Figure 3. ^{13}C NMR of isolated compound X

Figure 4. DEPT of isolated compound X

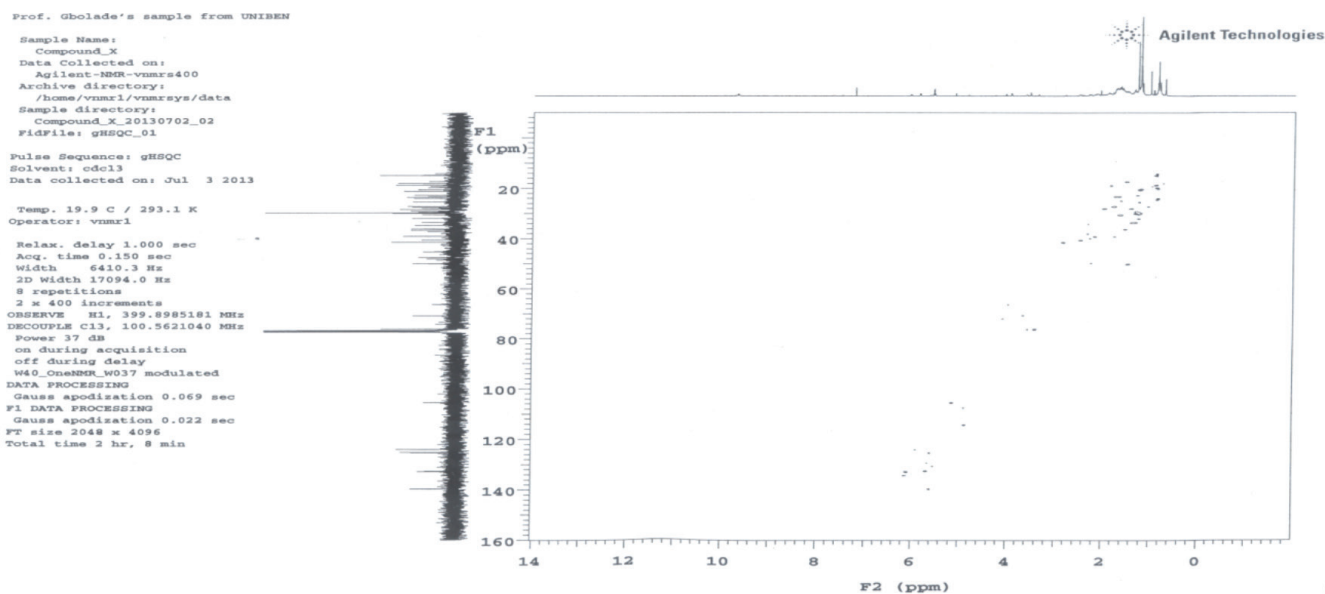


Figure 5. HMBC of isolated compound X

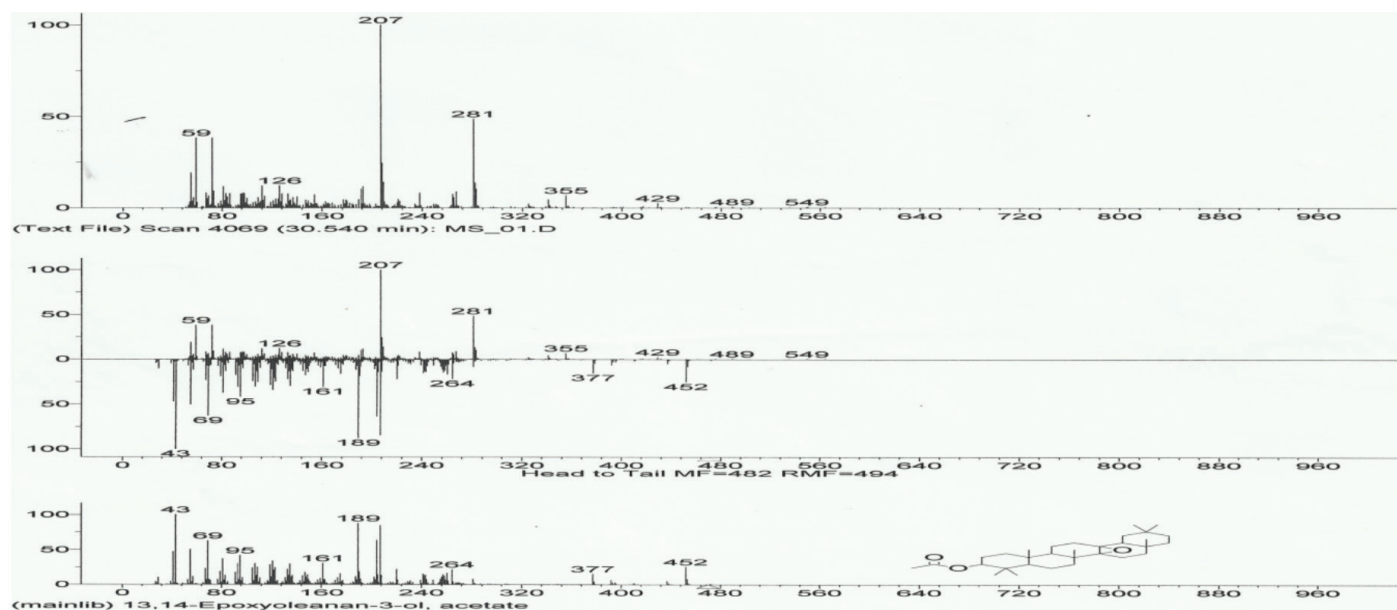


Figure 6. GC-MS of isolated compound X

GC-MS: Gas chromatography-mass spectrometry

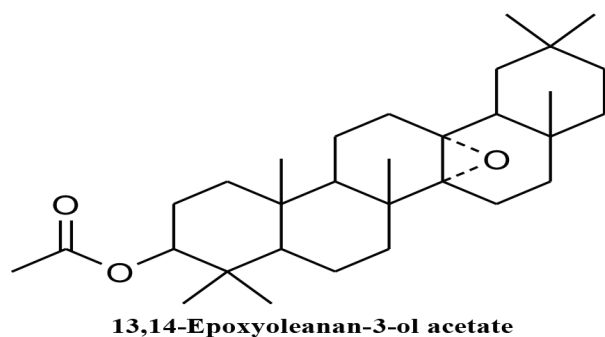


Figure 7. Suggested structure of compound X

of the plant as an aphrodisiac by the people of Esan Central Local Government Area of Edo State in Nigeria.

ACKNOWLEDGEMENTS

The authors are grateful to the Rev. Fr. Anslem Adodo and Paxherbal Laboratories, Ewu, Edo State, for access to laboratory facilities. We also thank the organizers of the WANNPRES 2014 congress for the opportunity given to present some findings of this research.

REFERENCES

- Guay AT, Spark RF, Bansal S, Cunningham GR, Goodman NF, Nankin HR, Petak SM, Perez JB; American Association of Clinical Endocrinologists Male sexual dysfunction task force. American Association of Clinical Endocrinologists medical guidelines for clinical practice for the evaluation and treatment of male sexual dysfunction: a couple's problem-2003 update. *Endocr Pract.* 2003;9:77-95. Erratum in: *Endocr Pract.* 2008;14:802-803.
- Patel DK, Kumar R, Prasad SK, Hemalatha S. Pharmacologically screened aphrodisiac plant- a review of current scientific literature. *Asian Pac J Trop Biomed.* 2011;(Suppl)S131-S138.
- Malviya N, Jain S, Gupta VB, Vyas S. Recent studies on aphrodisiac herbs for the management of male sexual dysfunction-a review. *Acta Pol Pharm.* 2011;68:3-8.
- Dandekar SP, Nadkarni GD, Kulkarni VS, Puneekar S. Lipid peroxidation and antioxidant enzymes in male infertility. *J Postgrad Med.* 2002;48:186-89; discussion 189-190.
- de Lamirande E, Gagnon C. Reactive oxygen species and human spermatozoa. I. effects on the motility of intact spermatozoa and on sperm axonemes. *J Androl.* 1992;13:368-378.
- Alvarez JG, Storey BT. Spontaneous lipid peroxidation in rabbit and mouse epididymal spermatozoa: dependence of rate on temperature and oxygen concentration. *Biol Reprod.* 1985;32:342-351.
- Singh R, Singh S, Jeyabalan G, Ali A, Semwal A. Medicinal plants used to treat sexual dysfunction: a review. *Int J Rec Adv Pharm Res.* 2013a;3:29-35.
- Singh R, Singh S, Jeyabalan G, Ali A. An overview of traditional medicinal plants as aphrodisiac agent. *J Pharmacogn Phytochem.* 2012;1:43-56.
- Gupta M, Sharma S, Guatam AK, Bhadauria R. *Momordica charantia* Linn. (Karela): nature's silent healer: a review. *Int J Pharm Sci Rev Res.* 2011;11:32-37.
- Kumar DS, Sharathnath KV, Yogeswaran P, Harani A, Sudhakar K, Sudha P and Banji D. A medicinal potency of *Momordica charantia*. *Int J Pharm Sci Rev Res.* 2010;1:95-100.
- Li QY, Chen HB, Liu ZM, Wang B, Zhao YY. Cucurbitane triterpenoids from *Momordica charantia*. *Magn Reson Chem.* 2007;45:451-456.
- Chen J, Tian R, Qiu M, Lu L, Zheng Y, Zhang Z. Trinorcucurbitane and cucurbitanetriterpenoids from the roots of *Momordica charantia*. *Phytochemistry.* 2008;69:1043-1048.
- Leung L, Birtwhistle R, Kotecha J, Hannah S, Cuthbertson S. Antidiabetic and hypoglycaemic effects of *Momordica charantia* (bitter melon): a mini review. *Br J Nutr.* 2009;102:1703-1708.

14. Chang CI, Chen CR, Liao YW, Cheng HL, Chen YC, Chou CH. Cucurbitane-type triterpenoids from *Momordica charantia*. J Nat Prod. 2006;69:1168-1171.
15. Chang CI, Chen CR, Liao YW, Cheng HL, Chen YC, Chou CH. Cucurbitane-type triterpenoids from the stems of *Momordica charantia*. J Nat Prod. 2008;71:1327-1330.
16. Yakubu MT, Akanji MA, Oladiji AT. Aphrodisiac potentials of aqueous extract of *Fadogia agrestis* (Schweinf. Ex Hiern.) stem in male Albino rats. Asian J Androl. 2005;7:399-404.
17. Luotola MT, Luotola JEI. Effect of α -tocopherol on the peroxidation of cod liver oil. Life Chem Reports. 1985;3:159-163.
18. Adedokun, OA, Gbolade, AA, Ayinde, BA. Effect of ethanol crude and solvent fractions of *Momordica charantia* Linn (Cucurbitaceae) on male sexual performance. Niger J Pharm Sci. 2021.
19. Murakami T, Emoto A, Matsuda H, Yoshikawa M. Medicinal foodstuffs. XXI. Structures of new cucurbitane-type triterpene glycosides, goyaglycosides-a, -b, -c, -d, -e, -f, -g, and -h, and new oleanane-type triterpene saponins, goyasaponins I, II, and III, from the fresh fruit of Japanese *Momordica charantia* L. Chem Pharm Bull. 2001;49:54-63.
20. Venkatesh P, Hariprasath K, Soumya V, Prince-Francis M, Sanker S. Isolation and aphrodisiac screening of the fruits of *Durio zibenthinus* Linn. Asian J Biol Sci. 2010;3:1-17.
21. Harinantenaina L, Tanaka M, Takoaka S, Oda M, Mogami O, Uchida M, Asakawa Y. *Momordica charantia* constituents and antidiabetic screening of the isolated major compounds. Chem Pharm Bull. 2006;54:1017-1021.
22. Liu Y, Ali Z, Khan IA. Cucurbitane-type triterpene glycosides from the fruits of *Momordica charantia*. Planta Med. 2008;74:1291-1294.
23. Nguyen XN, Phan VK, Chau VM, Ninh KB, Nguyen XC, Le MH, Bui HT, Tran HO, Nguyen HT, Kim YH. Cucurbitane-type triterpene glycosides from the fruits of *Momordica charantia*. Magn Reson Chem. 2010;48:392-386.
24. Tajuddin, Ahmad S, Latif A, Qasmi IA. Effect of 50% ethanolic extract of *Syzygium aromaticum* (L.) Merr. & Perry. (clove) on sexual behaviour of normal male rats. BMC Complement Altern Med. 2004;4:17.
25. Ratnasooriya WD, Dharmasiri MG. Effects of *Terminalia catappa* seeds on sexual behaviour and fertility of male rats. Asian J Androl. 2000;2:213-219.
26. Lin KW, Yang SC, Lin CW. Antioxidant constituents from the stem and fruits of *Momordica charantia*. Food Chem. 2011;127:609-614.
27. Talukder EU, Aklima J, Bin Emran T, Islam S, Rahman A, Bhuiyan RH. *In vitro* antioxidant potential of *Momordica charantia* fruit extracts. Br J Pharm Res. 2013;3:963-971.



Chitosan-Based Microparticle Encapsulated *Acinetobacter baumannii* Phage Cocktail in Hydrogel Matrix for the Management of Multidrug Resistant Chronic Wound Infection

Margaret O. ILOMUANYA^{1*}, Nkechi V. ENWURU², Emmanuella ADENOKUN¹, Abigail FATUNMBI¹, Adebawale ADELUOLA²,
 Cecilia I. IGWILLO¹

¹University of Lagos, Faculty of Pharmacy, Department of Pharmaceutics and Pharmaceutical Technology, Lagos, Nigeria

²University of Lagos, Faculty of Pharmacy, Department of Pharmaceutical Microbiology and Biotechnology, Lagos, Nigeria

ABSTRACT

Objectives: Multi-drug resistant bacteria have been implicated in various debilitating infections that have led to life loss. This study developed an approach to tackle multidrug resistant *Acinetobacter baumannii* infection in a chronic wound model through *A. baumannii* phage encapsulation with resuspension in hydrogel.

Materials and Methods: Two isolates of *A. baumannii*-specific lytic phases ϕ AB140 and ϕ AB150 alone, in combination (cocktail) encapsulated within a chitosan (CS) microparticle was suspended in CS hydrogel and evaluated for their therapeutic efficacy to ensure bacterial clearance in *A. baumannii* induced diabetic wound infection. Microencapsulation of the phage was carried out using ionic gelation techniques. Biological characterization *via* cell cytotoxicity, *in vivo* wound healing, histology and histomorphometry was carried out.

Results: Two characterized *A. baumannii* phages (ϕ AB140 and ϕ AB150), specific to twenty *A. baumannii* isolates, were isolated. The encapsulated CS microparticle hydrogel exhibited a pH of 5.77 ± 0.05 . The wound size reduction was most pronounced in formulation C2, which showed statistically significant wound size reduction on days 4 and 7, $56.79 \pm 2.02\%$ and $62.15 \pm 5.11\%$, respectively. The optimized concentration of C2 was not toxic to the cells as it adequately supported cell growth with a proliferation rate of $215 \pm 7.89\%$ compared to control ($107.32 \pm 4.55\%$).

Conclusion: Microparticle carrier technology was used to show the lytic activity against multi drug-resistant *A. baumannii*. *In vivo* results showed significant wound size reduction that was most pronounced in formulation C2 on day 4.

Key words: ϕ AB140 and ϕ AB150 phage, microparticle hydrogel, chronic wound, cytotoxicity

INTRODUCTION

Wound healing requires collagen synthesis, cell migration, angiogenesis, blood clotting, extracellular matrix adhesion, and immune/inflammatory response,¹ amongst other complex biological processes to ensure the complete restructure of the skin in the area where the wound occurred.² Diabetic wound healing is however mitigated by both systemic and local factors. Systemic factors include the use of steroids, antineoplastic agents and non-steroidal anti-inflammatory drugs, deficiencies of vitamins A, C and E, magnesium, zinc and

copper; nutritional status, associated illnesses/immunity and patient age.³ Blood glucose level, diabetic neuropathy, immune system deficiencies, infections, mechanical stress, chemical stress and pressure are some of the local factors affecting diabetic wound healing.³ Diabetic wounds are also promoted by the presence of microorganisms antimicrobial-resistant.

Infection of diabetic wounds impairs the inflammatory phase of natural wound healing.³ This is due to pathogenic microbes competing with macrophages and fibroblasts for limited

*Correspondence: milomuanya@unilag.edu.ng, Phone: +234 8033295077, ORCID-ID: orcid.org/0000-0001-8819-1937

Received: 22.05.2021, Accepted: 16.08.2021

©Turk J Pharm Sci, Published by Galenos Publishing House.

resources, hence impairing neutrophil function, chemotaxis, phagocytosis and decreased T-cell response, leading to necrosis in the wound bed; sepsis and perhaps death.⁴ In a bid to combat antimicrobial resistance, encapsulation of bacteriophage has been used to tackle systemic infections caused by *Staphylococcus* sp. and *Mycobacterium* sp.^{4,5} Liposome entrapment of bacteriophages has been used as a veritable approach for treating bacterial associated infections after encapsulation of phage cocktail facilitated tissue healing in a diabetic excision wound infection associated with *Staphylococcus* sp.⁵

The prevalence of antibiotic resistant infections in individuals living with diabetes was measured and compared against non-diabetics and found to be 63.4% in patients with diabetes as against 50% in non-diabetics.⁶⁻⁹ Multidrug-resistant organisms (MDRO) were more prevalent in the population with diabetes and co-infections were also higher. In a more recent study by Lee et al.⁷, high levels of antibiotic resistance and MDRO were observed to limit the treatment options of individual with diabetic wound ulcers.¹⁰ Chitosan (CS)-based hydrogels have been used as carriers for other therapeutic molecules in enhancing diabetic wound healing.¹¹ They are ideal to promote wound healing as they serve as both wound dressings and drug delivery systems.¹² Different polymeric and oil-based drug delivery platforms have been examined for delivery of bacteriophages, however, these drug delivery platforms for bacteriophage delivery of ϕ AB140 and ϕ AB150 have not been documented.⁸⁻¹¹ A simplified stepwise system for drug delivery involving bacteriophages for translation to bedside use in the management of chronic life threatening and debilitating infections is currently unavailable. This study presents a novel attempt to encapsulate ϕ AB140 and ϕ AB150. This study developed an approach to tackle MDR *Acinetobacter baumannii* infection in a chronic wound model through *A. baumannii* phage (ϕ AB140 and ϕ AB150 phage) encapsulation resuspension in hydrogel.

MATERIALS AND METHODS

Chemicals and reagents

CS (MW 80,000 g/mol, degree of deacetylation 80%), polyether sulfone, sodium chloride, polyethylene glycol, sodium tripolyphosphate (TPP), alloxan monohydrate and DNase (were obtained from Sigma-Aldrich, St. Louis, USA), glutaraldehyde, acetic acid, tween 80, and hydrochloric acid were obtained from Fluka, Steinheim, Germany, pepsin, KH_2PO_4 , sodium hydroxide, pancreatin, and BCA solution were obtained from (Macklin Biochemical Co. Ltd, Pudong China). Ketamine and xylazine were obtained from Tocris Bioscience Bio-Techne Corporation MN, USA. High performance liquid chromatography acetonitrile and phosphate buffered saline (Merck Darmstadt, Germany). The water used in formulation development was Milli-Q water. All other chemical reagents were of analytical grade and were used without further purification. Ethical approval was obtained from the Health Research Ethics Committee, College

of Medicine, University of Lagos (approval number: CMUL/HREC/09/19/676).

Bacterial strains

Fifty wound samples were collected from Medical Microbiology Laboratory of Teaching Hospital in Lagos University, Nigeria. The samples were subcultured on varying media including MacConkey and blood agar at 37°C with time equals 24 hrs. Bacteria strain was identified by conventional methods and confirmed using microbact 12A and B system.^{6,13} The identified *A. baumannii* isolates were confirmed using microbact 12A and B system.

Antibiotic susceptibility test

Kirby-Bauer method was used to undertake antibiotic susceptibility screening of the *A. baumannii* isolates. Seventeen antibiotics in various concentrations including but not limited to 10 µg imipenem, 30 µg cefepime, 10 µg levofloxacin, 10 µg meropenem, 30 µg amikacin etc. were used in this study in line with the procedure from Tanner.¹³

Phage isolation and purification

Ten MDR *A. baumannii* strains were selected for the isolation of *A. baumannii*-specific phage. Sewage and canal water samples were used for phage isolation. Sewage water was collected from sewage treatment plant of the Department of Works and Services, University of Lagos, while the canal water sample was collected from the canal behind Teaching Hospital of Lagos University. The phage was isolated using enrichment protocol as previously described.¹⁴

Two clonal differences in the *A. baumannii* isolates (ϕ AB140 and ϕ AB150) that showed very distinct and clear plaques were picked for further purification tests. The phage was purified through optimization and biokinetic measuring process as previously described.⁸ The phage was amplified against their specific host bacterial stains and titer quantified; this was followed by storage at 4°C.

Chitosan microparticle encapsulating *Acinetobacter baumannii* phage cocktails (ϕ AB140 and ϕ AB150) in hydrogel matrix

CS (0.1% w/w) was dissolved in 10 mL acetic acid (4% v/v). Fifty microliter of *A. baumannii* phage cocktails (1×10^{11} PFU/mL) was added to the CS solution under magnetic stirring and continuous sonication to obtain a homogenized fluid at $25 \pm 0.5^\circ\text{C}$. Using a gauge 25 needle, 20 mL of the phage-CS dispersion was then added drop wise into 100 mL of 2% w/v TPP with continuous sonication. The droplets instantaneously gelled into discrete Phage-CS microcapsules upon contact with the crosslinking agent. The microparticle suspension was subsequently centrifuged for 25 min (2750 rpm). The pellet was resuspended in Milli-Q water to wash the microparticles and centrifuged again. This washing procedure was repeated twice and the encapsulated phage was stored overnight in an amber glass vial.¹⁵

To prepare the plain gel to be used as the control, CS (0.1% w/v) was dispersed in Milli-Q water and 0.1% v/w acetic acid. The

gel was homogenized at 200 rpm for 1 h and 50 μ L of the phage cocktail (1×10^{11} PFU/mL) was mixed with 20 mL of the gel and homogenized at 100 rpm for 30 min and then stored in a glass vial at $25 \pm 0.5^\circ\text{C}$.

Formulation C1 contained 20 mL hydrogel alone whilst formulation C2 contained 20 mL of hydrogel and 50 μ L of bacteriophage component comprising *A. baumannii* phage cocktail.

Physical evaluation and morphological characterization of the gels

The hydrogels were evaluated for homogeneity. The pH of the gel was recorded in triplicate and the viscosity was also examined with the use of a DV-E digital viscometer, Brookfield viscometer at 25°C , 20 rpm using spindle 04. Scanning electron microscopy (SEM) using JEOL JSM-6360\L instrument was used to determine approximate shape, size, and uniformity of the microparticles.

Microparticle entrapment and yield determination

Microparticle suspension (10 mL) was centrifuged ($20,000 \times g/30$ min), followed by supernatant decantation from the microparticle pellets. The pellets were freeze-dried to ensure that all residual moisture was removed. Dried microparticle powder was weighted and percentage microparticle yield determined by dividing the weight of the microparticles by the cumulative weight of total solids including CS, TPP. The weight of the phage particles was excluded from the microparticle yield calculation (equation 1).

$$\text{Microparticle yield (\%)} = \frac{\text{microparticle weight}}{\text{Total solids (CS + TPP - 1) weight}} \times 100$$

Equation 1

A. baumannii phage microparticle suspension was evaluated for entrapment efficiency. Under centrifugal force of $21700 \times g$ for 15 min. Aided the concentration in the supernatant was determined by bicinchoninic assay where the supernatant from CS nanoparticles is used as the blank sample. Using bicinchoninic assay the phage entrapment efficiency was determined using equation 2.

$$\% \text{ Entrapment efficiency} = \frac{(\text{Total phage} - 1) - (\text{free phage} - 1)}{\text{total phage} - 1} \times 100$$

Equation 2

Fourier-transform infrared spectra (FTIR)

Using a Shimadzu 8400 FTIR spectrophotometer, FTIR spectra of free and vacuum dried encapsulated phage in CS containing samples were recorded. FTIR analysis was done at Agilent Technology to determine the various bands and compounds in the CS molecule. Twenty scans *per* spectra were recorded between 4000 and 400 cm^{-1} .

Accelerated stability studies

The stability of CS microparticle encapsulating *A. baumannii* phage cocktails (ϕ AB140 and ϕ AB150) in hydrogel matrix (formulation C1 and C2) was determined by the resuspension

of the formulation in sterile distilled water at the concentration of 20% w/w using a modified method of Pirnay et al.¹⁴ The hydrogel was incubated at $25^\circ\text{C} \pm 2^\circ\text{C}$ and analysed for their size different time intervals (0, 10, 15, 30, 60, and 90 days) using SEM as previously described.

Accelerated stability testing of the CS microparticle encapsulating *A. baumannii* phage cocktails (ϕ AB140 and ϕ AB150) in the hydrogel matrix was then evaluated using the ICH guidelines ($40^\circ\text{C}/75\% \text{ RH}$). Formulations C1 and C2 were stored in amber colored vials and kept in a stability chamber with set temperature and relative humidity. The formulations were subjected to accelerated stability testing at both room temperature and at 40°C and parameters were recorded on days 0, 10, 15, 30, and 90. The formulations were evaluated for pH, homogeneity, appearance, and viability of the phage within the formulation using earlier described methodology.

Biological characterization

Antimicrobial determination of A. baumannii encapsulated phage hydrogel in vitro

To investigate the lytic activity of *A. baumannii* phage cocktail (ϕ AB140 and ϕ AB150) hydrogel against multi drug-resistant *A. baumannii* isolates, a spot test was performed. Bacterial lawn was prepared using double layer agar plate method with Luria Bertani agar. The lawn was allowed to set and four microparticles of formulation C1 and C2 were spotted on the bacterial lawns, the plates were left uncovered within aseptic zone for 5 min to allow the spots to dry and incubated (37°C for 24 h) and lytic activity observed. Draize tests were performed to ensure non-reactivity of the developed hydrogels on intact skin.¹⁶

In vitro release study

ϕ AB140 and ϕ AB150 release from CS microparticle encapsulating *A. baumannii* phage cocktails in the hydrogel matrix was determined 25 mg microparticles were transferred to a tube with 5 mL 50 mM phosphate buffered saline maintained at pH 7 and $37^\circ\text{C} \pm 1^\circ\text{C}$. At predetermined time intervals (2, 4, 6, 8, 10, 12, and 24 h), 2 mL sample was removed after centrifugation at $21,700 \times g$ for 30 min, and 2 mL of the supernatant removed was replaced with fresh 50 mM phosphate buffered saline. The sample from each time interval was analysed by bicinchoninic acid (BCA) assay to determine the concentration of the released protein.

Cell toxicity assessment

Using the method of Iloмуanya et al.¹⁷, double enzymatic digestion, isolation of keratinocytes obtained from human (a waste product of male circumcision) was carried out. The formulation was carried using aseptic technique and, hence, it was not necessary to conduct sterilization. The CS-based microparticles were also cultured to ensure that no bacterial contamination occurred in line with good quality control measures.¹⁷ 3-(4,5-Dimethylthiazol-2-yl)-2,5-diphenyltetrazolium bromide assay was carried out using CS-based microparticle-encapsulated *A. baumannii* phage at concentrations of (0, 0.05, 0.1, 0.25, 0.5, 0.75, and 1 mg/mL). Cell cultured in wells devoid of phage was taken as control.

In vivo wound healing

Sixty thirteen-week-old rats breed specifically for research without exposure to medications and weighing between 150 and 165 g were used for the study after a seven-day acclimatization period. The animals were housed at a steady thermostatically controlled condition (12 hr night/day cycle; $29 \pm 2^\circ\text{C}$; $45 \pm 10\%$ RH). Standard feeding conditions were provided in line with international best practices, as stated within the study ethical approval (CMUL/HREC/09/19/676).

Experimental timelines (Figure 1) show that the wound healing study was conducted within a 14 day period. Diabetes was induced using 150 mg/kg body weight alloxan monohydrate in 2 day time lapse in the fasted rodents.¹⁸ After the alloxan injection was administered rats having fasting blood glucose levels above 190.5 ± 8.1 mg/dL with the random blood glucose levels of above 350 mg/dL were considered severely diabetic and selected for infection studies.¹⁸

Wound model

Overnight culture of MDR *A. baumannii* isolates corresponding to 1×10^9 CFU/mL was prepared. Diabetic rats were taken and distributed in four different groups of six animals each randomly distributed. Epilation was carried and the skin cleaned with rubbing alcohol before wounding through the skin to the panniculus carnosus using a 5 mm diameter punch. The wounds in group 1, 2, 3 and 4 were left open and inoculated with 0.1 mL of *A. baumannii* (1.5×10^8 CFU/mL) suspension. The animals were given ibuprofen suspension (5 mg/kg bwt) to reduce pain. The infection was allowed to take hold for 24 h before the treatment protocol started as follows.

Group 1: The infected rats that received no medication.

Group 2: The infected rats were treated with gentamicin ointment twice a day.

Group 3: Formulation C1 was applied on infected wounds, twice a day.

Group 4: Formulation C2 was applied on infected wounds, twice a day.

Wound size was determined using a digital camera with an image calibration capacity and calculated using relative wound size reduction measurements was calculated based difference in wound diameter A_o and A_t ; on treatment time in days *i.e.* initial wound diameter and diameter at predetermined time intervals respectively (equation 3).

$$\text{Relative wound size reduction \%} = \frac{A_o - A_t}{A_o} \times 100 \quad \text{Equation 3}$$

Bacterial load in wounds

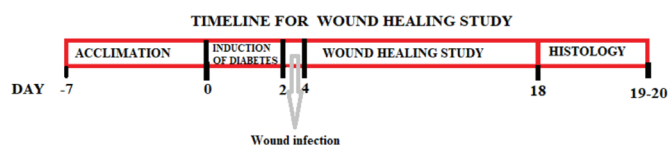


Figure 1. Experimental timelines

MDR *A. baumannii* on the surface of the wound, samples were collected from the wound surface using a sterile swab stick for three times on day 7, 10, and 14. The samples were processed *via* nutrient broth inoculation and a 12 hour incubation at 37°C before identification and evaluation of the presence of MDR *A. baumannii*.^{18,19}

Histology

Fourteen days post-treatment of the infected wound, skin sections fixed in 10% formaldehyde was stained using hematoxylin/eosin and Masson's trichome and histological profiles recorded using a microsystems microscope (Mannheim, Germany).²

Histomorphometry

DML-300 camera (South Korea) was used as the Image analyser was used to evaluate the histological skin samples. Percentage re-epithelialization was calculated as in equation 4.

$$\text{Re-epithelialization \%} = \frac{[\text{Total wound length (mm)} - \text{Desquamated epithelium region (mm)}]}{\text{Total wound length (mm)}} \times 100 \quad \text{Equation 4}$$

Statistical analysis

Graph pad prism software ver. 5 was used for statistical analysis using data obtained in triplicate. All reported date is expressed as mean \pm standard deviation of experimental values for each variable.

RESULTS

Phage isolation and purification

MRD *A. baumannii* was used in the study. Five *A. baumannii*-specific phages were isolated among ten *A. baumannii* strains used for phage isolation. However, two unique phages (ϕAB140 and ϕAB150) were selected for the study amongst the five-phage library based on high lytic activity, broad host range and the plaque size formation (Figure 2A, B). The encapsulated phage was freely released and highly sensitive to host bacteria (10^8 CFU/mL, 1×10^9 CFU/mL) when tested using spot method on double agar layer technique (Figure 2C).

Physical evaluation and pH determination of the gels

The encapsulated CS microparticle hydrogel exhibited pH of 5.77 ± 0.05 , however after encapsulation of *A. baumannii* phage (ϕAB140 and ϕAB150) the pH of the formulation increased

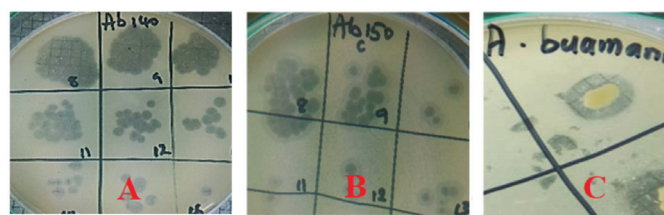


Figure 2. Plate A and B showed the lytic activity and the titer of *Acinetobacter baumannii* phage (ϕAB140 and ϕAB150) on double agar layer spot test. Plate C showed lytic activity of chitosan-based microparticle encapsulated *A. baumannii* phage cocktails (ϕAB140 and ϕAB150) on host strains

to 6.54 ± 0.03 . This pH is still in tandem with the range of formulation pH required for the management of chronic wounds. The viscosity of the C2 (1099 ± 2.15 MPa) was slightly lower than that of C1 (1120 ± 1.09 MPa). The viscosity of the formulations promotes ease of application as well as deters run-off of the formulation from the site of application.

Morphological characterization

SEM analysis showed that CS-based microcapsule presented as spheres of 30–40 μm in size. The shape was uniform throughout the sample and microparticles existed as discrete particles. As shown in Figure 3C, CS-based microparticle encapsulated *A. baumannii* phage presented as spherical shape approximately 40–60 μm in size (Figure 3A). The microparticles were suspended in hydrogel matrix to obtain formulation C1 and C2 and the SEM shows homogeneity of the microparticles within the hydrogel matrix (Figures 3B and D).

Microparticle entrapment and yield determination

The microparticle yield of CS microparticles and CS-based microparticle encapsulated *A. baumannii* phage was $87.12 \pm 2.93\%$ and $80.99 \pm 3.66\%$ respectively. Entrapment efficiency of *A. baumannii* phage into CS microparticles was found to be $60.72 \pm 3.09\%$.

Fourier-transform infrared spectroscopy

The development of CS-based microparticle-encapsulated *A. baumannii* phage using plain CS microparticles as reference was analysed evaluated using FTIR. Sample C1 contained plain CS microparticles showed C-H stretches at 2875 cm^{-1} with corresponding stretch vibration at 3283 cm^{-1} reflecting-NH hydroxyl linkages (Figures 4A and B). The presence of the encapsulated *A. baumannii* phage caused a slight shift from 2128 cm^{-1} to 2105 cm^{-1} and shows eminent microparticle protein entrapment. The various bands seen include 1066 and 1021 cm^{-1} , which represent a C-O bending vibration accompanied by a peak, 1215 cm^{-1} a representation of stretching vibration of P=O with a peak being observed, the bending of C-H formation is given within the range of 1457 – 1483 cm^{-1} , gives-H bending deformation, the carbonyl group of the amide bond is given as 1632 cm^{-1} with a trough, C=O, the amine bond present N-H is given as 1580 cm^{-1} , and the C-H vibration stretch at 2867 cm^{-1} . The broad band N-H from the spectrum in Figure 4A, B is represented majorly as 3290 cm^{-1} and 3253 cm^{-1} .

Accelerated stability studies

Formulations C1 and C2 were seen to be stabile after resuspension and storage at different time intervals at $25^\circ\text{C} \pm 2^\circ\text{C}$. There was no change in the morphology of the microparticle. C1 and C2 were stable, when challenged with accelerated stability testing. There was no statistically significant variation in pH, lytic activity of the formulation and viscosity when exposed to ICH guidelines of $40^\circ\text{C}/75\% \text{RH}$ (Table 1).

In vitro antimicrobial determination of encapsulated *A. baumannii* phage in hydrogel matrix

Bacterial load in wounds

The *A. baumannii* infection was observed after 2, 7, 10, and 14th days on the wound surface in the no treatment (NT), control

treatment (CT) and CS microparticle suspended in hydrogel group C1 and C2. *A. baumannii* contamination infection was not detected on days 7, 10, and 14 in the groups receiving the microparticle encapsulated *A. baumannii* phage hydrogel as in Table 2.

In vitro release study

The cumulative release of ϕAB from CS microparticle encapsulating *A. baumannii* phage cocktails in the hydrogel matrix was found to be $72.9 \pm 7.09\%$ after 24 h of incubation. An initial release 32.76 at 2 h followed by burst release of 72.24 which was sustained from 6 h to 24 h as shown in Figure 5.

Cell toxicity assessment

Microparticle encapsulated *A. baumannii* phage (ϕAB140 and ϕAB150) were non-toxic to the cells at all concentration utilized.

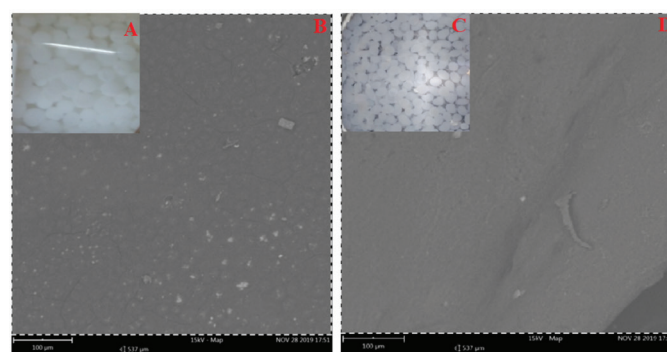


Figure 3. SEM images of chitosan-based microparticle encapsulated *Acinetobacter baumannii* phage cocktail (ϕAB140 and ϕAB150) (A) in hydrogel C2 (B), encapsulated chitosan microparticles (C) in hydrogel C1 (D)

SEM: Scanning electron microscopy

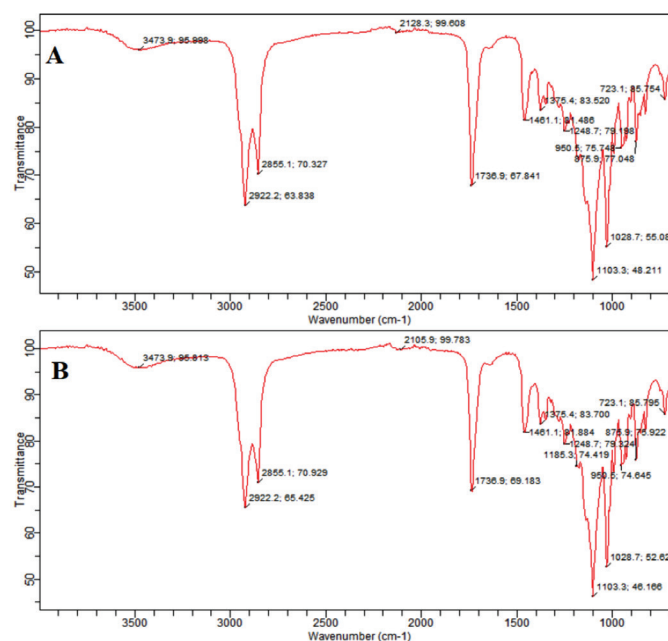


Figure 4. FTIR spectra encapsulated phage in chitosan containing samples (A) C1 and (B) C2 containing *Acinetobacter baumannii* phage cocktail (ϕAB140 and ϕAB150)

Table 1. Accelerated stability testing on the microparticle encapsulated *Acinetobacter baumannii* phage cocktail in hydrogel ($p \leq 0.05$)

Time (duration)	Formulation	pH	Lytic activity of formulation	Viscosity (mPas at 40 rpm)
Day 0	C1	5.77 ± 0.05	Absence of lytic activity	1120 ± 1.09
	C2	6.54 ± 0.03	Presence of lytic activity	1099 ± 2.15
Day 10	C1	5.79 ± 0.10	Absence of lytic activity	1120 ± 2.05
	C2	6.53 ± 0.04	Presence of lytic activity	1098 ± 2.31
Day 15	C1	5.79 ± 0.09	Absence of lytic activity	1119 ± 1.72
	C2	6.53 ± 0.10	Presence of lytic activity	1101 ± 2.00
Day 30	C1	5.78 ± 0.07	Absence of lytic activity	1121 ± 1.18
	C2	6.5 ± 0.11	Presence of lytic activity	1100 ± 1.45
Day 60	C1	5.77 ± 0.07	Absence of lytic activity	1119 ± 1.11
	C2	6.55 ± 0.05	Presence of lytic activity	1097 ± 1.33
Day 90	C1	5.79 ± 0.02	Absence of lytic activity	1121 ± 0.98
	C2	6.55 ± 0.04	Presence of lytic activity	1100 ± 1.32

Table 2. The assessment of the colonization of drug resistant *Acinetobacter baumannii* on the wound surface

Group	Treatment protocol	Chemotherapy utilized	Presence of multi drug resistant <i>A. baumannii</i> at			
			Day 2	Day 7	Day 10	Day 14
1	NT	No treatment	Positive	Positive	Positive	Positive
2	CT	Gentamicin ointment	Positive	Positive	Positive	Positive
3	C1	Chitosan microparticle suspended in hydrogel	Positive	Positive	Positive	Positive
4	C2	Microparticle encapsulated <i>A. baumannii</i> phage cocktail in hydrogel	Positive	Negative	Negative	Negative

NT: No treatment, CT: Conventional treatment

At the highest concentration of 1 mg/mL, C1 and C2 showed similar percentage ($117 \pm 8.01\%$ and $121 \pm 2.83\%$ respectively, after 24 hours following $183.03 \pm 3.77\%$ and $215 \pm 7.89\%$ after 120 hrs) of cell proliferation with control. With respect to % cell proliferation, both hydrogels exhibited statistically significant difference at 120 hours compared to the value at $t=24$ hr. The optimized concentration of C2 adequately supported cell growth with a proliferation rate of $215 \pm 7.89\%$ compared to control ($107.32 \pm 4.55\%$) showing a lack of cell toxicity.

In vivo wound healing

The cumulative release of ϕ AB from CS microparticle encapsulating *A. baumannii* phage cocktails in hydrogel matrix was found to be $72.9 \pm 7.09\%$ after 24 h of incubation. An initial release 32.76 at 2 hours followed by burst release of 72.24 which was sustained from 6 hours to 24 hours as shown in Figure 5.

Histology and histomorphometry

There was an absence of hemorrhaging seen on the infected wounds in all groups including the control post product application on the infected wound surface. The wound size reduction was most pronounced in formulation C2 that showed statistically significant wound size reduction on days 4 and

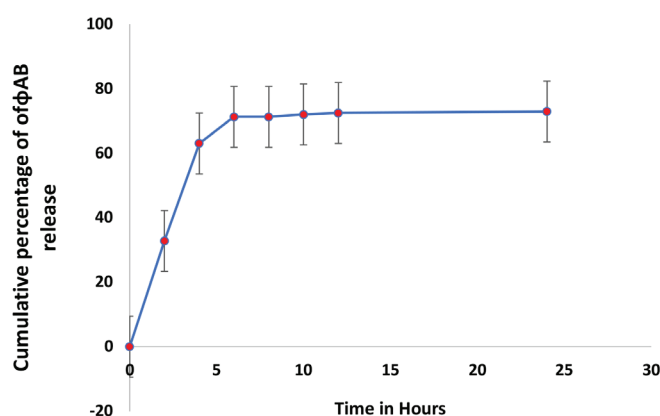


Figure 5. Release profile of ϕ AB from chitosan-based microparticle encapsulated *Acinetobacter baumannii* phage (ϕ AB140 and ϕ AB150) cocktail (C2) at pH 7 at different time intervals

7, 56.79 ± 2.02 and $62.15 \pm 5.11\%$, respectively. C1 containing plain hydrogel and CT showed a wound size reduction of $31.766 \pm 3.07\%$ and $31.28 \pm 2.63\%$ respectively. On day 14th, only C2 showed completed wound closure with wound size reduction of 100% (Figure 6). Histologic section of tissue of animals in

the NT group showed skin with dermis containing oil glands, as well as presence of clusters of inflammatory red cells (Figure 6A). Histologic section of tissue of animals treated with C2 reflected an absence of abnormalities after at day 14th. The desquamated epithelial region for C1 measured at 1.55 mm that was statistically lower than control C1 and conventional drug measured at 2.91 ± 0.01 mm and 3.9 ± 0.03 mm, respectively. NT group had desquamated epithelial region measured at 6.7 ± 0.10 mm due to increased inflammation in the dermis (Figure 7). The thickness of epidermis to the dermis in C2 was significantly higher than C1 (Figure 7B). The thickness of the central region in C1 (2.45 ± 0.09) was a clear indication of facilitated re-epithelization pathway that was not impaired by drug-resistant *A. baumannii* infection. Re-epithelization rates were highest for C2 at $83.44 \pm 2.17\%$ compared to $32.78 \pm 0.11\%$, $23.68 \pm 1.01\%$, and $11.99 \pm 0.97\%$ for C1, conventional drug and NT groups, respectively (Figure 7C).

DISCUSSION

This study developed encapsulated *A. baumannii* phage cocktails (ϕ AB140 and ϕ AB150) using chitosan and resuspended the microparticles in hydrogel to treat chronic wounds. *A. baumannii* phages were encapsulated using CS and then suspended in a hydrogel matrix. *A. baumannii* phages exhibited bactericidal activity *in vitro*. More so, *in vivo* lytic activity of the CS-based microparticle-encapsulated *A. baumannii* phage cocktails in hydrogel matrix against methicillin-resistant *A. baumannii* was studied in an animal model. In the *in vivo* animal wound experiment, we demonstrated that the phage cocktail in hydrogel was not toxic in the rodent model used in this study. Phage application in wound infections effectively reduced

the number of bacteria isolates from the treated animal and all visible infection symptoms (red, swollen-purulent wound) disappeared. MDR *A. baumannii* is a rapidly emerging pathogen in the healthcare setting, it causes bacteremia, pneumonia, meningitis, urinary tract, and wound infection.^{20,21} The organism's ability to survive under various environmental conditions and to persist for extended time on surfaces make it a frequent cause of outbreaks of infection. It also promotes its endemicity hence making it a healthcare-associated pathogen.¹⁰ The developed microparticle phage formulation containing bacteriophages were stable and exhibited good organoleptic properties suitable for use as a wound healing formulation. There was also an absence of irritation displayed on intact skin when tested before the wound healing study. The encapsulation of the phages followed by resuspension in a biomimetic hydrogel base ensured phage preservation within the drug delivery platform whilst aiding ease of usage in the clinical setting. Additionally, the use of CS based microparticle-encapsulated phage cocktail in hydrogel matrix sufficiently solved the problem of dropping of phage titer and inactivation of phage by immune cells around wound sites. Similarly, Colom et al.²² encapsulated *Salmonella* spp. phages that were stable showed excellent bioavailability in the intestine thus increasing its therapeutic effect.

The animals treated with C2 containing bacteriophage exhibited bacterial clearance as there was an absence of colonization drug-resistant *A. baumannii* on the wound surface. Kim et al.²³ evaluated safety tests of phage lysis reflecting success in systemic infection clearance of *A. baumannii*. This study,

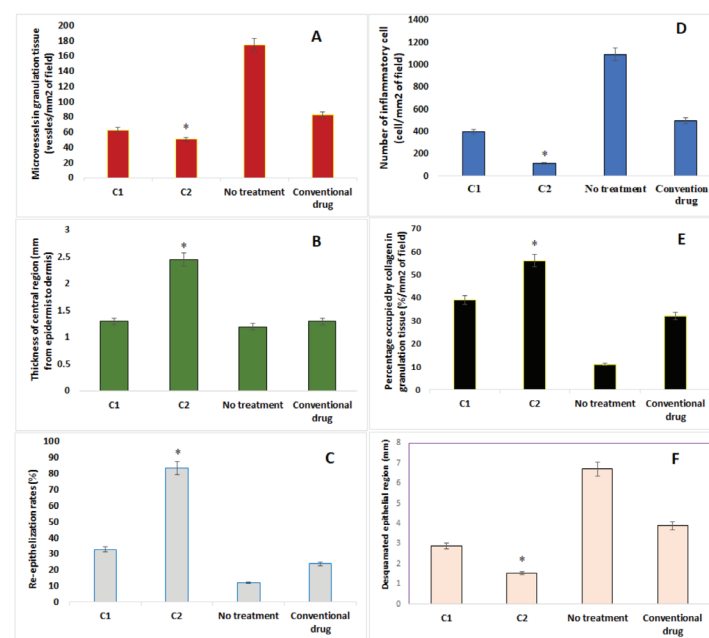


Figure 7. Histomorphometrical values showing (A) microvessels in granulation tissue (vessels/mm² of field), (B) thickness of central region (mm from epidermis to dermis) (C) re-epithelisation rates (%), (D) number of inflammatory cells (cell/mm² of field), (E) percentage occupied by collagen in granulation tissue (%/mm² of field), (F) desquamated epithelial region (mm). Treatments were compared with control and conventional drug (hydrogel without bacteriophage) * $p < 0.05$. The compositions of hydrogels C1 and C2 are provided in Table 1

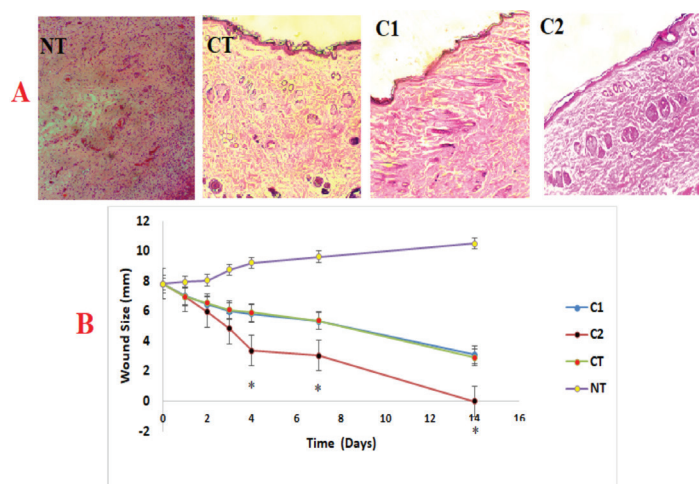


Figure 6. (A) Representative sections stained with hematoxylin and eosin after post treatment. (B) Wound size/biometric analysis (mm) of wound area of *Acinetobacter baumannii* (1.5×10^8 CFU/mL). Infected animals ($n = 6$, each group) following NT, CT with gentamicin ointment, C1 and C2. Wound area was measured on various days post-infection. Error bars represent the standard deviation from three independent values. * $p < 0.05$ indicate statistically significant differences between infected control and treated groups

NT: No treatment, CT: Conventional treatment

however, showed that hastened lysis of *A. baumannii* resulting in septic shock when 500 µg of phage was used. The encapsulation of the phage that was carried out in this study ensured that bacterial clearance occurred *via* sustained release of the phage through the microparticles.

The microparticle phage formulation C2 could facilitate complete wound closure by day 14. Similarly, Vinod Kumar et al.²⁴ *Staphylococcus aureus* clearance from wounds in immune compromised rats eight days post-treatment with phage. The presence of drug-resistant *A. baumannii* in the wound bed preclude the control drug and C1 treatment from achieving wound closure due to the inability of the formulation achieve bacterial clearance due to lack of sensitivity and specificity for *A. baumannii* clearance. Cell proliferation and collagen deposition facilitate angiogenesis in the development of granulation tissue. The animals treated with formulation C2, displayed an increase in granulation tissue with evidenced fewer inflammatory cells and increased collagen deposition. The percentage of granulation tissue which was collagen occupied was increased in C2 compared to C1 with increased fibroblast agglomeration seen in the tissue. The enhanced collagen deposition seen in animal treated with C2 was associated with well-organized collagen bands found within thin barrier blood vessels largely distributed throughout the granulation tissue with C2 exhibiting 50 microvessels within the granulation tissue. Weak scaffolds of collagen fibers accompanied by a low number of microvessels at the tissue surface was observed for C1 and conventional drug treatment groups. C1 contained CS hence its ability to stimulate wound bed re-epithelization comparable with that seen in the convention treatment. The utilization of the hydrogel matrix as well has been seen to facilitate wound healing in contrast untreated wounds exhibited incomplete maturation of epidermal layer few fibroblasts, reduced number of microvessels, and irregularly arranged collagen fibers that appeared coarse and lacking a compact structure.

The cytotoxicity of the microparticles is crucial for their *in vivo* use in clinical setting. CS-based microparticle-encapsulated *A. baumannii* phage cocktail was studied for their *in vitro* cytotoxicity on human keratinocyte cells and showed high cell viability (1 mg/mL) of microparticles. The present study corroborated that C2 was non-toxin on human keratinocyte cells. The use of phage cocktail provides an effective solution which readily delivered the wounded animals without any delay, making cocktail phage therapy potentially more effective clinically than mono-phage therapy. Similarly, Chhibber et al.²⁵ demonstrated that fast reduction in bacterial concentration and hastened wound healing occur in an animal model treated with phage cocktail therapy.

CONCLUSION

Microparticle carrier technology was used to show the lytic activity against multi drug-resistant *A. baumannii* phage. *In vivo* results showed significant wound size reduction that was most pronounced in formulation C2 on day 4. Complete clearance of *A. baumannii* isolates was detected on days 7, 10, and 14

in all groups that received the microparticle encapsulated *A. baumannii* phage hydrogel as treatment. The optimized concentration of C2 is safe, non-toxic and effect in complete clearance of MDR *A. baumannii* infection from the wound bed.

Ethics

Ethics Committee Approval: Ethical approval was obtained from the Health Research Ethics Committee, College of Medicine University of Lagos approval number: CMUL/HREC/09/19/676.

Informed Consent: This was not required.

Peer-review: Externally peer-reviewed.

Authorship Contributions

Concept: M.O.I., Design: M.O.I., N.V.E., Data Collection or Processing: E.A., A.F., A.A., Analysis or Interpretation: M.O.I., N.V.E., E.A., A.F., C.I.I., Literature Search: M.O.I., A.F., E.A., Writing: M.O.I., N.V.E., E.A.

Conflict of Interest: No conflict of interest was declared by the authors.

Financial Disclosure: The authors declared that this study received no financial support.

REFERENCES

1. Sorg H, Tilkorn DJ, Hager S, Hauser J, Mirastschijski U. Skin wound healing: an update on the current knowledge and concepts. *Eur Surg Res.* 2017;58:81-94.
2. Elegbede RD, Ilomuanya MO, Sowemimo AA, Nneji A, Joubert E, de Beer D, Koekemoer T, van der Venter M. van. Effect of fermented and green *Aspalathus linearis* extract loaded hydrogel on surgical wound healing in Sprague Dawley rats. *Wound Medicine.* 2020;29:100186.
3. Hourelid NN. Shedding light on a new treatment for diabetic wound healing: a review on phototherapy. *Sci World J.* 2014;398412.
4. de Oliveira S, Rosowski EE, Huttenlocher A. Neutrophil migration in infection and wound repair: going forward in reverse. *Nat Rev Immunol.* 2016;16:378-391.
5. Chhibber S, Kaur J, Kaur S. Liposome entrapment of bacteriophages improves wound healing in a diabetic mouse MRSA infection. *Front Microbiol.* 2018;9:561.
6. Trivedi U, Parameswaran S, Armstrong A, Burgueno-Vega D, Griswold J, Dissanaik S, Rumbaugh KP. Prevalence of multiple antibiotic resistant infections in diabetic *versus* nondiabetic wounds. *J Pathog.* 2014;2014:173053.
7. Lee NY, Ko WC, Hsueh PR. Nanoparticles in the treatment of infections caused by multidrug-resistant organisms. *Front Pharmacol.* 2019;10:1153.
8. Rohde C, Wittmann J, Kutter E. Bacteriophages: a therapy concept against multi-drug-resistant bacteria. *Surg Infect (Larchmt).* 2018;19:737-744.
9. Keen EC. Phage therapy: concept to cure. *Front Microbiol.* 2012;3:238.
10. Jassim SA, Limoges RG. Natural solution to antibiotic resistance: bacteriophages 'The Living Drugs'. *World J Microbiol Biotechnol.* 2014;30:2153-2170.
11. Masood N, Ahmed R, Tariq M, Ahmed Z, Masoud MS, Ali I, Asghar R, Andleeb A, Hasan A. Silver nanoparticle impregnated chitosan-PEG

- hydrogel enhances wound healing in diabetes induced rabbits. *Int J Pharm.* 2019;559:23-36.
12. Iloмуanya MO. Chapter 23 - Hydrogels as biodegradable biopolymer formulations. In *Biopolymer-Based Formulations*. 2020, pp. 561-585.
 13. Tanner H. Verification of the cepheid Xpert Carba-R assay for the detection of carbapenemase genes in bacterial isolates cultured on alternative solid culture media. *J Hosp Infect.* 2017;97:254-257.
 14. Pirnay JP, Blasdel BG, Bretaudeau L, Buckling A, Chanishvili N, Clark JR, Corte-Real S, Debarbieux L, Dublanchet A, De Vos D, Gabard J, Garcia M, Goderdzishvili M, Górski A, Hardcastle J, Huys I, Kutter E, Lavigne R, Merabishvili M, Olchawa E, Parikka KJ, Patey O, Pouilot F, Resch G, Rohde C, Scheres J, Skurnik M, Vaneechoutte M, Van Parys L, Verbeken G, Zizi M, Van den Eede G. Quality and safety requirements for sustainable phage therapy products. *Pharm Res.* 2015;32:2173-2179.
 15. Furuie T, Komoto D, Hashimoto H, Tamura H. Preparation of chitosan hydrogel and its solubility in organic acids. *Int J Biol Macromol.* 2017;104(Pt B):1620-1625.
 16. National Research Council (US) Committee for the Update of the Guide for the Care and Use of Laboratory Animals. *Guide for the Care and Use of Laboratory Animals*. 8th ed. Washington (DC): National Academies Press (US); 2011.
 17. Iloмуanya MO, Adebona AC, Wang W, Sowemimo A, Eziegbo CL, Silva BO, Adeosun SO, Jourbert E, Beer DD. Development and characterization of collagen-based electrospun scaffolds containing silver sulphadiazine and *Aspalathus linearis* extract for potential wound healing applications. *SN Applied Sciences.* 2020;2:881.
 18. Mendes JJ, Leandro CI, Bonaparte DP, Pinto AL. A rat model of diabetic wound infection for the evaluation of topical antimicrobial therapies. *Comp Med.* 2012;62:37-48.
 19. Rahimzadeh G, Gill P, Saeedi M, Ghasemi M, Rokni GR, Rostamkalaei SS, Ghara AAG, Rezai MS. Evaluation of bacteriophage products against burn wound methicillin-resistant *Staphylococcus aureus* (MRSA) infections. *Wound Medicine.* 2020;28:100182.
 20. Lood R, Winer BY, Pelzek AJ, Diez-Martinez R, Thandar M, Euler CW, Schuch R, Fischetti VA. Novel phage lysin capable of killing the multidrug-resistant gram-negative bacterium *Acinetobacter baumannii* in a mouse bacteremia model. *Antimicrob Agents Chemother.* 2015;59:1983-1991.
 21. Turner D, Wand ME, Briers Y, Lavigne R, Sutton JM, Reynolds DM. Characterisation and genome sequence of the lytic *Acinetobacter baumannii* bacteriophage vB_AbaS_Loki. *PLoS One.* 2017;12:e0172303.
 22. Colom J, Cano-Sarabia M, Otero J, Aríñez-Soriano J, Cortés P, Maspoch D, Llagostera M. Microencapsulation with alginate/CaCO₃: a strategy for improved phage therapy. *Sci Rep.* 2017;7:41441.
 23. Kim S, Lee DW, Jin JS, Kim J. Antimicrobial activity of LysSS, a novel phage endolysin, against *Acinetobacter baumannii* and *Pseudomonas aeruginosa*. *J Glob Antimicrob Resist.* 2020;22:32-39.
 24. VinodKumar CS, Srinivasa H, Basavarajappa KG, Patil U, Bandekar N, Patil R. Abrogation of *Staphylococcus aureus* wound infection by bacteriophage in diabetic rats. *Int J Pharm Sci Drug Res.* 2011;3:202-207.
 25. Chhibber S, Kaur T, Sandeep Kaur. Co-therapy using lytic bacteriophage and linezolid: effective treatment in eliminating methicillin resistant *Staphylococcus aureus* (MRSA) from diabetic foot infections. *PLoS One.* 2013;8:e56022.



Creatine and Alpha-Lipoic Acid Antidepressant-Like Effect Following Cyclosporine A Administration

✉ Mehdi ALIOMRANI¹, ✉ Azadeh MESRIPOUR^{2*}, ✉ Abolfazl Saleki MEHRJARDI¹

¹Isfahan University of Medical Sciences, School of Pharmacy and Pharmaceutical Sciences, Department of Pharmacology and Toxicology, Isfahan, Iran

²Isfahan University of Medical Sciences, School of Pharmacy and Pharmaceutical Sciences, Isfahan Pharmaceutical Sciences Research Center, Isfahan, Iran

ABSTRACT

Objectives: Cyclosporine A (CYA), is an immunosuppressant drug used to prevent graft rejection, but it may initiate neuropsychological problems such as depression. The aim was to evaluate the antidepressant-like effects of creatine (Crt), a mediator of oxidative phosphorylation, and alpha-lipoic acid (ALA), a cofactor for the mitochondrial respiratory chain following CYA administration.

Materials and Methods: Female mice (27 ± 2 g) were used, immobility time during the forced swimming test (FST) was measured, and hippocampal brain-derived neurotrophic factor (BDNF) level was evaluated. CYA 20 mg/kg, ALA 40 mg/kg, fluoxetine 20 mg/kg, and Crt 10 mg/kg (oral) were administered for 6 consecutive days, and the tests were performed on day 7.

Results: ALA, but not Crt, treatment alone decreased immobility in the FST (*i.e.*, decreases depression-like behavior). CYA administration increased immobility in the FST (175.1 ± 13.16 s, vs. vehicle 130.9 ± 13.5 s, $p = 0.0364$), and this depression-like behavior was prevented by co-administrating, ALA (100 ± 15.9 s, $p = 0.020$) or Crt (93.5 ± 16.6, $p = 0.009$) and the positive control, fluoxetine. Notably, there was a synergistic effect of Crt-ALA co-administration since CYA-induced immobility was lower in this group than in the groups pretreated with Crt or ALA. These behavioral changes were observed without treatment effects on locomotor activity in an open field. CYA treatment increased hippocampal BDNF protein levels prevented by co-administration of ALA (with or without Crt) or fluoxetine.

Conclusion: CYA-induced depression-like behavior might be related to hippocampal mitochondrial dysfunction as ALA and Crt prevented the development of this behavioral phenotype. ALA, similar to fluoxetine, prevented BDNF alteration and its possible neurological changes.

Key words: Cyclosporine, depression, creatine, alpha-lipoic acid, brain-derived neurotrophic factor

INTRODUCTION

Calcineurin, a calcium-dependent protein phosphatase enzyme, is well known for its effect as a modulator of the immune response. It also participates in neurotransmission, neuronal structure, and neuronal excitability.^{1,2} Calcineurin inhibiting drugs, such as cyclosporine A (CYA), are immunosuppressive drugs that have developed the organ transplantation process by extensively reducing allograft rejection rates in individuals.^{3,4} However, some patients that receive these agents suffer from neuropsychological problems such as depression, anxiety, confusion, and tremor.⁵ Peripheral administration of high dose (60 mg/kg) CYA has decreased the release of serotonin and dopamine and caused prefrontal cortex dysfunction that could be responsible for the increased anxiety and social behavior

disturbance.⁶ Additionally, CYA may induce neurotoxicity by interaction with brain mitochondria functioning.⁵ Brain-derived neurotrophic factor (BDNF) belongs to the neurotrophin family; it is the most plentiful neurotrophin in the central nervous system (CNS) and is related to neural cell survival and neural transmission.⁷ Reduction of BDNF expression in hippocampal neurons would cause severe stress and influence learning, inspiration, and mood.^{8,9}

Creatine (*N*-aminoiminomethyl-*N*-methylglycine; Crt) can be endogenously synthesized by the liver, kidney, pancreas, and to some extent in the brain from the amino acids arginine, glycine, and methionine. Crt is also provided in diets having meat or fish.¹⁰ Adenosine triphosphate (ATP) is the primary energy source in the brain that is closely joined to phosphocreatine

*Correspondence: a_mesripour@yahoo.com, Phone: +0989131000614, ORCID-ID: orcid.org/0000-0003-3150-5581

Received: 27.06.2021, Accepted: 16.08.2021

©Turk J Pharm Sci, Published by Galenos Publishing House.

(PCr). The isoenzymes of Crt kinase are specially localized in high-demanding ATP sites like the neurons to regenerate ATP *in situ* via PCr.¹⁰ Therefore, oxidative phosphorylation and Crt/PCr system prepare high energy that is critical for CNS function.¹¹ Crt has various properties in the CNS, including antioxidant, anti-inflammatory, anti-apoptotic, and neuromodulatory activity.^{10,12} These effects have provoked further research regarding Crt monohydrate efficacy for treating neurological disorders.

Alpha-lipoic acid (ALA) naturally occurs in vegetables like broccoli, spinach, and tomatoes.¹³ ALA is an essential cofactor for mitochondrial respiratory chain enzymes α -keto-dehydrogenase complexes.¹⁴ ALA and its reduced metabolite dihydrolipoic acid have been noticed as antioxidants against hydroxyl radicals and an inhibitor of lipid and protein oxidation. Interestingly, this free-radical quenching antioxidant, in contrast to vitamin E (fat-soluble), is soluble in both fat and water; thus, it deactivates free radicals in both fatty and watery areas of cells. ALA can readily spread into CNS and induce protective effects on the nervous system, leading to its promising therapeutic effects on brain disorders.¹⁴

Since CYA might induce depression side effects and administrating prophylactic antidepressant drugs would expose the individual to unnecessary medication and polypharmacy, the aim was to introduce an alternative medicine. Therefore, treatment with two supplements, ALA (cofactor for mitochondrial respiratory chain) and Crt (mediator of mitochondria oxidative phosphorylation), was evaluated on mice's CYA-induced behavior changes. Novelty of the study was that the antidepressant effects of Crt and ALA were evaluated following CYA administration in mice, and finally, the BDNF levels were assessed in mice brains.

MATERIALS AND METHODS

Animals

Female NMRI mice (weighing 27 ± 2 g, 6–8 weeks old) were housed six in each cage and kept at room temperature $21 \pm 2^\circ\text{C}$ on a 12 h light and 12 h dark cycle (lights on at 06:00 AM); standard mice chow and tap water *ad libitum*. Cages were placed in the behavioral laboratory 24 h prior to the experiments to acclimatize. The experiments were carried out according to the Care and Use of Laboratory Animals Guidelines Issued by The National Ethical Committee of Vice-Chancellor in Research Affairs-Medical University of Isfahan (ethical no: IR.MUI.RESEARCH.REC.1399.200). All the attempts were made to reduce animal distress and the number of animals used in the research.

Drug administration

CYA (Sandimmun, 50 mg/mL; Novartis, Switzerland) 20 mg/kg was injected intraperitoneal (IP) after diluted in 2% v/v EtOH/normal saline.¹⁵ Crt monohydrate (Karen Pharma and Food Supplement, Iran) 10 mg/kg was administered by daily gavage feeding tube.¹⁶ ALA (Sigma Aldrich, India) 40 mg/kg was injected IP.¹⁷ A selective serotonin reuptake inhibitors (SSRIs) fluoxetine (Sigma-Aldrich, Germany) 20 mg/kg was

injected IP.¹⁵ Control groups were injected with normal saline or received normal saline by gavage feeding tube. In a separate group of mice, Crt and ALA were co-administration with CYA. The volume for all of the injections was 10 mL/kg.

Experiment design

Totally 9 groups of animals consisting of 6 mice in each group were studied. Groups included: groups that received each of the drugs (ALA, Crt) alone and the control group that received normal saline (data for IP injection and gavage were similar; therefore, one group was considered here). The CYA alone group and the vehicle group (2% v/v EtOH/normal saline). Three groups that received ALA, Crt or fluoxetine (the positive control) concomitantly with CYA; finally, a group that was treated with ALA+Crt together with CYA. All the treatments were administered for 6 consecutive days, and the tests were performed on day 7. The locomotor and forced swimming tests (FST) for measuring animal despair behavior were performed on each animal. After the animals were decapitated, the brain was carefully removed on ice and stored in -70°C for BDNF evaluation.

Locomotor test

The locomotor activity of mice was assessed in an open arena (45×45 cm) (Borj Sanat, Iran) divided into 15 zones by red beams. Mice were allowed to explore the field for 3 min;^{18,19} by passing through the beams, the number of zone entries (horizontal exploration) was counted automatically, while rears on back-legs (vertical exploration) were recorded manually. The total activity for each animal was calculated, which was the sum of zone entries and rears on the back legs.

Forced swimming test

During FST, mice were forced to swim in 25°C water in a 2-liter Pyrex beaker (diameter 12.5 cm, depth 12 cm) for 6 min; the first 2 min was considered for habituation.²⁰ The animals' despair behavior was evaluated by measuring the immobility time during the last 4 min of the trial. It was considered when animals had no additional activity required to keep the animals' heads above the water. Swimming behavior, defined as horizontal movement throughout the beaker, which involved at least two limbs, and climbing behavior, defined as upward movements of the forepaws along the side of the beaker, was also recorded. The entire experiment was recorded by a camera and analyzed later. After 6 min, the mice were dried carefully to avoid hypothermia and returned to their home cage.

Brain BDNF enzyme-linked immunosorbent assay (ELISA)

Mice were rapidly decapitated after CO_2 euthanasia, and the whole brain was quickly removed, weighed, and the hippocampus was dissected on a cold tile. After that, the frozen samples were kept at -70°C until further assay. Hippocampus of each sample was homogenized for 30 sec with ice-cold extraction buffer containing 50 mM Tris-HCl, 0.6 M NaCl, 0.2% Triton-X 100, 1% bovine serum albumin, 0.1 mM benzethonium chloride, 1 mM benzamidine, and 0.1 mM phenylmethylsulfonyl fluoride at pH 7.4. According to the manufacturer's instructions, a mice BDNF ELISA kit (Picokine TM ELISA, catalog no:

EK0309, Boster Biological Technology, Canada) was used. Briefly, the homogenates were centrifuged (10,000×g, 25 min, 4°C), and the supernatant was separated.²¹ After dilution, 100 µL of samples were added to each empty well and incubated at 37°C for 90 minutes. After washing the wells, 100 µL of biotinylated anti-mice BDNF antibody working solution was added and incubated at 37°C for 60 minutes. Then all of the wells were washed three times with poly(butylene succinate) and incubated with avidin-biotin-peroxidase complex working solution at 37°C for 30 minutes. Finally, TMB color was added to each well and kept in the dark for 30 minutes. After changing the color to yellow following TMB stop solution addition, the plate optical density absorbance was read at 450 nm using a Synergy HTX microplate reader (BioTek, USA). All of the tests were run in duplicate. The standard curves ranged from 9.5 to 380 pg/mL BDNF with a 4 pg/mL sensitivity. The intra-assay coefficient of variation varied from 2.5 to 5.1%, and the inter-assay coefficient of variation varied from 4.8 to 6.3%. BDNF levels were calculated as pg/mg of total protein.

Statistical analysis

Results were expressed as group mean ± standard error of the mean. All behavior results were analyzed by One-Way ANOVA, followed by Tukey's multiple comparison tests. BDNF results were analyzed by One-Way ANOVA, followed by Tukey's multiple comparison tests. *P* values less than 0.05 were considered significant. Excel 2010 and GraphPad Prism (version 8) used the software programs for data analysis and making graphs.

RESULTS

Effect of Crt, ALA, and CYA on the behavioral tests

The locomotor activity results in Figure 1a show no statistically important difference in the total activity between Crt and ALA alone groups compared with the control group [*F* (2, 15)=3.544, *p*= 1.724]. Also, there was no significant difference in the total activity between CYA and the pretreatments with Crt, ALA, or fluoxetine groups compared with the vehicle group [*F* (5, 30)=1.445, *p*= 2.055]. The results of immobility time during FST are presented in Figure 1b; Crt insignificantly reduced immobility time in normal animals while ALA significantly reduced immobility time (81.6 ± 15.9 s vs. control 142 ± 9.7 s, *p*= 0.0094). CYA significantly increased immobility time (175.1 ± 13.16 s, vs. vehicle 130.9 ± 13.5 s, *p*= 0.0364), and by pretreatments, with ALA (100 ± 15.9 s, *p*= 0.020) or Crt (93.5 ± 16.6, *p*= 0.009) the immobility time significantly decreased compared to CYA alone. By co-administration of ALA-Crt following CYA injection, immobility time dropped dramatically (12.2 ± 2.59 s, *p*<0.001 vs. CYA). The result was significantly lower than pretreatment with ALA (*p*= 0.0022) or Crt separately (*p*= 0.0052). Fluoxetine as the reference antidepressant drug reduced immobility in CYA-treated animals (47.7 ± 18.8 s, *p*<0.001 vs. CYA group).

According to Table 1, swimming time during the FST following ALA administration was significantly higher than control (141 ± 13.9 s vs. control 76.9 ± 11 s, *p*= 0.002) Crt also slightly increased swimming time. By administering Crt and CYA, swimming time was significantly higher (*p*= 0.0393) than CYA alone.

Similarly, co-administrating ALA-Crt increased swimming time compared to CYA alone (*p*= 0.0030). The table also shows that treating with ALA-Crt significantly increased the climbing time compared to CYA alone (*p*= 0.0298). Climbing time was also significantly higher in animals treated with fluoxetine than CYA alone (*p*<0.001).

Brain BDNF level

The results of brain BDNF levels are depicted in Figure 2. BDNF level was not different following administering ALA or Crt compared to the control group (571 ± 43.1 pg/mg protein). Interestingly CYA significantly increased BDNF levels compared with vehicle (1059 ± 81.0 pg/mg protein, *p*= 0.0093). Treatment with Crt did not change the result, while treatment with ALA similar to fluoxetine significantly reduced BDNF levels compared with CYA alone (684 ± 103 pg/mg protein, *p*= 0.0454). Administering ALA-Crt also significantly decreased BDNF levels compared with CYA alone (*p*= 0.0413). Table 2

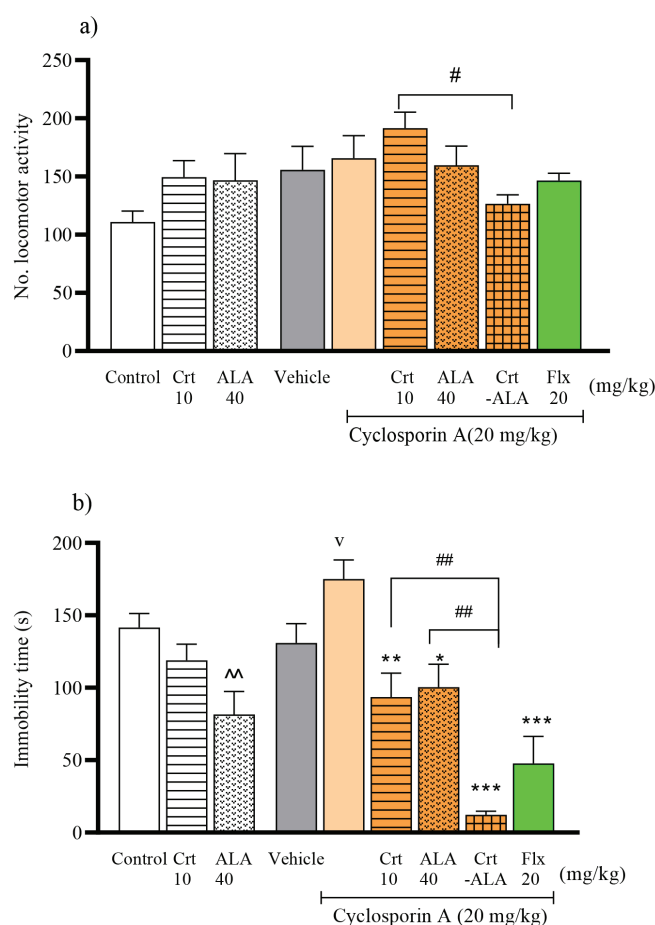


Figure 1. Effect of Crt, and ALA, on mice behavior following CYA administration. Total activity during locomotor test = (horizontal + vertical) exploration (a), and immobility time during FST (b). The control and vehicle groups received normal saline and 2% v/v EtOH/normal saline. Results are expressed as group mean ± SEM and analyzed by ANOVA followed by Tukey's comparison test (*n*= 6). **p*<0.05, compared with the control; **p*<0.05, compared with the vehicle. ***p*<0.01, and ****p*<0.001 compared with CYA group. ##*p*<0.01 as shown

ALA: Alpha-lipoic acid, Crt: Creatine, CYA: Cyclosporine A, SEM: Standard error of the mean

Table 1. Swimming and climbing time during the FST

Groups (n= 6)	Swimming time (s)	Climbing time (s)
Control	76.9 ± 11	21.14 ± 12.01
ALA	141 ± 13.9 [^]	17.50 ± 10.16
Crt	113 ± 9.65	8.50 ± 3.26
Vehicle	76.3 ± 17.4	1.66 ± 0.91
CYA	69.7 ± 18.3	3.16 ± 1.68
CYA+ALA	117 ± 10.1	22.50 ± 9.60
CYA+Crt	132 ± 18.2 [*]	20.17 ± 8.64
CYA+ALA+Crt	174 ± 18.1 ^{**v}	54.17 ± 18.67 [*]
CYA+fluoxetine	84.2 ± 21.2	91.50 ± 15.51 ^{***}

The control and vehicle groups received normal saline and 2% v/v EtOH/normal saline. Results are expressed as group mean ± SEM and analyzed by ANOVA followed by Tukey's comparison test (n= 6). [^]: $p < 0.05$, compared with the control; ^v: $p < 0.01$, compared with the vehicle. ^{*}: $p < 0.05$, ^{**}: $p < 0.01$, compared with CYA group. FST: Forced swimming test, ALA: Alpha-lipoic acid, Crt: Creatine, CYA: Cyclosporine A, SEM: Standard error of the mean

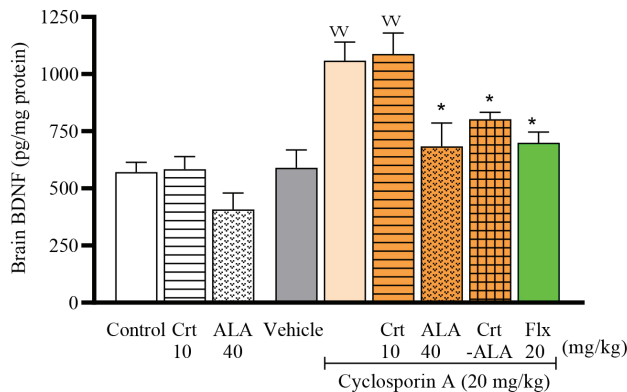


Figure 2. Normalized brain-derived BDNF level. The control and vehicle groups received normal saline and 2% v/v EtOH/normal saline. Results are expressed as group mean ± SEM and analyzed by ANOVA followed by Tukey's comparison test (n= 6). ^v $p < 0.01$, compared with the vehicle; ^{*} $p < 0.05$, compared with the CYA group

BDNF: Brain-derived neurotrophic factor, SEM: Standard error of the mean, CYA: Cyclosporine A, ALA: Alpha-lipoic acid, Crt: Creatine

shows the percentage of the hippocampus to whole-brain tissue; in CYA treatments, it was significantly higher than the vehicle group, and ALA and Crt reversed it, but not fluoxetine.

DISCUSSION

This research proved that the complementary drugs, ALA and Crt, prevent depressive-like behavior initiation by CYA in mice, and ALA-Crt showed a synergistic antidepressant effect. While CYA increased the brain BDNF level, treatment with Crt did not change the BDNF level, and ALA reduced it. This study was carried out on female mice since it was shown previously that Crt effects on depressive behavior in FST are sex-dependent, and female rats had shown better antidepressant-like response.²²

Table 2. Hippocampus to whole-brain percentage

Groups (n= 5)	% Hippocampus to the whole brain
Control	9.02 ± 0.44
ALA	7.15 ± 1.22
Crt	6.31 ± 0.52 [^]
Vehicle	8.06 ± 0.32
CYA	10.34 ± 0.54 ^v
CYA+ALA	7.42 ± 0.98 [*]
CYA+Crt	8.58 ± 0.51
CYA+ALA+Crt	8.22 ± 0.76
CYA+fluoxetine	11.31 ± 0.31 ^v

The control and vehicle groups received normal saline and 2% v/v EtOH/normal saline. Results are expressed as group mean ± SEM and analyzed by ANOVA followed by Tukey's comparison test (n= 6). [^]: $p < 0.05$, compared with the control; ^v: $p < 0.05$, compared with vehicle; ^{*} $p < 0.05$, compared with the CYA group. ALA: Alpha-lipoic acid, Crt: Creatine, CYA: Cyclosporine A, SEM: Standard error of the mean

FST is the most commonly used behavior test used for antidepressant screening.²³ Rodents perform a typical immobile posture following initial escape attempts movements in the inescapable water-filled beaker. Immobility time during FST was measured as a certain depressive-like phenotype that is despair behavior. The locomotor activity was evaluated prior to the FST since no noticeable difference was observed between different therapies and normal animals; thus, changes in the immobility time in FST could be interpreted as animal depressive-like behavior. CYA administration increased immobility time, indicating animal despair behavior. It was also reported previously that following CYA single-dose injection, immobility time measured after 4 h and 24 h in separate groups of animals increased in FST.¹⁵ After nephrotoxicity, neurotoxicity is the most severe CYA-related side effect that was proved to be related to drug interface with brain mitochondria.⁵

In the following experiment, Crt prevented CYA-induced despair behavior, as the immobility time was significantly lower than the CYA group. It has been proven that Crt could protect neurons against neurotoxic substances such as harmful excitatory amino acid glutamate levels by buffering ATP levels.²⁴ The mitochondrion and Crt and PCr establish a critical system in energy homeostasis in high energy demanding organs, such as the brain. Crt buffers against ATP depletion since it increases PCr as a substrate for Crt kinase, which converts adenosine diphosphate to ATP and, therefore, exerts its neuroprotection effect.²⁵ Therefore, by stimulating the rate of ATP synthesis and producing high amounts of PCr, Crt may have prevented the CYA-induced neurotoxicity and depressive-like behavior in mice. Pretreatment with Crt also increased the swimming time, although neurotransmitters were not measured on the downside of the study; according to previous studies, the

serotonergic system may be involved in the antidepressant-like effects. The SSRI drugs increase the swimming time while the catecholamine-related antidepressants increase the climbing time.²⁶ However, the pretreatment of fluoxetine with CYA showed unexpected results as the climbing time was significantly higher than control because of the interaction between CYA and fluoxetine. It was shown previously that high dose CYA decreases serotonin release.⁶

Pretreatment with ALA also reduced CYA-induced depression-like behavior, as immobility time was reduced significantly. ALA has been recognized as a potent antioxidant naturally found in diets; indeed, there would be increased functional capacity when given as a supplement.²⁷ ALA antioxidant capacity could be the reason for its protective effects against CYA-induced depression. In support of our study, animal studies have shown that ALA, along with reducing neurodegeneration in the hippocampus, reduced peripheral oxidative damage by increasing total anti-oxidative potential.²⁸ In addition, supplemented ALA in old rats has increased mitochondrial membrane capacity and declined oxidative damage.²⁹ Therefore ALA has prevented CYA neurotoxicity through interaction with brain mitochondria functioning.⁵ The most exciting finding was that co-administrating ALA-Crt had a synergistic antidepressant-like effect as immobility time during FST reduced dramatically. Meanwhile, climbing and particularly swimming time significantly increased. It was supposed that serotonin and mitochondria have a close interconnection since by improving mitochondrial functioning, swimming time increased. Variable mitochondrial activity equals energy demand to energy supply throughout the neurons and controls replacing mitochondria in the periphery.³⁰ Researchers have found that serotonin and 5-HT_{1A} receptors in hippocampal neurons are involved in mitochondrial trafficking.³¹

In the present study, brain BDNF levels almost doubled following CYA administration, and ALA similar to fluoxetine prevented this effect. BDNF and its receptor tyrosine kinase receptor B play essential roles in cell survival, neurogenesis, synaptic plasticity, and neuron survival during life.³² Previous studies have shown that chronic administration of CYA in rats for 30 days reduced brain BDNF levels that could be responsible for the depressant effect of CYA.⁸ It was observed that following 14 days of treatment with fluoxetine, BDNF expression was decreased.³³ However, following 21 days of fluoxetine administration, BDNF expression was upregulated.³⁴ It was also reported that BDNF level increased in an animal model of schizophrenia, and it was suggested that this elevation is in response to toxic materials as a defensive mechanism.^{35,36} After 7 days of BDNF infusions into the ventral tegmental area, latency to immobility in the FST declined, suggesting a depressive-like behavior against the BDNF role proposed in the hippocampus.³⁷ In addition, some studies have shown that increased BDNF level is related to depression.³⁸ According to these studies, different therapies and exposure time could influence brain BDNF levels. In our study, after depressive-like behavior initiated by CYA, BDNF levels increased, that might be related to CYA neurotoxic effect. However, although Crt pretreatment had an anti-immobility

effect in FST, it did not alter the rise in BDNF levels. Only ALA pretreatment reduced BDNF levels similar to fluoxetine, and probably, ALA is more effective in preventing CYA neurotoxic initiation; this warrants further investigation. In addition, the higher hippocampus to whole-brain ratio and elevation of BDNF level in CYA treated groups are related to the increased immobility during FST.

CONCLUSION

In conclusion, the present study showed that mitochondrial antioxidant ALA and Crt prevented CYA-induced depressive-like behavior. Therefore, it was postulated that at least part of CYA induced depressive effect is mediated by mitochondrial dysfunction neurotoxicity. Also, we observed that ALA could hinder BDNF alteration and its possible neurological changes as effective as fluoxetine.

ACKNOWLEDGEMENTS

This work was supported by the School of Pharmacy and Pharmaceutical Sciences Research Council, Isfahan University of Medical Sciences (grant number 399189, 1/05/2020).

Ethics

Ethics Committee Approval: Care and Use of Laboratory Animals Guidelines Issued by The National Ethical Committee of Vice-Chancellor in Research Affairs-Medical University of Isfahan (ethical no: IR.MUI.RESEARCH.REC.1399.200).

Informed Consent: Not applicable.

Peer-review: Externally peer-reviewed.

Authorship Contributions

Concept: M.A., A.M., Design: A.M., M.A., Data Collection or Processing: A.S.M., A.M., Analysis or Interpretation: A.M., M.A., Literature Search: A.M., M.A., A.S.M., Writing: A.M., M.A.

Conflict of Interest: No conflict of interest was declared by the authors.

Financial Disclosure: This research was supported by the Research Council, Isfahan University of Medical Sciences, Iran.

REFERENCES

- Buttini M, Limonta S, Luyten M, Boddeke H. Differential distribution of calcineurin A isoenzyme mRNA's in rat brain. *Naunyn Schmiedeberg Arch Pharmacol*. 1993;348:679-683.
- Mansuy IM. Calcineurin in memory and bidirectional plasticity. *Biochem Biophys Res Commun*. 2003;311:1195-1208.
- Musson RE, Cobbaert CM, Smit NP. Molecular diagnostics of calcineurin-related pathologies. *Clin Chem*. 2012;58:511-522.
- Kahl AL, Kirchhof J, Fütting A, Hütter BO, Wilde B, Witzke O, Benson S, Hadamitzky M, Schedlowski M. Acute administration of cyclosporine A does not impair attention or memory performance in healthy men. *Behav Pharmacol*. 2017;28:255-261.
- Serkova NJ, Christians U, Benet LZ. Biochemical mechanisms of cyclosporine neurotoxicity. *Mol Interv*. 2004;4:97-107.

6. Sato Y, Takayanagi Y, Onaka T, Kobayashi E. Impact of cyclosporine upon emotional and social behavior in mice. *Transplantation*. 2007;83:1365-1370.
7. Lewin GR, Barde YA. Physiology of the neurotrophins. *Annu Rev Neurosci*. 1996;19:289-317.
8. Chen CC, Hsu LW, Huang LT, Huang TL. Chronic administration of cyclosporine a changes expression of BDNF and TrkB in rat hippocampus and midbrain. *Neurochem Res*. 2010;35:1098-1104.
9. Pakzad D, Akbari V, Sepand MR, Aliomrani M. Risk of neurodegenerative disease due to tau phosphorylation changes and arsenic exposure via drinking water. *Toxicol Res (Camb)*. 2021;10:325-333.
10. Andres RH, Ducray AD, Schlattner U, Wallimann T, Widmer HR. Functions and effects of creatine in the central nervous system. *Brain Res Bull*. 2008;76:329-343.
11. Nasrallah F, Feki M, Kaabachi N. Creatine and creatine deficiency syndromes: biochemical and clinical aspects. *Pediatr Neurol*. 2010;42:163-171.
12. Gualano B, Artioli GG, Poortmans JR, Lancha Junior AH. Exploring the therapeutic role of creatine supplementation. *Amino Acids*. 2010;38:31-44.
13. Deng C, Sun Z, Tong G, Yi W, Ma L, Zhao B, Cheng L, Zhang J, Cao F, Yi D. α -Lipoic acid reduces infarct size and preserves cardiac function in rat myocardial ischemia/reperfusion injury through activation of PI3K/Akt/Nrf2 pathway. *PLoS One*. 2013;8:e58371.
14. Bist R, Bhatt DK. The evaluation of effect of alpha-lipoic acid and vitamin E on the lipid peroxidation, gamma-amino butyric acid and serotonin level in the brain of mice (*Mus musculus*) acutely intoxicated with lindane. *J Neurol Sci*. 2009;276:99-102.
15. Mesripour A, Golbidi M, Hajhashemi V. Dextromethorphan improved cyclosporine-induced depression in mice model of despair. *Res Pharm Sci*. 2020;15:447-453.
16. Alraddadi EA, Lillico R, Vennerstrom JL, Lakowski TM, Miller DW. Absolute oral bioavailability of creatine monohydrate in rats: debunking a myth. *Pharmaceutics*. 2018;10:31.
17. Zou J, Gan X, Zhou H, Chen X, Guo Y, Chen J, Yang X, Lei J. Alpha-lipoic acid attenuates cardiac hypertrophy via inhibition of C/EBP β activation. *Mol Cell Endocrinol*. 2015;399:321-329.
18. Hemsley KM, Hopwood JJ. Development of motor deficits in a murine model of mucopolysaccharidosis type IIIA (MPS-III A). *Behav Brain Res*. 2005;158:191-199.
19. Azimi Fashi Y, Mesripour A, Hajhashemi V. Evaluation of the effect of soybean diet on interferon- α -induced depression in male mice. *Avicenna J Phytomed*. 2017;7:436-443.
20. Mesripour A, Meshkati A, Hajhashemi V. A synbiotic mixture augmented the efficacy of doxepin, venlafaxine, and fluvoxamine in a mouse model of depression. *Turk J Pharm Sci*. 2020;17:293-298.
21. Paknejad B, Shirkhanloo H, Aliomrani M. Is there any relevance between serum heavy metal concentration and BBB leakage in multiple sclerosis patients? *Biol Trace Elem Res*. 2019;190:289-294.
22. Allen PJ, D'Anci KE, Kanarek RB, Renshaw PF. Chronic creatine supplementation alters depression-like behavior in rodents in a sex-dependent manner. *Neuropsychopharmacology*. 2010;35:534-546.
23. Deussing JM. Animal models of depression. *Drug Discovery Today: Disease Model*. 2006;3:375-383.
24. Brustovetsky N, Brustovetsky T, Dubinsky JM. On the mechanisms of neuroprotection by creatine and phosphocreatine. *J Neurochem*. 2001;76:425-434.
25. Matthews RT, Ferrante RJ, Klivenyi P, Yang L, Klein AM, Mueller G, Kaddurah-Daouk R, Beal MF. Creatine and cyclocreatine attenuate MPTP neurotoxicity. *Exp Neurol*. 1999;157:142-149.
26. Cryan JF, Markou A, Lucki I. Assessing antidepressant activity in rodents: recent developments and future needs. *Trends Pharmacol Sci*. 2002;23:238-245.
27. Anthony RM, MacLeay JM, Gross KL. Alpha-lipoic acid as a nutritive supplement for humans and animals: an overview of its use in dog food. *Animals (Basel)*. 2021;11:1454.
28. Cui X, Zuo P, Zhang Q, Li X, Hu Y, Long J, Packer L, Liu J. Chronic systemic D-galactose exposure induces memory loss, neurodegeneration, and oxidative damage in mice: protective effects of R- α -lipoic acid. *J Neurosci Res*. 2006;83:1584-1590.
29. Liu J, Head E, Gharib AM, Yuan W, Ingersoll RT, Hagen TM, Cotman CW, Ames BN. Memory loss in old rats is associated with brain mitochondrial decay and RNA/DNA oxidation: partial reversal by feeding acetyl-L-carnitine and/or R- α -lipoic acid. *Proc Natl Acad Sci U S A*. 2002;99:2356-2361.
30. Schwarz TL. Mitochondrial trafficking in neurons. *Cold Spring Harb Perspect Biol*. 2013;5:a011304.
31. Chen S, Owens GC, Crossin KL, Edelman DB. Serotonin stimulates mitochondrial transport in hippocampal neurons. *Mol Cell Neurosci*. 2007;36:472-483.
32. Webster MJ, Herman MM, Kleinman JE, Shannon Weickert C. BDNF and trkB mRNA expression in the hippocampus and temporal cortex during the human lifespan. *Gene Expr Patterns*. 2006;6:941-951.
33. Miró X, Pérez-Torres S, Artigas F, Puigdomènech P, Palacios JM, Mengod G. Regulation of cAMP phosphodiesterase mRNAs expression in rat brain by acute and chronic fluoxetine treatment. An in situ hybridization study. *Neuropharmacology*. 2002;43:1148-1157.
34. De Foubert G, Carney SL, Robinson CS, Destexhe EJ, Tomlinson R, Hicks CA, Murray TK, Gaillard JP, Deville C, Xhenseval V, Thomas CE, O'Neill MJ, Zetterström TS. Fluoxetine-induced change in rat brain expression of brain-derived neurotrophic factor varies depending on length of treatment. *Neuroscience*. 2004;128:597-604.
35. Hirota K, Lambert DG. Ketamine: its mechanism(s) of action and unusual clinical uses. *Br J Anaesth*. 1996;77:441-444.
36. Guo C, Yang Y, Su Y, Si T. Postnatal BDNF expression profiles in prefrontal cortex and hippocampus of a rat schizophrenia model induced by MK-801 administration. *J Biomed Biotechnol*. 2010;2010:783297.
37. Eisch AJ, Bolaños CA, de Wit J, Simonak RD, Pudiak CM, Barrot M, Verhaagen J, Nestler EJ. Brain-derived neurotrophic factor in the ventral midbrain-nucleus accumbens pathway: a role in depression. *Biol Psychiatry*. 2003;54:994-1005.
38. Branchi I, D'Andrea I, Sietzema J, Fiore M, Di Fausto V, Aloe L, Alleva E. Early social enrichment augments adult hippocampal BDNF levels and survival of BrdU-positive cells while increasing anxiety- and "depression"-like behavior. *J Neurosci Res*. 2006;83:965-973.



Potential Inhibitors of SARS-CoV-2 from *Neocarya macrophylla* (Sabine) Prance ex F. White: Chemoinformatic and Molecular Modeling Studies for Three Key Targets

Amina Jega YUSUF^{1*}, Musa Ismail ABDULLAHI¹, Aliyu Muhammad MUSA², Hassan ABUBAKAR³, Abubakar Muhammad AMALI⁴,
 Asma'u Hamza NASIR²

¹Usmanu Danfodiyo University, Department of Pharmaceutical and Medicinal Chemistry, Sokoto, Nigeria

²Ahmadu Bello University, Department of Pharmaceutical and Medicinal Chemistry, Zaria, Nigeria

³Sokoto State University, Department of Chemistry, Sokoto, Nigeria

⁴Usmanu Danfodiyo University, Department of Pharmacology and Toxicology, Sokoto, Nigeria

ABSTRACT

Objectives: The novel coronavirus disease-2019 (COVID-19) that emerged in China, is a highly transmittable and pathogenic viral infection caused by the severe acute respiratory syndrome-coronavirus-2 (SARS-CoV-2); the disease has been declared by the World Health Organization as a Public Health Emergency of International Concern. The unavailability of approved therapeutic agents or vaccines is of great concern. This study performed molecular docking and absorption, distribution, metabolism, excretion and toxicity (ADMET) analysis of some compounds isolated from *Neocarya macrophylla* (Sabine) Prance ex F. White (Chrysobalanaceae) against three targets of SARS-CoV-2 proteins (3C-like protease, spike protein, and papain-like protease).

Materials and Methods: Phytoconstituents isolated from *N. macrophylla* were screened against key targets of SARS-CoV-2 using Auto Dock Vina, while the ADMET analysis was performed using swiss ADME and pkCSM ADMET descriptors algorithm protocols.

Results: The *in silico* computational studies revealed that the compounds (catechin, catechin-3-rhamnoside, quercetin, and epicatechin) isolated from *N. macrophylla* can effectively bind with high affinity and lower energy values to the three target proteins of SARS-CoV-2. ADMET analysis was used to predict important pharmacokinetic properties of the compounds, such as aqueous solubility, blood-brain barrier, plasma protein binding, CYP2D6 binding, intestinal absorption, and hepatotoxicity.

Conclusion: The findings of this study have shown that *N. macrophylla* contains potential leads for SARS-CoV-2 inhibition and thus, should be studied further for development as therapeutic agents against COVID-19.

Key words: *Neocarya macrophylla*, SARS-CoV-2, flavonoids, ADMET, COVID-19

INTRODUCTION

Coronavirus disease-2019 (COVID-19) is a major public health problem. From December 2019, when it was first presented in Wuhan, China,¹ it rapidly spread to several countries around the world, necessitating the declaration of the disease as a Public Health Emergency of International Concern by World Health Organization on the 30th January 2020.² The life cycle

of coronavirus mediates its infection in few typical steps *viz.*; (i) attachment that must do with transmission inside the human body as well as binding of the virus spike protein with angiotensin-converting enzyme-2 (ACE-2) receptors of the cell membrane, (ii) penetration, which involves membrane fusion of the virus through endocytosis and release of the viral genome inside the cell, (iii) biosynthesis, which encompasses the

*Correspondence: amina.yusuf@udusok.edu.ng, Phone: +2348036386793, ORCID-ID: orcid.org/0000-0002-4557-859X

Received: 28.04.2021, Accepted: 16.08.2021

©Turk J Pharm Sci, Published by Galenos Publishing House.

synthesis of replication-transcription complex and replication of viral RNA, (iv) maturation *i.e.* transcription of subgenomic mRNAs, (v) release that must with the translation of the viral proteins, assembly of new virions, and release of the virion from infected cells *via* exocytosis and infect new healthy cells.^{3,4} There is presently no specific drug or vaccine targeted at the severe acute respiratory syndrome-coronavirus-2 (SARS-CoV-2) virus but different classes of drugs, including anti-viral, anti-inflammatory, steroids, or anti-coagulants are employed for the symptomatic treatment. There is thus, an urgent need for research to develop an alternative, effective and safe therapy for managing COVID-19, and natural products have been known historically as a veritable source of medicines.

Few studies have reported the potential of medicinal plants as a novel approach for the effective management of the COVID.⁵ There are several anecdotal accounts of the use of plant extracts, including *Artemisia annua* L., *Pyrrosia lingua* (Thunb.) Farw., *Lindera aggregata* (Sims) Kosterm., *Zingiber officinale* Roscoe, *Syzygium aromaticum* (L.) Merr. & L.M.Perry, and *Allium sativum* L., singly or as a combination for managing COVID-19.⁶ A recent *in silico* drug repurposing study identified several natural product compounds with excellent binding affinity against the three selected COVID-19 viral protein targets.^{6,7} Phytochemicals containing biologically active polyphenols have been reported as effective agents against COVID-19 disease.⁸

Neocarya macrophylla (Sabine) Prance ex F. White is a West African plant species belonging to the Chrysobalanaceae family. It has been used in ethnomedicine to treat different diseases such as pulmonary troubles, inflammations, breathing disorders, internal troubles, and other gastrointestinal tract (GIT) related issues.⁹ Chemically, steroids, flavonoids, and glycosides are the major secondary metabolites found in the plant.¹⁰ Based on the anecdotal uses and some observed biological effects¹⁰ of *N. macrophylla*, this has strengthened us to perform molecular docking and absorption, distribution, metabolism, excretion, and toxicity (ADMET) analysis of some compounds isolated from the plant against three targets of SARS-CoV-2 proteins [3C-like protease, spike protein, and papain-like protease (PL^{pro})].

MATERIALS AND METHODS

Ligand selection and preparation

Catechin, catechin-3-rhamnoside, epicatechin, and quercetin (Figure 1) were previously isolated from the stem bark and leaves of *N. macrophylla* using a combination of silica gel and a Sephadex LH-20 column. The structures of the compounds were established using one-dimensional (1D) and two-dimensional (2D) nuclear magnetic resonance spectroscopic analysis and by direct comparison of data obtained with those reported in the literature.^{11,12} The SDF files of catechin (CID: 9064), catechin-3-rhamnoside (CID: 21626704), epicatechin (CID: 72276), and quercetin (5280343) were retrieved from PubChem (<https://pubchem.ncbi.nlm.nih.gov/>). The structures were prepared and converted to protein data bank (PDB) format using Chimera 1.14.¹³

Protein preparation

Crystallography structures of the SARS-CoV-2 main protease (PDB: 6LU7), spike protein (PDB ID: 6LZG), and PL^{pro} (PDB: 6W9C) were retrieved from the PDB (<https://www.rcsb.org>). The 3D structures of the proteins were prepared by removing all water molecules and non-standard residues to alleviate errors and as a cleanup of a PDB file retaining only ATOM and TER records and it was modified by adding hydrogens and minimized.¹³

Molecular docking

Molecular docking studies were conducted to estimate the binding energies of the compounds isolated from *N. macrophylla* against the three protein targets of SARS-CoV-2 using AutoDock Vina software.¹⁴ The prepared proteins and the ligands were converted into PDB partial charge, and atom type format using AutoDock tools. The grid box dimensions for each protein were noted as indicated in Table 1. Molecular docking was performed using AutoDock tools in PyRx software and post docking analysis was conducted using the BIOVIA Discovery studio visualizer 2020 and Chimera 1.14.¹³

In silico ADMET and drug-likeness prediction

The physicochemical properties of the compounds (catechin, catechin-3-rhamnoside, epicatechin, and quercetin) and their ADME and toxicity were determined using swiss ADME and pkCSM ADMET descriptors algorithm protocol.^{15,16} The drug-likeness properties of the compounds were predicted using the Molinspiration Cheminformatics free web service (<https://www.molinspiration.com/cgi-bin/properties>) by inserting the Canonical SMILES of the compounds.

No statistical data were used for this study.

RESULTS

Molecular docking data

The four compounds (catechin, catechin-3-rhamnoside, epicatechin, and quercetin) isolated from *N. macrophylla* were screened against three important protein targets of SARS-CoV-2, including main protease, spike protein, and PL^{pro} by conducting a molecular docking analysis using AutoDock Vina

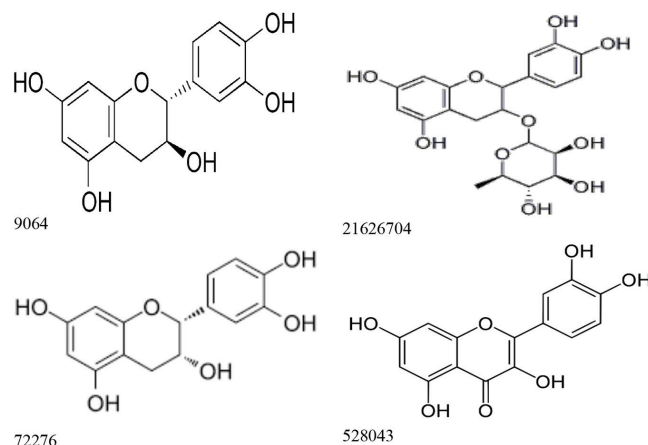


Figure 1. 2D-structures of the ligands isolated from *Neocarya macrophylla*

tools in PyRx. The docking scores of the four ligands at the active sites of the three proteins are shown in Table 2.

Based on the analysis of the docking results (Figure 2), interactions between the ligands (*i.e.* catechin, catechin-3-rhamnoside, epicatechin, and quercetin) and the binding sites of the main protease of the SARS-CoV-2 were consistent; the binding energies for the best pose against the SARS-CoV-2 main protease ranged from -8.0 to -6.9 kcal/mol with catechin-3-rhamnoside having the highest docking score. All the ligands interacted with key active site residues such as HIS41 and CYS145. Catechin formed five conventional hydrogen bonds with GLU166, ARG188, and THR190. Quercetin formed a hydrogen bond with GLU166 only and catechin-3-rhamnoside formed hydrogen bonds with THR26, LEU141, ASN142, GLY143, and MET165, while epicatechin interacted with LEU141, HIS163, and GLN189 *via* H-bond (Table 3).

The interaction of the spike protein with the compounds is shown in Figure 3. The ligands exhibited lower binding energies ranging from -7.1 to -6.3 kcal/mol. Catechin-3-rhamnoside indicated the highest affinity (-7.1) toward the receptor, while epicatechin had the least affinity (Table 2). All the compounds interacted with similar amino acid residues of clinical importance such as TYR505 (active site residue). Catechin-3-rhamnoside formed a conventional hydrogen bond with TYR449, and GLY496. Quercetin was found to form four conventional hydrogen bonds with TYR505, ASN501, GLY496 and GLN493. Catechin formed a hydrogen bond with ASN501 and GLY496, while epicatechin interacted (H-bond) with TYR505 at the active sites (Table 3).

The interaction formed between the ligands and the PL^{pro} of SARS-CoV-2 coronavirus is shown in Figure 4. Epicatechin had the lowest docking score and highest affinity while catechin was the least. Catechin-3-rhamnoside formed five hydrogen bonds with residues ARG166, ASP164, TYR264, TYR268, and GLY163. Epicatechin formed three hydrogen bonds with ASP302, ASN267, TYR264, and TYR268. Also, pication was built between the ligand and ARG166. Two hydrogen bonds were formed with residues ASP302 and ARG166 for catechin, whereas quercetin formed only one hydrogen bond with ARG166 (Table 3).

In silico ADMET and drug-likeness evaluation

The results of the *in silico* ADMET screening and drug-likeness of the compounds are presented in Tables 4 and 5. The analysis of different parameters, including physicochemical properties, ADMET and drug-likeness was performed.

DISCUSSION

COVID-19, a highly transmissible disease, has rapidly spread all over the world.^{17,18} This necessitated the need for research to develop effective and safe therapy for managing the disease in the absence of therapeutic drug(s) and vaccine. Natural products, either singly or in combination, have proven to be effective in the management of COVID-19.^{5,19} *N. macrophylla* has been used traditionally to treat pulmonary troubles, inflammations, breathing disorders, internal issues, and other GIT related issues.⁹ In this study, we selected three important coronavirus protein targets

i.e. the main protease, spike protein, and PL^{pro}, which were docked with four compounds isolated from *N. macrophylla* (catechin, catechin-3-rhamnoside, epicatechin, and quercetin) as ligands.⁹⁻¹² The spike glycoprotein (SGp) of coronavirus attaches to ACE-2 receptor, thereby allowing viral entry.²⁰ Viral genome replication will thereafter set in by RNA-dependent RNA polymerase (*RdRP*) gene.²¹ The main proteinase (3CL^{pro}) and PL^{pro} facilitates the process of proteolysis of the viral polyprotein into functional units.⁴ In order words, the proteins SGp, ACE-2, 3CL^{pro}, PL^{pro}, and RdRP are directly involved in either the establishment of the disease, translation, and replication or facilitate the proliferation of the virus in the host cell.²⁰

The docking scores of the compounds against the individual proteins revealed binding energies ranging from -6.3 to -8.0 kcal/mol, which was higher compared to the docking scores reported for remdesivir, hydroxychloroquine, ribavirin, and arbidol that were used as control.¹⁷ All the ligands interacted with key active site residues of the SARS-CoV-2 main protease, such as HIS41 and CYS145.²² Shah et al.²³ reported that the OH group of lopinavir interacted with GLU166 and HIS41. Besides, remdesivir and methisazone have also been reported to form H-bond with GLU166, ASN142, and THR190 for the main protease. Peterson¹⁶ also reported a higher docking score (-7.7 kcal/mol) for quercetin. The main protease plays a vital role in viral replication. Thus, inhibiting the activity of the main protease could block the replication of the coronavirus inside infected cells. Hence, based on the results of our study, phytoconstituents of *N. macrophylla* may be potential inhibitors of the main protease of SARS-CoV-2.

SGp of SARS-CoV-2 plays an important role in facilitating the viral attachment, fusion, and viral entry into the host cells.²⁰ Phytoconstituents with lower binding energy toward the receptor could serve as a potential drug for further studies. The ligands demonstrated lower binding energy and have a higher affinity for the spike glycoprotein. Non-covalent interactions of the compounds detected by AutoDock Vina tools in PyRx revealed that all compounds interacted with catalytic residue TYR505 (active site) of the spike protein. Chikhale et al.²⁴ reported similar docking results and interactions for quercetin-3-O-galactosyl-rhamnosylglucoside, hydroxychloroquine, and lopinavir. However, the binding affinities of the tested ligands (catechin, catechin-3-rhamnoside, epicatechin, and quercetin) were higher than those of hydroxychloroquine (-3.57 kcal/mol), remdesivir (-4.41 kcal/mol), and lopinavir (-4.22 kcal/mol).²⁴ Pandey et al.²⁵ also reported a lower binding affinity of -5.6 for hydroxychloroquine.

The PL^{pro} plays a vital role in processing viral polyproteins to generate a functional replicase complex and enable viral spread^{26,27} and it is also implicated in cleaving proteinaceous post-translational modifications on host proteins as an evasion mechanism against host antiviral immune responses.²⁸⁻³⁰ The selected ligands could dock into an entirely different binding pocket of PL^{pro} with lower binding energy compared to the standard inhibitor, α -ketoamide 13 b (-8.24 kcal/mol) as reported by Gurung et al.¹⁹

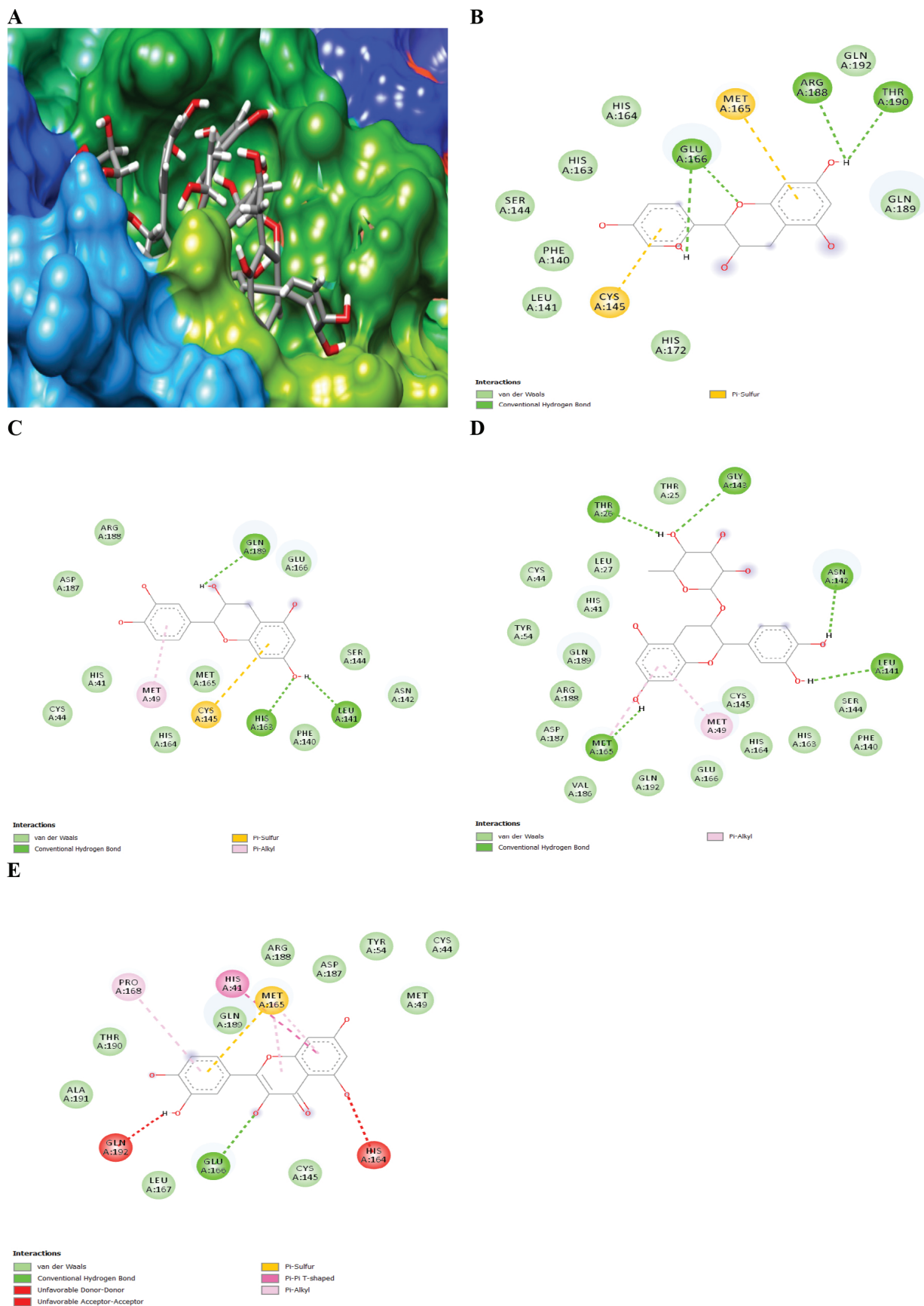


Figure 2. A) Docking pose at the active site of the main protease of SARS-CoV-2 for the compounds. 2D animated poses between the compounds and main protease of coronavirus B) catechin, C) epicatechin, D) catechin-3-rhamnoside, E) quercetin

The ADMET analysis of catechin, catechin-3-rhamnoside, epicatechin, and quercetin was predicted by Swiss ADME and pkCSM ADMET descriptors algorithm protocol.^{15,16} The important parameters related to ADMET properties such as Lipinski's³¹ rule of five, the solubility of drug, pharmacokinetic properties, molar refractivity, and drug likeliness were evaluated. According to the rule, molecules should have molecular weight ≤ 500 , hydrogen bond donors ≤ 5 and acceptors ≤ 10 , calculated octanol-water and -partition coefficient, and $\log p \leq 5$ possess good membrane permeability and molar refractivity should be between 40-130.³¹ The ADMET and drug-likeness results indicated that all compounds have satisfied the limitations and drug-likeness. The study assisted in screening the best compound(s) with drug-likeness in a biological system and the compounds were considered to be well absorbed based on the predicted values of intestinal absorption, which were $>30\%$ and Caco2 permeability values were also normal. Human VDss

of the compounds ranged from -1.559 to 2.001 L/kg that was within the range; thus, values of 0.71 L/kg are considered low and 2.81 L/kg as high. Blood-brain barrier (BBB) permeability $\log BB$ of <-1 is considered as poorly absorbed, while a value

Table 1. Grid box dimensions

S/no	Name of the protein (PDB ^a ID)	Grid box center	Grid dimension
1	Main protease (PDB: 6LU7)	-25.8 x 13.3 x 56.2	54 x 69 x 64
2	Spike protein (PDB ID: 6LZG)	-32.1 x 28.0 x 21.2	44 x 54 x 61
3	Papain-like protease (PDB: 6W9C)	-22.3 x -2.84 x 24.3	44 x 74 x 77

^aPDB: Protein data bank

Table 2. Docking scores of the compounds against three target proteins SARS-CoV-2

Compound name	Compound ID	Docking scores (kcal/mol)		
		Main protease	Spike protein	Papain-like protease
Catechin	9064	-7.0	-6.6	-6.4
Catechin-3-rhamnoside	21626704	-8.0	-7.1	-6.9
Epicatechin	72276	-6.9	-6.3	-7.1
Quercetin	528043	-6.9	-6.7	-7.0

Table 3. Interactions of the compounds against the three target proteins of SARS-CoV-2

Compound name	Interactions		
	Main protease	Spike protein	Papain-like protease
Catechin	H-bond: GLU166, ARG188, THR190 Others: PHE140, LEU141, SER144, LYS145, HIS163, HIS164, MET165, HIS172, GLN189, GLN192	H-bond: GLY496, ASN501 Others: ARG403, GLU406, LYS417, TYR453, PHE497, TYR495, GLN498, TYR505	H-bond: ARG166, ASP302 Others: LEU162, GLY163, ASP164, VAL165, MET208, SER245, ALA246, PRO248, SER262, TYR264, ASN267, TYR268, TYR273, THR301
Catechin-3-rhamnoside	H-bond: THR26, LEU141, ASN142, GLY143, MET165 Others: THR25, LEU27, HIS41, CYS44, MET49, TYR54, PHE140, SER144, CYS145, HIS163, HIS164, GLU166, ASP187, VAL186, ARG188, GLN189, GLN192	H-bond: TYR449, GLY496 Others: ARG403, TYR453, SER494, TYR495, PHE497, GLN498, ASN501, GLY502, TYR505	H-bond: GLY163, ASP164, ARG166, TYR264, TYR268 Others: VAL165, LEU162, MET208, PRO248, TYR273, ASN267, THR301
Epicatechin	H-bond: LEU 141, HIS163, GLN189 Others: HIS41, CYS44, MET49, PHE140, ASN142, SER144, CYS145, HIS164, MET165, GLU166, ASP187, ARG188,	H-bond: TYR505 Others: ARG403, GLU406, LYS417, TYR453, LEU455, TYR495, GLY496, PHE497, GLN498, ASN501	H-bond: ASN267, TYR268, ASP302 Others: VAL165, ASP164, ARG166, MET208, MET243, SER245, ALA246, PRO248, SER262, TYR264, GLY266, TYR273, THR301
Quercetin	H-bond: GLU166 Others: HIS41, CYS44, MET49, TYR54, CYS145, HIS164, MET165, LEU167, PRO168, ASP187, ARG188, GLN189, THR190, ALA191, GLN192	H-bond: GLN493, GLY496, ASN501, TYR505 Others: ARG403, TYR453, GLN493, TYR495, SER494, GLN496, PHE497, GLN506	H-bond: ARG166 Others: LEU162, ASP164, GLY163, MET208, SER245, PRO248, ASN267, TYR268, TYR273, THR301, ASP302

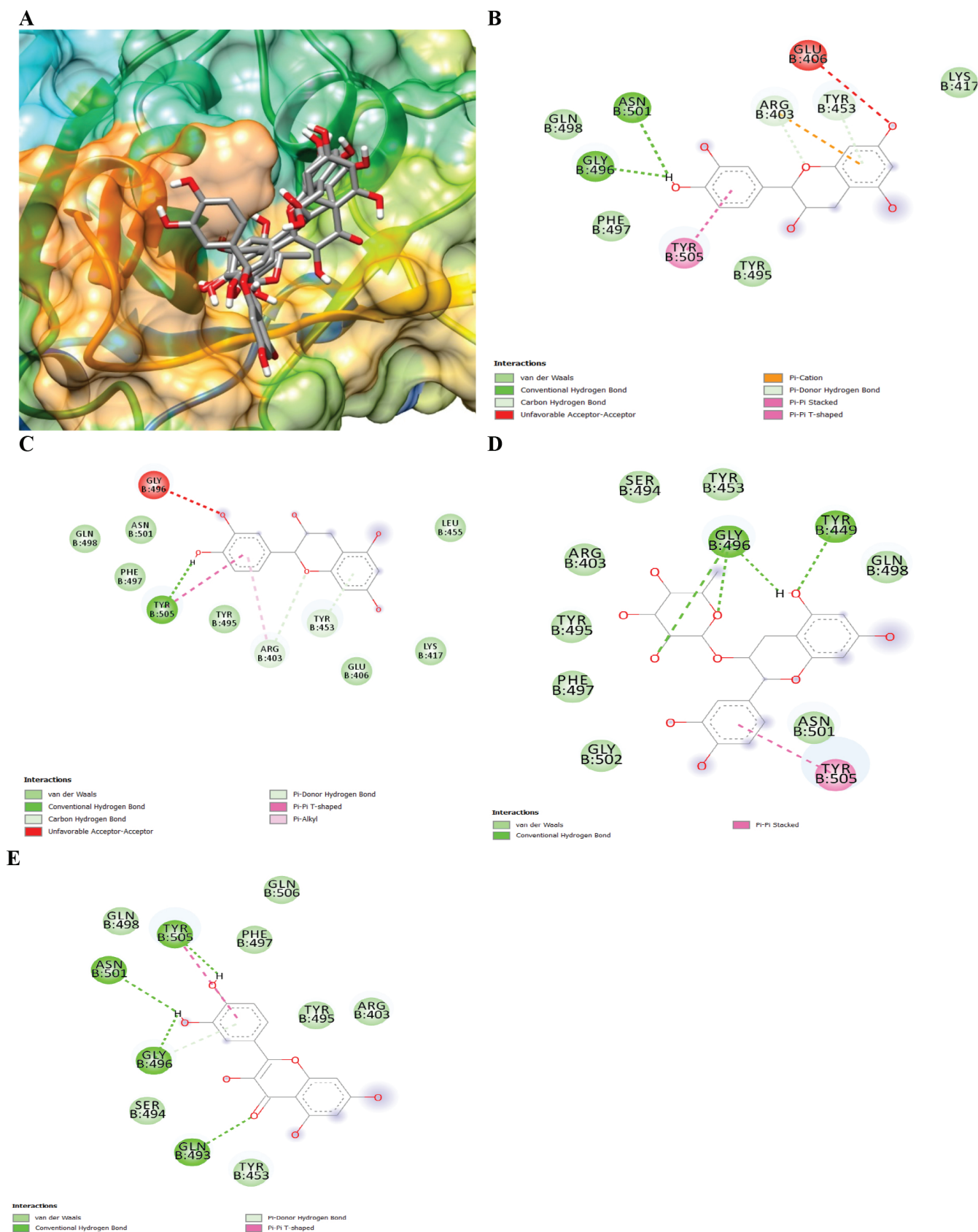


Figure 3. A) Docking pose at the active site of the main spike protein of SARS-CoV-2 for the compounds. 2D animated poses between the compounds and spike protein of coronavirus B) catechin, C) epicatechin, D) catechin-3-rhamnoside, E) quercetin

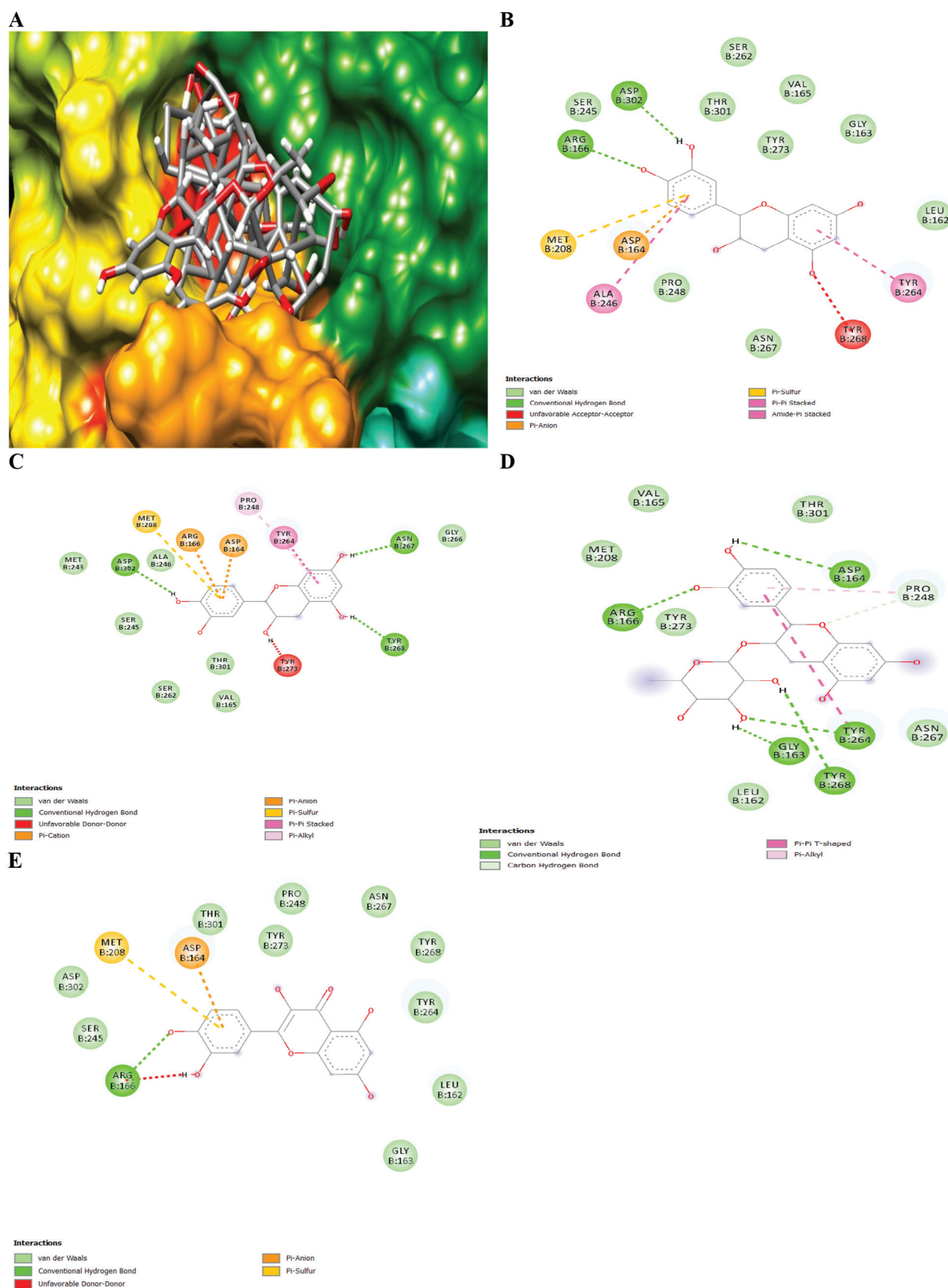
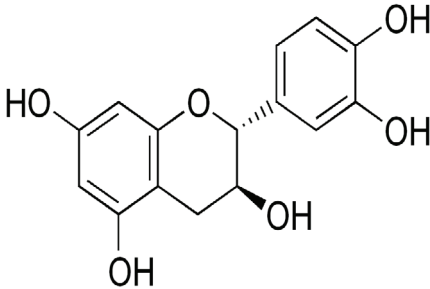
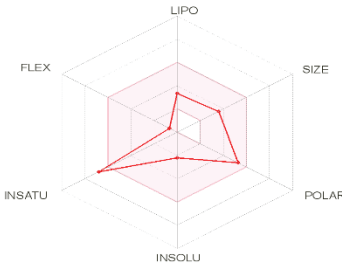
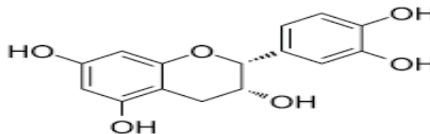
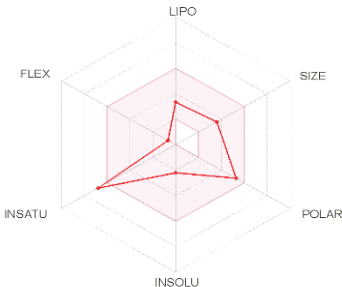
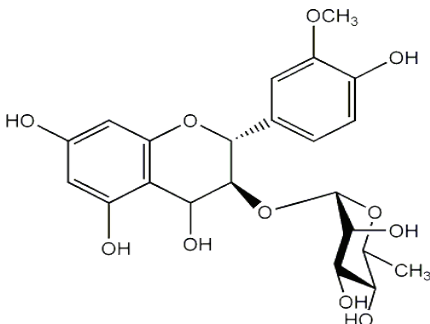
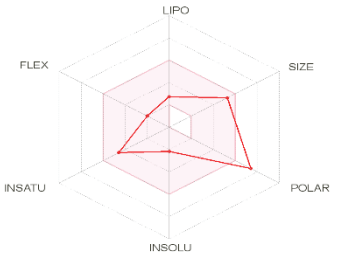
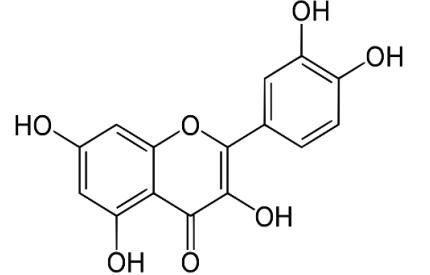
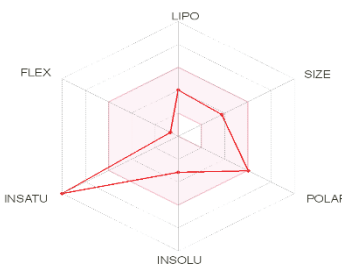


Figure 4. A) Docking pose at the active site of the papain-like protease of SARS-CoV-2 for the compounds. 2D animated poses between the compounds and spike protein of coronavirus B) catechin, C) epicatechin, D) catechin-3-rhamnoside, E) quercetin

Table 4. *In silico* ADMET properties of compounds from *Neocarya macrophylla*

Properties	Quercetin	Catechin	Epicatechin	Catechin-3-rhamnoside
Physicochemical properties				
Formula	C ₁₅ H ₁₀ O ₇	C ₁₅ H ₁₄ O ₆	C ₁₅ H ₁₄ O ₆	C ₂₁ H ₂₄ O ₁₀
Molecular weight (g/mol)	302.24	290.27	290.27	436.41
Fraction Csp3	0.00	0.20	0.20	0.43
H-bond donor	5	5	5	7
H-bond acceptor	7	6	6	10
Molar refractivity	78.03	74.33	74.33	105.56
TPSA	131.36 Å ²	110.38 Å ²	110.38 Å ²	169.30 Å ²
Absorption				
Water solubility (log mol/L)	-2.925	-3.117	-3.117	-2.98
Caco2 permeability (log Papp in 10 ⁻⁶ cm/s)	-0.229	-0.283	-0.283	-0.002
Intestinal absorption (human) (% absorbed)	77.207	68.829	68.829	48.902
Skin permeability (log Kp)	-2.735	-2.735	-2.735	-2.735
P-glycoprotein substrate	Yes	Yes	Yes	Yes
P-glycoprotein inhibitor I	No	No	No	No
P-glycoprotein inhibitor II	No	No	No	No
Distribution				
VDss (human, log L/kg)	-1.559	1.027	1.027	2.001
Fraction unbound human (Fu)	-0.206	0.235	0.235	0.309
BBB permeability (log BB)	-1.098	-1.054	-1.054	-1.345
CNS permeability (log PS)	-3.065	-3.298	-3.298	-3.988
Metabolism				
CYP2D6 substrate	No	No	No	No
CYP3A4 substrate	No	No	No	No
CYP1A2 inhibitor	Yes	No	No	No
CYP2C19 inhibitor	No	No	No	No
CYP2C9 inhibitor	No	No	No	No
CYP2D6 inhibitor	No	No	No	No
CYP3A4 inhibitor	No	No	No	No
Excretion				
Total clearance (log mL/min/kg)	0.407	0.183	0.183	-0.393
Renal OCT2 substrate	No	No	No	No
Toxicity				
Maximum tolerated dose (human) (log mg/kg/day)	0.499	0.438	0.438	0.449
Oral rat acute toxicity (LD ₅₀) (mol/kg)	2.471	2.428	2.428	2.446
Oral rat chronic toxicity (LOAEL) (log mg/kg_bw/day)	2.612	2.500	2.500	2.808
Hepatotoxicity	No	No	No	No
<i>Tetrahymena pyriformis</i> toxicity (log µg/L)	0.288	0.347	0.347	0.285
Minnow toxicity (log mM)	3.721	3.585	3.585	6.116
Drug-likeness				
MiLogP	1.68	1.37	1.37	0.69
TPSA	131.35	110.37	110.37	169.30

Table 5. Boiled-egg model for ADMET/drug-likeness of the compounds from *Neocarya macrophylla*

Compounds	2D structure	Boiled egg model for ADMET/drug likeness
Catechin		
Epicatechin		
Catechin-3-rhamnoside		
Quercetin		

of >0.3 is considered as well. A drug can penetrate central nervous system, when the $\log PS$ is >-2 , however, $\log PS$ of <-3 is considered as poor. A compound is considered toxic, when *Tetrahymena pyriformis* value is >-0.5 $\mu\text{g/L}$ and high acute toxicity for compounds can as well be attributed to a minnow toxicity LC_{50} of <-0.3 Mm .²⁰

All the compounds had five hydrogen bonds except catechin-3-rhamnoside, which had seven and the hydrogen bond acceptors were within the range. The hydrophilicity of the compounds determined by calculating the $\log p$ value indicated

that the compounds have good absorption. Thus, higher $\log p$ values result in poor absorption. The calculated polar surface area (PSA) was within the range of 7.0–200.0 Å. One violation of Lipinski's rule (PSA, molecular weight, number of hydrogen donors, and acceptors) was observed for catechin-3-rhamnoside, which indicates the compound's potential as a drug-like molecule.

Boiled-egg for ADMET/drug-likeness is an accurate predictive model used to estimate various stages of drug discovery; it works by computing the lipophilicity and polarity of small

molecules.³² The pink area represents the optimal range for each property constituting lipophilicity, molecular weight, polarity, solubility, saturation, flexibility among others.

CONCLUSION

In conclusion, we have screened four compounds (catechin, catechin-3-rhamnoside, epicatechin, and quercetin) isolated from *N. macrophylla* using molecular docking, *in silico* ADMET, and drug-likeness prediction. The findings of this study have shown that the plant *N. macrophylla* may contain potential leads for SARS-CoV-2 inhibition and thus, should be studied further for development as effective therapeutic agents against COVID-19.

ACKNOWLEDGMENTS

We acknowledge the efforts of the staff of JARIS Computational Biology Center, Jos, Nigeria, for providing the softwares.

Ethics

Ethics Committee Approval: Not applicable.

Informed Consent: Not applicable.

Authorship Contributions

Concept: A.J.Y., Design: A.J.Y., M.I.A., A.M.M., H.A., A.M.A., A.H.N., Data Collection or Processing: A.J.Y., M.I.A., A.M.M., H.A., A.M.A., A.H.N., Analysis or Interpretation: A.J.Y., A.H.N., Literature Search: A.J.Y., M.I.A., A.M.M., H.A., A.M.A., A.H.N., Writing: Amina A.J.Y., H.A.

Conflict of Interest: No conflict of interest was declared by the authors.

Financial Disclosure: The authors declared that this study received no financial support.

REFERENCES

- Lupia T, Scabini S, Mornese Pinna S, Di Perri G, De Rosa FG, Corcione S. 2019 novel coronavirus (2019-nCoV) outbreak: A new challenge. *J Glob Antimicrob Resist*. 2020 Jun;21:22-27.
- World Health Organization. Coronavirus: overview, prevention and symptoms 2020. [Online]. Retrieved 6th September 2020 from https://www.who.int/health-topics/coronavirus#tab=tab_1
- Yuki K, Fujiogi M, Koutsogiannaki S. COVID-19 pathophysiology: a review. *J Clin Immunol*. 2020;215:108427.
- Kilianski A, Mielech AM, Deng X, Baker SC. Assessing activity and inhibition of Middle East respiratory syndrome coronavirus papain-like and 3C-like proteases using luciferase-based biosensors. *J Virol*. 2013;87:11955-11962.
- Kadioglu O, Saeed M, Gretten HJ, Efferth T. Identification of novel compounds against three targets of SARS CoV-2 coronavirus by combined virtual screening and supervised machine learning. *Comput Biol Med*. 2021;133:104359.
- Li SY, Chen C, Zhang HQ, Guo HY, Wang H, Wang L, Zhang X, Hua SN, Yu J, Xiao PG, Li RS, Tan X. Identification of natural compounds with antiviral activities against SARS-associated coronavirus. *Antiviral Res*. 2005;67:18-23.
- Chojnacka K, Witek-Krowiak A, Skrzypczak D, Mikula K, Młynarz P. Phytochemicals containing biologically active polyphenols as an effective agent against COVID-19-inducing coronavirus. *J Funct Foods*. 2020;73:104146.
- Peterson LE. COVID-19 and flavonoids: *in silico* molecular dynamics docking to the active catalytic site of SARS-CoV and SARS-CoV-2 main protease. 2020. doi: 10.13140/RG.2.2.22294.50246.
- Yusuf AJ, Abdullahi MI, Haruna AK, Idris AY, Musa AM. Isolation and characterization of stigmasterol and bis-(5,7-diacetyl-catechin-4'- α -rhamnopyranoside) from the stem bark of *Neocarya macrophylla* (Sabine) Prance (Chrysobalanaceae). *Nig J Basic Appl Sci*. 2015;21:15-22. <https://www.ajol.info/index.php/njbas/article/view/120053>
- Yusuf AJ, Abdullahi MI, Musa AM, Haruna AK, Mzozoyana V, Biambo AA, Abubakar HA. Bioactive flavan-3-ol from the stem bark of *Neocarya macrophylla*. *Sci Afr*. 2020;7:e00273.
- Yusuf AJ, Abdullahi MI, Musa AM, Haruna AK, Mzozoyana V, Abubakar H. Bioactive (+)-catechin-3'-O-rhamnopyranoside from *Neocarya macrophylla* (Sabine) Prance (Chrysobalanaceae). *Egypt J Basic Appl Sci*. 2019;124-136.
- Yusuf AJ, Abdullahi MI, Musa AM, Haruna AK, Mzozoyana V, Abubakar H. Anti-snake venom activity and isolation of quercetin from the leaf of *Neocarya macrophylla* (Sabine) Prance ex F. White (Malpighiales: Chrysobalanaceae). *Braz J Biol Sci*. 2019;6:381-389. doi:10.21472/bjbs.061306.
- Johnson TO, Odoh KD, Nwonuma CO, Akinsanmi AO, Adegboyega AE. Biochemical evaluation and molecular docking assessment of the anti-inflammatory potential of *Phyllanthus nivosus* leaf against ulcerative colitis. *Heliyon*. 2020;6:e03893.
- Trott O, Olson AJ. AutoDock Vina: improving the speed and accuracy of docking with a new scoring function, efficient optimization, and multithreading. *J Comput Chem*. 2010;31:455-461.
- Han Y, Zhang J, Hu CQ, Zhang X, Ma B, Zhang P. *In silico* ADME and toxicity prediction of ceftazidime and its impurities. *Front Pharmacol*. 2019;10:434.
- Peterson L. *In silico* molecular dynamics docking of drugs to the inhibitory active site of SARS-CoV-2 protease and their predicted toxicology and ADME. <https://chemrxiv.org/engage/api-gateway/chemrxiv/assets/orp/resource/item/60c74a49bb8c1af2c83dafb6/original/in-silico-molecular-dynamics-docking-of-drugs-to-the-inhibitory-active-site-of-sars-co-v-2-protease-and-their-predicted-toxicology-and-adme.pdf>
- Yu R, Chen L, Lan R, Shen R, Li P. Computational screening of antagonists against the SARS-CoV-2 (COVID-19) coronavirus by molecular docking. *Int J Antimicrob Agents*. 2020;56:106012.
- Hussain A, Kaler J, Tabrez E, Tabrez S, Tabrez SSM. Novel COVID-19: a comprehensive review of transmission, manifestation, and pathogenesis. *Cureus*. 2020;12:e8184.
- Gurung AB, Ali MA, Lee J, Farah MA, Al-Anazi KM. Unravelling lead antiviral phytochemicals for the inhibition of SARS-CoV-2 M^{pro} enzyme through in silico approach. *Life Sci*. 2020;255:117831.
- Boopathi S, Poma AB, Kolandaivel P. Novel 2019 coronavirus structure, mechanism of action, antiviral drug promises and rule out against its treatment. *J Biomol Struct Dyn*. 2021;39:3409-3418.
- Vardhan S, Sahoo SK. *In silico* molecular docking study on searching potential inhibitors from limonoids and triterpenoids for COVID-19. *Comput Biol Med*. 2020;124:103936.

22. Rahman MM, Saha T, Islam KJ, Suman RH, Biswas S, Rahat EU, Hossen MR, Islam R, Hossain MN, Mamun AA, Khan M, Ali MA, Halim MA. Virtual screening, molecular dynamics and structure-activity relationship studies to identify potent approved drugs for COVID-19 treatment. *J Biomol Struct Dyn*. 2021;39:6231-6241.
23. Shah B, Modi P, Sagar SR. *In silico* studies on therapeutic agents for COVID-19: Drug repurposing approach. *Life Sci*. 2020;252:117652.
24. Chikhale RV, Sinha SK, Patil RB, Prasad SK, Shakya A, Gurav N, Prasad R, Dhaswadikar SR, Wanjari M, Gurav SS. *In-silico* investigation of phytochemicals from *Asparagus racemosus* as a plausible antiviral agent in COVID-19. *J Biomol Struct Dyn*. 2021;5033-5047.
25. Pandey P, Rane JS, Chatterjee A, Kumar A, Khan R, Prakash A, Ray S. Targeting SARS-CoV-2 spike protein of COVID-19 with naturally occurring phytochemicals: an *in silico* study for drug development. *J Biomol Struct Dyn*. 2021;39:6306-6316.
26. Lim KP, Ng LF, Liu DX. Identification of a novel cleavage activity of the first papain-like proteinase domain encoded by open reading frame 1a of the coronavirus Avian infectious bronchitis virus and characterization of the cleavage products. *J Virol*. 2000;74:1674-1685.
27. Harcourt BH, Jukneliene D, Kanjanahaluethai A, Bechill J, Severson KM, Smith CM, Rota PA, Baker SC. Identification of severe acute respiratory syndrome coronavirus replicase products and characterization of papain-like protease activity. *J Virol*. 2004;78:13600-13612.
28. Devaraj SG, Wang N, Chen Z, Chen Z, Tseng M, Barretto N, Lin R, Peters CJ, Tseng CT, Baker SC, Li K. Regulation of IRF-3-dependent innate immunity by the papain-like protease domain of the severe acute respiratory syndrome coronavirus. *J Biol Chem*. 2007;282:32208-32221.
29. Frieman M, Ratia K, Johnston RE, Mesecar AD, Baric RS. Severe acute respiratory syndrome coronavirus papain-like protease ubiquitin-like domain and catalytic domain regulate antagonism of IRF3 and NF-kappaB signaling. *J Virol*. 2009;83:6689-6705.
30. Bailey-Elkin BA, Knaap RC, Johnson GG, Dalebout TJ, Ninaber DK, van Kasteren PB, Bredenbeek PJ, Snijder EJ, Kikkert M, Mark BL. Crystal structure of the Middle East respiratory syndrome coronavirus (MERS-CoV) papain-like protease bound to ubiquitin facilitates targeted disruption of deubiquitinating activity to demonstrate its role in innate immune suppression. *J Biol Chem*. 2014;289:34667-34682.
31. Lipinski CA. Lead- and drug-like compounds: the rule-of-five revolution. *Drug Discov Today Technol*. 2004;1:337-341.
32. Daina A, Michielin O, Zoete V. SwissADME: a free web tool to evaluate pharmacokinetics, drug-likeness and medicinal chemistry friendliness of small molecules. *Sci Rep*. 2017;7:42717.



Simple and Sensitive RP-HPLC and UV Spectroscopic Methods for the Determination of Remogliflozin Etaborate in Pure and Pharmaceutical Formulations

Nandeesh ITIGIMATHA¹, Kailash S. CHADCHAN², Basappa C. YALLUR¹, Manjunatha D. HADAGALI^{3*}

¹Visvesvaraya Technological University, Ramaiah Institute of Technology, Department of Chemistry, Bangalore, India

²BLDEA's V.P. Dr. P.G. Halakatti College of Engineering and Technology, Department of Chemistry, Karnataka, India

³Davangere University, Department of Studies in Chemistry, Karnataka, India

ABSTRACT

Simple, novel and selective reverse phase-high performance liquid chromatography (RP-HPLC) and ultraviolet (UV) spectroscopic methods have been developed and optimized for the determination of remogliflozin etaborate (RMZ) in bulk and dosage forms. In the HPLC method, the principal peak and internal standard peak were eluted separately at different retention times (RT) with the chromatographic conditions such as, mobile phase consisting of 0.02 M ammonium acetate buffer (pH was adjusted to 4.0 by 1.0 M ortho phosphoric acid), acetonitrile and tetrahydrofuran in the ratio 50:45:05, respectively (v/v) and the stationary phase used was C18, 5 μ m, 4.6 mm x 250 mm kromasil column. The flow rate was 2.0 mL min⁻¹, sample injection volume was 10 μ L, and the wavelength of detection was fixed at 228 nm. In case UV spectroscopic method, the RMZ was diluted with pure ethanol. The RMZ showed a maximum absorbance at 228 nm. Hence throughout analysis 228 nm was used for the determination of RMZ. The RT of RMZ and internal standard, atorvastatin (ATST) were 6.2 min and 7.0 min, respectively. The resolution between the peaks was found to be more than 2.0. The total run time was fixed at 10 min. The linearity range for RP-HPLC method was found to be 10 μ g mL⁻¹ to 50 μ g mL⁻¹, at a fixed concentration of ATST. The linearity range for the UV spectroscopic method was found to be in the range of 100 to 250 μ g mL⁻¹. Regression coefficients (R²) were found above 0.999 for both of the techniques. The limit of detection and quantification for RMZ were found to be 1.0 μ g mL⁻¹ and 3.5 μ g mL⁻¹ respectively, in RP-HPLC method and 10.0 μ g mL⁻¹ and 40 μ g mL⁻¹, respectively, in UV spectroscopic method. The developed methods were found to be simple, accurate, reproducible, and precise. The RMZ can be analyzed in dual techniques, *i.e.*, chromatographic and UV spectroscopic methods for its routine analysis.

Key words: Remogliflozin etaborate, RP-HPLC, UV spectroscopy, bulk and dosage forms

INTRODUCTION

Remogliflozin etaborate (RMZ) (Figure 1) chemically known as (5-methyl-4-[4-(1-methylethoxy) benzyl]-1-(1-methylethyl)-1H-pyrazol-3-yl 6-O-(ethoxycarbonyl)- β -D glucopyranoside), belongs to the gliflozin category. It is a pro-drug of gliflozin, which is used mainly for the non-alcoholic steatohepatitis and type 2 diabetes. RMZ helps reduce the sodium-glucose, transport proteins, and it is accountable for glucose re-inclusion in the kidney.^{1,2}

Thorough literature review revealed that few methods were developed and validated by different analytical instruments for the determination of RMZ.^{1,3-10} An analytical method has been developed by ultra-performance liquid chromatography (UPLC) in bulk and in formulations for the simultaneous estimation of RMZ and metformin hydrochloride. The mobile phase used was phosphate buffer (pH: 4.5) and acetonitrile in the ratio 60:40 v/v.¹ An ultraviolet (UV) spectrophotometric method was developed for the simultaneous estimation of empagliflozin

*Correspondence: manjunathdh@gmail.com; manjunathdh@davangereuniversity.ac.in, Phone: +91-9886646232, ORCID-ID: orcid.org/0000-0002-0634-6198

Received: 19.12.2020, Accepted: 05.04.2021

©Turk J Pharm Sci, Published by Galenos Publishing House.

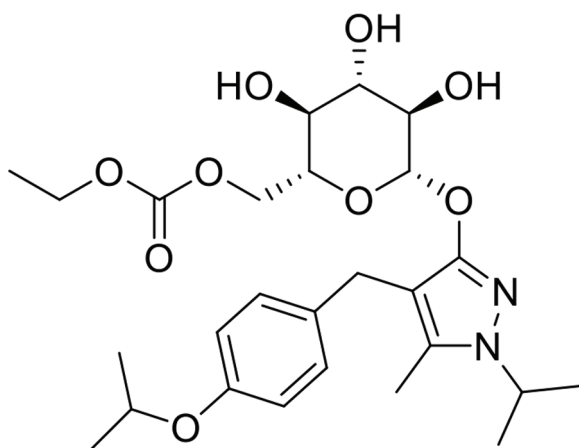


Figure 1. Chemical structure of RMZ

and metformin hydrochloride in bulk and dosage forms.³ The method showed that there were two methods, *i.e.* A and B, in method A the absorption was measured at 272 nm and 234 nm for empagliflozin and metformin hydrochloride, respectively. Method B used the absorbance ratio (Q-analysis), in which the absorbance was measured at 254 nm and 226 nm for empagliflozin and metformin hydrochloride, respectively.³ A liquid chromatographic method was developed and validated for simultaneous estimation of metformin, pioglitazone, and glimepiride in dosage forms.⁴ This method determined the diabetic drugs except RMZ. reverse phase-high performance liquid chromatography (RP-HPLC) method has been developed for the simultaneous determination of dapagliflozin and saxagliptin in the bulk and pharmaceutical dosage forms.⁵ Stability indicating HPLC method was developed for the determination of saxagliptin and metformin in the bulk forms.⁶ A RP-HPLC method was developed and validated for the simultaneous determination of metformin and saxagliptin in the formulations.⁷ The simultaneous estimation of metformin hydrochloride and canagliflozin by stability-indicating RP-HPLC method was developed by Kommineni et al.⁸ An assay method was developed and validated for simultaneous determination of metformin hydrochloride and canagliflozin by RP-HPLC instrument.⁹ Ayoub developed spectrophotometric and chemometric methods for the simultaneous determination of empagliflozin and metformin in the pharmaceutical formulations.¹⁰ An UV derivative spectrophotometric method was developed for the simultaneous determination of metformin and remogliflozin by Attimarad et al.¹¹ A thorough statistical data analysis of the reported methods and proposed methods are given in Table 1. The reported methods were not simple in a way that they have a long run time or having a complicated mobile phase. The UPLC instrument is sophisticated, but expensive so that the small-scale industries and laboratories cannot afford. Keeping these points in view, we proposed the RP-HPLC and UV spectroscopic methods for the determination of RMZ in bulk and formulations. The results of the proposed methods

indicated that the HPLC and UV spectroscopic methods for the determination of RMZ in pure and dosage forms are simple, accurate and rugged. The RP-HPLC method was developed with atorvastatin (ATST) as an internal standard. For the proposed UV spectroscopic method, the absorbance was measured at 228 nm. Both the methods were validated according to the ICH guidelines.¹²

MATERIALS AND METHODS

Instruments

The proposed method was developed and validated using Shimadzu prominence-i HPLC, which consists of an auto-injector, UV detector with a deuterium lamp as the source of light and a quaternary pump. The output signal and chromatographic data were processed using lab solution software. Eutech pH meter was used for measuring the pH of the buffer solution. An ultrasonic sonicator bath was used to degas the solvents and a nylon membrane of 0.45 μ m filter paper was used for filtration. For UV-spectroscopic method, agilent UV-visible spectrophotometer (carry 60 model), which consists of a deuterium lamp as a source of light was employed. The spectra were monitored and processed by Win lab software. The solvents used in the experiment were degassed using an ultrasonic bath.

Chemicals and reagents

RMZ and ATST compounds (>98% purity) were provided by Karnataka Antibiotics and Pharmaceutical Ltd. (Bengaluru, India) as gift samples. HPLC grade ammonium acetate, tetrahydrofuran (THF), and ethanol (99.9% purity) were purchased from SD Fine-Chem Ltd. (India). Acetonitrile and ortho-phosphoric acid were procured from Merk Ltd. (India). The ultra-purified water was prepared by Siemens purifier instrument (India). Column Kromasil, C18, 5 μ m, 4.6 mm x 250 mm, was obtained from Waters Ltd. for the UV spectroscopic method development, pure ethanol was used as the diluent.

Preparation of mobile phase, standard solutions and dilutions

The mobile phase was prepared by mixing 0.02 M ammonium acetate buffer (pH adjusted to 4.0 using 1.0 M ortho-phosphoric acid), acetonitrile and THF, in the ratio of 50:45:05, respectively (v/v/v). The standard solution was prepared by transferring accurately weighed 100 mg RMZ to 100 mL standard flask, followed by making up to the mark with the mobile phase. The concentration of the resultant stock solution was 1000 μ g mL⁻¹. From this stock solution, 0.1 mL solution was pipetted out into another 100 mL standard flask and made up to the mark with the mobile phase. The concentration of the resulting working standard solution was 1.0 μ g mL⁻¹. Similarly, to obtain a linearity graph, the stock solution was diluted to get the concentrations ranging from 10 to 50 μ g mL⁻¹. A 30 μ g mL⁻¹ of internal standard (ATST) was prepared in the mobile phase. For the development of the UV spectroscopic method, a similar procedure was followed. The standard stock solution and working standard solutions were prepared by taking ethanol as the diluent.

Chromatographic conditions

The mobile phase was composed of a buffer solution consisting of 0.02 M ammonium acetate buffer (pH adjusted to 4.0 with 1.0 M ortho-phosphoric acid), acetonitrile and THF in the ratio of 50:45:05, respectively (v/v/v). The flow rate of the mobile phase was maintained at 1.0 mL min⁻¹. The column temperature was

kept at 25°C and the stationary phase was kromasil column (C18, 5 µm, 4.6 mm x 250 mm). The wavelength of detection was fixed at 228 nm. The sample injection volume was 10 µL. The retention times (RT) of RMZ and ATST were 6.2 and 7.0 min, respectively.

Table 1. Comparison of the statistical data of the reported methods and proposed methods

Ref. no.	Analytical method	Drug(s) analyzed	Result(s)	Remarks
1	UPLC/PDA	Simultaneous determination of RMZ and metformin hydrochloride	Linearity range: 10-100 ng mL ⁻¹ LOD: 5 and 10 ng mL ⁻¹ LOQ: 10 and 50 ng mL ⁻¹	UPLC is very expensive; small scale industries and laboratories cannot afford
3	UV-spectrophotometric	Simultaneous determination of empagliflozin and metformin hydrochloride	Linearity range: 5-25 and 2-12 µg mL ⁻¹ LOD: Not available LOQ: Not available	Gliflozine pro-drug used for determination with metformin Not included RMZ
4	Liquid chromatography	Simultaneous determination of RMZ and metformin hydrochloride	Linearity range: 1-20 µg mL ⁻¹ LOD: 0.180 µg mL ⁻¹ LOQ: 0.560 µg mL ⁻¹	Narrow linearity range
5	RP-HPLC	Simultaneous determination of dapagliflozin and saxagliptin	Linearity range: 20-70 and 20-70 LOD: 0.109 and 0.58 µg mL ⁻¹ LOQ: 0.332 and 1.77 µg mL ⁻¹	Gliflozine pro-drug used for determination Not included RMZ
6	HPLC	Simultaneous determination of saxagliptin and metformin	Linearity range: 5.00-125.00 and 2.50-62.50 µg mL ⁻¹ LOD: 0.45 and 0.19 µg mL ⁻¹ LOQ: 1.50 and 0.66 µg mL ⁻¹	Other than RMZ drug determined Not included RMZ
7	RP-HPLC	Metformin hydrochloride and sitagliptin phosphate	Linearity range: 10-50 and 20-100 µg mL ⁻¹ LOD: 0.016 and 0.14 µg mL ⁻¹ LOQ: 0.048 and 0.42 µg mL ⁻¹	Other than RMZ drug determined
8	RP-HPLC	Metformin hydrochloride and canagliflozin	Linearity range: 25-150 and 2.5-15 µg mL ⁻¹ LOD: 0.17 and 0.50 µg mL ⁻¹ LOQ: 0.01 and 0.50 µg mL ⁻¹	Other than RMZ drug determined
9	RP-HPLC	Metformin hydrochloride and canagliflozin	Linearity range: 25-150 and 2.5-15 µg mL ⁻¹ LOD: 0.134 and 0.124 µg mL ⁻¹ LOQ: 0.406 and 0.376 µg mL ⁻¹	Other than RMZ drug determined
10	Spectrophotometric and Chemometric methods	Empagliflozin and metformin	Linearity range: LOD: 0.20 and 0.19 µg mL ⁻¹ LOQ: 0.59 and 0.58 µg mL ⁻¹	Other than RMZ drug determined
11	UV derivative Spectrophotometric Methods	Metformin and RMZ	Linearity range: 1-20 and 2.5-35 µg mL ⁻¹ LOD: 0.180 and 0.660 µg mL ⁻¹ LOQ: 0.560 and 1.850 µg mL ⁻¹	Derivative method Narrow linearity range
Proposed methods	RP-HPLC and UV spectroscopic	Remogliflozin etabonate	HPLC method Linearity range: 10-50 µg mL ⁻¹ LOD: 1.00 µg mL ⁻¹ LOQ: 3.50 µg mL ⁻¹ UV spectroscopic method Linearity range: 100-250 µg mL ⁻¹ LOD: 10.00 µg mL ⁻¹ LOQ: 40.00 µg mL ⁻¹ R ² : 0.999	Employed internal standard. Simple, sensitive and rugged

UPLC: Ultra-performance liquid chromatography, UV: Ultraviolet, RP-HPLC: Reverse phase-high performance liquid chromatography, RMZ: Remogliflozin etabonate, LOD: Limit of detection, LOQ: Limit of quantification

Spectroscopic conditions

The stock solution of RMZ was scanned between 200 - 400 nm, which showed maximum absorbance at 228 nm by a UV spectrophotometer. Further, to confirm the analysis, different concentrations of RMZ drug solutions were scanned. The source of the detector contained a deuterium lamp and quartz cuvettes were used as sample holders.

RESULTS

Method development

The mobile phase equilibrium was primarily conceded using a stationary phase column (kromasil). Initially, the mobile phase used for different trials was ammonium acetate and acetonitrile with different concentrations and ratios. In another experiment, 0.02 M ammonium acetate buffer (pH adjusted to 4.0 with 10% dilute acetic acid) and methanol in the ratio 50:50 was tried. In this trial, it was possible to detect peaks, but elution was inaccurate. Further trials were carried out with different ratios of 0.02 M ammonium acetate (pH: 4.0), acetonitrile and THF. However, with the mobile phase of ratio 50:45:05, respectively (v/v/v), the peaks of RMZ and ATST internal standard were eluted with good shape and resolution. Hence, the mobile phase of the ratio 50:45:05 was considered for the entire RP-HPLC method development and validation. The flow rate of the mobile phase was kept at 1.0 mL min⁻¹. With these experimental trials, the resulting peaks were eluted as satisfactory, in accordance with ICH guidelines. In this method, the total run time was 10 min for the elution of both peaks. For detecting the eluted peaks, the wavelength of detection was fixed at 228 nm. The proposed method was validated as per the ICH guidelines.¹¹

The UV spectroscopic method development was carried out by scanning the RMZ drug in the UV region ranging between 200 nm to 380 nm at different concentrations in the scan mode. The RMZ showed a maximum absorbance at 228 nm. Hence, λ_{max} of 228 nm was fixed for the entire method development process. The RMZ solution was subsequently diluted with the ethanol to obtain different concentrations according to the desired parameters. All the obtained results are satisfactory and are tabulated in Table 2. The parameters were well within the limits as specified in the ICH guidelines.¹¹ For the proposed research, the ethics committee approval is not required. Since we have not used any matrices for human beings and animals. The statistical data (obtained results of all parameters) was revealed in tables form with respect to the parameter results.

System suitability

The proposed HPLC method has consistent RT for RMZ and ATST at 6.2 and 7.0 min, respectively. There were no changes in the RT throughout the analysis. The percentage of relative standard deviation % (RSD) from six individual spikes (analytes) was found to be less than 2.0% at least concentrations, i.e., 0.74% and 0.82% for the RMZ and ATST, respectively. The system suitability data are tabulated in Table 2 and the characteristic chromatograms are shown in Figure 2A. The

resultant data indicate that the developed method has good sensitivity for RMZ. The limit of detection (LOD) and limit of quantification (LOQ) was found to be 1.0 µg mL⁻¹ and 3.5 µg mL⁻¹, respectively, and S/N ratios found for LOD and LOQ were 6.5 and 21, respectively. The results were found to be satisfactory and within the limits as shown in Table 3.

In the case of the UV spectroscopic method, the percentage of RSD was found to be less than 2.0%. The LOD and LOQ were found to be 10 µg mL⁻¹ and 40 µg mL⁻¹ respectively. The results were found to be satisfactory and are tabulated in Table 3.

Table 2. RP-HPLC system suitability parameters

Parameter	RMZ	ATST	Limit
Number of theoretical plates	6269	6465	NLT* 2000
Retention time (t _R) in min	6.10	7.00	-
Resolution	-	2.90	NLT* 2.0
Peak asymmetry (A _s)	1.06	1.09	NMT** 2.0
% RSD [#]	0.74	0.82	NMT** 2.0

*NLT: Not less than, **NMT: Not more than, [#]Average of 6 injections, RP-HPLC: Reverse phase-high performance liquid chromatography, RMZ: Remogliflozin etabonate, ATST: Atorvastatin, RSD: Relative standard deviation

Table 3. Calibration curve results, limit of detection and limit of quantification

Parameter	RP-HPLC	UV-spectroscopy
Linear dynamic range (µg mL ⁻¹)	10-50	100-250
Regression equation (Y ^a)	-	-
Slope (b)	0.028	0.003
Intercept (c)	-0.015	-0.131
Correlation coefficient (r)	0.999	0.999
LOD (µg mL ⁻¹)	1.00	10.00
LOQ (µg mL ⁻¹)	3.50	40.00
% RSD*	0.24	0.92

Y^a = bX + c, where X is concentration of drug in µg mL⁻¹, *Average of 6 injections and/or scans. RP-HPLC: Reverse phase-high performance liquid chromatography, LOD: Limit of detection, LOQ: Limit of quantification, UV: Ultraviolet, RSD: Relative standard deviation

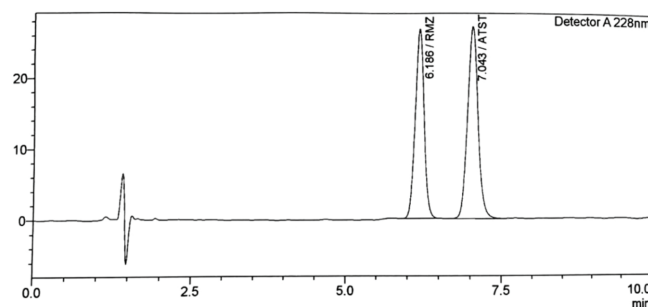


Figure 2A. A typical HPLC chromatogram of the RMZ and ATST

Linearity

In UV spectroscopic method development, five different concentrations of RMZ solutions ranging from 100 to 250 $\mu\text{g mL}^{-1}$ were scanned using a UV spectrophotometer. RMZ is absorbed at a maximum absorbance at 228 nm. The resulting linearity overlay spectra are shown in Figure 2B and the linearity graph was plotted by the absorbance against the concentration of RMZ and the regression coefficient (R^2) was found to be more than 0.999. The results are tabulated in Table 3.

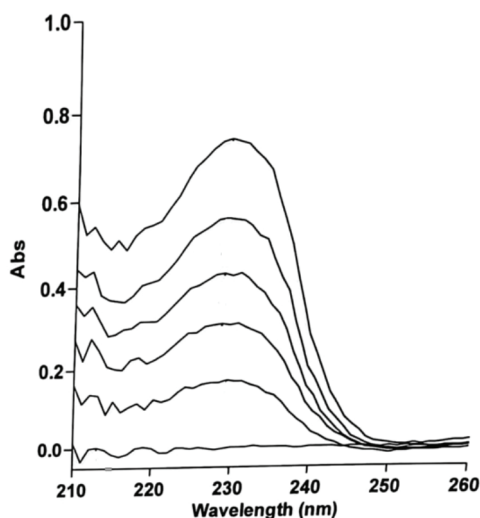


Figure 2B. Overlapped linearity graphs of UV-spectroscopic method

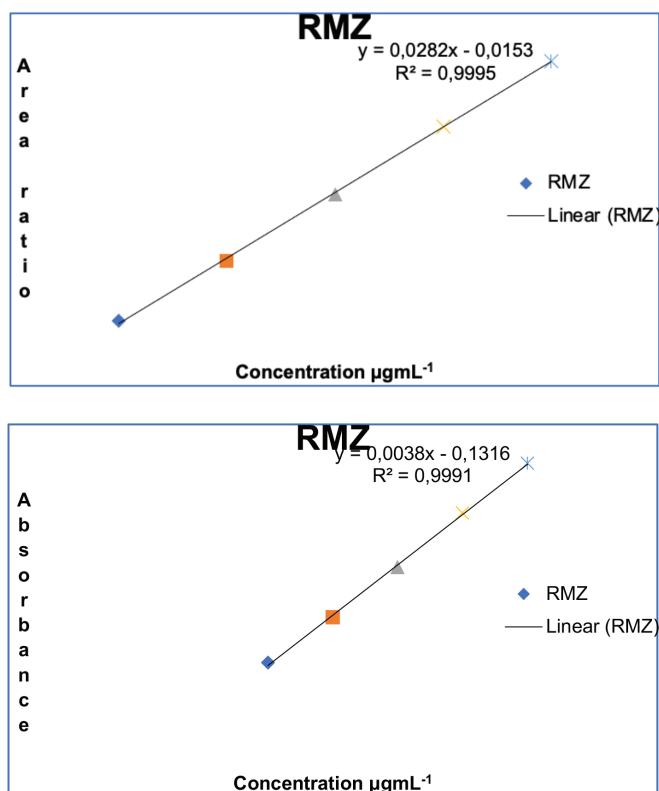


Figure 3. Linearity graphs plotted by RP-HPLC data (A) and UV-visible spectroscopy data (B)

In case of HPLC method, RMZ and ATST peaks were eluted at different time intervals. The working standard solutions of RMZ ranging between 10 $\mu\text{g mL}^{-1}$ to 50 $\mu\text{g mL}^{-1}$ were eluted along with the internal standard ATST. The concentration of the ATST was fixed at 30 $\mu\text{g mL}^{-1}$. The linearity graph was plotted by taking the values of the peak area ratio of RMZ to ATST. With the resulting straight line obtained from the linearity graph as shown in Figures 3A and B, we could validate the precision of the analyst using this method. The regression coefficient (R^2) value was found to be more than 0.999, following the equation $Y = MX + C$. The results are tabulated in Table 3.

Recovery

This parameter shows that the study of accuracy estimation accomplished by the standard solution of the lower, middle, upper and blank, spiked at 60, 80, and 120% against 100%. The results were calculated using the standard procedures and the recovery data were found to be satisfactory. The values were shown in Table 4. The accepted limits of recovery were in the range of 98-102%. All the observed outcomes were within the range. Hence, the proposed method can be adopted in industry units and in educational labs for the assay of RMZ.

The recovery parameter in spectroscopic method was performed by the standard solution of the lower, middle, upper and blank, spiked at 60, 80, and 120% against 100%. The outcomes were found to be satisfactory. The results are tabulated in Table 4.

Precision

Precision results of the developed methods were found to be good and in compliance with ICH guidelines. Based on the results of the precision parameter, the HPLC method was found to be precise. The results are revealed in Table 4. Repeatability testing was performed by six individual spikes. The outcomes of inter-day and intra-day analysis revealed that there was not much deviation in the results and RSD% was found to be less than 2.0%. Therefore, the system suitability of the proposed HPLC method was excellent and thereby precision of the system. The results are shown in Table 4.

In the spectroscopic method, intra-day and inter-day precision was studied by estimating the consistent responses at three different time intervals on the same day and on three different days by taking different working standard solutions. The percentage of RSD was found to be less than 2.0% *i.e.*, 0.96, and 0.85 for the intraday and inter-day, respectively, which indicates good reproducibility. These results, which are tabulated in Table 4, indicated that the precision of the UV spectroscopic method is good.

Robustness studies

The robustness of the HPLC method was studied by a slight deviation in the boosted conditions of the method by injecting a solution of a known concentration. The distinctive conditions correspond to variation of flow rate in the mobile phase ranging from 0.9 mL min^{-1} to 1.1 mL min^{-1} and change the column oven temperature at 25°C and 30°C. The results are tabulated in Table 5, which revealed that robustness values are satisfactory and there was not much variance in results and therefore,

Table 4. Recovery and precision data

Concentration	Amount of the drug is taken	RP-HPLC				UV spectroscopy		Limit
		RMZ	% RSD*	ATST	% RSD*	RMZ	% RSD**	
60%	60 mg mL ⁻¹	99.50	0.95	101.00	0.60	98.50	0.85	98%-102%
80%	80 mg mL ⁻¹	99.00	0.82	99.00	0.65	98.80	0.92	98%-102%
120%	120 mg mL ⁻¹	98.50	0.75	99.50	0.74	99.50	0.97	98%-102%
Intraday			0.65		0.72		0.96	NMT-2.0
Interday			0.59		0.65		0.85	NMT-2.0

*Average of 6 injections, **Average of 6 scans, RSD: Relative standard deviation, RMZ: Remogliflozin etabonate, UV: Ultraviolet, ATST: Atorvastatin

Table 5. Robustness evaluation parameters

Parameter	Variations	RMZ retention time	ATST retention time
Flow rate	1.9 mL min ⁻¹	6.45	7.32
	2.0 mL min ⁻¹	6.10	7.00
	2.1 mL min ⁻¹	5.85	6.64
Temperature	25°C	6.10	7.10
	30°C	6.20	7.20

RMZ: Remogliflozin etabonate, ATST: Atorvastatin

Table 6. Assay results

Name of the drug	Instruments	Label claims of market sample in mg per tablet	Obtained result in mg per tablet	Assay values (%)	Limit
RMZ	HPLC	200	199	99.5	98.00%-102%
	UV spectroscopy	200	197	98.5	98.00%-102%

HPLC: High performance liquid chromatography; RMZ: Remogliflozin etabonate, UV: Ultraviolet

the projected method can be used under different conditions. However, in the case of UV spectroscopic method, the robustness parameter was performed by a slight modification in the detection wavelength by ± 2 nm and outcomes were found to be satisfactory.

Ruggedness

In the ruggedness parameter, standard working solutions were examined by the same chromatographic system on different days using the same column. It was observed from the results that there was a small variation in the peak area and there were no large differences in the RT. The percentage of RSD was found to be less than 2.0% for RMZ. The resulting data revealed that the developed method is rugged. In the alternate days, the same detector responses were observed and it was successfully found that the projected method is capable of achieving results with great precision on different days. Also, ruggedness was determined using different HPLC instruments by injecting a known concentration of a solution. The detector response, good reproducibility, and no variations in RT indicated that the method is fundamentally rugged. In the spectroscopic method, the ruggedness parameter was examined using

different concentrations of the solution and a slight change in the wavelength. The percentage of RSD did not diverge much with the absorbance value. Hence, the developed method was rugged and can be adopted for the assay of RMZ.

Specificity

Assay

This parameter was carried out by successive separation of RMZ and ATST, which was established against placebo, which contains potential excipients. In the assay parameter, sss interference found and both peaks were sharp and separated at the baseline. It was found that no interference of the excipients in the test solution. Therefore, the projected HPLC method was established specifically. The obtained results were found to be satisfactory and are shown in Table 6.

In the case of the spectroscopic method, no interferences were found by the placebo of tablet formulations. Thus, the obtained results were acceptable and the results are shown in Table 6.

DISCUSSION

Most of the diabetic drug formulations contain pro-drug of gliflozin derivatives like RMZ to prevent diabetic disorder.

Several formulations of the diabetic drug contain glioflozin derivative drugs. The literature survey revealed that few analytical methods have been developed and validated for the determination of RMZ, viz., UPLC, HPLC and UV spectroscopic methods. But most of these methods have one or the other drawbacks. For example, the UPLC is very expensive and hence small-scale industries and laboratories cannot afford. Some HPLC and UV spectroscopic methods were developed for the determination of pro-drugs of gliozzi but not included RMZ. Through statistical data analysis (Table 1) of the reported methods, it was planned to develop and validate HPLC and UV spectroscopic methods for the assay of RMZ. These analytical methods are simple, sensitive, rapid, rugged, use inexpensive chemicals, involve small sample volumes, and show good recovery. The results of the parameters comply with ICH guidelines.

CONCLUSION

A few RP-HPLC methods have been developed for the determination of gliozzi derivatives such as canagliflozin, empagliflozin, and metformin hydrochloride. These methods were carried out for the determination of either one or two of the above-mentioned drugs or a single drug along with other combinations. The projected methods are distinctive from the reported methods. In RP-HPLC method, the total run time was 10 min. The linearity range for RP-HPLC method was found to be from 10 $\mu\text{g mL}^{-1}$ to 50 $\mu\text{g mL}^{-1}$ and for the UV spectroscopic method, it was found to be in the range of 100 to 250 $\mu\text{g mL}^{-1}$. The values of regression coefficients (R^2) were found to be more than 0.999 for both techniques. The LOD and LOQ values for the UV and HPLC methods were found to be 10.0 $\mu\text{g mL}^{-1}$ and 1.0 $\mu\text{g mL}^{-1}$ and 40 $\mu\text{g mL}^{-1}$ and 3.5 $\mu\text{g mL}^{-1}$, respectively. The developed methods were found to be simple, accurate, reproducible and precise. The obtained data of both the methods clearly showed that RP-HPLC method was relatively more sensitive than the UV spectroscopic method.

Ethics

Ethics Committee Approval: The ethics committee approval not required for the proposed research. We were not used any kind of human being and animal matrices.

Informed Consent: Not applicable

Authorship Contributions

Concept: M.D.H., Design: M.D.H., Data Collection or Processing: N.I., Analysis or Interpretation: B.C.Y., M.D.H., Literature Search: K.S.C., Writing: N.I., M.D.H., B.C.Y.,

Conflict of Interest: No conflict of interest was declared by the authors.

Financial Disclosure: The authors declared that this study received no financial support.

REFERENCES

1. Tammisetty MR, Challa BR, Puttagunta SB. A novel analytical method for the simultaneous estimation of remogliflozin and metformin hydrochloride by UPLC/PDA in bulk and formulation application to the estimation of product traces. *Turk J Pharm Sci.* 2021;18:296-305.
2. Hussey EK, Kapur A, O'Connor-Semmes R, Tao W, Rafferty B, Polli JW, James CD Jr, Dobbins RL. Safety, pharmacokinetics and pharmacodynamics of remogliflozin etaborate, a novel SGLT2 inhibitor, and metformin when co-administered in subjects with type 2 diabetes mellitus. *BMC Pharmacol Toxicol.* 2013;14:25.
3. Padmaja N, Babu Sharath M, Veerabhadram G. Development and validation of UV spectrophotometric method for simultaneous estimation of empagliflozin and metformin hydrochloride in bulk drugs and combined dosage forms. *Sch Res J.* 2016;8:207-213.
4. Pandit V, Pai RS, Devi K, Singh G, Narayana S, Suresh S. Development and validation of the liquid chromatographic method for simultaneous estimation of metformin, pioglitazone, and glimepiride in pharmaceutical dosage forms. *Pharm Methods.* 2012;3:9-13.
5. Aswini R, Eswarudu MM, Babu PS. A novel RP-HPLC method for simultaneous estimation of dapagliflozin and saxagliptin in bulk and pharmaceutical dosage form. *Int J Pharm Sci Res.* 2018;12:5161-5167.
6. Caglar S, Alp AR. A Validated high performance liquid chromatography method for the determination of saxagliptin and metformin in bulk. A stability indicating study. *J Anal Bioanal Tech.* 2014;12(Suppl):1-5.
7. Prasad PBN, Satyanarayana K, Krishnamohan G. Development and validation of a method for simultaneous determination of metformin and saxagliptin in formulation by RP-HPLC. *Am J Analyt Chem.* 2015;5:737-742.
8. Kommineni V, Chowdary KP, Prasad SM. Development of a new stability indicating RP-HPLC method for simultaneous estimation of metformin hydrochloride and canagliflozin and its validation as per ICH guidelines. *Int J Pharm Sci Res.* 2017;8:3427-3435.
9. D'Douza S, Muddu K, Gude Sai S, Vasantharaju SG. Stability indicating assay method development and validation to simultaneously estimate metformin hydrochloride and canagliflozin by RP-HPLC. *Curr Trends Biotechnol Pharm.* 2016;10:334-342.
10. Ayoub BM. Development and validation of simple spectrophotometric and chemometric methods for simultaneous determination of empagliflozin and metformin: Applied to recently approved pharmaceutical formulation. *Spectrochim Acta Part A Mol Biomol Spectros.* 2016;168:118-122.
11. Attimarad M, Nair AB, Sreeharsha N, Al-Dhubiab BE, Venugopala KN, Shinu P. Development and validation of green UV derivative spectrophotometric methods for simultaneous determination of metformin and remogliflozin from formulation: evaluation of greenness. *Int J Environ Res Public Health.* 2021;18:448.
12. International Council of Harmonization. Q2B Validation of analytical procedures: methodology and availability. Federal Register; 1997. <https://www.fda.gov/media/71725/download>



A Brief Discussion of Multi-Component Organic Solids: Key Emphasis on Co-Crystallization

Braham DUTT¹, Manjusha CHOUDHARY², Vikas BUDHWAR^{1*}

¹Maharishi Dayanand University, Department of Pharmaceutical Sciences, Haryana, India

²Kurukshetra University, Institute of Pharmaceutical Sciences, Department of Pharmacy, Kurukshetra, India

ABSTRACT

Co-crystallization (CCs) is a less studied phenomenon related to its applicability and reliability as it is directly related to the generation of newer multicomponent solids like co-crystals (CS), eutectic, salts or solid solutions *etc.* having improved physicochemical properties compared to their pure components. Further, the design and structural aspects of these multicomponent systems remain hindered compared to other techniques such as nanotechnology or solid dispersion. CC is a newer technique to modify the physicochemical as well as pharmaceutical characteristics of various drugs having issues like solubility, stability, *etc.* without altering or hindering their pharmacological activities. For drug delivery purpose, CC process has numerous advantages over nanotechnology and solid dispersion drug delivery techniques. CCs can modify the physicochemical properties of active pharmaceutical ingredients (API) have issues like sensitivity toward environmental hazards like temperature, moisture, or photostability issues. The availability of large numbers of conformers makes this technique favorable for the researchers in designing CS of newer and older. Although, solid dispersion and nanotechnology techniques are being utilized to a larger extent still there are some drawbacks of these techniques like stability, toxicological factors and protection from environmental factors need to be considered, while the CCs process drastically modifies the various pharmaceutical parameters without altering the pharmacological properties of API's. Salts, design of CS, their methods of preparation, and their application in various fields with special emphasis on their applicability in the pharmaceutical industry.

Key words: Co-crystals, eutectic, salts, cocrystallization, chromophores, cosmetic

INTRODUCTION

Since the last decade, the interest of pharmaceutical scientists shifted toward co-crystallization (CC) process, because of their interest in improvising the physicochemical characteristics of an active pharmaceutical ingredients (API) without any alteration in its pharmacological activity, which led them to be a better option for patents and for development of these drugs into a newer marketable formulation.¹ But a proper definition of co-crystals (CS) is still a matter of debate because there are only a few studies available, which significantly made differences between CS, eutectic or salts as a products of CCs.² In most of the studies, it has been assumed that when heteromolecular interaction between two molecules compensate or balance the homo-molecular interactions, the resultant product will be a CS, on the other hand, when homo-molecular interaction comes into action, then chances of eutectic formation increased. Some studies also concluded that eutectic were

similar to solid solutions and they called it as “conglomerates of solid solutions” formed due to interactions between couples of molecules lacking geometrical fit and on the other point CS were found to be more stable compared to eutectic as these are geometrically fir components and various studies related to the CCs process have settled various parameters, which govern the formation process of CS, while in case of eutectic, solid solutions or salts, much literature is not available.³

On the basis of literature, most of the studies conclude that CS are component solids carrying a crystalline structure.⁴ The latest guidelines of United States Food and Drug Administration (FDA) related to CS, these are “Crystalline materials composed of two or more molecules within the same crystal lattice”.⁵ There are numerous publications, which have provided a more constricted definition as these are crystalline substances, whose components remain solids in their pure states under ambient circumstances and all the components should be

*Correspondence: vikaasbudhwar@yahoo.com, Phone: +919466673246, ORCID-ID: orcid.org/0000-0003-4331-0116

Received: 04.05.2020, Accepted: 03.12.2020

©Turk J Pharm Sci, Published by Galenos Publishing House.

present in a fixed stoichiometric ratio of drug and coformers (CFs).⁶ A recent perspective, authored by 46 scientists, provided a different explanation about CS as “CS are solids that are crystalline single-phase materials composed of two or more different molecular and/or ionic compounds generally in a stoichiometric ratio, which are neither solvates nor simple salts”. In this context, the definition of pharmaceutical CS is different compared to the definition of CS, as in the case of pharmaceutical CS, one component is drug and the other is CFs.⁶ In the crystal engineering technique, the pharmaceutical properties of drugs are changed without disturbing their inherent structures. Presence of various chemical groups viz. carboxylic acids, carbohydrates, amides, amino acids and alcohols in the co-crystal formers lead to the formation of CS with different drugs.

Synthons are responsible for holding the molecules, when the formation of a compound occurs through non-covalent interactions. Due to their strength, directionality and higher rate of recurrence, hydrogen bonds are often used for designing co-crystals. In 1991, Etter gave three rules for hydrogen bonding pattern⁷ every available hydrogen molecule could be used in the formation of bonding, every acceptor of hydrogen bond could participate, if an H bond acceptor is present there as well as the H bonding is possible when a good acceptor and donor H bond are present in the molecule. The formation of synthons is governed by the strength of hydrogen bonding between co-crystal formers, not by the total number of groups available. With the use of the above discussed rules, we can predict the formation of synthons within different functional groups. Synthons are essential structural entities between supramolecules that formed *via* non-covalent bonding and are made up of molecular fragments and supramolecular links among them. Supramolecular synthons could be classified into two categories: Supramolecular homosynthons and heterosynthons. The first one is composed of self-complementary functional groups, while the second one is composed of dissimilar but complementary functional groups. Supramolecular heterosynthons formation occur by non-covalent interactions between various drugs that leads to a co-crystal formation. The concept of the supramolecular approach is used for CS screening but now-a-days Cambridge Structural Database (CSD) is used for the selection of suitable CFs for various drugs.

So, in broad terms, CCs is the process of generation of newer crystalline substances by manipulating the intermolecular interactions of two components, which remain solids in their pure states at ambient conditions and interact with each other in a fixed stoichiometric ratio. But CS are not the only target during CCs, there are different multicomponent solids are also present viz. eutectic, salts, polymorphs, hydrates, solvates *etc.*, which are the side products of the CC process.⁸ In the case of CS, the interaction between drug and CFs occurred through non-covalent interactions like hydrogen bonding or ionic interaction. While in case of eutectic, mostly weak van der Waals interactions occurred in an unfit geometric pattern, and that's why eutectic became less stable compared to CS.⁹ So, here

in this review, we have briefly discussed various significant factors and chemistry involved during the CCs process along with the differences between CS, salts and eutectic. Screening methods for CS, their methods of preparation, and their applications CS in pharmaceutical and allied industries are been discussed in later sections.

Co-cocrystals vs. eutectic

The literature is full of studies related to the development of newer drug delivery techniques to improvise the pharmaceutical properties of API's including dissolution profile, ss thermostability, material compressibility during tablet production process.⁸ When we discuss crystal engineering, the most useful point is understanding of supramolecular synthon formation. These are the fundamental building blocks of the products obtained during the CCs process. When there is an interaction between two similar functional groups like the -COOH functional group of the drug and API interact, formation of homosynthons occurred, while interactions between two different functional groups lead to the generation of heterosynthons. As we discussed above in the introduction section, the chances of CS or eutectic formation depends upon these two synthons. Generally, it has been hypothesized that, heterosynthon formation leads to the generation of CS, while homosynthon formation goes to generate eutectic, but recent studies proved this wrong as numerous CS has been reported *via* homosynthon formation.⁹

Eutectics are basically multi-component crystalline solids closely related to solid solutions.¹⁰ Both are well-documented in inorganic systems as alloys.¹¹ There are numerous studies in the literature, which have defined eutectic on the basis of their lower melting point patterns and on the basis their compositions. The term eutectic was derived from the Greek term “*eutectos*”, which means fused.¹² Yet the formation of eutectic has not much studied compared to solid solutions,¹³ as these are defined on the basis of their composition or arrangements of solutes and solvents in the crystalline lattice.¹⁴ The detailing of internal structural composition *via* X-ray diffraction (XRD) studies of eutectic are rarely available compared to solid solutions. A deep analysis of structural detailing is required for eutectic in pharmaceutical scenarios the famous tin-lead eutectic was studied by inorganic chemists.¹⁵ In the past eutectic have been considered solid solutions and recently it has been considered CS for pharmaceuticals and organic systems.¹⁶ However, CS has been reported to form eutectic and solid solutions¹⁷ and some studies considered eutectic as an intermediate step between CS and solid solutions, which is crucial for the formation of CS, but the exact mechanism for eutectic formation still remains a matter of discussion.^{18,19} Thus, CS, eutectic and solid solutions are correlated with each other but most of the studies that differentiate them focused on the phase diagram studies and binary composition properties of multicomponent crystalline studies. We discussed the inter-relationships of these multicomponent solids on the basis of their intermolecular interactions and structural inter-relationships and proposed

that detailed structural data are required to differentiate between eutectic, solid solutions and CS.²⁰

Cocrystals vs. salts

The development of a multicomponent system into CS or salts depends upon the degree of proton transfer within a hydrogen bonded synthon. To form a multicomponent crystalline system, interactions between different components at the molecular or ionic level are necessary and for multicomponent systems like CS, salts or any other type, such interactions should be non-covalent and supramolecular.^{21,22} The level of interactions and the geometrical arrangements between two isolated molecules (gaseous phases) comparably remain open, which makes them easy to understand, while in the case of a closed and 3D packing system, it becomes a challenging task to understand it.²³ Finally, the methods like computational crystal structure prediction (CSP) methods retain the key to resolving the problems by understanding the full and clear spectrum of interactions at the intermolecular level within a crystalline system. Undeniably, it becomes the only reliable source for understanding the influence of every short- or long-range interaction made by the molecules in a crystal and this leads to predicting the most stable crystal compound.²⁴ Even after this, the various stages in crystal developments like nucleation and growth considerations play their important roles, which cannot be explained by the experimental level studies; hence, it must understand intermolecular interactions at all points of crystal development stages. For understanding such developments, CSP method²⁵ is not a sufficient tool, but recently, Cambridge blind tests provided some significant approaches for this.²⁶ In case of the CSP method, the presence of additional degrees of freedom leads to the generation of a possible structure enabled by the occurrence of the second component and this made the CSP method a more discouraging technique²⁷ while to understand the development of multicomponent systems, we required gathering of more empirical and rationalized data. However, the more precise calculation, understanding of various associated modes and inclusion of empirical data during the study, could help in the prediction of CS or salt formation.^{28,29} Recently, engineering of ternary CS been designed on the understanding of pKa values, supramolecular synthon history and hydrogen bond basicity. Ternary CS system like acridine-3-hydroxybenzoic acid· 2-amino-4,6-dimethylpyrimidine, due to its smaller size of proton, its causes transfer of protons with small steric significance and leads to the protonation of the base by an acid. This phenomenon was a great example of understanding the electronic factors along with the solvation characteristics of acid, base and their salt.³⁰ The pKa value represents the pH value at which all the solubilised-ionisable components are fifty percent charged and fifty percent remained protonated and it depends upon the acidic or basic strength of the molecule.¹ The concept of prediction of salt and CS formation mainly depends upon the difference in pKa values of acid and base, which has been explained in detail in screening methods. By using the pKa value, the equilibrium concentration of ions can be calculated, and if the difference in pKa values of acidic and basic components is found to be more than 2 or 3

units, in that case proton transfer takes place³¹ and the chances of salt formation increase, but currently, newer theoretical and high pressure techniques based studies exhibited that proton transfer in pyridine-formic acid system depends upon the concentration of formic acid present in the solution.³² The charged ions and the polar molecules of the aqueous medium interact with each other, which makes salts more hygroscopic, especially in case of anions, they are found to be conjugated bases of strong acids like chloride and sulfates. In terms of interactions at the intermolecular level, the rationalization becomes easier in at least in broad terms (Figure 1).⁴

Methods of cocrystal preparation

Numerous methods for the formulation of CS, but traditional crystallization was carried *via* solution with suitable degrees of super saturation *viz.* cooling, evaporation and includes substances having properties of the solubility lowering. CCs with the solvent evaporation technique did not provide favorable results.³⁰ Generally, two methods are used for CCs: solution-based and grinding-based techniques. Solution-based methods are generally preferred because of the formation of CS, which can qualify the testing with a single XRD (SXRD). The grinding-based techniques include neat-grinding and solvent drop-grinding techniques. Currently, newer techniques are available, *viz.* hot-stage microscopy, ultrasound assisted and CCs *via* supercritical fluid.³¹

Grinding method

CC products usually prepared with grinding method are consistent compared to those prepared from a solution. The main drawback of this method is its inability to prepare significant arrangements of CS before due to the stability of early phases. The solvent method is better than the grinding method in another way also as grinding method leads to solvent inclusion in supramolecular structure stabilization. Solvent drop grinding might enhance the kinetics and assist the formation of CS leading to increased interest as a CC technique.³¹

Neat-grinding technique can be performed by vibratory mills, mechanical-grinding or manual-grinding, while the solvent drop-

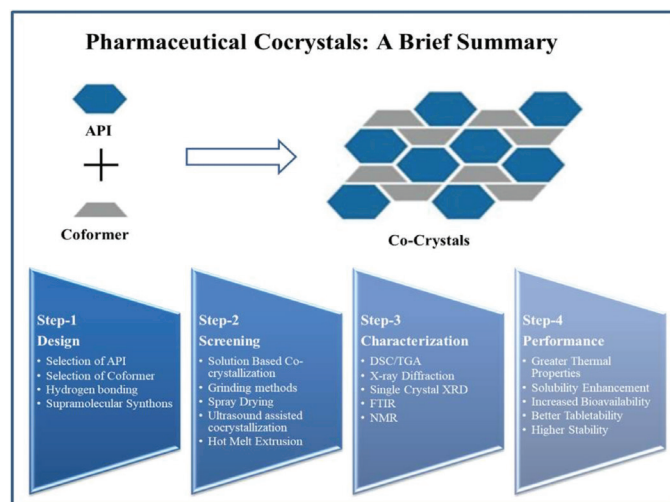


Figure 1. An overview of pharmaceutical cocrystals

grinding can be performed by the addition of suitable solvent at regular intervals with grinding ensure that the solvent should be capable of dissolving the solid material. Caffeine-glutaric acid CS polymorph compared with the solvent evaporation technique is cost effective, eco-friendly, and effective for CS formation.³¹

Solid state-grinding

In solid state grinding, the particulate size reduced with increased covalent reactivity within the mixture. This technique helps in improving in simplicity and selectivity over solution-based CCs technique.³⁰ Six CS formulations of sulfadimidine with salicylic acid using solid state grinding technique while with grinding anthranilic acids were prepared and studied. Anthranilic acid replaced salicylic acid due to the general arrangement of hydrogen bonds of both CS. In this technique, the major shortcoming is that the polymorphic transition leads to serious side effects, causing product withdrawal by the market.³²

Solvent drop-grinding

It is almost same as solid state grinding method with the introduction of the solvent in a smaller quantity. Here solvent act as catalytic agent.³³ Primarily, CS formation occurred via a solution crystal growth manner. Most of the crystals grow faster with the solid grinding technique while others proceed further slowly. For those crystals, solvent drop method was found to be effective.³¹ For the preparation of CS of caffeine and glutaric acid solvent drop grinding technique was found to be suitable compared to solid state grinding. Preparation of succinic acid (SA):anthranilic acid and indomethacin:saccharine was done with solvent drop-grinding method and optimum outcomes of studies revealed an increment in physical stability and dissolution rates.³²

Co-crystallization from the solution

Here the key requirement is the same solubility profile for both compounds undergoing CCs, otherwise the least soluble compound will get precipitated out completely from the solution. While similar solubility profile of both components could not promise a positive result. It is probably beneficial to trust polymorphic complexes that occur in additionally compared to solitary crystalline arrangement as CC compounds. When a molecular component occurs in various polymorphic states, it reveals a structure-based tractability and cannot be locked into a packing model.³³ For large-scale production, water-jacketed vessel with a circulating water bath facility for temperature control was being used. Teflon blades were used for continues to stir. The drug and CFs were dissolved in alcoholic solvent at 70°C under reflux for 1 h. The reduction in temperature with 10°C rate was done to precipitate out the co-crystals. Literary to increase solid retrieval reduced the surplus heat.³¹

Solvent evaporation

This is the most traditional method used for CCs, including super saturation of solution by cooling, evaporating, and solvent addition having solubility changing properties. It is assumed that molecules undergo hydrogen bonding, when mixed in appropriate quantities. CS of fluoxetine hydrochloride

with different CFs viz. fumaric acid, SA, and benzoic acid was prepared using this method for enhancing their intrinsic solubility.³¹ In another study, CS of norfloxacin with malonic acid, maleic acid and isonicotinamide was also prepared with improved physicochemical properties.³³

Slurry crystallization

The process of addition of a suitable crystallization solvent to the API and its co-former is known as slurry crystallization, the use of this process is governed by the physical stability of the crystallization solvent compared to that of the API and CFs. The synthesis of CS through slurry crystallization was used with sixteen CS system.³¹ Different solvents can be used for slurry crystallization, around 100 mL of liquid solvent is poured and for a few days, stirring was done to the suspension room temperature. The suspension was then allowed to decant and the CS was dried under nitrogen.³³ Examples of slurry polymerization include CS of trimethoprim and sulfamethoxazole using distilled water. Slurry crystallization possess one major disadvantage is that it requires a large amount of solvent.³¹

Hot melt extrusion

Hot melt extrusion is an efficient CS synthesis method, which does not require any solvents; however, the selection of this process depends on the thermodynamic stability of the API and CFs. Holt melt extrusion can be optimized using the solvent drop extrusion technique, which an extra advantage to conduct hot melt at the lowest temperature. Examples include carbamazepine nicotinamide CS.³¹

Sonocrystallization method

The use of sonocrystallization to synthesize CS is very rarely explored, this method is suitable for the preparation of nanocrystals. The ultrasound method was used for the preparation of caffeine-maleic acid CS, theophylline and L-tartaric acid as a CFs.³²

Screening of co-crystals

Various methods for screening of CS are discussed below:

ΔpK_a rule is widely used for CS screening by using the following equation.

$$\Delta pK_a = [pK_a(\text{base}) - pK_a(\text{acid})]$$

When the difference in pKa values is >2-3, transfer of proton will occur between acids and bases. pKa values less than 0 exhibit the formation of CS, while more than 2-3 value revealed the formation of salts.^{34,35} In CSD 6465 possible CS were studied to validate and quantify this rule. The increment in the pKa value of free base to one digit directly increased one unit of pH_{max} . To attain this condition practically, we need to modify the drug molecule. In the same way one-digit increment in the intrinsic solubility profile of a free base affects directly one-unit increment in pH_{max} again. This also required modification in drug molecule.³⁶ While one decrement in salt solubility leads to an increment of one unit in pH_{max} . This characteristic can be modified using a counter ion with different properties and if salt

Table 1. Relation of pKa values with possibility of formation of complexes³²

Possibility of formation of complexes	pKa values
Non-ionized complexes	$\Delta pK_a < -1$
Ionized complexes	$\Delta pK_a < 4$
	(Ionizable complex formation possibility increases by 17% by increasing ΔpK_a by 1 unit from 10% at $\Delta pK_a = -1$ to 95% at $\Delta pK_a = 4$)

Table 2. Relation of cocrystal formation with DSC screening³⁷

Endothermic peak	Cocrystal formation
Three endothermic and a couple of exothermic peaks	CS with stoichiometric variety
Two endothermic and one exothermic	One CS formation with certain molar ratio
One endothermic	No CS formation

DSC: Differential scanning calorimetry, CS: Cocrystals

formation occurred, it would be stable over a greater pH range but having a lower solubility profile (Table 1).

Fabian's method used molecular descriptors, *viz.* (atom, functional groups, bond, hydrogen donor-acceptors, size, shape, molecular and surface area descriptors *etc.*) for calculation and screening of CS. In this method, mostly polarity and shape descriptors are used to predict the possible formers of CS. Other molecular descriptors are also important as well for prediction of CS formers.³⁶

Conductor-like screening model for real solvents was used for checking the miscibility of CFs with super cooled liquid (melt) phase. The excess enthalpy, between the pure compounds and the mixture of drug and CFs reveals the capability of CCs between the drug and CFs.³⁷

Calculated gas phase MEPS technique used the difference in energy ΔE difference between CS and pure solids in various stoichiometries, to determine the possible formation of CS between the two solids. The outcome of the study revealed that, when ΔE is more than 11 kJ/mol, chances of CS formation are enhanced by 50% more. Over 1000 compounds were screened to validate this method including (caffeine and carbamazepine) and the results were satisfactory enough.²¹

Co-crystal cocktail method is a very useful and smaller time-consuming method. In this method, more than three CFs were simultaneously grounded with the drug leading to the formation of homo or heterosynthons between the drug and CFs, which could be analyzed with thermal analysis methods by checking their endothermic peaks.²⁴

Differential scanning calorimetry (DSC) is a rapid thermal method for screening of CCs.²⁴ In this method, we check the endothermic peaks for the formation of CS by heating the mixture of drug and CFs in DSC pans. We hypothesized that CS formation is an exhibition of three endothermic and a couple of exothermic peaks in thermogram represent the formation of CS with stoichiometric variety.³⁸ In the case of thermal techniques, it is a general hypothesis that during CCs, the melting point of CS remains between the melting points of the drug and CFs while in case of a eutectic mixture, generally the melting point

of product comes before the melting point of both the drug and CFs. But there are numerous studies present in literature, where the melting point of CS comes before and after the melting points of parent components. In a study related to the behavior of melting point in CCs, Schultheiss and Newman²⁷ in 2009 determined that around 51% of CS possess a melting points between drugs and CFs, while 6% possess greater melting points and around 39% possess lower melting points compared to drug and CF respectively. The melting point of CS is generally altered by the melting point of CFs. If we choose a CF with a higher melting point, the resultant product should possess a higher melting point and vice versa. This technique can be applied to those drugs, which have thermostability problems (Table 2).⁴

Hot stage microscopy or the Kofler contact method offers a visualization of the total phase number that is exhibited by the system when two compounds are heated. When the high melting point compounds start melting and recrystallization occurs before other melted compounds comes in contact with it leading to the formation of zone of mixing.^{39,40}

Saturation solubility technique involved the measurement of the saturation solubility of API's and conformer separately at the reference temperature. The saturation temperature of the solvent system is measured by heating with a rate of 0.3°/min. If the increase in saturation temperature is more than 10° compared to reference temperature, chances for co-crystal formation increases.^{41,42} The study of carbamazepine and nicotinamide-based CS revealed that the solubility profile of drug directly depends upon the concentration of CS in the drug and CF solution. This study concluded that the solubility of a drug could be increased only when it gets complexed with CFs during the CC process, otherwise the free drug had no impact on the increment of solubility profile of the parent components.⁴

Applications of co-crystallization

Pharmaceuticals

The interest of pharmaceutical industry and researchers have shifted toward CCs and many drugs, including newer and older APIs have been included in the preparation of CS and eutectic

as these formulations improvise the pharmaceutical issues related to these drugs without altering or modifying their therapeutic activities.^{43,44} The enhancements in solubility,⁴⁵ stability⁴⁶ and aqueous solubility have been reported after CCs of various. With the drastically improved pharmaceutical characteristics of API's, CC process has been considered the most effective technique to improvise the bioavailability of drugs.⁴⁷ It is evident from literature that by developing a CS of fluoxetine hydrochloride with different CFs, the solubility of each formulation was increased. The solubility of fluoxetine hydrochloride was found to be 11.6 mg/mL while its CS with fumaric acid and SA were found to be 14.8 mg/mL and 20.2 mg/mL respectively.⁴⁸ In another study, the solubility profile of CS of tegafure was found to be much higher compared to the its pure amorphous state.⁴⁹ Here, the important point is the increment in its solubility without affecting the stability of the pure amorphous form of the drug. A vast literature is available containing such examples where the solubility and dissolution behavior of various drugs have been modified without changing their original therapeutic properties.^{50,51} If we talk about eutectic, the drug: drugs eutectic have been reported in literature like 1:1 eutectic mixture of pyrazinamide and isoniazid exhibiting enhanced solubility profiles, while in some examples, polyethylene glycol and different APIs are revealing enhanced pharmaceutical characteristics.^{46,52,53} Eutectic mixture of ibuprofen-menthol showed an improved dissolution behaviour.⁴⁶ The similar improved dissolution behavior was recognized in the case of 2-[4-(4-chloro-2-fluorophenoxy) phenyl] pyrimidine-4-carboxamide: glutaric acid CS.³ These examples revealed the effects of CCs in improvement of solubility behavior along with bioavailability improvement of drugs.⁵⁴ The 1:1 danazol: vanillin CS showed increased solubility compared to poorly soluble pure danazol. The stability of drugs is also improved by CCs like carbamazepine CS revealed enhanced hydrostability in caparison susceptibility hydrate formation property of carbamazepine.⁵⁵ An improved humidity stability of theophylline and oxalic acid CS have been reported compared to their pure state (Figure 2).

Mechanical properties

In the CCs process, the API's and CFs create new crystalline

structures through non-covalently bonding resulting to a higher mechanical property. This is evident from previous studies like caffeine: Methyl gallate CS exhibited improved tableting characteristics compared to pure caffeine, while an enhanced compressibility and mechanical strength during tableting were observed in acetaminophen CS compared to pure acetaminophen. The plasticity and compressibility of theophylline: methyl gallate CS was found to be much higher than theophylline alone. All these properties were improved due to the layered structures of their CS.⁵⁶

Compression behaviors

The poor compression and compaction of powdered API's and ingredients is a bigger problem faced by drug formulation scientists because the compression is required at the roller stage to prepare granules, while compaction is the major requirement for making tablets by reducing the volume of powders under pressure. The compactness is the ability to compress the free flow powder in the form of a solid unit dosage form having the desired tensile strength. Therefore, the understanding of material's characteristics becomes an important key to developing and designing newer formulations with desired physical and chemical properties. Where, a higher dose or higher amount of drug is required, than compressibility and compaction become critical parameters to study.⁵⁷ To date, the focus of CS researchers mainly focused on improvement of solubility issue and tableting property area did not get much attention. some handful examples in the literature where this area of research touched like CS of carbamazepine with nicotinamide and saccharin were found to have increased tensile strength of 2.00 and 2.19 times, respectively, at 1500 lb/cm³. But the dissolution rate of these CS was found to be lesser compared to pure drugs. This signifies the relationship of higher tensile strength is directly proportional to a lower dissolution profile.⁵⁸

Formulation and dissolution

CS tend to have higher dissolution rates than the corresponding drugs, due to their higher solubility. However, most studies have focused on the powder dissolution profile as an indicator of CS performance. These studies did not comment on the CS solubility behavior or explain the reasons for improved dissolution rates in some. Further, suggested approaches or a mechanistic understanding of overcoming transformation challenges during dissolution were not discussed. One of the early examples is CS of itraconazole with a carboxylic acid, *i.e.*, fumaric acid, SA, malic acid, and tartaric acid,⁵⁹ all of which had higher dissolution rates than that of the crystalline drug and similar rates to that of the amorphous form of the drug.

The dissolution of fluoxetine hydrochloride was compared with that of CS made with benzoic acid, fumaric acid, or SA. The dissolution rate of the alt was about twice as high as that of the benzoic acid CS, similar to that of the fumaric acid CS and at least 3 times lower than that of the SA CS.⁵² Celecoxib-NIC CS had a higher dissolution rate than the drug alone. The dissolution rate of CS developed with 2% sodium dodecylsulfate and polyvinylpyrrolidone was better than that of the drug alone

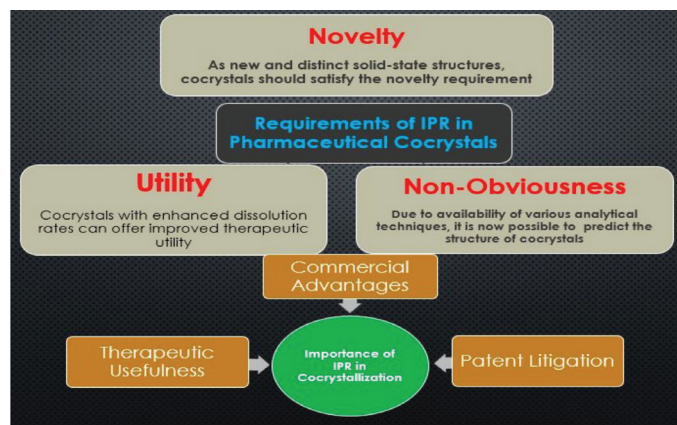


Figure 2. Application of intellectual property rights in cocrystallization

Table 3. Various drugs and coformers used for cocrystals formation and chemistry involved in their formation

Drug(s)	Coformer (s)	Method of Preparation	Method of Analysis	Important Points
Ezetimibe ⁵⁷	L-proline and imidazole	Wet-grinding and solution crystallization	Raman spectroscopy, Infrared spectroscopy, DSC, TGA, PXRD, SCXRD	Proline exists as zwitter ion in the crystal lattice of EZT-PRO. Carbonyl group of EZT formed C-H...O hydrogen bond with imidazole. Co-former was selected on the basis of pKa and complementary structure. Improved solubility and solid-state stability
Paracetamol ⁵⁸	Citric acid	Slow evaporation	Raman spectroscopy, DSC, TGA, PXRD, SCXRD	Two paracetamol molecules forms hydrogen bonds with citric acid molecule, one of these phenolic-OH acts as hydrogen bond donor while other as acceptor
Sildenafil ⁵⁹	Acetyl salicylic acid	Solution crystallization	PXRD, HPLC, DSC, ATR-IR, NMR	Sil: asa are held together by C-H...O and C-H... forces. 75% improved Intrinsic dissolution rate
6-mercaptopurine ⁶⁰	Isonicotinamide	Reaction crystallization method	DSC, TGA, DVS, FT-IR, PXRD, SCXRD	CS produced were less hygroscopic. CS attained maximum solubility in 5-10 minutes
Theophylline ⁶¹	Oxalic, malonic, maleic and glutaric acid	Solid state-grinding and solution precipitation	SCXRD	Theophylline also possesses a good N-H hydrogen bond donor. N-H...O hydrogen bond is formed between N-H donor of a theophylline by linking with carbonyl oxygen from an adjacent theophylline. This interaction between N-H and O forms hydrogen-bonded dimers in a cyclic motif. Improvement of physical properties and avoidance of hydration
Caffeine ⁶²	Maleic acid	Ultrasonic assisted solution co-crystallization	Raman spectroscopy, PXRD	CCs with maleic acid increases solubility of caffeine which decreases supersaturation
Myricetin ⁶³	Acetamide	Solvent drop grinding	PXRD, morphological analysis, TGA, dissolution studies, IR and NMR spectroscopy	4 times increased dissolution rate
Tropium chloride ⁶⁴	Urea	Solvent evaporation	PXRD, SCXRD, NMR, Karl Fischer coulometric titration, TGA, DSC	Electronegative chloride anion accepts an H-bond from the best H-bond donor, a hydroxyl group in tropium molecule. Urea molecules form an infinite chain on which chloride anions hang over tropium. Increased intrinsic dissolution rate
Theophylline ⁶⁵	Urea, saccharin, gentisic acid, salicylic acid, glutaric acid, sorbic acid, oxalic acid, maleic acid and nicotinamide	Supercritical fluid-enhanced atomization	PXRD, DSC, SEM, solubility and dissolution studies	Low soluble CFs produce theophylline CS with a low dissolving rate while use of high soluble CFs produce faster dissolving CS.
Diffunisal ⁴⁵	Nicotinamide	Supercritical fluid antisolvent precipitation	XRD, DSC, FT-IR, Electron microscopy, dissolution studies	Acetone was chosen as a solvent for diffunisal and nicotinamide. pH 7.4 phosphate buffer was used to carry out dissolution studies
Indomethacin ⁶⁶	Saccharin	Anti-solvent crystallization, solvent evaporation	XRD, DSC, DVS, Near-IR spectroscopy	N-H...O bonding was formed between the carboxylic acid dimer of IMC and SAC imide dimer

Itraconazole ⁶⁷	L-Malic acid	Gas antisolvent crystallization	HPLC, solubility studies, XRD, DSC, SEM, powder composition study, dissolution studies	The CS obtained by this method were suspected to contain unquantified amount of amorphous material. GAS CCs may have improved itraconazole bioavailability
Sulfamethazine ⁶⁸	Theophylline	Neat-cogrounding, solvent drop-cogrounding and slow evaporation	DSC, TGA, raman, PXRD, and DVS techniques	The sulfamethazine molecules form a dimer through the intermolecular O...H--N, and two O...H--N and N...H-N keeping theophylline molecule attached
Carbamazepine ⁶⁹	Saccharin	Cogrounding	ATR-FTIR, PXRD, DSC	Grinding induced amorphous phases are followed by CS formation. High relative humidity exposure increases rate of CCs
2-[4-(4-chloro-2-fluorophenoxy)phenyl]pyrimidine-4-carboxamide ⁷⁰	Glutaric acid	Solvent crystallization	Raman spectroscopy, SCXRD, intrinsic dissolution studies, pharmacokinetic evaluation, particle size evaluation	<i>In vivo</i> bioavailability was increased. CS was found to be physically and chemically stable. Increased dissolution rate
Ethenzamide ⁷¹	Gentisic acid	Slow evaporation	DSC, hot-stage microscopy, PXRD, SCXRD	The primary amide anti-N-H of the ofEthenzamide and the 2-hydroxy group ofGentisic acid forms two intramolecular N-H...O and O-H...O hydrogen bonds. Dissolution rate of ethenzamide was improved by a factor of 2
Artemisinin ⁷²	Orcinol and resorcinol	Liquid-assisted grinding	DSC, FT-IR, PXRD	The interaction of trimeric units is through a vast network of C-H...O bonds. Every synthon comprises of O-H...O hydrogen bonds formed between the OH group of resorcinol and the carbonyl moiety of artemisinin
Gabapentin ⁷³	C-propan-3-ol pyrogallol[4]areneand C-butyl pyrogallol[4]arene	Slow evaporation-aided with sonication	XRD	Reported CS exhibit bilayer structures comprising of networks of extensive hydrogen bonding networks between the pyrogallol[4]arene, gabapentin molecules
S-naproxen and RS-naproxen ⁷⁴	D-Proline	Liquid-assisted grinding	DSC, TGA, PXRD, SCXRD	Synthon part is mainly composed of zwitterionic entity. The crystalline network in the four CS formed is guided by the amino acid prolinium
Pyrazine ⁷⁵	Dicarboxylic acid, terephthalic, phthalic, fumaric and succinic acids.	Pyrazine CS were synthesised by neat grinding. Samples of the pyr:fum CS (50 mg), which were prepared by grinding were dissolved in a minimum amount of acetonitrile	SCXRD, PXRD, DSC and TGA measurements IR spectroscopy	Pyridine-carboxylic acid synthon-based h-bonded chains is the backbone of the structure
Theophylline ⁷⁶	Benzoic acid	Both neat-riding and liquid-assisted grinding	X-ray diffraction	Carbonyl group of theophylline and the carboxyl group of benzoic acidforms an O-H...O hydrogen bond. Another hydrogen bond is formed between acidic imidazolic nitrogen atom of theophylline and the carboxyl oxygen atom of benzoic acid

DVS: Dynamic vapor sorption, PXRD: Powder X-ray diffraction, SCXRD: Single-crystal X-ray diffractometry, HPLC: High performance liquid chromatography, ATR-IR: Attenuated total reflectance-infrared

developed with similar excipients, and similar to that of the amorphous formulation. This was only an empirical formulation study and the mechanics of the effect of the excipient on CS behavior have not been investigated.⁵⁸

The dissolution of CS of exemestane with maleic acid and megestrol acetate with saccharine was studied in fasted state simulated intestinal fluid. The transformation of the exemestane CS to the drug was fast and dissolution rate was similar to that of the drug when the particles were fine, whereas higher dissolution rates than those of the drug were achieved for larger particle sizes (106-150 and 150-300 m).⁵⁹ The transformation of megestrol acetate CS was slow and the dissolution rate of the fine particles was much faster than for the drug, whereas that of the larger particles was similar to that of the drug.

In another study, the bioavailability of IND-saccharine CS was investigated in beagle dogs and compared with the bioavailability of both the marketed product of IND (Indomee®) and the physical mixture of drug and CFs.⁴⁵ The CS had similar pharmacokinetic data to the marketed product but significantly improved performance compared to the physical mixture. After preparing and characterizing CS of AMG517, CS of AMG517 with sorbic acid was studied *in vivo* in Sprague-Dawley rats at different doses and compared with 500 mg/kg doses of the free base form of the drug. The result indicated dose-dependent pharmacokinetics (C_{max} and area under the curve) for the CS.^{61,62}

Cosmetics

In the cosmetic formulation development, the focus remains on the formulation of a stable and easily applicable preparation using active ingredients. CCs and eutectic mixtures provide these basic facilities to the formulation developers. The inclusion of solid cologne in these cosmetic preparations is a challenge because a higher temperature must melt these solid components, which may directly affect the thermostability of other ingredients used. Some eutectic mixtures of standard cologne in solid form with benzophenone were developed which in result convert into liquid form and could be easily included in the formulation. The flexibility and alterability of these varieties of binary preparations were evaluated through binary formulations of solid fragrances and benzoquinone.⁶³ The eutectic mixture based upon above idea was prepared using 12-hydroxystearic acid, as well-known benefit of 12-hydroxystearic acid on skin having a higher melting point and inadequate bioavailability. The other key benefit of CCs is availing a higher melting point crystalline substance having more stability. But higher melting point substances could be a problem for other lower melting point ingredients.⁶⁴ CS-based formulation of 3-iodopropynyl butylcarbamate, an antifungal agent reported in the literature. These CS formulations exhibit higher physical and chemical stability profiles along with higher aqueous solubility and thermostability.⁶⁵ These systems also provide higher flowability to powders and better compressibility during tablets or capsule formulation process. Nicotinamide: p-coumaric acid CS formulations were reported in the literature to treat acne.⁶⁶ In another study, the CS of hair dye colorants exhibit better stability on hair compared to pure

colorant.⁶⁷ CS could be an important formulation development system in cosmetic scenario, but the higher melting point of CS plays a key role and that's why, in the cosmetic industry, the main focus areas become eutectic systems. Butyl methoxy-dibenzoylmethane an ultraviolet (UV) B absorbing agent, included in the eutectic mixture with and without 12-hydroxystearic acid to overcome the challenge of the higher melting points of both components.⁶⁸ An anti-sun eutectic formulation based on *n*-butylphthalamide and isopropylacrylamide with 1,3,5-triazine derivatives was prepared revealing higher stability.⁶⁹ The eutectic mixture preparation of monoethanolamine used in scalp itching treatment exhibits higher deposition compared to pure compound.⁷⁰

Agricultural applications

In the agrochemical sector, there are plentiful patents that have been completed on CS, which mainly include fertilizers, insecticides, and fungicides, *etc.* CS-based fungicide patent was filled containing two fungicides, namely metalaxyl and prothioconazole.⁷¹ In this preparation, the aqueous solubility of metalaxyl was drastically decreased compared with that of the pure component. The reason given behind reduced solubility was the decrement to a surplus of the fungicide in the ground water streams along with higher efficacy and less requirement of fungicides for the desired action. This CS-based formulation is a significant example of the synergistic action of two active fungicide ingredients. The CS of herbicide 3,6-dichloro-2-methoxybenzoic acid with different nitrogenous heterocycles was also reported less water solubility and higher stability.⁷² But there are some examples of various herbicides suffer from the Ostwald effect (large size crystals growth) with time, which has deleterious effects during the storage and processability of product in production and efficacy during use. Here CS provides significant improved stability to overcome these issues. 4-Hydroxybenzoic acid-based CS with different agrochemicals effectively overcome the above discussed problems.⁷³ The increased melting points insecticides were reported by CCs of these insecticides with oxalic acid. The higher melting point provides shelf stability and prevents the clumping or Ostwald effect on pure insecticides with time. A recent patent on CS of 4-[(6-chloropyrid-3-yl) methyl] (2,2-difluoroethyl) amino} furan- 2(5H)-one with salicylic acid was filled higher melting point and stability.^{74,75}

Chromophores

Pigments are a principally fascinating chromophore application of CS. According to Skořepová et al.⁶³ it is impossible to prepare novel pigments in high amounts only through solvent methods, it can be prepared in high yield through mechanochemical grinding. The three-colour tuned fluorescein CS formulation supports this argument mainly. Chromophore CS of titanyl fluoroalanine with titanyl fluorocytosine was developed by dry milling and heating. The novel CS has a novel spectrum along with enhanced sensitivity toward electrophotography and less dark decay. Bicomponent diazo eutectic was prepared as red textile pigments. These eutectic pigments exhibit an equal performance compared to highly toxic dyes in relation

to thermostability, color fastness, acidic and alkali resistance, and solubility profile. In another study, proved that CS can be utilized at a much higher level than just tuning the solubility, stability, and colour of chromophores. They formulated a series of CS based upon stilbene-type molecules with different CFs. The results exhibited a significant and remarkable change in the form of UV or visible absorbance, quantum yield, and luminescence emissions.⁶³

Food industry

CS has created a place in food additives. The yerba mate (an antioxidant) along with sucrose induce CS show a better flow property and good hygroscopicity during the production process compared to their pure state.⁵⁹ It is also evident that the antioxidant properties of yerba mates remain stable in their CS form. In another example, ethyl much vanilla are required in mixture form to provide a better taste and fragrance, but during the manufacturing process, clumping occurred in a simple mixture of both these substances. But CCs of these compounds at the individual level provide their powder form carrying good flow properties and weak clump formation tendency. Menthol: xylitol-based CS is another good example of CS having optimum flow properties used for fragrance.^{52,53} These CS revealed a higher solubility profile compared to pure menthol and lesser hygroscopicity compared to pure xylitol.

Solubilization of cocrystals

CS has risen as a method for the modification of dissolvability, disintegration, bioavailability, and other physicochemical properties of drugs, without changing their pharmacological properties.⁵³ CS are a class of multicomponent solids containing at least two diverse crystalline components in a solitary homogenous system in a fixed stoichiometry ratio. They are distinguished from solvates in that the CS components are solids at room temperature. Pharmaceutical CS are generally made of a hydrophobic drug molecule and a hydrophilic CFs molecule.⁵⁴ The mechanism by which CS go into solution involves three main steps: (1) Breaking intermolecular bonds in the CS, (2) breaking intermolecular bonds in the solvent, and (3) forming intermolecular bonds between the CS molecules and solvent molecules. The limiting step in dissolving the CS of hydrophobic drug molecules in aqueous media has been shown to be solvation and not breaking away from the crystal lattice. CFs appear to decrease the solvation barrier of CS of hydrophobic drugs to an extent proportional to that of the pure CFs. Consequently, CF aqueous solubility is correlated with CS solubility. However, melting points are not good indicators of CS aqueous solubility, since it is drug hydrophobicity and not CS lattice strength that limits solubility (Table 3).⁵⁵

CONCLUSION

In the crystal engineering technique, the pharmaceutical properties of drugs are changed without disturbing their inherent structures. Presence of various chemical groups' viz. carboxylic acids, carbohydrates, amides, amino acids, and alcohols in the co-crystal formers lead to the formation of CS with different drugs. So, in CC studies, the presence of a carboxylic acid functional group plays an admirable role.

Synthons are responsible for holding the molecules, when the formation of a compound occurs through non-covalent interactions. Due to their strength, directionality and higher rate of recurrence, hydrogen bonds are often used for the design of CS. Generally, two methods are used for CCs: Solution-based techniques and grinding based techniques. Solution-based methods are generally preferred because of the formation of CS, which can qualify the testing with a SXRD. The grinding techniques include neat-grinding and solvent drop-grinding techniques. Currently, newer techniques are available viz. hot-stage microscopy, ultrasound-assisted, and CCs *via* supercritical fluid. CS offers numerous commercial applications, which are under study or less developed. In spite of their less patent activities, these are potentially critical binary systems because of their prominent effects. CCs can be used in almost all API's including acidic, basic, or non-ionic drugs. The availability of a large number of CFs allowed this technique to be used broadly. It is evident from previous and recent studies that CC materials carry higher electrical conductivity compared to their parent components. So, this is an area of research because of its potential in the power production sector.

ACKNOWLEDGMENTS

Authors want to thank the Department of Pharmaceutical Sciences, Maharishi Dayanand University, Rohtak, for providing all necessary facilities to conduct this work.

Ethics

Peer-review: Externally peer-reviewed.

Authorship Contributions

Concept: B.D., Design: V.B., Data Collection or Processing: B.D., Analysis or Interpretation: M.C., Literature Search: B.D., Writing: B.D.

Conflict of Interest: No conflict of interest was declared by the authors.

Financial Disclosure: The authors declared that this study received no financial support.

REFERENCES

1. Cherukuvada S, Nangia A. Eutectics as improved pharmaceutical materials: design, properties and characterization. *Chem Comm (Camb)*. 2014;50:906-923.
2. Berry DJ, Steed JW. Pharmaceutical cocrystals, salts and multicomponent systems; intermolecular interactions and property based design. *Adv Drug Deliv Rev*. 2017;117:3-24.
3. Blagden N, Berry DJ, Parkin A, Javed H, Ibrahim A, Gavan PT, De Matos LL. Current directions in cocrystal growth. *New J Chem*. 2008;32:1659-1672.
4. Brittain HG. Cocrystal systems of pharmaceutical interest. *Cryst Growth Des*. 2012;12:5823-5832.
5. Cherukuvada S, Row TNG. Comprehending the formation of eutectics and cocrystals in terms of design and their structural interrelationships. *Cryst Growth Des*. 2014;14:4187-4198.

6. Ross SA, Lamprou DA, Douroumis D. Engineering and manufacturing of pharmaceutical co-crystals: a review of solvent-free manufacturing technologies. *Chem Commun (Camb)*. 2016;52:8772-8786.
7. Shayanfar A, Jouyban A. Physicochemical characterization of a new cocrystal of ketoconazole. *Powder Technol*. 2014;262:242-248.
8. Ganduri R, Cherukuvada S, Sarkar S, Row TNG. Manifestation of cocrystals and eutectics among structurally related molecules: towards understanding the factors that control their formation. *Cryst Eng Comm*. 2017;19:1123-1132.
9. Sreekanth BR, Vishweshwar P, Vyas K. Supramolecular synthon polymorphism in 2: 1 co-crystal of 4-hydroxybenzoic acid and 2,3,5,6-tetramethylpyrazine. *Chem Commun (Camb)*. 2007;2375-2377.
10. Cherukuvada S, Kaur R, Row TNG. Co-crystallization and small molecule crystal form diversity: from pharmaceutical to materials applications. *Cryst Eng Comm*. 2016;18:8528-8555.
11. Merz K, Vasylyeva V. Development and boundaries in the field of supramolecular synthons. *Cryst Eng Comm*. 2010;12:3989-4002.
12. Aakeröy CB, Rajbanshi A, Li ZJ, Desper J. Mapping out the synthetic landscape for recrystallization, cocrystallization, and salt formation. *Cryst Eng Comm*. 2010; 12: 4231-4239.
13. Ying Hsi KH, Chadwick A, Fried M, Kenny AS, Myerson AS. Separation of impurities from solution by selective co-crystal formation. *Cryst Eng Comm*. 2012;14:2386-2388.
14. Fábíán LS. Cambridge structural database analysis of molecular complementarity in cocrystals. *Cryst Growth Des*. 2009;9:1436-1443.
15. Stevens JS, Byard SJ, Schroeder SLM. Characterization of proton transfer by X-Ray photoelectron spectroscopy (XPS). *Cryst Growth Des*. 2010;10:1435-1442.
16. Stevens JS, Byard SJ, Schroeder SLM. Salt or cocrystal? determination of protonation state by X-ray photoelectron spectroscopy (XPS). *J Pharm Sci*. 2010;99:4453-4457.
17. Good DJ, Rodríguez-Hornedo N. Cocrystal eutectic constants and prediction of solubility behaviour. *Cryst Growth Des*. 2010;10:1028-1032.
18. Mohammad MA, Alhalaweh A, Bashimam M, Al-Mardini MA, Velaga S. Utility of hansen solubility parameters in the cocrystal screening. *J Pharm Pharmacol*. 2010;62:1360-1362.
19. Huang N, Rodríguez-Hornedo N. Effect of micellar solubilization on cocrystal solubility and stability. *Cryst Growth Des*. 2010;10:2050-2053.
20. Moore MD, Wildfong PLD. Aqueous solubility enhancement through engineering of binary solid composites: pharmaceutical applications. *J Pharm Innov*. 2009;4:36-49.
21. Childs SL, Stahly GP, Park A. The salt-cocrystal continuum: the influence of crystal structure on ionization state. *Mol Pharm*. 2007;4:323-338.
22. Cannon AS, Warner JC. Noncovalent derivatization: green chemistry applications of crystal engineering. *Cryst Growth Des*. 2002;2:255-257.
23. Aitipamula S, Banerjee R, Bansal AK, Biradha K, Cheney ML, Choudhury AR, Desiraju GR, Dikundwar AG, Dubey R, Duggirala N, Ghogale PP, Ghosh S, Goswami PK, Goud NR, Jetli RRRK, Karpinski P, Kaushik P, Kumar D, Kumar V, Moulton B, Mukherjee A, Mukherjee G, Myerson AS, Puri V, Ramanan A, Rajamannar T, Reddy CM, Rodríguez-Hornedo N, Rogers RD, Guru Row TN, Sanphui P, Shan N, Shete G, Singh A, Sun CC, Swift JA, Thaimattam R, Thakur TS, Thaper RK, Thomas SP, Tothadi S, Vangala VR, Variankaval N, Vishweshwar P, Weyna DR, Zaworotko MJ. Polymorphs, salts, and cocrystals: what's in a name? *Cryst Growth Des*. 2012;12: 2147-2152.
24. Cruz-Cabeza AJ. Acid-base crystalline complexes and the pKa rule. *Cryst Eng Comm*. 2012;14:6362-6365.
25. Babu NJ, Reddy LS, Nangia A. Amide N-oxide heterosynthon and amide dimer homosynthon in cocrystals of carboxamide drugs and pyridine N-oxides. *Mol Pharm*. 2007;4:417-434.
26. Etter MC, Reutzel SM. Hydrogen bond directed cocrystallization and molecular recognition properties of acyclic imides. *J Am Chem Soc*. 1991;113:2586-2598.
27. Schultheiss N, Newman A. Pharmaceutical cocrystals and their physicochemical properties. *Cryst Growth Des*. 2009;9:2950-2967.
28. Kuroda R, Imai Y, Tajima N. Generation of a co-crystal phase with novel coloristic properties via solid state grinding procedures. *Chem Commun (Camb)*. 2002;23:2848-2849.
29. Cherukuvada S, Nangia A. Fast dissolving eutectic compositions of two anti-tubercular drugs. *Cryst Eng Comm*. 2012;14:2579-2588.
30. Vitthalrao MA, Kumar FN, Radheshyam BK. Cocrystallization: an alternative approach for solid modification. *J Drug Deliv Ther*. 2013;3:166-172.
31. Raghuram Reddy Kothur AS, Swetha NPB. An outline of crystal engineering of pharmaceutical co-crystals and applications: a review. *Int J Pharm Res Dev*. 2012;4:84-92.
32. Sevukarajan M, Thamizhvanan K, Sodanapalli R, Sateesh Babu JM, Naveen KB, Sreekanth Reddy B, Sethu KJ, Vivekananda U, Sarada K, Hyndavi N. Crystal engineering technique – an emerging approach to modify physicochemical properties of active pharmaceutical ingredient. *Int J Chem Pharm Sci*. 2012;3:15-29.
33. Trask AV, Motherwell WD, Jones W. Solvent-drop grinding: green polymorph control of cocrystallisation. *Chem Commun (Camb)*. 2004;7:890-891.
34. Friscic T, Jones W. Recent advances in understanding the mechanism of cocrystal formation via grinding. *Cryst Growth Des*. 2009;9:1621-1637.
35. Aakeröy CB, Grommet AB, Desper J. Co-crystal screening of diclofenac. *Pharmaceutics*. 2011;3:601-614.
36. Swapna B, Maddileti D, Nangia A. Cocrystals of the tuberculosis drug isoniazid: polymorphism, isostructurality, and stability. *Cryst Growth Des*. 2014;14:5991-6005.
37. Bhogala BR, Basavoju S, Nangia A. Tape and layer structures in cocrystals of some di- and tricarboxylic acids with 4,4-bipyridines and isonicotinamide. From binary to ternary CS. *Cryst Eng Comm*. 2005;7:551-562.
38. Laszlo F. Cambridge structural database analysis of molecular complementarity in cocrystals. *Cryst Growth Des*. 2009;9:1436-1443.
39. Kumar S, Nanda A. Pharmaceutical cocrystals: an overview. *Indian J Pharm Sci*. 2017;79:858-871.
40. Musumeci D, Hunter CA, Prohens R, Scuderi S, McCabe JF. Virtual cocrystal screening. *Chem Sci*. 2011;2:883-890.
41. Yamamoto K, Tsutsumi S, Ikeda Y. Establishment of cocrystal cocktail grinding method for rational screening of pharmaceutical cocrystals. *Int J Pharm*. 2012;437:162-171.
42. Lu E, Rodríguez-Hornedo N, Suryanarayanan R. A rapid thermal method for cocrystal screening. *Cryst Eng Comm*. 2008;10:665-668.
43. Trask AV, Motherwell WDS, Jones W. Physical stability enhancement of theophylline via cocrystallization. *Int J Pharm*. 2006;320:114-123.

44. Rahman Z, Agarabi C, Zidan AS, Khan SR, Khan MA. Physico-mechanical and stability evaluation of carbamazepine cocrystal with nicotinamide. *AAPS PharmSciTech*. 2011;12:693-704.
45. Kasim NA, Whitehouse M, Ramachandran C, Bermejo M, Lennernäs H, Hussain AS, Junginger HE, Stavchansky SA, Midha KK, Shah VP, Amidon GL. Molecular properties of WHO essential drugs and provisional biopharmaceutical classification. *Mol Pharm*. 2004;1:85-96.
46. Jain S. Mechanical properties of powders for compaction and tableting: an overview. *Pharm Sci Technol Today*. 1999;2:20-31.
47. Hiestand EN. Dispersion forces and plastic deformation in tablet bond. *J Pharm Sci*. 1985;74:768-770.
48. Hiestand EN. Tablet bond. I. a theoretical model. *Int J Pharm*. 1991;67:217-229.
49. Hiestand EN, Smith DP. Tablet bond. II. Experimental check of model. *Int J Pharm*. 1991;67:231-246.
50. Blagden N, Coles SJ, Berry DJ. Pharmaceutical cocrystals- are we there yet? *CrystEngComm*. 2014;16:5753-5761.
51. Sun CC, Hou H. Improving mechanical properties of caffeine and methyl gallate crystals by cocrystallization. *Cryst Growth Des*. 2008;8:1575-1579.
52. Rahman Z, Samy R, Sayeed VA, Khan MA. Physicochemical and mechanical properties of carbamazepine cocrystals with saccharin. *Pharm Dev Technol*. 2012;17:457-465.
53. Desiraju GR. Crystal and cocrystal. *CrystEngComm*. 2003;2:466-467.
54. Dunitz JD. Crystal and cocrystal: a second opinion. *CrystEngComm*. 2003;4:506.
55. Bond AD. What is a cocrystal? *CrystEngComm*. 2003;9:833-834.
56. Shimpi MR, Childs SL, Boström D, Velaga SP. New cocrystals of ezetimibe with L-proline and imidazole. *Cryst Eng Comm*. 2014;16:8984-8993.
57. Elbagerma MA. Analytical method development for structural studies of pharmaceutical and related materials in solution and solid state. An investigation of the solid forms and mechanisms of formation of cocrystal systems using vibrational spectroscopic and X-ray diffraction techniques. (Doctoral dissertation, University of Bradford). 2010.
58. Zegarac M, Lekšić E, Šket P, Plavec J, Bogdanović MD, Bučar DK, Dumic M, Meštrović E. A sildenafil cocrystal based on acetylsalicylic acid exhibits an enhanced intrinsic dissolution rate. *CrystEngComm*. 2014;16:32-35.
59. Wang JR, Yu X, Zhou C, Lin Y, Chen C, Pan G, Mei X. Improving the dissolution and bioavailability of 6-mercaptopurine via co-crystallization with isonicotinamide. *Bio Med Chem Lett*. 2015;25:1036-1039.
60. Trask AV, Motherwell WD, Jones W. Physical stability enhancement of theophylline via cocrystallization. *Int J Pharm*. 2006;320:114-123.
61. Aher S, Dhumal R, Mahadik K, Paradkar A, York P. Ultrasound assisted cocrystallization from solution (USSC) containing a non-congruently soluble cocrystal component pair: caffeine/maleic acid. *Eur J Pharm Sci*. 2010;41:597-602.
62. Mureșan-Pop M, Chiriac LB, Martin F, Simon S. Novel nutraceutical myricetin composite of enhanced dissolution obtained by co-crystallization with acetamide. *Compos B Eng*. 2016;89:60-66.
63. Skořepová E, Hušák M, Čejka J, Zámotný P, Kratochvíl B. Increasing dissolution of trospium chloride by co-crystallization with urea. *J Crystal Growth*. 2014;399:19-26.
64. Padrela L, Rodrigues MA, Tiago J, Velaga SP, Matos HA, de Azevedo EG. Tuning physicochemical properties of theophylline by cocrystallization using the supercritical fluid enhanced atomization technique. *J Supercrit Fluids*. 2014;86:129-136.
65. Cuadra IA, Cabañas A, Cheda JAR, Martínez-Casado FJ, Pando C. Pharmaceutical co-crystals of the anti-inflammatory drug diflunisal and nicotinamide obtained using supercritical CO₂ as an antisolvent. *J CO₂ Util*. 2016;13:29-37.
66. Chun NH, Wang IC, Lee MJ, Jung YT, Lee S, Kim WS, Choi GJ. Characteristics of indomethacin-saccharin (IMC-SAC) co-crystals prepared by an anti-solvent crystallization process. *Eur J Pharm Biopharm*. 2013;85:854-861.
67. Ober CA, Montgomery SE, Gupta RB. Formation of itraconazole/L-malic acid cocrystals by gas antisolvent cocrystallization. *Powder Technol*. 2013;236:122-131.
68. Lu J, Rohani S. Synthesis and preliminary characterization of sulfamethazine-theophylline co-crystal. *J Pharm Sci*. 2010;99:4042-4047.
69. Jayasankar A, Somwangthanaroj A, Shao ZJ, Rodríguez-Hornedo N. Cocrystal formation during cogrinding and storage is mediated by amorphous phase. *Pharm Res*. 2006;23:2381-2392.
70. McNamara DP, Childs SL, Giordano J, Iarriccio A, Cassidy J, Shet MS, Mannion R, O'Donnell E, Park A. Use of a glutaric acid cocrystal to improve oral bioavailability of a low solubility API. *Pharm Res*. 2006;23:1888-1897.
71. Aitipamula S, Wong AB, Chow PS, Tan RB. Pharmaceutical cocrystals of ethenzamide: structural, solubility and dissolution studies. *CrystEngComm*. 2012;14:8515-8524.
72. Karki S, Friščić T, Fábán L, Jones W. New solid forms of artemisinin obtained through cocrystallisation. *CrystEngComm*. 2010;12:4038-4041.
73. Fowler DA, Tian J, Barnes C, Teat SJ, Atwood JL. Cocrystallization of C-butyl pyrogallol [4] arene and C-propan-3-ol pyrogallol [4] arene with gabapentin. *CrystEngComm*. 2011;13:1446-1449.
74. Tilborg A, Springuel G, Norberg B, Wouters J, Leyssens T. On the influence of using a zwitterionic coformer for cocrystallization: structural focus on naproxen-proline cocrystals. *CrystEngComm*. 2013;15:3341-3350.
75. Arhangelskis M, Lloyd GO, Jones W. Mechanochemical synthesis of pyrazine: dicarboxylic acid cocrystals and a study of dissociation by quantitative phase analysis. *CrystEngComm*. 2012;14:5203-5208.
76. Heiden S, Tröbs L, Wenzel KJ, Emmerling F. Mechanochemical synthesis and structural characterisation of a theophylline-benzoic acid cocrystal (1:1). *CrystEngComm*. 2012;14:5128-5129.



Challenges Faced by Hospital Pharmacists in Low-Income Countries Before COVID-19 Vaccine Roll-Out: Handling Approaches and Implications for Future Pandemic Roles

Rajeev SHRESTHA^{1*}, Sunil SHRESTHA², Binaya SAPKOTA³, Saval KHANAL⁴, Bhuvan KC²

¹Lamjung District Community Hospital, Department of Pharmacy, Lamjung, Nepal

²Monash University Malaysia, School of Pharmacy, Selangor, Malaysia

³Nobel College, Department of Pharmaceutical Sciences, Kathmandu, Nepal

⁴University of Warwick, Warwick Medical School, Department of Health Sciences, Coventry, United Kingdom

ABSTRACT

Coronavirus disease-2019 (COVID-19) is one of the greatest pandemics of modern times. More than one hundred eleven million global deaths have already been associated with COVID-19. The incidence of COVID-19 as well as morbidity and mortality due to COVID-19 have increased in low-income countries (LICs). COVID-19 has further weakened health systems in LICs, that are already distressed by inadequate funding, lack of human resources, and poor infrastructure and service delivery. Despite the resource crunch, hospital LICs have been instrumental in treating COVID-19 patients. Pharmacists working in hospitals play an indispensable role in providing pharmaceutical services for infection prevention and control. This study discusses the contribution of hospital pharmacists and the challenges faced by them for treating COVID-19 patients in LICs before the COVID-19 vaccine roll-out.

Key words: COVID-19, hospital pharmacy, hospital pharmacist, low-income countries, pharmacy service, pharmacist

INTRODUCTION

Coronavirus disease-2019 (COVID-19) is a current ongoing global threat. It is one of the fatal pandemics in the history of humankind. As *per* the World Health Organization (WHO), as of March 3, 2021, there were 114,140,104 confirmed cases and 2,535,520 deaths globally. Similarly, 828,461 confirmed cases and 14,749 deaths in low-income countries (LICs).¹ Among 31 LICs, coronavirus deaths are found in 30 countries, and 83.87% of countries had community transmission, too.¹ LICs are those countries that have a very low, *i.e.* \$1,035 or less gross national income in 2019.²

Vaccines against COVID-19 have been developed and rolled over in many countries. Before that, the non-pharmacological interventions to contain the virus, such as social distancing

and personal hygiene, were only mechanisms that prevent the transmission. The LICs, often have a huge population concentrated in a few cities, living in overcrowded conditions.³ It is difficult to maintain social distancing for people. Furthermore, people did not have access to adequate hand sanitizer and other protective measures required for preventing transmission.³ Healthcare systems LICs were traditionally developed to deliver basic health services and treatment of some life-threatening infective diseases. These systems are already overstretched and struggling to cope with the increasing burden of non-communicable diseases.⁴ During this transition phase, the emergence of COVID-19 had presented significant challenges to LICs where the accessibility of quality and affordable health services is poor.^{5,6}

*Correspondence: rajiv2stha@gmail.com, Phone: +977-9845445205, ORCID-ID: orcid.org/0000-0003-1822-3969

Received: 27.10.2020, Accepted: 19.03.2021

©Turk J Pharm Sci, Published by Galenos Publishing House.

All healthcare professionals and health institutions must strengthen themselves against the COVID-19 or any pandemic situation. Like other healthcare professionals, hospital pharmacists also play a significant role in preventing and controlling pandemic. The International Pharmaceutical Federation (FIP) has developed guidelines for hospital pharmacists considering their imperative value during the disaster and pandemic control.^{7,8} Various studies have identified the importance of pharmacists' roles in providing pharmaceutical care and services during infection control and managing disaster complications.^{9,10} Pharmacists are the third largest healthcare professionals in the world after physicians and nurses,¹⁰ but they are still struggling to prove their value in the healthcare systems of LICs.¹¹ The current review discusses the hospital pharmacists' potential contributions in the management of disasters and the challenges they faced in LICs. The discussion is based on the situation before the development of COVID-19 vaccines. The reflection will help different stakeholders to understand how essential pharmacists are to healthcare delivery during pandemics and how they can effectively use hospital pharmacists during any future pandemics.

METHODS

We performed a narrative review of the existing literature known to the authors. The literature was searched in PubMed, MEDLINE, ScienceDirect and Google Scholar from its inception up to and including May 2020. Key search terms included were "pharmacist," "COVID-19," "low-income countries," "pharmacy," "hospital" and "developing countries." Along with this, various synonyms or combinations of these terms have been used. The authors viz. R.S., S.S. are working as the hospital and clinical pharmacists in the hospital. S.K., B.S. and B.K.C. are in academia, but had experience working as a pharmacists in the past. We have themed potential activities and challenges into different headings to improve readability. The potential role of hospital pharmacists is mainly based on FIP and Nepal (a lic) guidelines for managing COVID-19. The main features of both guidelines are presented in Table 1.

RESULTS

Potential role of hospital pharmacists in the management of COVID-19 and pandemics

The healthcare systems in LICs differs from one country to another. Therefore, it would be difficult to generalize what exactly a hospital pharmacist can provide in general. However, we propose these activities (Figure 1), which may be possible in many LIC jurisdiction under the existing legal and professional framework. These are the recommended role; some of these might not be legal in some countries. The role presented in Figure 1 is described below individually in subsequent sections.

Pharmaceutical management

Access to adequate, qualitative, and affordable essential medicines is challenging in LICs.¹³ Medicine accessibility has

been a problem during COVID-19 because of the disruption in manufacture, distribution and logistics. Hospital pharmacists played an important role in this situation *via* handling of medicine logistics *via* appropriate forecasting, stocking, quality maintenance, and optimum usage of resources.

In close consultation with clinicians, pharmacists can develop a strategy for using available therapeutic alternatives, such as converting the oral dosage form to intravenous, selecting equivalent alternative medicine to tackle drug shortage.^{14,15} Hospital pharmacies use detailed information about their regular patients through electronic billing systems or other record-keeping forms. Therefore, they can estimate and transfer the required medications of their patients appropriately. Pandemic has broadly taught about keeping patient's medication record practice. It must be started if many hospital pharmacies do not have a system of keeping patient's medication record. Medication records are essential not only for better logistics and distribution but also for measuring patient's adherence to medication therapy and effective management of therapy.^{16,17}

Drug information service

Access to reliable information is crucial to the public and healthcare professionals during a pandemic. Fake or incomplete information is dreadful. It can even cause severe accidents, when the public figure personnel become a medium of rumor.

Similarly, more than 700 people in Iran died in about two months after injecting methanol following the manipulation of information raised by another misinformation by an influential global leader regarding the possibility of injecting disinfectant to cure COVID-19.¹⁸ Therefore, the correct information should be transmitted to both the general public and healthcare professionals. Pharmacists have a fundamental professional responsibility to continuously evaluate the existing literature and make health professionals and public awareness of the pandemic and its medicinal management by providing accurate, unbiased information.¹⁹⁻²¹ Currently, several medicines and vaccines are under trial for COVID-19 treatment. Pharmacists can be a part of the clinical trial team to manage and provide information on medicine or vaccine under trial. The pharmacist can also use various informative pictures, pamphlets, and information sheets to make patient aware, when they visit hospitals.

Patient screening and triaging

Social distancing is one of the most crucial approaches to pandemic control. Consequently, the initial screening of patients visiting the hospital could save unwanted contact with the hospital staff and patients. The pharmacy department and hospital pharmacists can play a significant role in initial screening and triage. The pharmacist can offer the initial evaluation of the patient. They can either recommend patients for clinician consultation or send them back home with OTC medications or non-pharmacological counseling in case of minor conditions. The pharmacist can also perform rapid diagnostic tests of suspected patients segregate immediately. These approaches could save unwanted clinician workload

Table 1. Guidelines for COVID-19 management by the hospital pharmacy and the pharmacists (FIP and Nepal)^{7,12}

Organization	Features of the guidelines
International Pharmaceutical Federation (FIP)	<ul style="list-style-type: none"> - Ensuring healthy inventory management of pharmaceutical products (both medicines and medical devices) and a good supply system - Liaising with other healthcare professionals in providing patient care and support - Promoting infection control mechanisms in hospitals - Promoting health education and counseling - Ensuring responsible and proper use of the pharmaceutical products and personal protective equipment supplied. - Providing pharmacovigilance services and monitoring treatment outcomes
Nepal Pharmaceutical Association	<ul style="list-style-type: none"> - Ensuring storage and supply of essential medicinal and surgical products, including mask, a thermometer, goggles - Co-ordinating with other healthcare professionals in patient care - Raising public awareness regarding COVID-19 prevention and control - Monitoring treatment outcomes and pharmacovigilance - Ensuring an inventory of medicine in both inpatients and outpatients with COVID-19 pandemic cases

COVID-19: Coronavirus disease-2019, FIP: International Pharmaceutical Federation

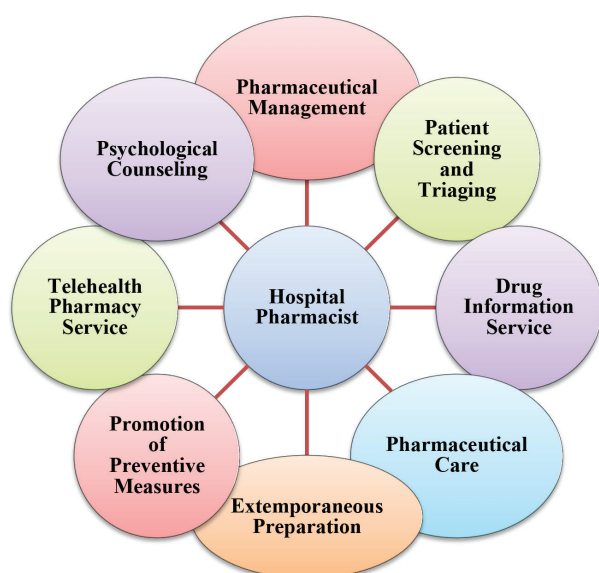


Figure 1. The role hospital pharmacists can play in COVID-19 and pandemic control in LICs

and prevent infection transmission possibility in the pandemic. The FIP has also made specific guidelines for pharmacists in disaster and pandemic situations.^{7,8} The guidelines instruct pharmacists to initial screening patients to provide first aid, triage, screening, and treating minor ailments.^{7,8} In some developed countries, pharmacists have adopted that role earlier, too.²² Therefore, LICs should also attempt to prepare, equip and use the pharmacy workforce optimally in disaster situations.

Pharmaceutical care

China implemented pharmaceutical care programs as substantial service in COVID-19 as it was reported to have a significant impact on patient outcomes.²³⁻²⁵ Pharmaceutical care is much needed care for the treatment and management of COVID-19 patients, especially for elderly patients and patients with chronic diseases as they are at a higher risk of developing drug interactions and adverse effects as well as their use of complex medication regimens.^{26,27} For instance, chloroquine, azithromycin, and hydroxychloroquine can cause

QT prolongation and the administration of these medicines to patients already suffering from cardiovascular conditions can make them worse.²⁸ Therefore, there was a need for close monitoring of patient medication status along with therapeutic outcomes. Hospital pharmacists should monitor and evaluate the medication dose, administration, drug interaction, and adverse effects to plan an appropriate medication formulary and medicine regimen in collaboration with other healthcare professionals.^{26,29,30} However, these clinical roles were not much emphasized in the guidelines made by LICs such as Nepal.¹²

Along with that, pharmacists have a responsibility to provide information on medication outcomes, assess polypharmacy issues and monitor the medication compliance of patients. Patients might not come for regular follow up their medical condition and require self-medication because of pandemic fears and movement control order and such restrictive provisions. Therefore, pharmacists must proactively identify these patients and get regular updates about their clinical condition and provide proper counseling and refer them to hospitals if needed.

Promotion of preventive measures

In many countries, community pharmacies were closed because of COVID-19; and the hospital pharmacies served as a primary source to get medicine and precautionary material like “masks” and “hand sanitizers” to the public. Therefore, hospital pharmacists are the most accessible and responsible health professionals in providing pharmacy and preventive and promotive healthcare services such as an aseptic way of using the mask, hand washing, social distance values, isolated coughing, sneezing, required in COVID-19 prevention (12.35).^{7,31} The study has previously shown a significant change in public health in controlling unhealthy behavior and promoting disease control, prevention, and drug abuse management through pharmacist involvement.^{24,32}

Extemporaneous preparation

Healthcare-associated infections result in complications and even death.³³ Simultaneously, simple hand hygiene can prevent diseases.³⁴ As pharmacists are trained to conduct

extemporaneous dispensing, pharmacist can prepare hand sanitizers, disinfectant liquids, *etc.*, for hospitals' internal use and the community at the time of medical goods scarcity due to disaster. There have been multiple reports about pharmacists preparing such products and contributing to society to fight against COVID-19 in this exceptional circumstance.³⁵

Telehealth pharmacy services (TPS)

Access to pharmacy services was challenging during the pandemic, when people were not allowed to leave their home. Approaching pharmacy services by using telecommunication technology can solve that challenge. Continuous pharmaceutical care is prominent, particularly for chronic disease patients who are at higher risk of infection and have already undertaken multiple medicines. Thus, TPS was a suitable way to reach the patient. TPS can serve people living in far-off places, self-quarantined and people unable to visit a hospital pharmacy using email, phone call, text message, or social media.^{36,37} Hospital pharmacists can collect patient's medicine and disease information and supply medicine to a respective patients with appropriate labeling and counsel on medicine administration through phone calls or any other online media.³⁶ Furthermore, pharmacists can advise patients on self-monitoring of medicine effectiveness and self-management of minor ailments and whether to continue their medicine or visit a center centre on a phone call or at the doorstep, while delivering medications.^{24,38} Good access to the internet and telecommunication is highly essential to providing TPS, which may be problematic in many villages of LICs.

Many developed countries have been using telepharmacy services.³⁷ In response to the pandemic, Australia enhanced its existing telepharmacy practices,³⁹ and China also emphasized the online pharmacy consultation for COVID-19.⁴⁰ Although online consultation and medicine delivery are difficult in LICs, the hospital pharmacist must attempt to start this approach in coordination with their hospital administration, at least in a disaster situation.

Psychological counseling

Because of the pandemic and lockdown, people could not move and were forced to confine themselves inside their home. The changing daily routine and the thought of death, pandemic, and growing disease progression affect people's thinking patterns, leading to anxiety, panic, and depression, to psychological problems.^{41,42} Psychological problems can be more pressing in mentally ill patients, low-socioeconomic groups, and cardiovascular diseases like chronic illness patients.^{43,44} Therefore, pharmacists should monitor the patient's emotional states and encourage them to perform stress-relieving activities.

Professional challenges of pharmacists and possible solutions in disaster management

Although we proposed some roles, they do not come without challenges. We have identified six challenges related to these roles and presented them in Figure 2. These problems and potential solutions are described in the different subheadings in this section of this manuscript.

Shortage of safety measures	<ul style="list-style-type: none"> Promoting local entrepreneurship Extemporaneous preparation of hand sanitizer Telehealth pharmacy services
Difficulty in adequate medication management	<ul style="list-style-type: none"> Need based minimal medicine prescribing Medicine substitution
Shortness of pharmacy manpower	<ul style="list-style-type: none"> Utilizing pharmacy students and medical personnel Long term planning on qualified pharmacy personnel development
Non-existent or less priority to pharmaceutical care	<ul style="list-style-type: none"> Promotion and utilization of pharmacy personnel in pharmaceutical care
Poor security to health care professionals	<ul style="list-style-type: none"> Assure basic need and health Site allocation and Ensure the safety of work place Appropriating training
Non-favourable legislation	<ul style="list-style-type: none"> Formulation of appropriate guideline for emergency prepared Promotion of appropriate education to developed skillful pharmacy personnel

Figure 2. Challenges and solutions

Shortage of safety measures

As *per* the WHO, the appropriate protective materials like surgical masks, eye protection and face shield, long-sleeved gowns, and gloves are the basic needs to work in a health institution during COVID pandemics.³¹ Hospital pharmacists were at a high risk of getting infected, and they could be a medium of transmission as they were in close contact with patients visiting the hospitals.⁷ However, the availability of precautionary safety materials to healthcare professionals, including pharmacists, has become challenging in LICs where there are no manufacturing companies for these protective supplies.^{31,45,46} Therefore, LICs should promote local entrepreneurs to produce personal protective equipment and mask-like protective measures without relying on imports from outside. Hospital pharmacists can contribute in this regard by extemporaneous compounding hand sanitizer gels, sprays, *etc.*

Difficulty in adequate medication management

Many LICs are not self-reliant and vastly depend on the import of medication from foreign countries. Thus, due to the possibility of a drug shortage or delayed supply chain system due to travel restrictions during a pandemic, adequate and timely access to essential medicine in healthcare settings can be challenging in many countries.⁴⁵ The situation may become more difficult for people with a chronic condition for whom missing a few doses of medication can be life-threatening. The hospital pharmacist had a responsibility to update the prescribers on available medicines and their inventory. This helped prescribers make appropriate prescribing decisions like prescribing only to the needed patients in minimum quantities to reduce the unnecessary wastage of medicine and prevent the medicine shortage. It also helped them decide whether to prescribe multiple refills to one patient or make a single refill to multiple patients. The appropriate quantification and stocking of medication-related to COVID-19, such as remdesivir and chloroquine, were essential based on the clinical practice. However, it came down to pharmacists' expertise to forecast the usage because overstocking may cause a shortage of these medications for those who require them regularly.⁴⁷

Furthermore, there might have been a problematic situation related to brand prescriptions, when patients rely on a particular

hospital for their continued medication. Brand prescribing is very common in LICs and a refill of a particular brand or searching for a particular brand for the patient is very tough, when there is a shortage due to the lockdown.⁴⁸ Also, there may come to some circumstances in disasters or pandemics, where the patient may not find a generic substitution and clinician consultation. Furthermore, pharmacists could only be an option to manage the patients. Therefore, the pharmacists should be allowed to substitute medicine for therapeutically equivalent alternatives in consultation with the prescribers, if they are accessible or without consultation if the prescribers are inaccessible to consult in a disaster situation. The FIP in 2016 made a guidelines focusing on pharmacy personnel's role in the disaster where pharmacists can also do some emergency prescribing if needed. That should be strongly taken into consideration by the responsible bodies in LICs. At least, pharmacists should be prepared to prescribe the essential medications during the pandemic and other similar disaster.⁸ However, it was not seen in the guidelines made by LICs,¹² which are quite hard to implement for LICs. Convincing with the local hospital administration and legal body would help solve this problem to some extent.

Shortage of pharmacy human resources

Pharmacists have been importing a significant role in providing pharmacy services in pandemic prevention and control.⁴⁹ COVID-19 has already caused the death of many health professionals in developed countries.⁵⁰ The situation could be even more devastating for LICs, where there is already a shortage of pharmacy human resources.^{51,52} The death, hospitalization or isolation of limited human resources would increase the workload. Eventually, it hampered the pharmaceutical services of patients. Therefore, the LICs should work proactively in developing and equipping sufficient human resources to defeat disaster challenges. Pharmacy students and non-pharmacy medical personnel can be used through immediate short-term training to cope with the current pharmacy workforce shortage in providing pharmaceutical services. Also, the pharmacy services can be provided to a large group by small human resources through the TPS approach.³⁶

Non-existent or less priority to pharmaceutical care

The pharmacy personnel in LICs are primarily focused on the product approach (procurement, inventory, and dispensing). Although pharmaceutical care has been determined as a vital aspect of treatment, the environment of providing pharmaceutical services and access to quality workforce still lacks in LICs.^{31,40,51,53} LICs should learn the importance of pharmaceutical care or the clinical service of pharmacy personnel. They must use the available pharmacy personnel in providing pharmaceutical care, at least, in this disaster. Eventually, LICs should make appropriate policies and guidelines to promote the pharmacist in a clinical role in the healthcare system.

Poor security to healthcare professionals

Healthcare professionals also need motivation and security during a disaster. Taking personal care of oneself, along

with continuous working for others' health, was relatively complicated. Healthcare personnel, including pharmacists, require appropriate motivation and support from the government and respective health centers. Pharmacists have been greatly appreciated even financially in developed countries like New Zealand for their remarkable contribution during pandemics.²⁵ The respective health institutions and governments of LICs should also learn from them and provide essential facilities such as food, lodging for them and their families during this disaster if they could not reward them as high-income countries did.

Similarly, protecting and preventing infection transmission to healthcare personnel is supremely essential because healthcare providers themselves can transmit others while serving. Previously, up to 10% of COVID cases in China and up to 9% in Italy were healthcare personnel.⁵⁰ Infection of healthcare personnel not only increases patient numbers but also reduces persons to care for patients. Therefore, stringent health approaches need to be adopted to prevent infection transmission. China made a strict guidelines for cleansing, disinfecting, and controlling human movements to prevent infection transmission.⁴⁰ Learning from them, LICs can create separate allocated places for COVID management, prepare disinfection guidelines and make designated sites for health personnel involved in COVID management.

Along with that, healthcare professionals, including hospital pharmacists, need to be aware and trained in following the safety procedures of work to prevent being infection and being a source of infection transmission.⁵⁰ The concerned government and hospital administrative body should provide appropriate training to ensure healthcare providers' safety, including hospital pharmacist.

Non-favorable legislation

LICs suffer from a lack of appropriate pharmacy education, skilled and qualified personnel, and professional guidelines for effective professional functioning.^{53,54} Though similar professionals have significantly impacted the health sector in developed countries, a pharmacist suffers due to the deficient role from the concerned authority in LICs.^{53,54} Unprepared pharmacy professionals cannot play a significant role in emergencies and disaster situations. The recent earthquake disaster in Nepal taught much about preparing pharmacy services for disaster management in LICs.⁵⁵ Many studies have already talked about the significant contributions pharmacists have made in pandemic and emergency disasters; therefore, along with the appropriate policy, pre-qualifying them through quality education and skill is the only necessity in LICs to defeat the disaster.^{49,56,57} Therefore, the LICs, where the pharmacists have not been adequately used to provide pharmaceutical services, should learn from the current COVID-19 pandemic and equip the pharmacy workforce to manage such possible future disasters through the appropriate formulation of guidelines and emergency training preparedness. Additionally, LICs or hospitals themselves can make separate guidelines for disaster situations by using FIP guidelines on responding to disasters for pharmacy personnel as a reference.⁸

CONCLUSION

The growing cases of COVID-19 have created significant challenges to the healthcare system and healthcare professionals of LICs. During COVID-19, hospital pharmacists were responsible for ensuring appropriate therapy outcomes, medication management, health promotion, pharmaceutical care of patients, and infection transmission prevention. The study recommends enhancing the hospital pharmacists' professional role in disaster and management for COVID-19 and other such disasters in the future.

ACKNOWLEDGMENTS

The authors want to thank Mrs. Nita Shrestha (Nepal Health Research and Innovation Foundation), Mr. Mandip Pokharel (Vennue Foundation) and Mr. Pankaj Vaidya (Nepal Cancer Hospital and Research Center) for their valuable suggestions and comments while developing the concept and overall writing.

Ethics

Peer-review: Externally peer-reviewed.

Authorship Contributions

Concept: R.S., S.S., Design: R.S., Data Collection or Processing: R.S., Analysis or Interpretation: R.S., S.S., B.S., B.K., S.K., Literature Search: R.S., Writing: R.S.

Conflict of Interest: No conflict of interest was declared by the authors.

Financial Disclosure: The authors declared that this study received no financial support.

REFERENCES

- World Health Organization. WHO coronavirus disease (COVID-19) Dashboard. Published 2020. <https://covid19.who.int/table>
- World Bank. World Bank Country and Lending Groups. Accessed February 25, 2021. <https://datahelpdesk.worldbank.org/knowledgebase/articles/906519-world-bank-country-and-lending-groups>
- WHO/UNICEF. Water, sanitation and hygiene in health care facilities: status in low- and middle-income countries and way forward. Published online 2019;1-52. https://apps.who.int/iris/bitstream/handle/10665/154588/9789241508476_eng.pdf;jsessionid=8BB20D0F383BB2585E35A2CEA1EF1457?sequence=1
- Hajat C, Stein E. The global burden of multiple chronic conditions: a narrative review. *Prev Med Rep*. 2018;12:284-293.
- McGregor S, Henderson KJ, Kaldor JM. How are health research priorities set in low and middle income countries? A systematic review of published reports. *PLoS One*. 2014;9:e108787.
- Agampodi TC, Agampodi SB, Glozier N, Siribaddana S. Measurement of social capital in relation to health in low and middle income countries (LMIC): a systematic review. *Soc Sci Med*. 2015;128:95-104.
- International Pharmaceutical Federation (FIP). COVID-19: Guidelines for Pharmacists and the Primary Workforce; 2020. Accessed May 7, 2020. <https://www.fip.org/files/content/priority-areas/coronavirus/COVID-19-Guidelines-for-pharmacists-and-the-pharmacy-workforce.pdf>
- International Pharmaceutical Federation (FIP). Responding to disasters: Guidelines for Pharmacy 2016. Published online 2016;46. <http://fip.org/files/fip/publications/2016-07-Responding-to-disasters-Guideline.pdf>
- Watson KE, Singleton JA, Tippet V, Nissen LM. Defining pharmacists' roles in disasters: a Delphi study. *PLoS One*. 2019;14:e0227132.
- Menighan TE. Pharmacists have major role in emergency response. *Pharm Today*. 2016;22:8.
- Ranjit E. Pharmacy practice in Nepal. *Can J Hosp Pharm*. 2016;69:493-500.
- Association NP. Covid-19: Guideline for pharmacists and pharmacy assistant. Accessed April 28, 2020. https://www.fip.org/files/content/priority-areas/coronavirus/mo-resources/NEPAL_Final_Guideline_COVID.pdf
- Ozawa S, Shankar R, Leopold C, Orubu S. Access to medicines through health systems in low-and middle-income countries. *Health Policy Plan*. 2019;34(Suppl 3):iii1-iii3.
- Dalton K, Byrne S. Role of the pharmacist in reducing healthcare costs: current insights. *Integr Pharm Res Pract*. 2017;6:37-46.
- AlRuthia YS, AlKofide H, AlAjmi R, Balkhi B, Alghamdi A, AlNasser A, Alayed A, Alshammari M, Alsuhailani D, Alathbah A. Drug shortages in large hospitals in Riyadh: a cross-sectional study. *Ann Saudi Med*. 2017;37:375-385.
- Lam WY, Fresco P. Medication adherence measures: an overview. *Biomed Res Int*. 2015;2015:217047.
- Barnsteiner JH. Chapter 38. Medication reconciliation. In: Hughes RG, ed. *Patient Safety and Quality - An Evidence-Based Handbook for Nurses*. 2008. <https://www.ncbi.nlm.nih.gov/books/NBK2648/>
- Aljazeera. Iran: Over 700 Dead after drinking alcohol to cure coronavirus. www.aljazeera.com/news/2020/04/iran-700-dead-drinking-alcohol-cure-coronavirus-200427163529629.html
- Ghaibi S, Ipema H, Gabay M; American Society of Health System Pharmacists. ASHP guidelines on the pharmacist's role in providing drug information. *Am J Health Syst Pharm*. 2015;72:573-577.
- Shrestha S, Khatiwada AP, Gyawali S, Shankar PR, Palaian S. Overview, challenges and future prospects of drug information services in Nepal: a reflective commentary. *J Multidiscip Healthc*. 2020;13:287-295.
- World Health Organization. Coronavirus disease (COVID-19) advice for the public: mythbusters. <https://www.who.int/emergencies/diseases/novel-coronavirus-2019/advice-for-public/myth-busters>
- Epp DA, Tanno Y, Brown A, Brown B. Pharmacists' reactions to natural disasters: from Japan to Canada. *Can Pharm J (Ott)*. 2016;149:204-215.
- Song Z, Hu Y, Zheng S, Yang L, Zhao R. Hospital pharmacists' pharmaceutical care for hospitalized patients with COVID-19: recommendations and guidance from clinical experience. *Res Social Adm Pharm*. 2021;17:2027-2031.
- Zheng SQ, Yang L, Zhou PX, Li HB, Liu F, Zhao RS. Recommendations and guidance for providing pharmaceutical care services during COVID-19 pandemic: a China perspective. *Res Social Adm Pharm*. 2021;17:1819-1824.
- Bukhari N, Rasheed H, Nayyer B, Babar ZU. Pharmacists at the frontline beating the COVID-19 pandemic. *J Pharm Policy Pract*. 2020;13:8.
- Shrestha S, Shrestha S, Khanal S. Polypharmacy in elderly cancer patients: challenges and the way clinical pharmacists can contribute in resource-limited settings. *Aging Med (Milton)*. 2019;2:42-49.
- Kurt M, Akdeniz M, Kavukcu E. Assessment of comorbidity and use of prescription and nonprescription drugs in patients above 65 years attending family medicine outpatient clinics. *Gerontol Geriatr Med*. 2019;5:2333721419874274.

28. Saleh M, Gabriels J, Chang D, Soo Kim B, Mansoor A, Mahmood E, Makker P, Ismail H, Goldner B, Willner J, Beldner S, Mitra R, John R, Chinitz J, Skipitaris N, Mountantonakis S, Epstein LM. Effect of chloroquine, hydroxychloroquine, and azithromycin on the corrected QT interval in patients with SARS-CoV-2 infection. *Circ Arrhythm Electrophysiol.* 2020;13:e008662.
29. Elden NM, Ismail A. The Importance of medication errors reporting in improving the quality of clinical care services. *Glob J Health Sci.* 2016;8:54510.
30. Velo GP, Minuz P. Medication errors: prescribing faults and prescription errors. *Br J Clin Pharmacol.* 2009;67:624-628.
31. Al-Quteimat OM MSc, BCOP, Amer AM RPh, MSc. SARS-CoV-2 outbreak: how can pharmacists help? *Res Social Adm Pharm.* 2021;17:480-482.
32. Agomo CO. The role of community pharmacists in public health: a scoping review of the literature. *J Pharm Heal Serv Res.* 2012;3:25-33.
33. Haque M, Sartelli M, McKimm J, Abu Bakar M. Health care-associated infections - an overview. *Infect Drug Resist.* 2018;11:2321-2333.
34. Mathur P. Hand hygiene: back to the basics of infection control. *Indian J Med Res.* 2011;134:611-620.
35. Di-Falco E, Bourbon J, Sbafe I, Kaiser J. Preparation of alcohol-based handrub in COVID-19 alsatian cluster. *Pharm Technol Hosp Pharm.* 2020. doi:10.1515/ptph-2020-0004.
36. Poudel A, Nissen LM. Telepharmacy: a pharmacist's perspective on the clinical benefits and challenges. *Integr Pharm Res Pract.* 2016;5:75-82. Erratum in: *Integr Pharm Res Pract.* 2016;5:83.
37. Le T, Toscani M, Colaizzi J. Telepharmacy: a new paradigm for our profession. *J Pharm Pract.* 2020;33:176-182.
38. Council on Credentialing in Pharmacy, Albanese NP, Rouse MJ. Scope of contemporary pharmacy practice: roles, responsibilities, and functions of pharmacists and pharmacy technicians. *J Am Pharm Assoc (2003).* 2010;50:35-69.
39. Department of Health AG. Fact sheet national health plan a guide for prescribers; 2020.
40. Association CP. Coronavirus 2019-nCoV infection: expert consensus on guidance and prevention strategies for hospital pharmacists and the pharmacy workforce (1st edition). First; 2020. Accessed April 24, 2020. <https://www.fip.org/files/content/priority-areas/coronavirus/CPA-CORONAVIRUS-2019-nCoV-Expert-Consensus-on-Guidance-and-Prevention.pdf>
41. Holmes EA, O'Connor RC, Perry VH, Tracey I, Wessely S, Arseneault L, Ballard C, Christensen H, Cohen Silver R, Everall I, Ford T, John A, Kabir T, King K, Madan I, Michie S, Przybylski AK, Shafraan R, Sweeney A, Worthman CM, Yardley L, Cowan K, Cope C, Hotopf M, Bullmore E. Multidisciplinary research priorities for the COVID-19 pandemic: a call for action for mental health science. *Lancet Psychiatry.* 2020;7:547-560.
42. Xiang YT, Yang Y, Li W, Zhang L, Zhang Q, Cheung T, Ng CH. Timely mental health care for the 2019 novel coronavirus outbreak is urgently needed. *Lancet Psychiatry.* 2020;7:228-229.
43. Mokdad AH, Mensah GA, Posner SF, Reed E, Simoes EJ, Engelgau MM; Chronic Diseases and Vulnerable Populations in Natural Disasters Working Group. When chronic conditions become acute: prevention and control of chronic diseases and adverse health outcomes during natural disasters. *Prev Chronic Dis.* 2005.
44. Dimsdale JE. Psychological stress and cardiovascular disease. *J Am Coll Cardiol.* 2008;51:1237-1246.
45. Kretchy IA, Asiedu-Danso M, Kretchy JP. Medication management and adherence during the COVID-19 pandemic: perspectives and experiences from low-and middle-income countries. *Res Soc Adm Pharm.* 2021;17:2023-2026.
46. Bong CL, Brasher C, Chikumba E, McDougall R, Mellin-Olsen J, Enright A. The COVID-19 pandemic: effects on low- and middle-income countries. *Anesth Analg.* 2020;131:86-92.
47. National Institute of Health NIH. Coronavirus disease 2019 (COVID-19) treatment guidelines; 2020. <https://files.covid19treatmentguidelines.nih.gov/guidelines/covid19treatmentguidelines.pdf>
48. Shrestha R, Prajapati S. Assessment of prescription pattern and prescription error in outpatient Department at tertiary care district hospital, Central Nepal. *J Pharm Policy Pract.* 2019;12:16.
49. Chin TW, Chant C, Tanzini R, Wells J. Severe acute respiratory syndrome (SARS): the pharmacist's role. *Pharmacotherapy.* 2004;24:705-712.
50. European Centre for Disease Prevention and Control. Infection Prevention and Control and Preparedness for COVID-19 in Healthcare Settings; 2020. Accessed April 29, 2020. <https://www.ecdc.europa.eu/sites/default/files/documents/nove-coronavirus-infection-prevention-control-patients-healthcare-settings.pdf>
51. Sakeena MHF, Bennett AA, McLachlan AJ. Enhancing pharmacists' role in developing countries to overcome the challenge of antimicrobial resistance: a narrative review. *Antimicrob Resist Infect Control.* 2018;7:63.
52. Koehler T, Brown A. A global picture of pharmacy technician and other pharmacy support workforce cadres. *Res Soc Adm Pharm.* 2017;13:271-279.
53. Alipour F, Peiravian F, Mehralian G. Perceptions, experiences and expectations of physicians regarding the role of pharmacists in low-income and middle-income countries: the case of Tehran hospital settings. *BMJ Open.* 2018;8:e019237.
54. Babar Z, Scahill S. Barriers to effective pharmacy practice in low-and middle-income countries. *Integr Pharm Res Pract.* 2014;52:25-27.
55. Shrestha S, Kandel P, Danekhu K, Bhuvan KC. Reflecting on the role of a pharmacist during the two major earthquakes of 2015: are we prepared for similar future disasters? *Res Soc Adm Pharm.* 2019;15:1500-1501.
56. Hannings AN, von Waldner T, McEwen DW, White CA. Assessment of emergency preparedness modules in introductory pharmacy practice experiences. *Am J Pharm Educ.* 2016;80:23.
57. Porter KE, Singleton JA, Tippet V, Nissen LM. Ready, willing and able: the role of pharmacists in natural and manmade disasters - can we do more? *Int J Pharm Pract.* 2018;26:195-196.

PUBLICATION NAME	Turkish Journal of Pharmaceutical Sciences
TYPE OF PUBLICATION	Vernacular Publication
PERIOD AND LANGUAGE	Bimonthly-English
OWNER	Onur Arman ÜNEY on behalf of the Turkish Pharmacists' Association
EDITOR-IN-CHIEF	Prof. İlkay Erdoğan Orhan, Ph.D
ADDRESS OF PUBLICATION	Turkish Pharmacists' Association, Mustafa Kemal Mah 2147.Sok No:3 06510 Çankaya/Ankara, TURKEY

Turkish Journal of

PHARMACEUTICAL SCIENCES

Volume: 19, No: 2, Year: 2022